Biology of the mountain pinhole borer, *Platypus subgranosus* Schedl, in Tasmania

by

Gregory
Steven G. Candy, B.Sc., Dip.Biom. (Sydney)

graduating 1991

Submitted in fulfilment
of the requirements of the degree of
Master of Agricultural Science
UNIVERSITY OF TASMANIA
HOBART
23rd February 1990.

This thesis contains no material which has been accepted for the award of any other degree or diploma in any university and, to the best of my knowledge and belief, this thesis contains no copy or paraphrase of material previously published or written by another person, except when due reference is made in the text of the thesis.

signed

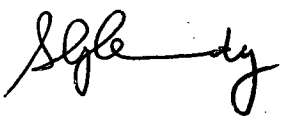

S.G. Candy

23rd February 1990.

Acknowledgements

Quite a few people have helped me during the life of this project and though it is not possible to mention everyone of them here, I am grateful for their assistance. I would especially like to thank my supervisors Dr. John Madden (University of Tasmania) and Dr. Humphrey Elliott (Forestry Commission). I am grateful to Drs. Elliott and Glen Kile for permission to use their previously unpublished data in this study. Dick Bashford has given me much practical assistance in the field work. Staff at the Geeveston district office of the Forestry Commission collected thermohydrograph sheets weekly over nearly two years and I am grateful for their help. Tony Morriss and Tom Kelly gave assistance in the use of the ARC/INFO software and Peter McQuillan gave assistance with scanning electron microscopy. I thank Dr. John Lawrence for identifying the *Hymaea succinifera* larva for me. I am also very grateful for the review of this thesis by Drs. Neil Gilbert, Humphrey Elliott, John Madden and Don Thompson. I would also like to thank the Forestry Commission for assistance in the work carried out for this special interest project. In particular, I would like to thank Drs. Murray Cunningham (former Commissioner), Marcus Higgs and Don Thompson for their encouragement and patience.

Finally, a special vote of thanks to my wife Chris and daughter Claire for their patience and encouragement during the many hours spent after work on this project.

Biology of the Mountain Pinhole Borer, *Platypus subgranosus* Schedl, in Tasmania

Contents

List of Figures

List of Tables

Summary

Information on the life cycle and associations of the mountain pinhole borer, *Platypus subgranosus* Schedl (Coleoptera : Curculionidae : Platypodinae) is reviewed. Existing unpublished data combined with data collected in this study are used to provide quantitative descriptions of aspects of *P.subgranosus* biology.

The within-tree spatial pattern of attack was found to be highly aggregated both at high and low density of attack. Aggregation was very high around host tissue infected with the pathogenic fungus *Chalara australis* Walker and Kile. A minimum spacing between pinholes of approximately one centimetre was indicated but densities were not sufficiently high for this to result in spatial regularity.

Use of larval head capsule width and body length in a non-hierarchical classification procedure confirmed the presence of five instars. Initial oviposition occurred when the gallery ranged between 5 and 25cm in length. The natality rate at initial oviposition was roughly one egg per centimetre beyond an initial length of 4cm. Initial oviposition in galleries established in the late summer/autumn period occurred at roughly the same date irrespective of establishment date. This was paralleled by a faster rate of gallery development for autumn compared to late summer establishment. Timing of emergence exhibited an analogous trend to that of initial oviposition. It is postulated that these trends as well as a trend for emergence and subsequent gallery establishment to occur less commonly in spring/early summer than late summer/autumn are a response to high mortality of eggs and early instars in summer from desiccation.

For a sample of galleries established in the late summer/autumn period, initial oviposition occurred in winter one to eight months after gallery establishment with eggs usually laid in a batch with median size of seven. First to third instars appeared through

the following spring and early summer with fourth and final instars appearing in summer and subsequently the final instar predominating through winter until pupation in the following spring. Emergence began in early summer.

A new model of insect phenology based on conditional probabilities is developed and compared to existing ordinal regression and gamma entry time models.

The sex ratio of emergents over the population is very close to unity but individual galleries can deviate markedly from this with an excess of either sex. The mean number of emergents per gallery was 19.7 with a maximum of 92. The gallery failure rate was 8% but negligible mortality of immature stages was observed.

Development time ranged from ten months to two years depending on the timing of gallery establishment as predicted by the linear day-degree model. Threshold temperature for development and total day-degrees above this threshold from gallery establishment to emergence, *DD*, were estimated from field data at 11°C and a mean of DD_{11} of 4047 respectively. A new estimation procedure based on maximum likelihood is developed to estimate the parameters of the day-degree model under ambient temperatures. Both gamma and inverse normal distributions were found to adequately describe the empirical distribution of DD_{11}. Only for the gamma, though, was the estimation algorithm successful.

The implications of *P.subgranosus* biology for rainforest ecology and management are discussed.

1. INTRODUCTION

Platypus subgranosus Schedl (Coleoptera: Curculionidae: Platypodinae) is a small brown cylindrical beetle commonly called the mountain pinhole borer. It is about 4mm long and 1mm in diameter and is typical of the platypodid beetles in shape and its habit of boring a system of tunnels, called a gallery, in the wood of trees or logs and introducing, feeding on, and rearing its brood on symbiotic (*ambrosia*) fungi which grow on the gallery walls. *P.subgranosus* belongs to the group of Coleoptera classified by this habit as *ambrosia* beetles. *P.subgranosus* appears to be endemic to Australia where it is common in the cool temperate rainforests of Tasmania and the Victorian central highlands. Its main host tree is myrtle beech, *Nothofagus cunninghamii* Oerst. It is similar in appearance and habits to other species of platypodid beetles, *P.apicalis* White, *P.gracilis* Broun and *P.caviceps* Broun (Milligan 1979), which attack *Nothofagus* spp. in cool temperate rainforests in New Zealand.

P.subgranosus was first described by Schedl (1936) from specimens contained in the South Australian Museum. The specimens examined by Schedl were collected from Waratah, Tasmania (Lea and Carter) (A.Simson collection) and from the Dividing Range, Queensland (Blackburn collection). Apart from the above Queensland collection *P.subgranosus* has only been recorded in or near temperate rainforests in Tasmania and Victoria. The first investigations of the biology of *P.subgranosus* were carried out by Hogan (1944,1948) in Victoria. Hogan (1948) described the immature stages, life history and habits, techniques for insectary rearing and observations on symbionts, parasites and predators of *P.subgranosus*. Webb (1945) identified the fungus *Leptographium lundbergia* from *P.subgranosus* gallery walls. After Hogan's work no other published studies on *P.subgranosus* have been found by the author until Howard (1973) gave the first report on a wilt disease affecting *N.cunninghamii* in Tasmania and observed that dying trees were attacked by an ambrosia beetle, *Platypus* sp., and had extensive discoloration of the stem sapwood. The wilt disease was given the colloquial

name 'myrtle wilt'. Elliott *et al.* (1983) established the important role ethanol plays as a primary attractant and boring stimulant for *P.subgranosus*. They established that ethanol is the major volatile produced by fermentation of logs under anoxic conditions. Later work has concentrated on the relationship between attack by *P.subgranosus*, myrtle wilt and infection of *N.cunninghamii* by the pathogenic hyphomycete *Chalara australis* Walker and Kile, a vascular stain disease, which has been identified as the cause of 'myrtle wilt' (Kile and Walker 1987, Kile and Hall 1988, Kile 1989, Kile *et al.* 1990a).

Death of *N.cunninghamii* due to myrtle wilt is virtually synonymous with attack by *P.subgranosus* (Elliott *et al.* 1987). Elliott *et al.* (1987) carried out an extensive survey of the incidence of *P.subgranosus* attack on *N.cunninghamii* in rainforests undisturbed by fire, roading or logging in Tasmania. They found that the cumulative death of *N.cunninghamii*, where the time since death was judged by the amount of dead foliage or fine branches remaining, ranged from 9 to 53% of the stand stocking with an average of 24.6% for the 20 sites surveyed. The average annual death rate was estimated to be 2.4 trees ha^{-1} or 1.6% of live trees. The incidence of attack was not found to be strongly related to stand or site variables with the exception of altitude where incidence decreased with increasing altitude and they suggested this relationship was determined by the effect of temperature on development of both *P.subgranosus* and *C.australis*. Attacked trees were also found to be clumped which was hypothesised to be the result of either or both of (i) the spread of *C.australis* via root grafts rendering freshly infected trees highly attractive to attack and (ii) the close proximity of a tree to a source of emerging beetles.

The possibility that *P.subgranosus* is a vector of *C.australis* rather than simply a secondary factor attacking trees already infected by *C.australis* was investigated by Kile and Hall (1988). Their work indicated that infection by *C.australis* is not primarily due to vectoring by *P.subgranosus*. The adult beetles were rarely found to be carrying

spores of *C.australis* and the fact that the saprophytic survival of the fungus is considerably shorter than the beetles life cycle suggested that emergent adults from infected trees would not be a source of infection for newly attacked trees. *P.subgranosus* is more probably (Kile *et al.* 1990a) an indirect source of infection through frass contaminated with conidia (Kile and Hall 1988), created by gallery excavations in infected tissue of live trees, producing air- or water-borne inoculum. This inoculum then enters the tree through wounds which in some cases could be pinholes produced by initial *P.subgranosus* attack. Another source of air- and water-borne inoculum are the conidia from mycelial felts on the bark of infected trees or other wood surfaces (Kile *et al.* 1990a). Wound infection can occur without beetle attack (Kile *et al.* 1990a) and the most likely cause of between-tree disease foci is wound infection, apparently without beetle attack, via air- and water-borne inoculum. Local spread is then likely to be due to below-ground spread via root grafting or attack by *P.subgranosus* (Kile *et al.* 1990a). The relative importance of *P.subgranosus* in the etiology of myrtle wilt is still unclear. As well as contributing to disease spread by the creation of tree wounds (pinholes) and liberation of infected host tissue (frass) Kile *et al.* (1990a) consider it likely that the development of *P.subgranosus* galleries promotes within-tree spread of *C.australis*. The importance of *P.subgranosus* probably depends most on the relative importance of infected frass as a source of air- and water-borne inoculum. Kile *et al.* (1990a) reported limited initial research by Kile showing that a summer peak in inoculum levels is indicated which corresponds to the peak in frass production by adults and final instar larvae (Hogan 1948). On the other hand, sporulating felts are produced most abundantly in the autumn-winter period. *P.subgranosus* adult frass is fibrous while that of the final instar larva is fine and granular (Hogan 1948) and whether this difference has any effect on the role of frass as a source of inoculum is yet to be investigated. However both types of frass, when produced more than approximately 2 years after tree death, have an infected proportion

decreasing to zero with time (Kile and Hall 1988).

P.*subgranosus* is the most important insect pest of Tasmania's rainforests (Elliott and deLittle 1984). The impact of myrtle wilt on rainforest adjacent to recent disturbances can be severe and the importance of *P.subgranosus* in the ecology and management of these forests is considerably increased if it contributes significantly to the spread of myrtle wilt. Kile *et al.* (1990a) in a survey of myrtle wilt using a line transect running perpendicular to a recently developed road in north-east Tasmania found that the incidence of myrtle wilt decreased significantly from about 70% at the roadside down to a 'background level' (i.e. that in the undisturbed forest) of about 5% at a distance of 500m or more from the road (Kile *et al.* 1990a).

Apart from its relationship with *N.cunninghamii* and myrtle wilt, *P.subgranosus* is also economically important as a borer of freshly cut logs on landings and marshalling yards in or near rainforests. Logs cut from eucalypts, radiata pine and rainforest species are all susceptible to attack (Elliott and deLittle 1984) which can result in the degrade of valuable saw and veneer logs.

Currently Tasmania's rainforests are not managed on a large scale for timber production and a moratorium on logging in rainforests is currently in force (Hickey and Felton 1987). Rainforests species forming an understorey to old-growth eucalypts are, however, logged in normal clearfall operations of the eucalypt overstorey. In any future management of commercial rainforest (Hickey and Felton 1987) (i.e. rainforest allocated primarily for wood production) harvesting operations and silvicultural treatment of stands, such as thinning stands of pole sized myrtle to allow production of sawlogs under rotations of around 100 years (Hickey and Felton 1987), will need to take into account the impact of *C.australis/P.subgranosus* on the residual stand's health. Also where rainforest is managed for nature conservation or recreation the health and appearance of stands will be affected by disturbances such as fires, roading, walking trails etc. increasing the incidence of myrtle wilt.

In view of the importance of *P.subgranosus* from both an ecological and economic point of view, the lack of quantitative information on its life cycle, particularly the immature stages, and the large amount of uncollated data collected previously by the Forestry Commission, this study was instigated to provide a comprehensive account of the basic biology of *P.subgranosus* in Tasmania by new field investigations and collation of existing data. Because of the nature and environment of *P.subgranosus* biology, data collection was restricted to the field since laboratory experimentation was impractical given the available time and equipment.

It was also intended that mathematical models be developed from these data for a number of reasons. First, to summarise the data to allow trends and features of *P.subgranosus* biology to be more easily seen; second, to provide, in some cases, a framework for hypothesis testing; and third, to provide models that can be incorporated in an overall simulation/prediction system of population dynamics. In the course of modelling the data in this study new techniques were developed to (i) model data on insect phenology and (ii) estimate the parameters of the linear day-degree model of development from field data. Also, generalised linear models (McCullagh and Nelder 1983) were used extensively because of the nature of the data which was often in the form of counts or proportions and an appendix is included giving a brief introduction to the theory of generalised linear models which emphasises their application in this study. Apart from the above cases, the statistical/mathematical techniques and models used are, for brevity, not described in general but instead are described as the results of their use are reported.

The other main organisational feature of this thesis is in Section 2 where a general description of *P.subgranosus* biology is given. This description is based on previously published work as well as the findings of this study. It therefore provides a more detailed summary of the results of this study than is given in the main summary and is useful for readers who do not wish to read through the detail of later sections.

Also results of this study which are more observational than quantitative in nature are given in Section 2.

2. GENERAL DESCRIPTION OF *P.SUBGRANOSUS* BIOLOGY

2.1 HOST TREES

The primary host tree of *P.subgranosus* is myrtle beech (*N.cunninghamii*) and apparently healthy trees of this species can be successfully colonised by the beetle. Damage, stress, fire scorch or close proximity to disturbances such as roading make myrtle beech more susceptible to attack by *P.subgranosus*. Trees smaller than 100mm diameter are not usually attacked unless damaged or fire-scorched. As well as *N.cunninghamii*, live but damaged or fire-scorched specimens of temperate rainforest species leatherwood, *Eucryphia lucida* (Labill.) Baill., sassafras, *Atherosperma moschatum* Labill., celery top pine, *Phyllocladus aspleniifolius* (Labill.) Hook.f., and horizontal, *Anodopetalum biglandulosum* A. Cunn. ex Hook.f., can also be attacked and galleries successfully established (Elliott and deLittle 1984) although brood production from these other rainforest species is not known. Apart from *N.cunninghamii* these species rarely die after attack by *P.subgranosus* and this can be attributed to the fact that only *N.cunninghamii* is naturally susceptible to the pathogenic fungus *C.australis* which produces 'myrtle wilt' and is closely associated with attack by *P.subgranosus* (Elliott *et al.* 1987, Kile and Walker 1987, Kile and Hall 1988). Hogan (1948) lists eucalypt species *E.regnans* F.Muell., *E.delegatensis* (*gigantea*) R.Baker, *E.obliqua* L'Her. and, *E.cypellocarpa* (*goniocalyx*) L.Johnson as sources of emergent *P.subgranosus* although the conditions under which these species were attacked was not stated. However, from the title of his work it is probable that his work was confined to attack on fire-killed or scorched eucalypts. Unhealthy radiata pine (*Pinus radiata* D.Don) is also attacked by *P.subgranosus* (Elliott and deLittle 1984). Even sawn timber and edgings of Huon pine [*Lagarostrobus franklinii* (Hook.f.) C.J.Quinn], a species which is noted for its resistance to insect attack, can be attacked. Attack of freshly sawn timber does not result in successful brood production because the timber dries out relatively quickly compared to the length of the life cycle, resulting in the desiccation

of eggs and larvae before new adults can be produced (Elliott and deLittle 1984).

2.2 DESCRIPTION

2.2.1 Adults

The adults have the typical elongate cylindrical form of platypodids with the female slightly longer than the male. The length and diameter of the adults is roughly 4mm and 1mm respectively (Fig 2.1). The sexes are dimorphic with the most obvious difference being the size and sculpturing of the elytra. In the male the elytral declivity forms an abrupt angle with the elytral disc (Fig 2.2a) while in the female the elytral declivity is feebly convex and perpendicularly aplanate at the apex of the elytra (Fig 2.2b). This difference between the sexes is easily discernable with the naked eye and can be used to sex individuals in the field. In the male the elytral declivity is densely covered with yellow setae while setae are much less dense on the apex of the elytra in the female. The elytra of the female is uniformly dark brown while for the male it is dark brown at the apex and light brown at the base. In both sexes the pronotum is light brown while the legs are light brown to yellowish in colour. Hogan (1948) provides details of adult morphology and a full description of the adults is given by Schedl (1936).

2.2.2 Immature stages

The eggs are featureless, oval, elongate and glistening white (Fig 2.3). They are roughly 0.7mm long and 0.4mm wide and are covered with a slightly sticky secretion which causes them to adhere to one another and to the gallery walls. Unless kept in air of high humidity they collapse within a few hours (Hogan 1948).

The larvae are apodous being legless and generally white with later instars white to creamy coloured. There are five instars in all (Hogan 1948, Section 5.1 this study). The mouthparts of the 1st instar are visible within the egg just prior to hatching. When freshly hatched the 1st instar is a translucent white colour becoming more opaque white with time. It is about the size of the egg with a head capsule width of

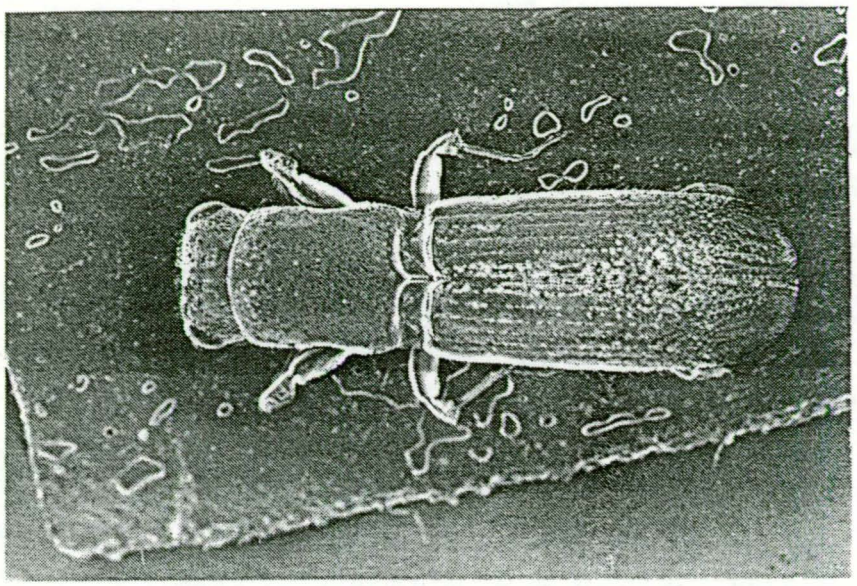

(2mm)

FIG 2.1(a) *Platypus subgranosus* adult male, dorsal view.

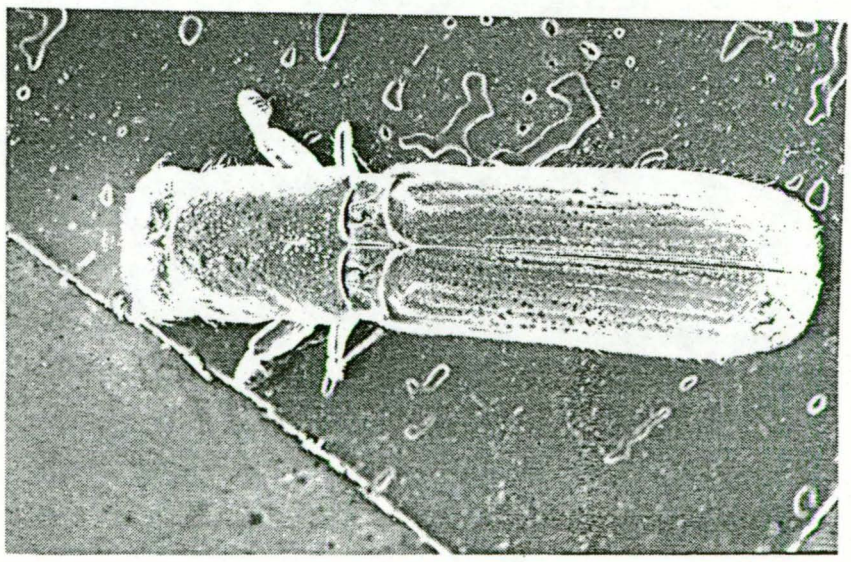

(2mm)

FIG 2.1(b) *Platypus subgranosus* adult female, dorsal view.

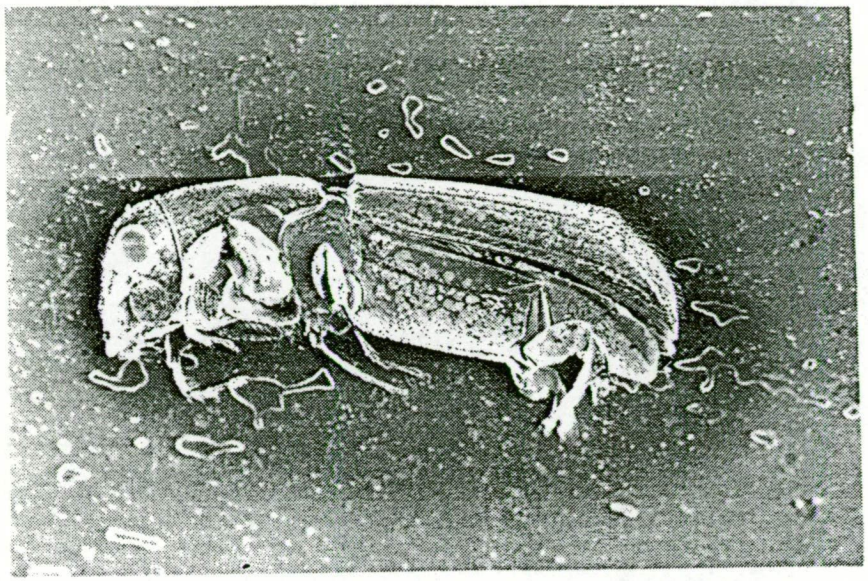

(2mm)

FIG 2.2(a) *Platypus subgranosus* adult male, lateral view.

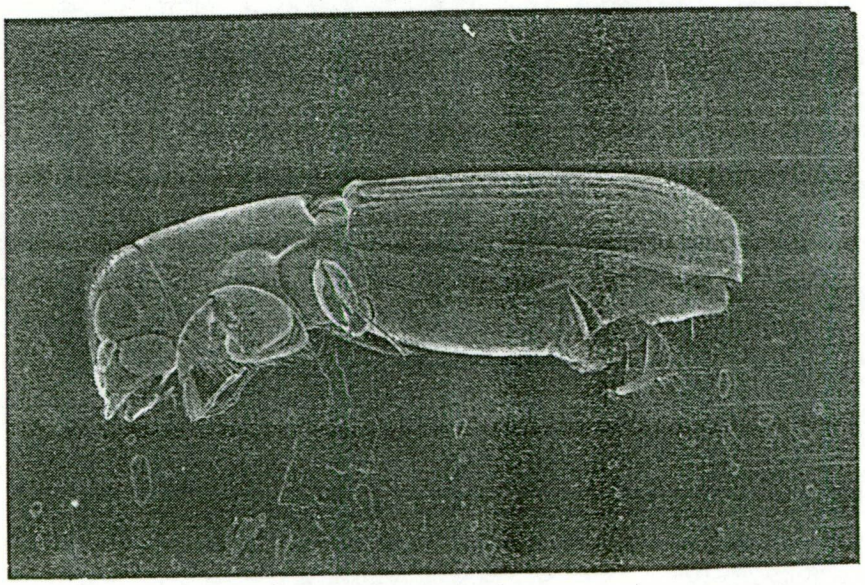

(2mm)

FIG 2.2(b) *Platypus subgranosus* adult female, lateral view.

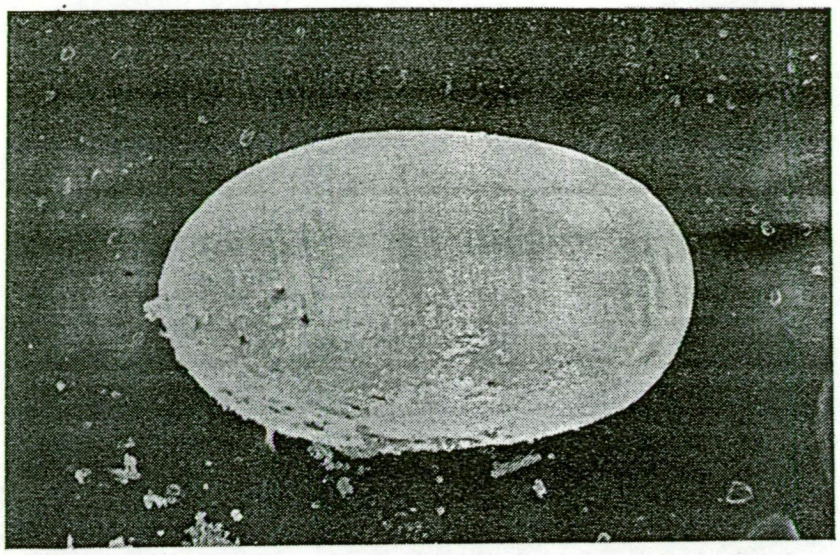

(500µm)

FIG 2.3 *Platypus subgranosus* egg

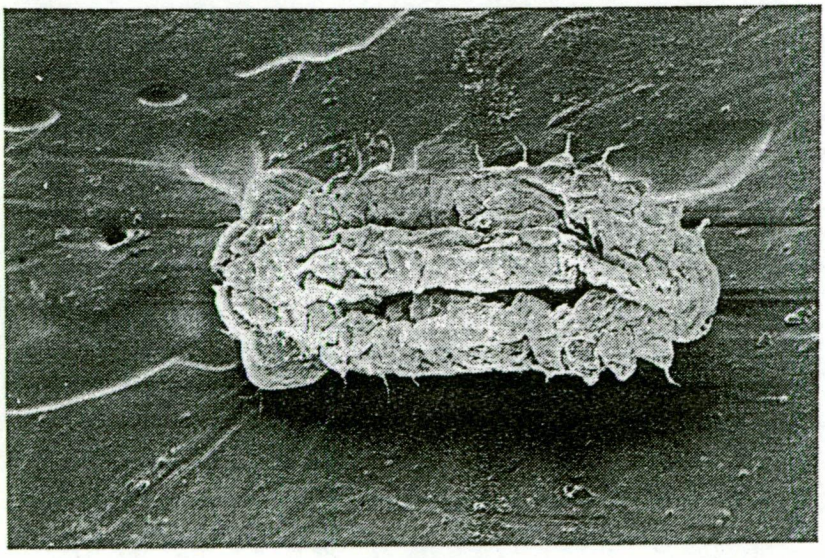

(500µm)

FIG 2.4 *Platypus subgranosus* first instar larva, ventral view.

around 0.36mm and it is roughly oval shaped and dorso-ventrally flattened with a lateral row of fleshy protuberances on either side of the body on the epipleurae (Fig 2.4). These protuberances increase in size towards the posterior of the body and each contains a single seta. The protuberances and setae are presumably an aid to locomotion within the tunnels.

The second instar is also dorso-ventrally flattened but the body is more pear-shaped narrowing towards the head. The fleshy protuberances are not as obvious as for the 1st instar and the body is slightly longer (0.8 to 1.7mm) with a head capsule width of approximately 0.44mm.

The third instar loses the flattened pear-shape and takes on the cigar shape of this and later instars with the epipleural proturberances further reduced. The prothoracic segment and an abrupt narrowing of the last few abdominal segments are now obvious in this and later instars (Fig 2.5). The third instar is 1 to 3mm long with a head capsule width of approximately 0.6mm.

The fourth instar is longer than the third (2 to 4mm) and is more of a bent cigar shape with a head capsule width of approximately 0.83mm. The fourth and fifth instars are very similar except for one main distinguishing feature. The fifth instar has a row of 4 chitinous loops on the dorsal surface of the prothoracic segment (Fig 2.6) which is absent in the fourth instar. These loops (Fig 2.7a) consist of back-pointing bristles (Hogan 1948) which are obviously aids to locomotion in the galleries and a means of gaining purchase on the tunnel walls while boring. The larvae although appearing, to the naked eye, to have a smooth surface are actually covered with setae and bristles (Fig 2.7b). Ocelli are absent and the antennae have been reduced to vestiges (Fig 2.7b). The full grown larva is between 5 and 6mm long with a head capsule width of approximately 0.96mm. The pupa are exarate and ivory white grading to a cream colour with mouthparts and elytra becoming more sclerotised with age.

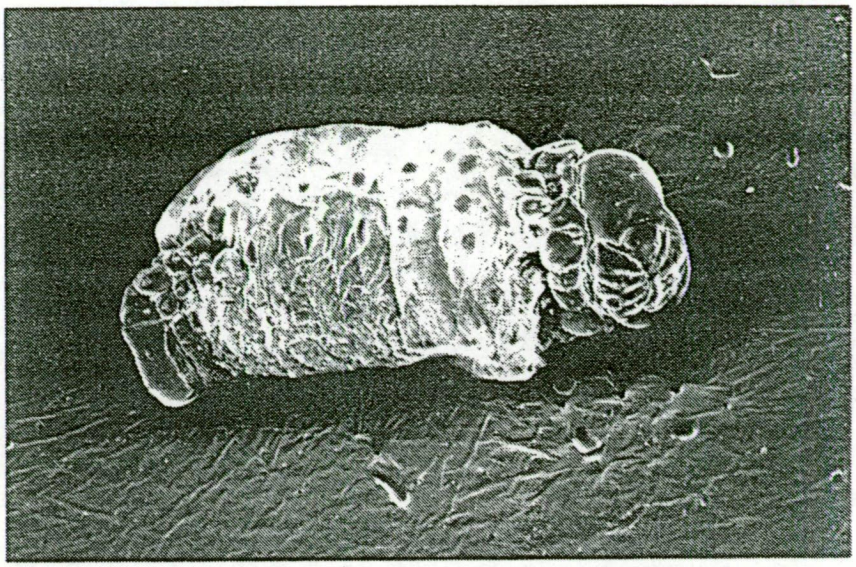

(1mm)

FIG 2.5 *Platypus subgranosus* third larval instar latero–ventral view.

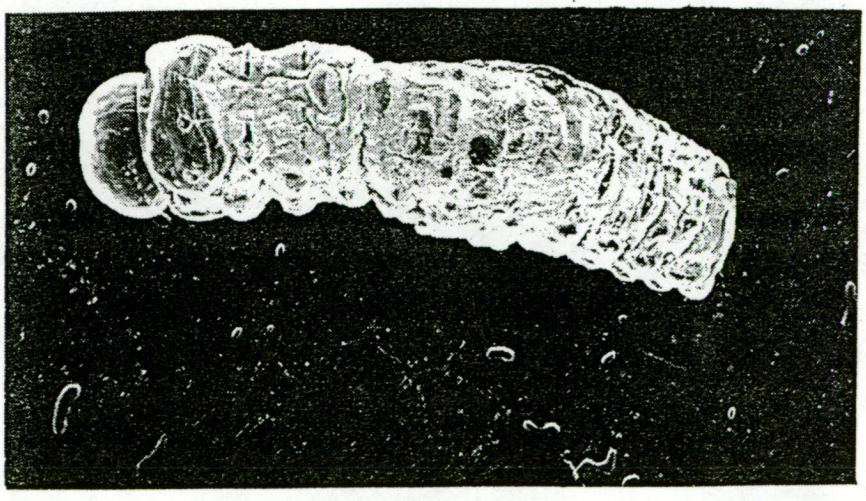

(2mm) .

FIG 2.6 *Platypus subgranosus* final instar larva, dorsal view.

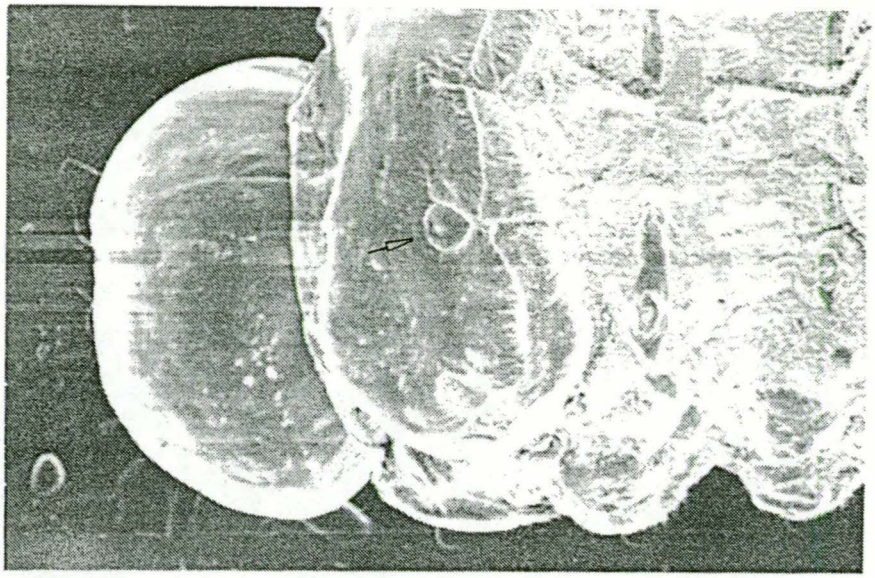

(500µm)

FIG 2.7(a) *Platypus subgranosus* final instar larva, dorsal view of head capsule and prothoracic segment showing chitinous loops.

(500µm)

FIG 2.7(b) *Platypus subgranosus* final instar larva, lateral view of head capsule.

2.3 LIFE HISTORY AND HABITS

2.3.1 Timing of adult emergence and flight

Emergence in Tasmania can begin as early as September and continue through until about April although a small number of individuals can be observed in the winter months. Most emergence occurs in the summer between January and March although the peak month varies from year to year (Section 6.3). There appear to be no definite brood flights. A similar timing was reported by Hogan (1948) for the Central Highlands of Victoria. Flight of both males and females is weak and slow and occurs on sunny days with few individuals observed when conditions are cold or wet. Males generally emerge in the late morning and afternoon of suitable days while females emerge in morning and are less readily trapped in flight (Hogan 1948, Section 6.7 this study). The males alight first on susceptible wood and are more commonly seen than females which are usually inside the wood before midday.

2.3.2 Host selection, density and pattern of attack

The density of attack on logs and trees has been observed on localised areas of the surface at up to 22 per 100cm^2 (Slade 1978) and over larger areas at 420 per m^2 (Section 4.1). Susceptible wood varies greatly in its attractiveness to attack. Elliott *et al.* (1983) demonstrated that ethanol can act as an attractant and boring stimulant on vigorous, uninfested trees which would not normally be attacked. They also identified ethanol as a naturally produced volatile in soaked myrtle beech logs. As mentioned above, *N.cunninghamii* is the most susceptible species in that apparently healthy trees are attacked which is probably a consequence of this species natural susceptibility to infection by the *C.australis* fungus (Kile and Walker 1987, Kile 1989) and the fact that trees infected by *C.australis* are rendered highly attractive to a *P.subgranosus* (Kile *et al.* 1990b, Section 4.2.1 this study). The within-tree pattern of attack appears to be aggregated at both low and high densities. Aggregation of attack is particularly intense around tissue infected by *C.australis*. A minimum spacing between galleries of roughly

one centimetre is suggested by this study (Section 4.2.1).

2.3.3 Construction of the gallery and development of immature stages

The initial entry point in the wood is made by the male which bores a hole roughly 1.5mm in diameter and 10mm deep in a few hours. The male then waits within the tunnel at its entrance for the arrival of a female which alights on the log and searches for a tunnel occupied by a male only. Pheromones are apparently emitted by the male attracting the female which moves directly from male to male without any random searching in between (Hogan 1948). The male then leaves the tunnel briefly to allow the female to enter and copulation occurs within the tunnel. Copulation on the surface has been observed occasionally (Hogan 1948). The species is monogamous and the parent beetles remain in the gallery until they die, the male only coming out of the tunnel temporarily to allow the next generation of adults to emerge.

The female takes over the development of the gallery while the male stays near the entrance of the tunnel clearing out frass generated by the female. Some unmated males were observed in this study in the spring following gallery initiation to have developed the gallery up to a length of about 8cm. A similar habit is documented for *P.apicalis* by Milligan (1979). The adult frass is fibrous while that of the final instar larva is fine and granular so that the type of frass expelled can be used to identify the activity within the gallery. The gallery consisting of the initial tunnel is extended radially across the grain and then tangentially along the sapwood/heartwood boundary until it reaches roughly 5 to 25cm in length at which time initial oviposition occurs (Fig 2.8a) (Section 5.2). At this stage, which takes between roughly 40 and 250 days from gallery establishment (Section 5.3), eggs are laid singly or more commonly in batches. Hogan (1948) gives an upper limit of 6 for the size of these batches but in this study single batches of between 10 and 16 were common and one group of 27 eggs was observed. The mean (standard deviation in brackets) of the number of eggs laid and length of gallery at initial oviposition was observed in this study to be 8.4 (6.6) and

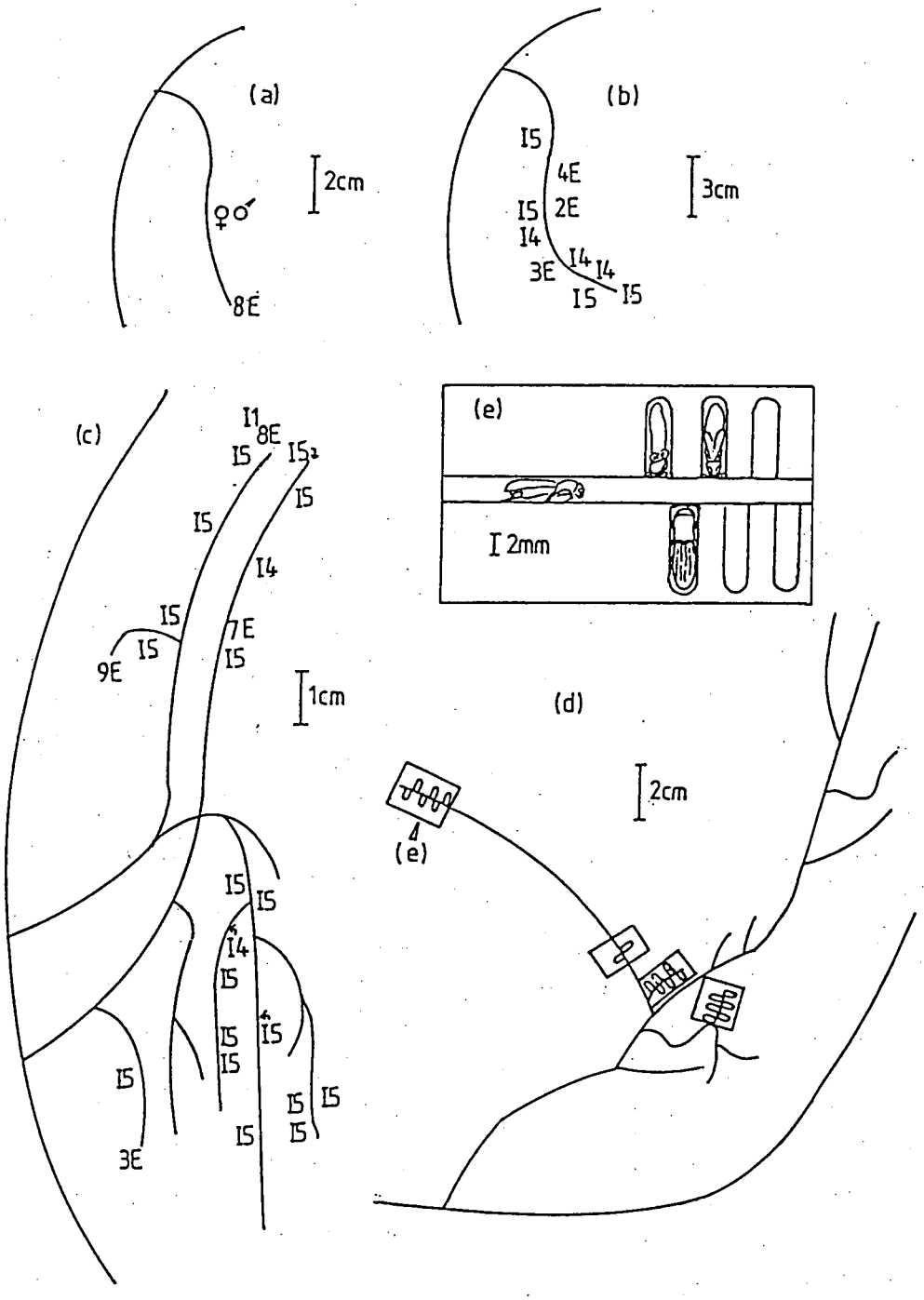

FIG 2.8 Example of gallery development after (a) 76 (b) 322 (c) 311 (d) 632 days: (No.)E – number of eggs, I1 to I5 larval instars (e) pupal cells running parallel to the wood grain.

12.1cm (3.9cm) respectively (Section 5.2). Slade (1978) recorded a maximum of 23 and minimum of 6 eggs per batch. The number of eggs laid in this initial oviposition is dependent on the length of the tunnel at a rate of roughly one egg for every centimetre beyond an initial length of 4cm (Section 5.2). The rate of gallery development for this initial section excavated by the adults ranges from roughly one centimetre for every 10 to 20 days. Attack late in the summer resulted in a slower rate than attack in autumn (Section 5.2). Earlier attack, however, was not found to produce a different length of gallery or number of eggs laid at initial oviposition. This trend was reflected in timing of emergence discussed later, where late summer attack, within the late summer/autumn period, did not result in first brood emergence, on average, any earlier than autumn attack. The explanation for this trend could be that oviposition is delayed until winter to minimise mortality of egg and early instar larvae due to desiccation.

Oviposition continues throughout the development of the gallery so that eggs can be found along with pupae and brood adults in the same gallery. These new adults must emerge and establish new galleries to begin the next brood so that generations can overlap across but not within galleries.

After initial oviposition the female, in most cases, does no further excavation of the gallery as evidenced externally by a long period when no adult frass is produced. In some cases, after an initial batch of eggs is laid the female extends the same unbranched tunnel one or two centimetres and may lay a second batch of eggs. Milligan (1979) reports that for New Zealand *Platypus* spp. after the initial batch of eggs is laid, the female excavates a branch off the main tunnel at its curvature and running again tangentially to the sapwood/heartwood boundary but in the opposite direction and then lays a second batch of eggs at the end of this branch before ceasing further gallery extensions. This habit was not observed for *P.subgranosus* in this study and the only branches to the main tunnel were found when final instar larvae were present. The larval instars develop within the initial section of gallery (Fig 2.8b) until

the final instar begins excavating tunnels branching from, and extending the main tunnel (Fig 2.8c). The variation in development rate of the gallery system and immature stages can be seen in Fig 2.8(b,c) where the two more developed galleries in (c) were established eleven days *before* that in (b) in logs from the same tree and of similar size and position on the ground.

Evidence of larval excavations is provided externally by the fine granular frass which usually collects on the bark below the gallery entrance. The female continues to lay eggs in the larval branches from, and extension to the original tunnel. During the gallery development larvae and adults feed on the ambrosia fungi discussed later.

The pupal cells are excavated by the final instar perpendicular to, and alternately on one side and then the other (i.e. top and bottom in a standing tree) of the tunnel with the long axis of the pupal cell running parallel to the grain of wood (Fig 2.8d). The larvae lie with their head facing the tunnel from which the cell was excavated with the entrance of the cell blocked with frass.

Roughly half the total number of eggs are laid at initial oviposition which occurs between late autumn and the following spring roughly 1 to 8 months after gallery establishment. Hogan (1948) describes oviposition as occurring in the warmer months with eggs and immature larvae relatively rare in winter although he does not say which stages are present in winter or qualify his observations with detail on the time of gallery establishment. In this study (Sections 5.3 and 7.3), where gallery establishment was in late summer and autumn, the egg stage was the only stage found in the first winter with early larval instars (1st to 3rd) appearing in the following spring, the 4th and final instars appearing in the following summer and the final instar then the main over-wintering stage until pupation in the second summer after gallery establishment (Fig 2.9). For galleries established in early summer (Nov-Dec) which can result in first brood emergence in the following summer (Section 7.4), the main over-wintering larval instar, assuming summer oviposition allows larvae to have

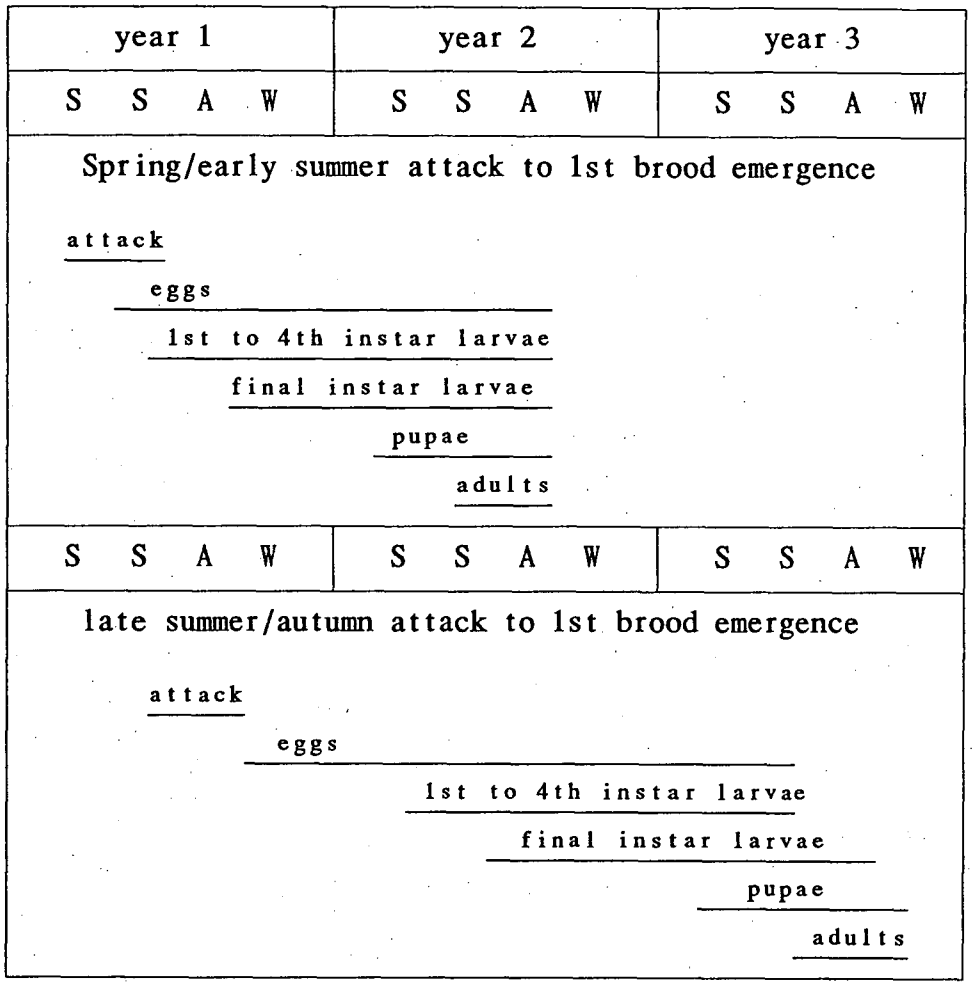

FIG 2.9 Life cycle of *P.subgranosus* for each of spring/early summer and late summer/autumn attack and gallery establishment.

developed by winter, has not been documented. In fact the timing of appearance of all immature stages in the case of spring/early summer attack and gallery establishment shown in Fig 2.9 is conjecture since no observations have been made for this case in this study. However, this description for one year development fits in well with Hogan's description above.

The difference in timing of the occurrence of the different immature stages, including variability in the over-wintering stage, is largely a function of the timing of gallery establishment (e.g. early, mid or late summer) in that such timing determines the accumulated temperature (day-degrees) that are available for development before winter when development slows down or ceases. No studies have been undertaken to establish the thermal requirements for development of each life stage separately largely because laboratory studies are not feasible with wood boring insects such as *P.subgranosus*. However, in this study (Section 7.3) an estimate of the lower threshold temperature and day-degrees above this threshold required for development from gallery establishment to emergence of the first brood was obtained using two sets of emergence data, in one case with emergence after a single year and the other, after two years (see below).

2.3.4 Length of Life Cycle

First emergence for a gallery usually begins in the second summer after gallery establishment although first emergence after as little as 10 months has been observed (Hogan 1948, Section 7.4.1 this study). The time taken to develop depends principally on the temperature individuals are exposed to. Using the simple day-degree model a lower threshold temperature for development was estimated to be roughly 11°C. Thermal requirements from gallery establishment to emergence and oviposition to emergence were estimated at approximately 4000 and 3400 day-degrees above 11°C respectively (Section 7.4). These estimates were based on ambient air temperatures

under the forest canopy and microsite variation such as direct exposure of gallery entrance to sunlight, aspect, topography, log or tree diameter and moisture content will all result in variability in the temperature individuals are exposed to. Also the timing of oviposition will affect the accumulated temperature exposure and as discussed above early summer gallery establishment is more likely to result in the first emergence occurring in the next summer. Emergence from the same gallery usually continues in the 3rd and 4th summer if attacked material does not dry out or is not overtaken by wood rot fungi. In this study (Section 6.5) 63% of total emergence occurred in the first summer of emergence (i.e. second summer after attack) with 36% and 1% occuring in the following two seasons respectively. Very similar observations on emergence of *P.apicalis* and *P.caviceps* are described by Milligan (1979).

Interestingly, the observation that the timing of gallery establishment, when this occurs in late summer/autumn, does not affect the timing of initial oviposition mentioned above was also found to hold for emergence. Of the galleries established in late summer/autumn, those established early in this period did not produce emergence any earlier on average than those established late (Section 7.5). However, galleries established in early summer produced emergence in the following summer (Section 7.3). Why early summer gallery establishment produces emergence after one year and establishment in late summer/autumn two years is explained in terms of the thermal requirements for development of *P.subgranosus* (Section 7.3).

For spring/early summer attack and gallery establishment to result in emergence in the following year initial oviposition presumably occurs in summer (Fig 2.9). However, the observation that such early attack occurs much less often than late summer/autumn attack fits in with the hypothesis that summer oviposition involves higher risk of egg and early instar larvae mortality due to desiccation. This disadvantage is offset to a degree by the reproductive advantage of producing brood adults in one rather than two years.

2.3.5 Number and sex ratio of emergents

The average number of emergents per gallery over the life of the gallery, which is usually three years (see above), was roughly 20 with a median of 15 and minimum of one and maximum of 92 (Section 6.1). The above average is very similar to that observed for *P.caviceps* emerging from *Nothofagus* in New Zealand by Holloway (W.A. Holloway, Forest Research Institute, unpublished data) who obtained an average of 21.4. The frequency distribution of total emergents per gallery is reverse J-shaped and not bell-shaped (Section 6.1) so that a small number of very productive galleries are responsible for the bulk of the population. A similar situation occurs for *Platypus* spp. in New Zealand (Milligan 1979).

Elliott *et al.* (1983) reported obtaining 11000 emergent *P.subgranosus* in a single summer from a 12 metre log of 60cm diameter which is equivalent to 900 per metre or 486 per m^2 of log surface. With a mean emergence of 20 per gallery, 11000 emergents equates to roughly 24 successful galleries per m^2. This is a low number of attacks per m^2 compared to some of the attacked material obtained in this study (Section 4.1).

The sex ratio is very close to one over the population although there is considerable heterogeneity between galleries in the sex ratio both significantly less than and greater than one. The most extreme case being a gallery which produced 41 males and only 14 females. There was a slight trend for males to predominant in the first week or two of emergence with females catching up by the end of the summer (Section 6.2). A similar trend was observed by Milligan (1979) for *P.gracilis* where 70% of emergents were male in the first two weeks of the flight season; the corresponding figure for *P.subgranosus* was 62% in the first 5 days and 53% in the first 10 days after emergence commenced for the gallery.

2.4 Symbionts

Platypodid beetles are called *ambrosia* beetles because of their habit of cultivating and feeding on *ambrosia* fungi (*xylomycetophagy*) which grow on the gallery walls obtaining nutrients and moisture from the wood. Hogan (1948) cites evidence that the frass from gallery excavations is not ingested by the beetle. In particular (a) in freshly opened galleries wood particles can occasionally be seen between the wall of the gallery and the abdomen of the female being passed back beneath the body; (b) in making the original entry the male passes wood particles out beneath the abdomen; (c) the frass ejected shows no evidence of maceration as would be the case if passed through the gut of the insect; and (d) against the possibility of only a portion of the wood being consumed is the fact that beetles go for prolonged periods, often six months or more without boring, and subsistence is evidently provided from substances within the gallery over this period. Further to these observations the author has observed, under a stereo light microscope in a freshly opened gallery, an adult *P.subgranosus* browsing, unperturbed, on the dark brown fungi attached to the gallery walls.

When freshly excavated the galleries soon develop a semi-translucent shining coating identified by Hogan (1948) and Milligan (1979) in the case of the New Zealand *Platypus* spp. as yeasts. As the gallery section ages the yeasts are replaced with dark coloured fungi (Hogan 1948, Milligan 1979) identified by Webb (1945) in *P.subgranosus* galleries as *Leptographium lundbergia* Lagerberg et Melin . Kile and Hall (1988) consistently isolated *Hormoascus platypodis* (Baker & Kreger-van Rij) von Arx and *Raffaelea* sp. from both the beetles and gallery walls and a species tentatively identified as a *Leptographium* sp. in galleries from *N.cunninghamii* which had been dead for two or more years (their disease categories 4-6). They found that scrapings from the light and moderately dark coloured gallery walls commonly contained conidiophores of *H.platypodis* and *Raffaelea* sp. while those from dark coloured walls

consisted of isolated conidiophores, conidia, hyphae, comminuted wood and amorphous debris.

The importance of these and other fungii isolated by Kile and Walker (1987) as *P.subgranosus* symbionts is not fully known but it appears that *H.platypodis* and *Raffaelea* sp. are probably the main symbionts. Many ambrosia beetles, such as *P.apicalis* and *P.gracilis* (Milligan 1979), carry their symbiotic fungi in specialised organs called *mycangia* which can be minute pits on the rear half of the prothorax (Francke-Grossmann 1967). However, Kile and Hall (1988) found no such specialised organs using scanning electron microscopy. Superficial pits on the pronotum were discounted as candidate mycetangia by Kile and Hall (1988) and they found that there were evidently no structural modifications or regular fungal deposits in other potential mycetangial areas such as coxal cavities, integumentary folds and the buccal cavity. Kile and Hall (1988) concluded that *P.subgranosus* carried the inoculum of the symbiotic associates largely on the dorsal cuticle of the body or possibly in mouthparts.

2.5 Predators and parasites

P.subgranosus appears to be largely free of major predators and parasites. This is partly due to the habit of the male of staying close to the gallery entrance with it's abdomen pointing outwards therefore providing an effective barrier to predators attempting to enter the gallery.

The bothriderid beetle *Oxylaemus leae* Grouvelle, which has recently been transferred to the genus *Teredolaemus* Sharp (Lawrence 1985), has been observed to emerge from *P.subgranosus* galleries. Hogan (1948) suggested that *T.leae* is a predator of *P.subgranosus* but Lawrence (1985) suggests that the mouthparts of the larvae of *T.leae* indicate a mycetophagous feeding habit (Pal and Lawrence 1986). This suggests that *T.leae* is an inquiline, feeding on the ambrosia fungi of *P.subgranosus*. Mass emergence tents (Section 3.2) produced only 203 emergent *T.leae* compared to 27,227 *P.subgranosus* although the bulk of the *T.leae* emerged in the 2nd and 3rd year of

P.subgranosus emergence and in these years was a higher percentage, ranging up to approximately 50%, of total emergence over the two species. No *T.leae* were found in emergence cages placed over individual gallery entrances or in dissections of galleries (Sections 3.1 and 3.2).

The buprestid beetle *Nascioides quadrinotata* Van de Poll has been collected in small numbers from mass emergence tents containing *N.cunninghamii* logs (Section 3.2) set up to obtain emergent *P.subgranosus* but it does not occupy *P.subgranosus* galleries and therefore is not associated directly with *P.subgranosus* (H.Elliott *pers.comm.*). Morgan (1966) reported the biology and behaviour of the buprestid *Nascioides enysi* Sharp which attacks *Nothofagus* spp. in New Zealand. Morgan associated *N.enysi* with a wilt disease of its host *Nothofagus*, similar to myrtle wilt. However, later work by Milligan (1972) discounted the possibility of *N.enysi* causing the wilt disease.

Hogan (1948) reported the presence of a parasitic mite, identified as belonging to the genus *Schiebea* OUDMS. of the *Rhizoglyphidae*, in *P.subgranosus* galleries. This mite was a problem for the insectary rearing of *P.subgranosus* when wood was taken from the field where *P.subgranosus* was numerous and had been established over a long time (Hogan 1948). In dissections of 381 galleries in this study (Section 3.1), a single mite was found in each of two galleries and in both cases was parasitising the parent female *P.subgranosus*. The mite was not identified but it could be that mentioned by Hogan (1948).

Parasitic nematodes have been recovered from dissected *P.subgranosus* but at an incidence of only roughly 1% of the sample of roughly 200 beetles (R.Bashford *pers.comm.*). These nematodes have been sent for identification. Zervos (1980) described a nematode, *Bispiculum inaequale*, parasitising the three New Zealand platypodid species. The incidence of parasitism was higher in the case of the New Zealand platypodids with around 50% of both males and females containing

B.inaequale.

In this study (Section 3.1) three specimens of the larva of the wingless, cucujoid beetle *Hymaea succinifera* Pascoe were found in *P.subgranosus* galleries. This larva (Fig 2.10) was roughly 10mm long and 1.7mm wide and flattened dorso-ventrally. When placed in a petri dish with live *P.subgranosus* final instar larvae it did not attack and consume the larvae but crawled over them harmlessly. When left overnight with the larva one *P.subgranosus* larva was observed to be bleeding body fluid but was still alive. Although it was not possible to induce *H.succinifera* larvae to feed they survived for a long period, at least a month or more, in a petri dish kept at a constant temperature of 10°C and at low humidity. A specimen of this larva was also observed in the field crawling on one of the logs of *N.cunninghamii* set up in this study (Section 3.1). It is possible that this larva is a facultative predator of *P.subgranosus* in that it opportunistically invades *P.subgranosus* galleries when the male dies and there is no longer any guard of the gallery entrance or when cracks in the log or tree allow entrance to exposed sections of the gallery. However, Dr. J.F. Lawrence (CSIRO Division of Entomology) believes it is more likely that the *H.succinifera* larvae feed primarily on fungi, perhaps the ambrosia fungi (Lawrence *pers. comm.*). Dr. Lawrence also obtained specimens of these larvae (Lawrence *pers. comm.*) in addition to *T.leae* larvae from dissections of *P.subgranosus* galleries in *N.cunninghamii* logs (Lawrence 1985).

The rate of gallery failure observed in this study due to either death of the parents, an unmated male or an abandoned gallery was 8%. Mortality in the larval stage was negligible and what little was observed could possibly be attributed to storage of discs awaiting dissection in coolstore for, in some cases, up to a month (Section 3.1.2).

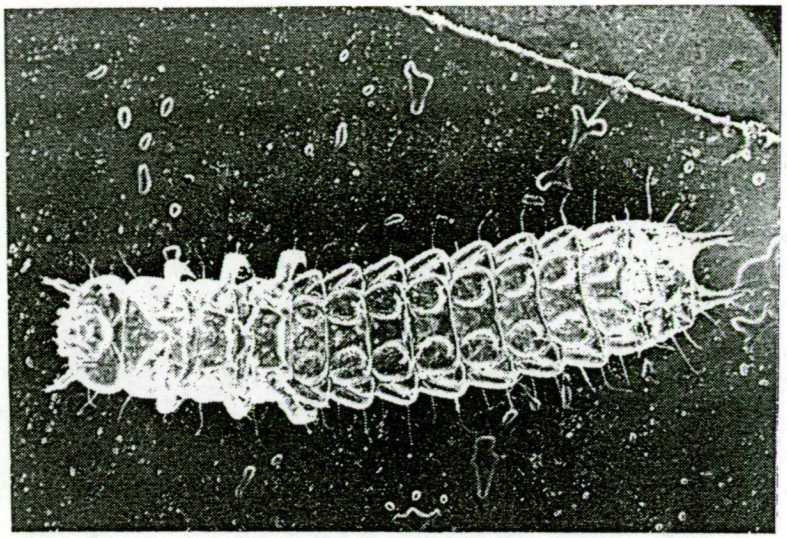

(5mm)

FIG 2.10(a) Larva of *H.succinifera*, ventral view.

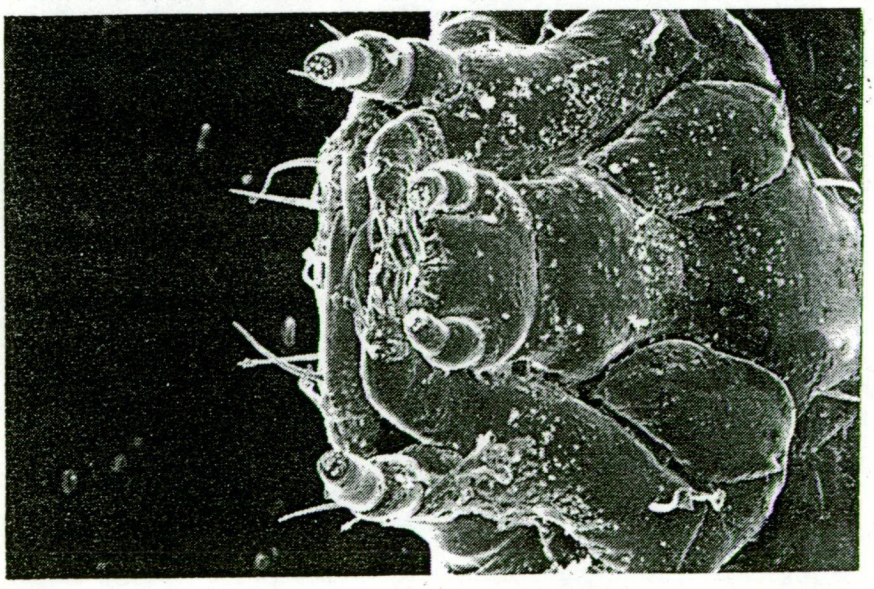

(200um)

FIG 2.10(b) Mouthparts of *H.succinifera* larva, ventral view.

3. MATERIALS AND METHODS

The data used for this thesis were obtained from a number of sources. Primarily data were obtained from the author's own experimental material. Unpublished data collected by researchers from the Silvicultural Research and Development Division (SILV) of the Forestry Commission, Tasmania (FC) and the Division of Forestry and Forest Products within CSIRO (DF&FP) were used with the kind permission of Dr.H.Elliott (SILV) and Dr.G.Kile (DF&FP).

3.1 Author's experimental material and methods

3.1.1 Study area, preparation of logs and attack

To provide information on the life cycle of *P.subgranosus* 9 healthy myrtle (*N.cunninghamii*) trees from the Arve study area (Fig 3.1a) were felled and cut into logs on 24/1/1984. The study area corresponds roughly to site 1 of Elliott *et al.* (1987) and is described in detail in Elliott *et al.* (1983). The site is at an altitude of 350 m with a gently sloping south-easterly aspect. The vegetation consists of an overstorey of mature eucalypts, *E.obliqua* and *E.regnans*, with a rainforest understorey consisting primarily of *N.cunninghamii*, sassafras (*A.moschatum*), leatherwood (*E.lucida*), celery top pine (*P.aspleniifolius*) and horizontal (*A.biglandulosum*). The rainforest community is described as *thamnic* using the classification of Jarman *et al.* (1984).

The felled myrtles had diameters, over bark, at felled height ranging from 15 to 43 cms and exhibited no evidence of attack by *P.subgranosus* or symptoms of myrtle wilt. The logs were arranged in a convenient way near where the tree had fallen. All the logs except those from tree 8 lay under the canopy where the removal of the subject tree had not drastically affected the light conditions. Tree 8 was located beside the Arve Loop road (Fig 3.1b) so that the logs for this tree were exposed to a much greater degree than those from the other subject trees. The logs obtained were of varying lengths (Table 3.1) and each log was painted with Hydroseal^{R} on each cut face and

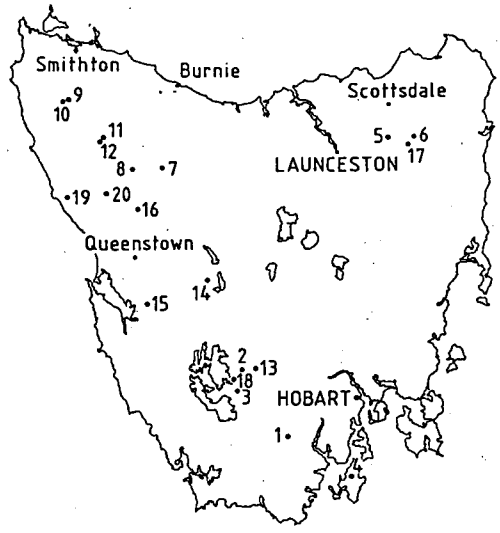

FIG 3.1(a) Fig.1 of Elliott *et al.* (1987) : Arve study area shown as site 1.

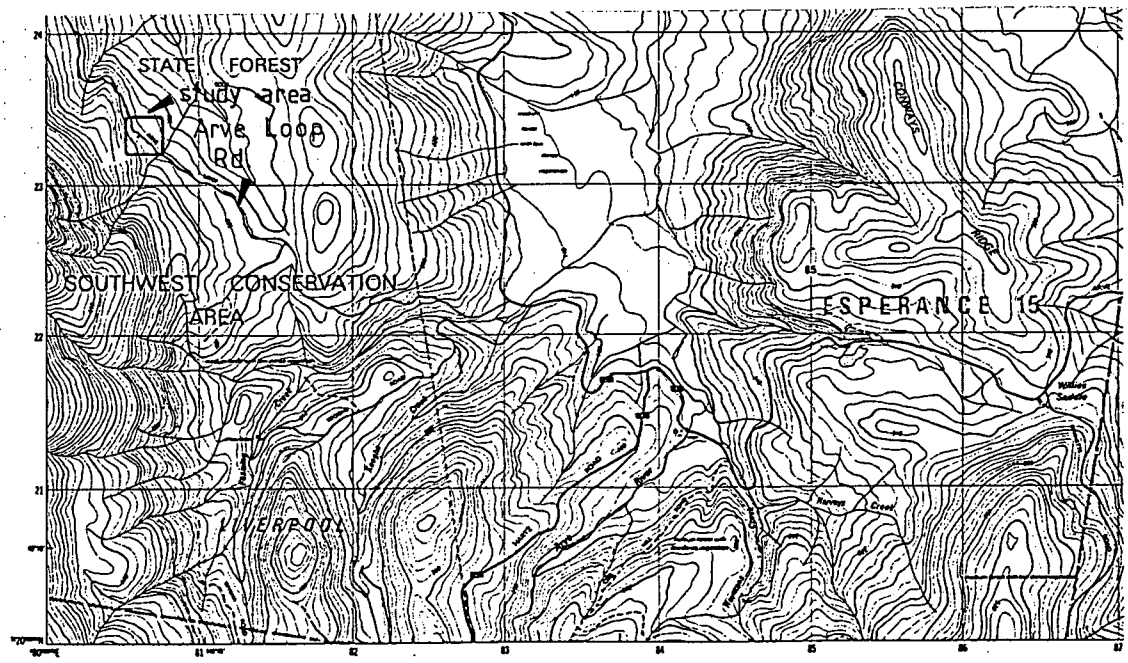

FIG 3.1(b) Section of Geeveston 1:25000 map (Tasmap 4822) showing the Arve study area.

Table 3.1 Details of logs prepared for this study

Tree	Log[a]	Diameter s.e. (cm) over-bark	Diameter l.e. over-bark	length (m)	surface area ($100cm^2$)	attack density (No/m^2)
5	1	15.0	17.7	1.39	71.4	35.0
	2	13.2	14.7	1.77	77.6	47.7
	3	12.7	12.9	1.60	64.3	23.3
6	1	36.4	43.2	1.03	128.8	25.6
	2	28.2	37.8	1.39	144.1	35.4
	3	27.9	28.2	1.36	119.9	65.1
	4	27.7	28.6	1.29	114.1	48.2
	5	17.7	27.5	1.46	103.7	94.5
	6	24.2	25.8	1.38	108.4	79.4
	7	16.7	17.2	1.37	73.0	39.8
	8	15.3	16.0	2.39	117.5	72.3
	9	16.5	17.5	1.05	56.1	42.8
	10	14.4	15.2	1.29	60.0	45.0
	11	15.6	17.4	1.91	99.0	66.7
	12	12.8	14.2	1.94	82.3	31.6
7	1	13.0	13.5	2.13	88.7	57.5
	2	17.7	19.7	1.53	89.9	81.2
	3	19.1	23.0	1.53	101.2	102.8
	4	20.8	24.4	1.09	77.4	56.9
	5	13.7	17.9	1.63	80.9	13.6
	6	26.5	33.0	0.87	81.3	16.0
8	1	33.5	35.0	0.92	99.0	77.8
	2	29.6	32.0	1.13	109.3	87.8
	3	28.6	29.2	2.04	185.2	83.7
	4	21.5	22.0	2.18	149.0	67.8
9	1	30.0	36.5	1.68	175.5	27.4
	2	28.7	31.0	2.00	187.6	31.5
	3	22.4	28.0	2.13	168.6	6.5
	4	13.1	16.2	2.53	116.4	24.9
	5	17.7	24.4	2.05	135.6	6.6

a. Logs were cut from forks and larger branches as well as the main stem and were numbered on the ground after they were conveniently organised so that log numbers do not necessarily represent an ascending sequence up the tree stem.

where any branches had been pruned off to prevent the log drying out and splitting at the ends. Each log was then labelled on each end using yellow spray paint with a tree and log number. The yellow paint did not induce *P.subgranosus* attack.

The logs were allowed to be attacked naturally by *P.subgranosus* and attack documented and labelled roughly weekly from when they were felled until the last labelling of attack on 7/5/84. At each measurement date, galleries that had been established since the last measurement were labelled with coloured drawing pins placed as close as possible to the entry hole without disturbing the activity of the male. The first attacks occurred in the week prior to 9/2/84. Only logs from trees 5 to 9 had sufficient numbers of galleries to be worthwhile studying and only logs from these six trees were used in this study. A thermohydrograph was placed in a Stephenson screen located under the canopy, midslope and in close proximity to the logs from trees 5 and 7. Traces were collected mostly weekly by Forestry Commission district staff. In all, 1673 galleries were labelled for 10 measurement dates.

3.1.2 Destructive sampling of galleries

For 5 sampling occasions at roughly 2 weekly intervals from the establishment of the logs until May 1984 a disc was cut from one or two logs which were selected in an *ad hoc* manner. Between June 1984 and December 1985, the logs were randomly sampled on 7 occasions. At each sampling occasion one log was sampled randomly from each one of the 5 trees. A further random number was drawn to determine whether the disc was to be taken from either the small or large end of the log. The discs were roughly 15 to 20 cm thick. After the disc was cut the face of the log was painted with Hydroseal. The discs were taken back to Hobart for dissection. Discs were split vertically along the grain using a hatchet, then sectioned horizontally using a bandsaw and finally, segments of galleries were exposed using a chisel. Individual galleries were tracked and their life stages collected up to and including the second last

(11th) sampling occassion in May 1985. However, by the time of the last sampling occasion in December 1985 the galleries were so well developed and involved so many branches due to larval excavations that many branches overlapped or even merged with branches from separate gallery systems. For this reason in a large number of cases it was impossible to determine to which gallery an exposed segment belonged. Combined with this was the task of keeping track of large numbers of slivers of wood and where they belonged in the 3-dimensional 'jigsaw puzzle'. So for these discs all labelled galleries were recorded for the disc and all individuals of each life stage obtained by dissecting the disc were recorded without tracking individual galleries. Discs awaiting dissection were kept in a coolstore at 5°C.

Each gallery was given a code and as individual life stages were found they were sexed in the case of adults and the diameter of the head capsule was measured transversely at its widest point for all larvae with the exception that only a sample of head capsules were measured on the final instar. The length of the larva was also measured where possible (i.e. if the body had not been damaged in the dissection of the gallery). Again only a sample of final instars were measured for body length. Measurements were taken live by using a fine camel hair brush to hold down the larva. An eyepiece micrometer on a stereo light microscope was used to make the measurements with a maximum error of 0.04mm (x25 magnification scale) for early and 0.083 (x12 magnification scale) for late instar larvae. To complement the individuals obtained above, the preserved specimens in the Forestry Commission collection were measured for head capsule width and body length at the x50 magnification scale. There were 50 preserved specimens of which 30 were final instar in the Forestry Commission collection.

The length of the section of the gallery excavated by the adults was approximated where possible by measuring widths of individual wood slivers containing sections of the gallery.

3.1.3 Emergence cages

On 6/2/85 for a sample of 72 labelled galleries, emergence cages were placed over the gallery exit. These cages used plastic sampling vials roughly 8cm long with a diameter of 2cm. A level area was made using a chisel where necessary to give a seal between the vial and the log. Gaps remaining between the log surface and vial were sealed using Bluetak^{R} around the base of the vial. The vial was secured to the log by means of wires passing through holes drilled through the vial at right angles to one another roughly half-way along the vial. The wires were then strained around nails hammered into the log which enabled a very strong attachment to be made. The space around the wire as it passed through the drill holes was large enough for air to circulate into the vial and any water to leak out but not large enough for emergents to escape.

The cages were checked weekly in summer and less regularly at other times of the year until the logs were relocated in the Forestry Commission insectary at Surrey House, Hobart. Half the logs were transported on 4/12/85 and the remainder on 10/12/85. No emergence had occurred up until 4/12/85. The first emergence (4 males, 1 female) occurred between the 4th and the 10th of December in one of the cages of tree 8. Since the cages were sealed at the end, the cage had to be removed to clear out frass and check for emergence. This had not been a problem before the logs were relocated since only a few traps needed to be cleared of frass. An advantage of the sealed vials over open-ended vials covered with gauze was that in this last case, cages pointing skywards can fill with water and flood the gallery. However, in the insectary for ease of clearing out emergents the ends of the vials were cut off and light gauze placed over the vial using elastic bands for attachment (Fig 3.2). The logs were placed on their ends in the insectary and traps checked and cleared daily from 12/12/85 to 30/12/85 and then weekly until 21/3/86 and finally on 6/5/86. The logs were regularly hosed with water during the 85/86 summer which combined with an exceptionally wet summer ensured that the logs remained wet and did not split. On the 16/12/85 a thermohydrograph was

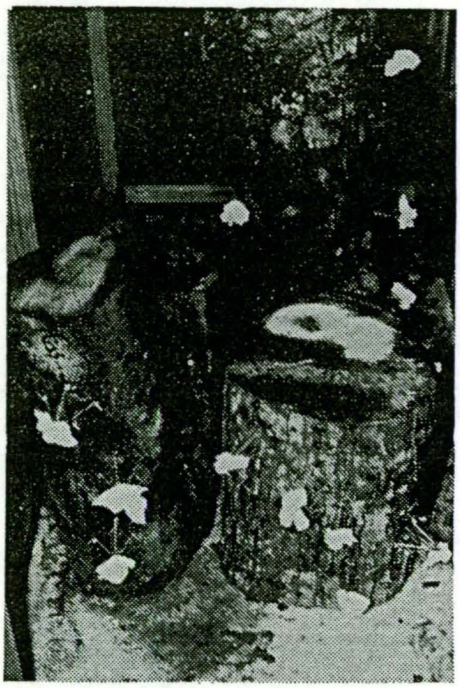

FIG 3.2 Emergence cages on logs in the Insectary

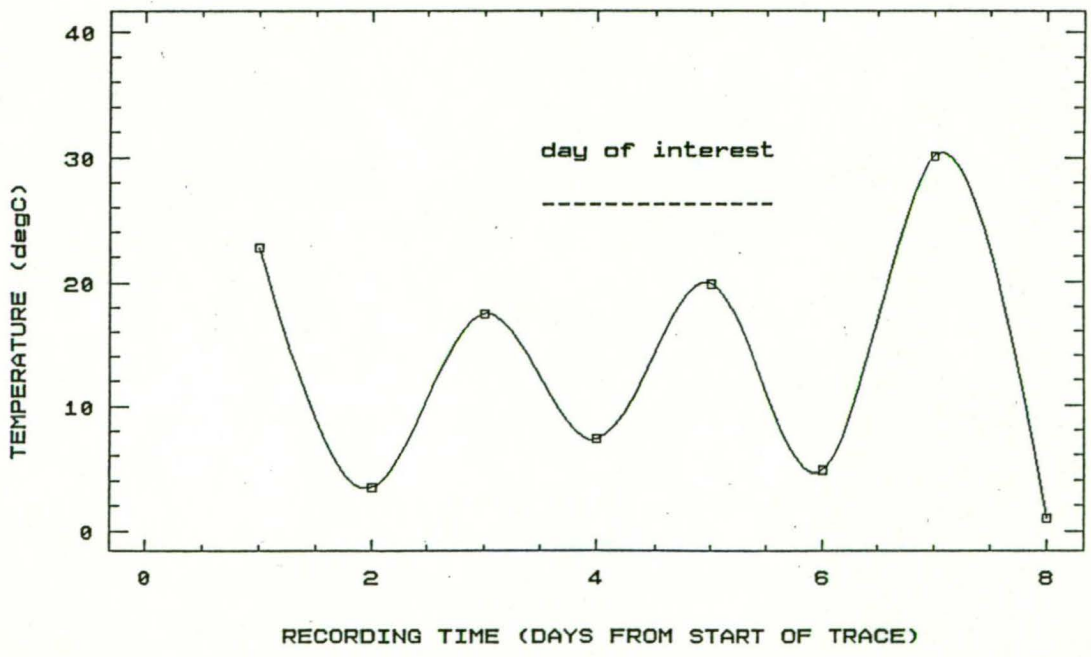

FIG 3.3 Section of estimated continuous temperature/time trace

placed in a Stephenson screen next to the insectary and a continuous trace of temperature and humidity taken until 6/5/86. Logs were checked for emergence in the 1986/87 summer but no emergence was observed and by this stage the logs had dried and cracked to a degree where survival of any later brood was highly unlikely.

3.2 Emergence experiments of Silviculture Division, Forestry Commission

Emergence data were also provided from emergence cages placed over individual galleries by H.Elliott and R.Bashford (SILV) over consecutive summers between the 79/80 and 82/83 summers in the Arve study area. A total of 58 cages were established, 12 of which had known date of attack in the 80/81 summer. Logs were kept at the study site and emergents were collected from summer 81/82 until summer 84/85. Cages were checked and cleared weekly in summer and intermittently at other times.

Mass emergence tents were also established in the Arve study area by Elliott and Bashford. Large numbers of emergents were obtained by placing heavily attacked logs under black plastic tents with a semi-transparent plastic collecting bottle attached to the tent. Five tents were established and emergents were collected over consecutive summers between the 81/82 and 83/84 summers.

Thermohydrograph recordings were made within a Stephenson screen from 5/11/81.

3.3 Calculation of day-degrees

To obtain the day-degrees for any period within the time from first attack (28/12/80) for the SILV cages until the last emergence for the author's cages (6/5/86) temperatures recorded using thermohydrographs at the study site and Hobart insectary were used. The temperature traces recorded at the Hobart insectary from the 17/12/85 to the 5/6/86 were digitized using a digitising tablet and FORTRAN 77 routines from the ARC/INFO (ESRI 1987) library with a temperature recorded approximately every 15 minutes. These data were integrated between measurement intervals using the

trapezoidal rule with adjustment for the arc of the recording arm of the thermohydrograph. Special purpose routines were written in APL*PLUS (STSC) to carry out the integration. Unfortunately there were too many gaps in the continuous tracings from the Arve study site to allow the day-degrees to be calculated by integrating the temperature/time trace directly. To overcome this problem an approximation to the cumulative day-degrees for any date after 28/12/80, starting from this date, until 16/12/85 was obtained as described below.

For the Arve study site thermohydrograph sheets obtained from the site covering the period 5/11/81 to 17/12/85 were available. Daily minimum and maximum temperatures for the Hastings Meterological Station for the period 1/1/79 to 31/10/87 were obtained from the Australian Meterological Bureau. From most of the sheets obtained by the author and those of Elliott and Bashford, a number of daily minimum and maximum temperatures were obtained and matched to the corresponding temperatures from the Hastings Station. One hundred and ninety (190) pairs of (maximum,minimum) were obtained and for 175 of these pairs the time of day (24 h clock) at which the maximum and minimum occurred was also recorded. Various linear and nonlinear regression models relating each of the study site minima and maxima (dependent variables) to those at the Hastings Station (predictor variables) were fitted using GENSTAT (Genstat 5 Committee 1987). The best model for study site maximum temperature (Y_{max}) was a simple linear regression

$$Y_{max} = \beta_1 + \beta_2 X_{max} \qquad (3.1)$$

where X_{max} is maximum temperature at Hastings Station. Fitting separate parameters for each of 'winter' (April to October) and 'summer' (November to March) was found to significantly ($P<0.01$) improve the model. The R^2 for this model was 0.82. Residual plots showed no serious problems with this model. The relationship for minimum temperature was not as good as that for maximum. After fitting various models the best was found to be

$$Y_{min} = \alpha_1 + \alpha_2 X_{min} + \alpha_3 \hat{Y}_{max} \qquad (3.2)$$

where Y_{min} and X_{min} have definitions corresponding to Y_{max} and X_{max} and $\hat{Y}_{max}$ is the predicted maximum from eqn (3.1). Eqn (3.1) can also be expressed as

$$Y_{min} = \gamma_1 + \gamma_2 X_{min} + \gamma_3 X_{max}$$

The R^2 for this model was 0.56 and again there were no trends evident in plots of residuals. Parameter estimates and their standard errors for eqns (3.1) and (3.2) are given in Tables 3.2 and 3.3 respectively.

The model used for the time of day of the maximum and minimum temperature was simply the monthly (i.e. January,February,...,December) mean time of day. These means are given in Table 3.4. It can be seen that these means follow a consistent trend for maximum temperature with the earliest time of about 1300 hours in winter increasing to a peak of roughly 1600 hours in summer. A trend is much less distinct in the case of time of minimum. Minima are generally found to be difficult to model due to topography and its effect on cold air drainage, wind chill and other local variables (M.Nunez, *pers. comm.*).

Using this database of maxima and minima and time of day (predicted if not obtained from thermohydrograph sheets directly) a cubic spline was fitted to these data in sets of 3 days (i.e. one day either side of the day of interest). An example of this fit is given in Fig 3.3. Points were taken off the predicted spline curve in 15 min intervals and integrated using the trapezoidal rule. To do this functions were written in APL*PLUS to read the daily maxima/minima data in sets of 3 days, fit the spline and integrate over the middle day to obtain day-degrees for this day. The results were accumulated so that total day-degrees could be obtained for any given period. In the above integration of the thermohydrograph trace and the fitted spline curve a number of different threshold temperatures were used. Starting from 0°C, each integer-valued threshold from 0 to 20°C was used so that if the temperature predicted from the spline curve or obtained directly from the thermohydrograph trace (i.e. after 17/12/85) was

Table 3.2 Regression parameters of daily maximum temperature model : eqn (3.1).

Season	β_1	β_2
Summer (Nov-Mar)	2.77 (1.12)	0.7530 (0.0515)
Winter (Apr-Oct)	-3.27 (1.08)	0.9609 (0.0742)

Table 3.3 Regression parameters of daily minimum temperature model : eqn (3.2).

α_1	α_2	α_3
-0.589 (0.708)	0.5763 (0.0901)	0.3855 (0.0581)

Table 3.4 Mean monthly time of day[a] of minimum and maximum temperature

Month	Mean Time[b] minimum		maximum		No. Obs
January	6.4	(0.2)	15.9	(0.1)	29
February	6.3	(0.2)	15.1	(0.2)	20
March	5.5	(0.4)	14.7	(0.2)	23
April	6.2	(0.4)	13.9	(0.3)	12
May	5.0	(0.5)	13.6	(0.2)	16
June	6.2	(1.0)	12.9	(0.8)	13
July	7.1	(0.8)	13.4	(0.3)	16
August	6.2	(1.0)	13.6	(0.4)	12
September	7.4	(0.4)	16.1	(0.7)	7
October	6.2	(1.3)	13.0	(0.4)	10
November	5.1	(0.3)	13.0	(0.6)	7
December	4.8	(0.5)	14.4	(0.3)	10

a. 24 h clock
b. Standard error of the mean given in brackets.

below the particular threshold temperature the corresponding time unit was excluded from the integration. As a result the accumulated day-degrees for each threshold from 1/1/79 to any later date up until 31/10/87 was available.

Other methods of calculating accumulated day-degrees using daily temperature minima and maxima have been used. A common method is to constrain a sine curve to pass through the daily minima and maxima (Baskerville and Emin 1969; Allen 1976; Stinner *et al.* 1974). The method of Stinner *et al.* (1974) allows the sine curve to be asymmetrical so that minima and maxima do not need to occur 12 h apart, however, the shape of the sine curve is fixed for all days. Dallwitz and Higgins (1978) used a linear interpolation method rather than a sine curve where typical 'cycle values' of the daily temperature cycle are used (Dallwitz and Higgins 1978; Samson 1984; Allsopp 1986). Using their method, which is implemented in the DEVAR computer programme (Dallwitz and Higgins 1978), the value of temperature at time t is given by T_t where

$$T_t = T_{min} + (T_{max} - T_{min})C_t \quad ,$$

T_{min} and T_{max} are the observed daily minimum and maximum under consideration, and C_t is the value of the cycle function ranging between 0 and 1. The value of C_t can be obtained by linearly interpolating between 'cycle points', c_i , which can be obtained as say, typical monthly values at 2 hourly intervals using a sample of days in each month. Such cycle points are calculated as

$$c_i = (T_i - T_l)/(T_u - T_l) \quad , i=1,...,12 \quad ,$$

where T_i is mean monthly temperature at the i^{th} time of day, T_l and T_u are the mean monthly minimum and maximum temperature respectively (Dallwitz and Higgins 1978, Samson 1984). The cycle points are used by the cycle function and temperature is integrated by DEVAR using the trapezoidal rule and the linearly interpolated values of T_t.

The method used here of fitting spline curves to daily minimum and maximum

temperatures using time of day of the minimum and maximum as the abscissa scale is more similar to the method of Dallwitz and Higgins (1978) than sine curve methods but differs from DEVAR in that nonlinear interpolation (i.e. cubic spline) between daily minima and maxima is used instead of linear interpolation to obtain T_t. Also the method here allows the time between minimum and maximum temperature to vary by month while DEVAR uses a fixed 12 h period. Both methods allow seasonal variation in the shape of the temperature curve between daily minima and maxima; DEVAR via the cycle points, c_i, and the method here via the time of day of minimum and maximum temperature. It was not possible given time constraints to compare the above methods to actual day-degrees (i.e. calculated via digitisation, as described above, or planimeter measurement of thermograph traces) however, the likely magnitude of the error in estimation of day-degrees is relatively small and given the use of day-degrees in this study is only a minor consideration.

3.4 Little Florentine experiment

An experiment to study the effect of various treatments applied to healthy, unattacked *N.cunninghamii* (a small number of *A.moschatum* were also included) on attractiveness to *P.subgranosus* attack and incidence of myrtle wilt was set up in December 1985 near the Little Florentine river in south-central Tasmania (study site 2 of Elliott *et al.* 1987) jointly by SILV and DF&FP. This experiment is described in detail as Experiment 2 of Kile *et al.* (1990b). For this study, 7 of the treated *N.cunninghamii*, of which 5 were treated by inoculation with *C.australis* and two were 'saprung' (i.e. tree 'ring-barked' with a chainsaw cut to the depth of the sapwood), and one *A.moschatum* (saprung) were selected because of the large amount of attacked they sustained. With assistance from SILV staff the author obtained co-ordinates of *P.subgranosus* pinholes established on the selected trees as follows.

A clear plastic sheet was wrapped around each tree from the base of the tree to a height of roughly 1.5 to 2.0 metres. Because of the buttressing of the tree bole and

uneveness of the ground around the base of the tree some triming of the plastic sheet was required. Attack had been marked weekly between 19/12/85 and 14/5/86 with coloured drawing pins, the colour designating the date when attack was recorded, by SILV and DF&FP researchers. The location of the drawing pins was recorded on the plastic sheet using waterproof marking pens. Dieline copies of the sheets were made and the locations digitised using a digitising tablet and ARC/INFO (ESRI 1987) routines. Boundaries of the sheet were also digitised to allow arc distances, both clockwise and anti-clockwise around the tree, to be calculated. Inoculation points and the saprung chainsaw cut were also recorded onto the plastic sheet and digitised.

3.5 Rotary trap collections

Between 24/2/86 and 26/3/86 rotary trap collections of flying *P.subgranosus* were carried out throughout the day on 8 separate days at the Little Florentine study site (site 2 of Elliott *et al.* 1987) by H.Elliott and R.Bashford (SILV). The trap was cleared hourly between 6.00am and 8.00pm and the number of male and female *P.subgranosus* collected were counted.

3.6 Work of A.Slade

The density of attack along the bole of standing *N.cunninghamii* was recorded on 50 trees by A.Slade (SILV) in 1978 in north-west Tasmania (sites 11 and 12 of Elliott *et al.* 1987). Myrtles suffering various degrees of myrtle wilt were selected and the maximum density per 100 cm^2 was recorded within 5 m sections of the bole to a maximum height of 28 m.

A number of *ad hoc* destructive samples of *P.subgranosus* galleries were carried out using a chainsaw cut made perpendicular to the wood grain to expose galleries.

4. ATTACK

4.1 Timing and density of attack

As described in Section 2.3.1, the flight season for *P.subgranosus* generally ranges from September to April. Variation in the timing and density of attack will depend on temporal and spatial variation in the timing of emergence, the presence of nearby trees and/or logs containing emerging beetles and the attractiveness of the trees and/or logs subject to attack. Fig 4.1 shows the rate of attack based on total attack for logs at the Arve study site (Section 3.1.1) and trees treated in the experiment at the Little Florentine site (Section 3.4). The dates give the times at which new pinholes were marked with coloured pins and the rate is the number of these pinholes for the previous period divided by the period length. In each case the experimental material was established after the potential start of the flight season and given that it takes some time for the material to become attractive to the beetles (Elliott *et al.* 1983) early attack seen in Fig 4.1 probably understates the potential attack at that time. Nevertheless, the peak of attack appears to be in February and March with a decline in April and May, although there is considerable variation in these trends and considerable attack can occur as late as May [Fig 4.1(a)]. This peak of attack occurs, as expected, around the peak time for emergence (Section 6.4).

The density of attack is defined here as the number per square metre of log or tree surface area. For a number of different sized logs, given they are equally attractive to *P.subgranosus* and equally close to a source of emerging beetles, it would be expected that the total number of attacks on a log would be proportional to its surface area. Fig 4.2 shows the number of attacks versus log surface area for the logs at the Arve study site (Section 3.1.1). For a particular tree there is a general trend for attack to increase with surface area although there is a large degree of variation about this trend. This variability probably reflects the differing attractiveness of the logs. No obvious relationship between density of attack (number m^{-2}) and log mid-diameter

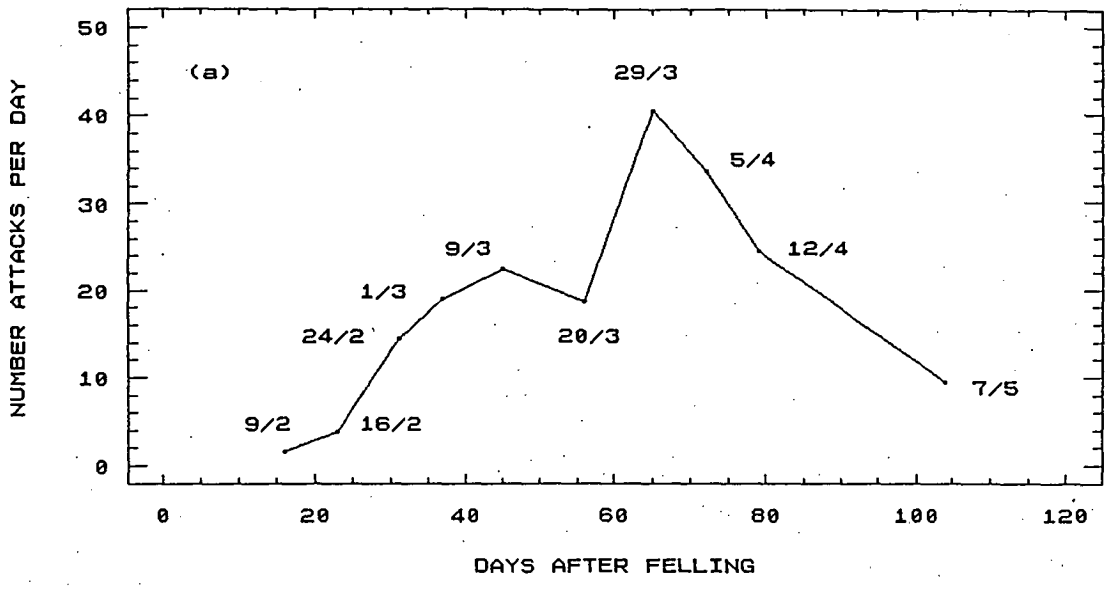

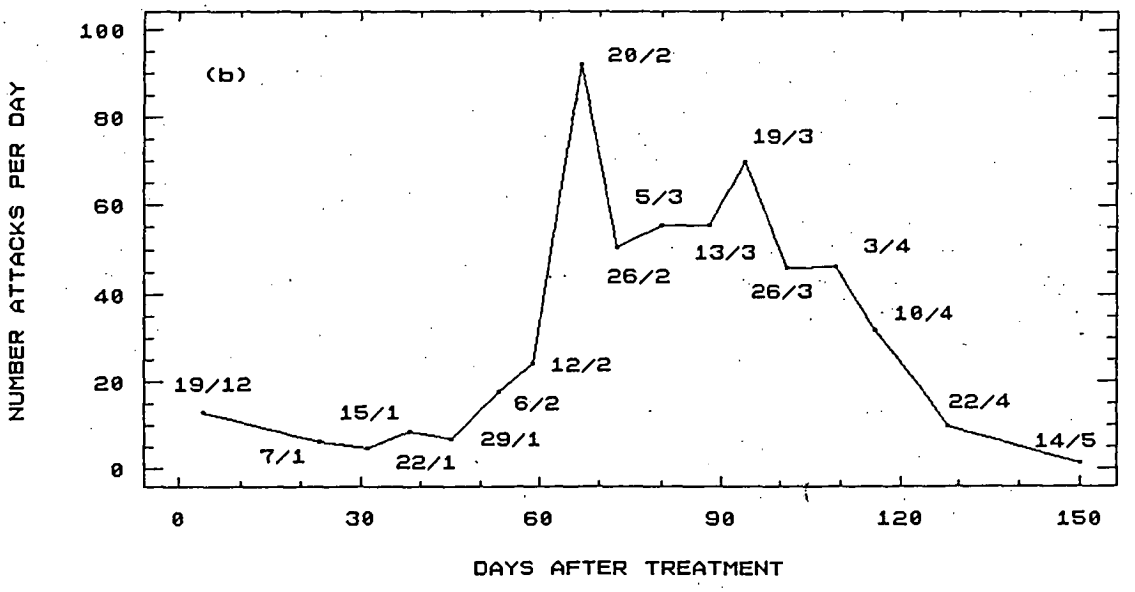

FIG 4.1 Number of attacks per day over the previous period versus days after (a) felling trees at the Arve study site (b) treatments at the Little Florentine study site

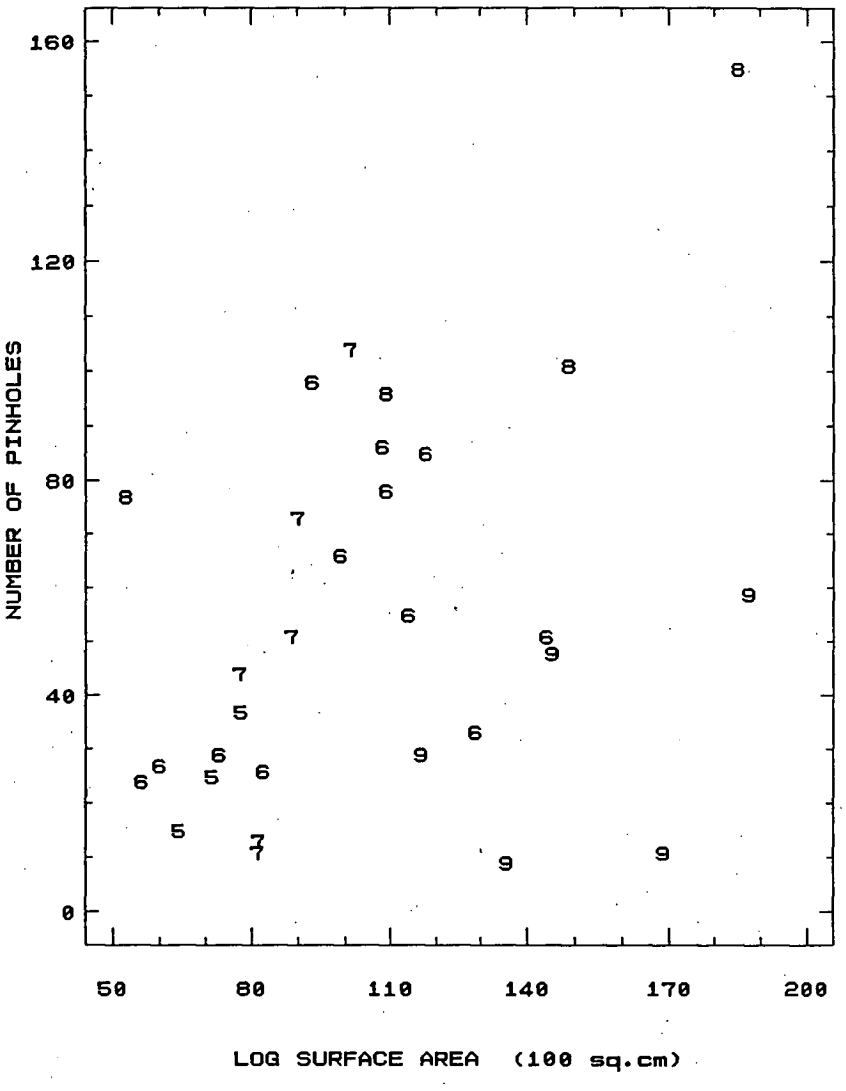

FIG 4.2 Number of pinholes versus log surface areas for trees 5 to 9

was found (graph not shown). The relationship between number of attacks and surface area will only be fully expressed when attack is so dense that beetles initially attracted to a log or tree must find an alternative site on another log or tree because the limit on space required for gallery establishment has been reached. Fig 4.3 shows the cumulative density of attack against time for several of the Arve logs and Little Florentine trees. The *C.australis* inoculated trees (Section 3.4) have been rendered highly attractive to *P.subgranosus* with attack reaching a density of 420 per square metre. This level of attack has not been sustained on the Arve logs (Section 3.1.1) which would explain the weak relationship in Fig 4.2. The plateauing of density of attack seen in Fig 4.3 is due largely to the petering out of emergence since new attack was observed, for both sets of material, in the following flight seasons but was not recorded. An idea of the limiting density of attack is obtained from the within-tree spatial pattern of attack.

4.2 Within-tree spatial pattern of attack

4.2.1 Mapped attack from the Little Florentine experiment

Maps of the within-tree spatial pattern of attack for 8 trees from the Little Florentine experiment (Section 3.4) are shown in Figs 4.4 and 4.5. Trees 11, 12 and 26 were ring-barked ('saprung') and the remaining trees were inoculated with *C.australis* (Section 3.4) with the inoculation point shown with an I in Fig 4.4. All the above trees including the ring-barked trees, with the exception of tree 11, showed symptoms of myrtle wilt. Tree 11 was the only *A.moschatum* with a significant amount of attack and for this reason was mapped. It provides a useful comparison to the *C.australis* infected *N.cunninghamii* trees. For all the inoculated trees with the exception of tree 9, the aggregation of attack around the spread of *C.australis* vertically within the vascular system of the tree is very obvious [Fig 4.4 (a-d)]. In ring-barked tree 12 [Fig 4.5(a)] such a pattern emanating from points along the ring barking is also obvious. Aggregation of attack is also fairly obvious in the case of ring-barked tree 26

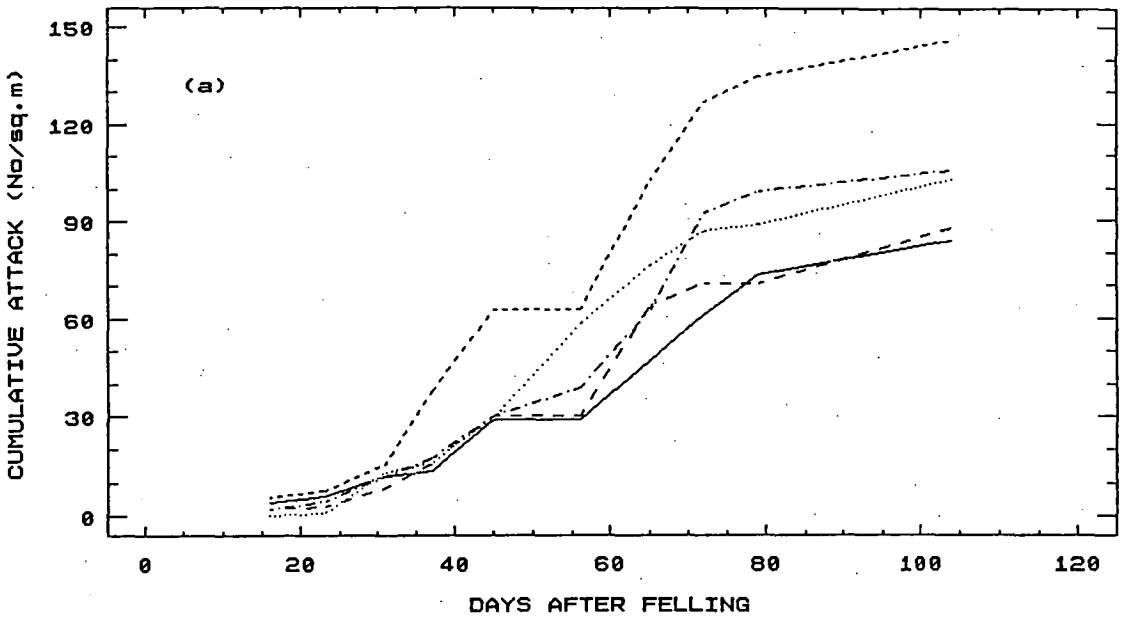

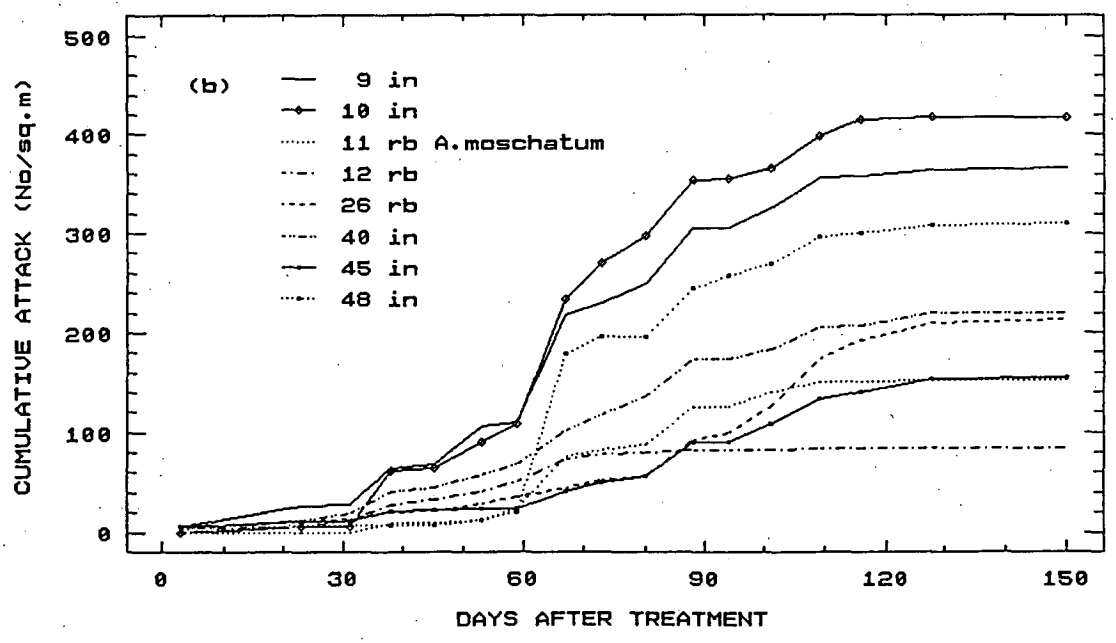

FIG 4.3 Cumulative density of attack for (a) 5 most heavily attacked logs from the Arve study site (b) trees treated by inoculation (in) and ring-barking (rb) at the Little Florentine study site

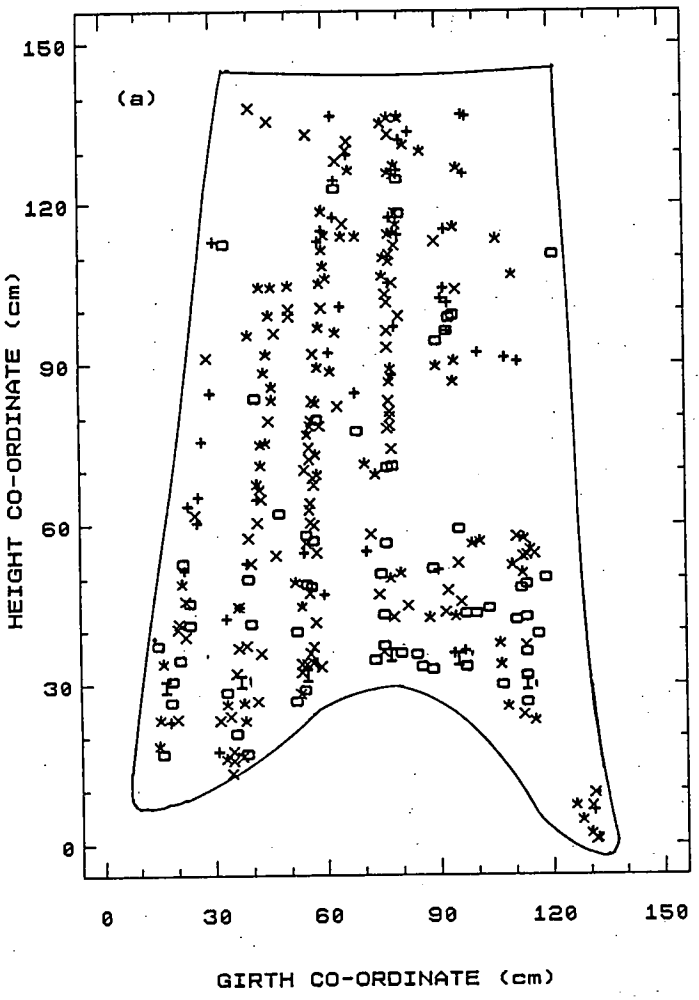

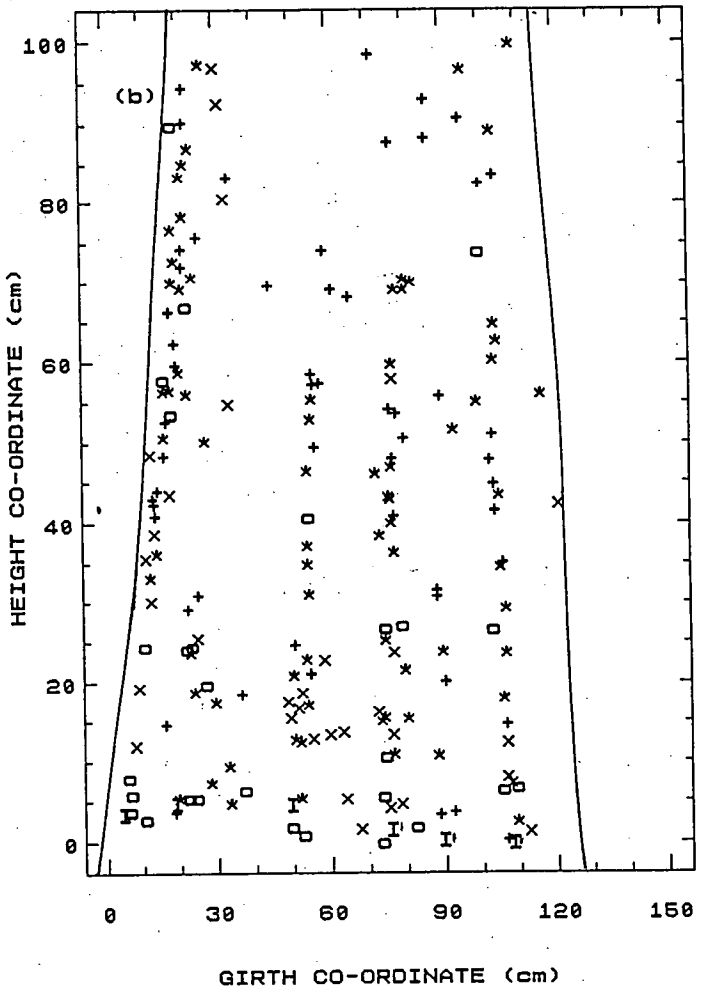

FIG 4.4 Inoculated trees : I inoculation point, o Jan, x Feb, * Mar, + after Mar

for trees (a) 40 (b) 45 (c) 48 (d) 10 (e) 9 (f) 9 Jan,Feb only

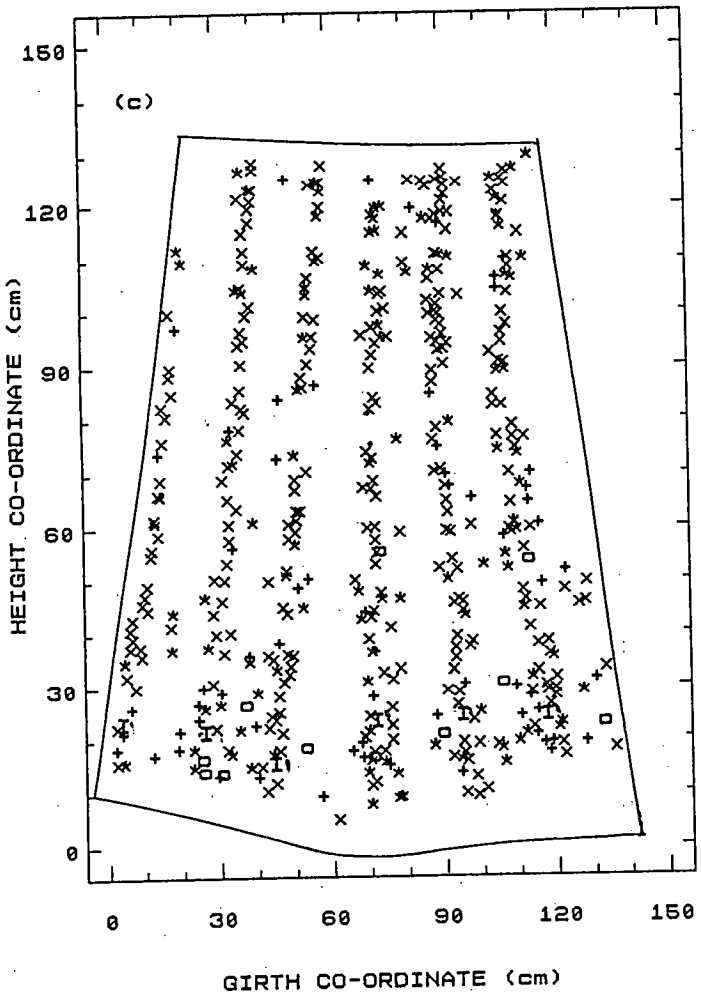
(c)
HEIGHT CO-ORDINATE (cm)
GIRTH CO-ORDINATE (cm)
0
30
60
90
120
150

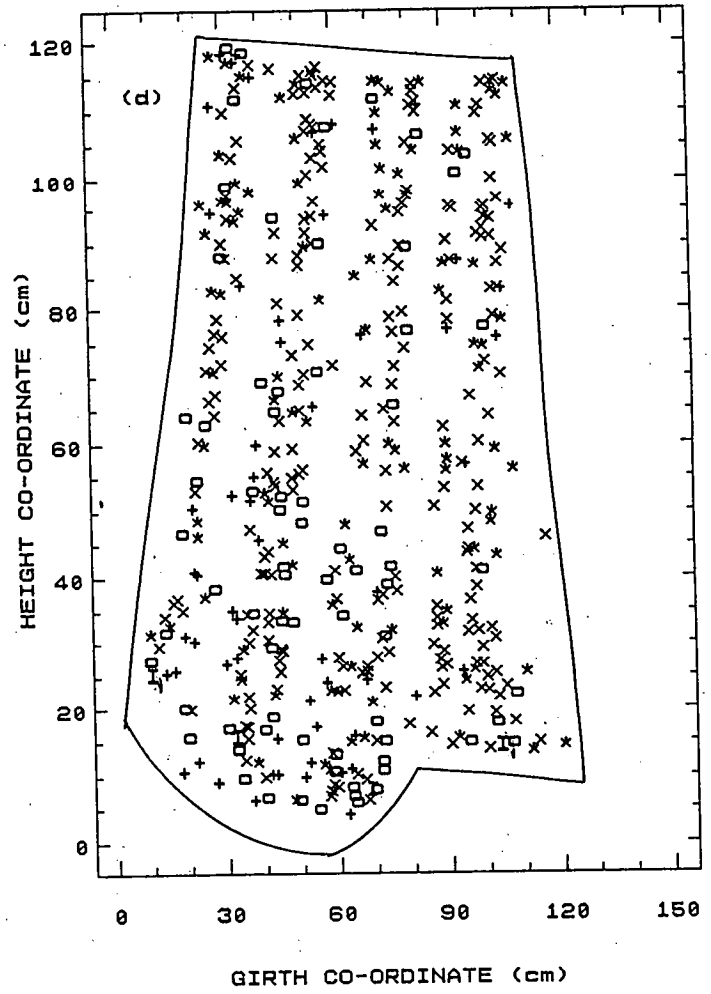
(d)
HEIGHT CO-ORDINATE (cm)
GIRTH CO-ORDINATE (cm)
0
20
40
60
80
100
120
30
90
150

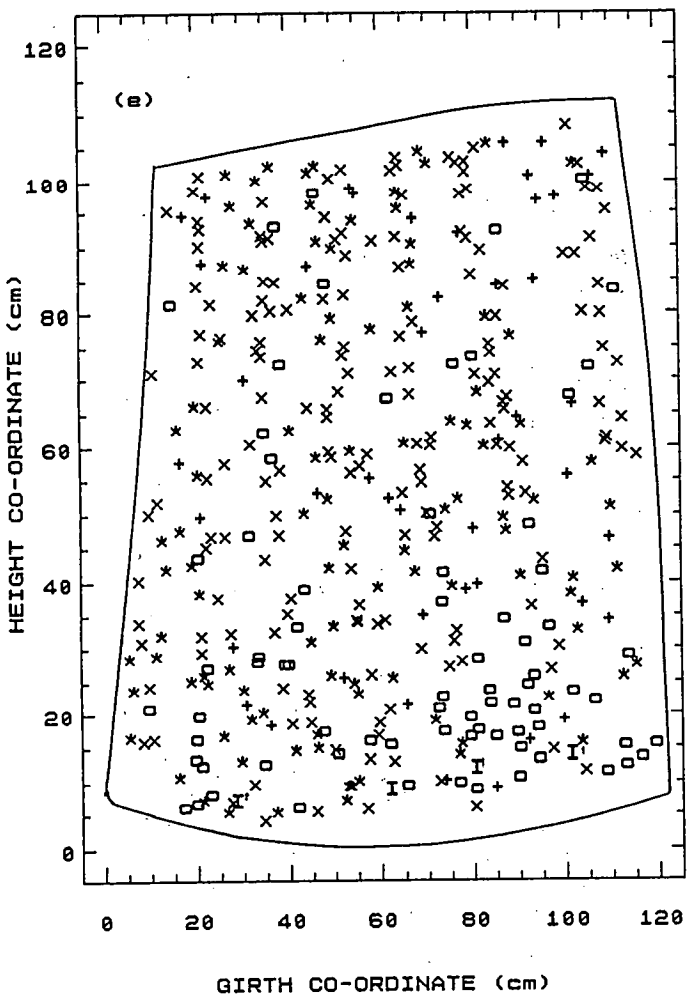
(e)
HEIGHT CO-ORDINATE (cm)
GIRTH CO-ORDINATE (cm)
0
20
40
60
80
100
120

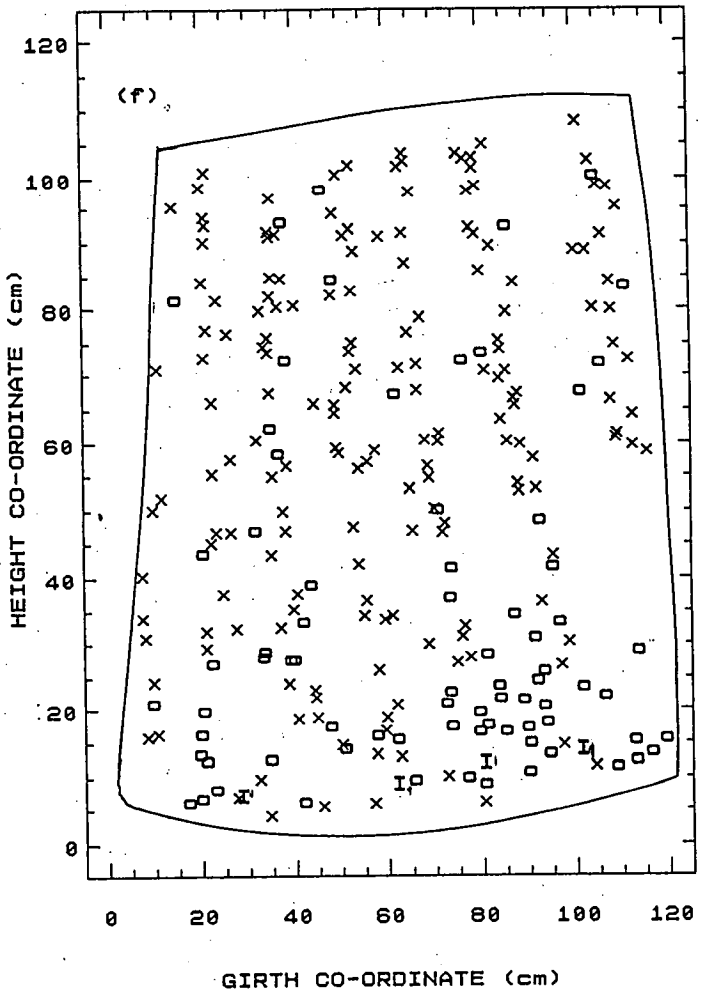
(f)
HEIGHT CO-ORDINATE (cm)
GIRTH CO-ORDINATE (cm)
0
20
40
60
80
100
120

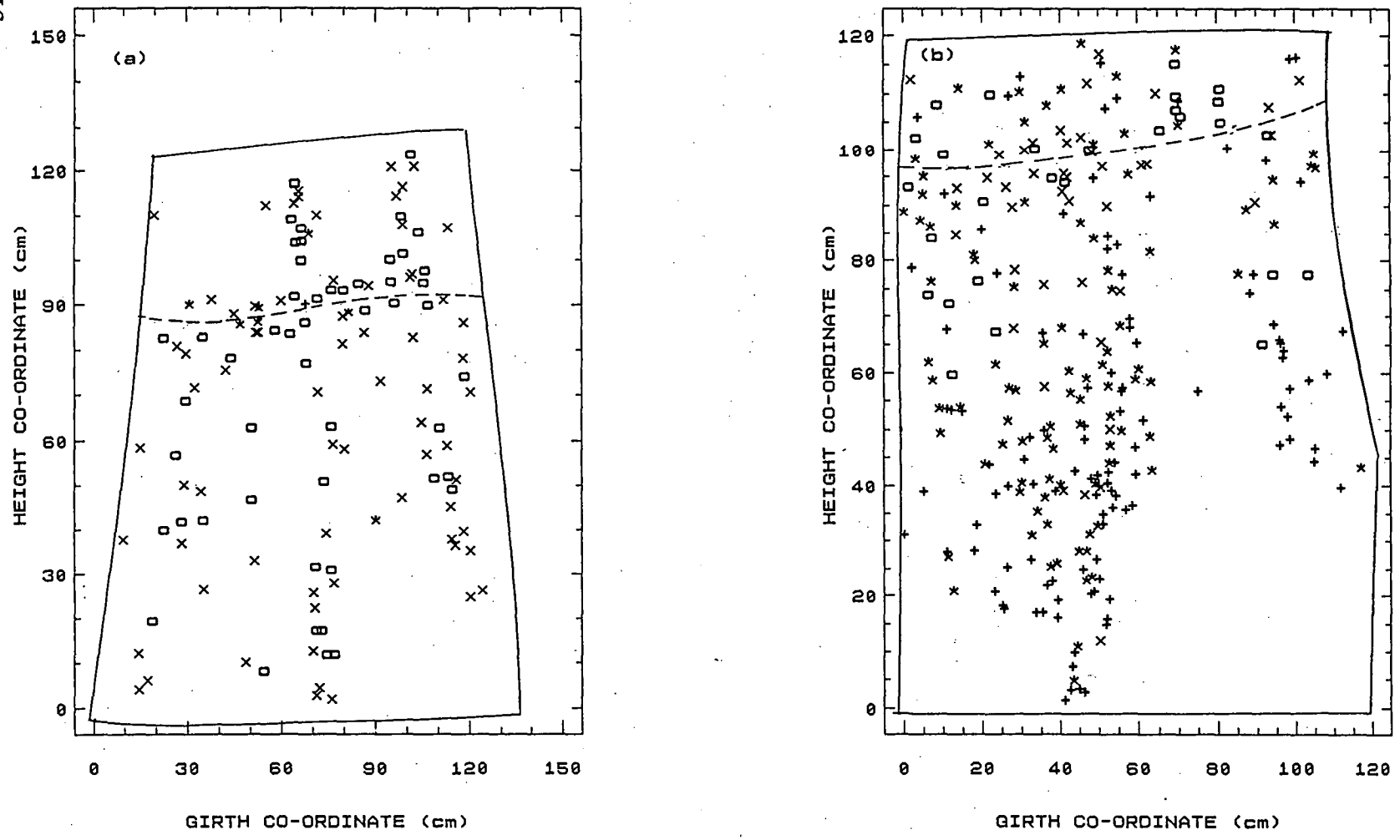

FIG 4.5 Saprung trees : ----- ring-barking for trees (a) 12 (b) 26 (c) 11

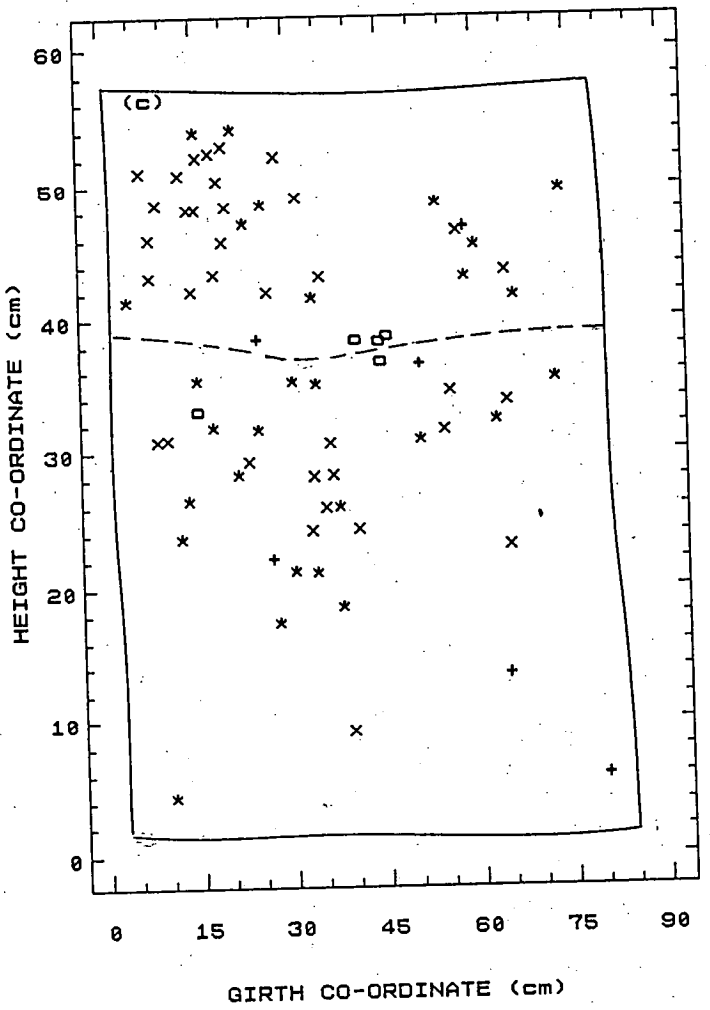
(c)
HEIGHT CO-ORDINATE (cm)
GIRTH CO-ORDINATE (cm)
0
10
20
30
40
50
60
0
15
30
45
60
75
90

[Fig 4.5(b)] although lines of *C.australis* spread/*P.subgranosus* attack are not as distinct. For tree 9 the overall attack does not appear obviously aggregated [Fig 4.4(e)] but considering only early attack (Jan,Feb) [Fig 4.4(f)] the streaming effect emanating from inoculation points is fairly obvious. Tree 9 appears to be exceptional in that later attack did not remain concentrated around the initial lines of attack created by the spread of *C.australis*.

4.2.2 Nearest neighbour distance for mapped attack

To quantify the spatial patterns of attack in Figs 4.4 and 4.5 nearest neighbour distances were calculated (Diggle 1983). Nearest neighbour distance (*nnd*) is the shortest distance from an event (a pinhole in this case) to the nearest event. Other methods of studying fully-mapped spatial point patterns such as point to nearest event (Diggle 1983) can be used but *nnd* is of intrinsic interest since the spacing mechanism between galleries is most likely to be related to the presence of galleries already established. For n pinholes there are $n(n\text{-}1)/2$ inter-event distances and these were calculated using the arc distance both clockwise and anti-clockwise around the tree (Section 3.4). So for a particular pinhole the $2(n\text{-}1)$ list of distances was used in a crude search to find the nearest neighbour of the pinhole under consideration. The empirical distribution function (EDF) of *nnd* (Diggle 1983) was obtained by calculating the frequency of *nnd* in classes of 0-1,1-2,2-3,3-4,4-5,5-6,>6 cm and then calculating the cumulative relative frequency which gives the EDF. The EDF of the observed *nnd* is given by $\hat{G}_1(y)$ where

$$\hat{G}_1(y) = n^{-1} \#(y_i \leq y) \qquad , i=1,...,n \qquad ,$$

y_i is observed *nnd*, y are values for tabulation of y_i (e.g. 1 to 6 cm classes above with last class calculated by difference) and # means "the number of". The observed EDF was compared to EDF's calculated for 49 Monte-Carlo simulations of a completely spatially random pattern (CSR) of n points on an area defined for each tree in Figs 4.4 and 4.5. EDF's can be calculated using the same values of y for each simulation so that

$\hat{G}_j(y)$, j=2,...,50 defines the simulated EDF's and $\bar{G}_1(y)$ is the sample mean of the simulated values for each class of y. Under a hypothesis of CSR all rankings of the $\hat{G}_j(y)$, j=1,...,50 are equi-probable so there is only a 2% chance of $\hat{G}_1(y)$ ranking either 1st or last if CSR is true. Thus the hypothesis of CSR can be tested graphically by inspecting the linearity of plot of $\hat{G}_1(y)$ versus $\bar{G}_1(y)$ compared to upper and lower simulation envelopes. The upper and lower envelopes are found simply by ranking, for each tabulated value of y, the values of $\hat{G}_j(y)$, j=2,...,50. If $\hat{G}_1(y)$ goes outside the bounds of the simulation envelope CSR is rejected at the 98% level (i.e. based on 49 simulations). If $\hat{G}_1(y)$ is under the lower envelope it indicates regularity in spatial pattern and above the upper envelope indicates an aggregated pattern.

Visual inspection of the mapped attack discussed above suggested that only for trees 9 and 11 was the pattern not obviously aggregated. To further investigate their pattern of attack EDF plots were constructed and these are shown in Fig 4.6 for tree 9 and Fig 4.7 for each of tree 11 and tree 48. Tree 48 was included for comparison even though CSR is overwhelmingly rejected simply by visual inspection of Fig 4.4(c). Fig 4.6(a) suggests that there is not a radical departure from CSR for all attack on tree 9 and if any, the departure is towards regularity and not aggregation. Fig 4.6(b) which shows the early attack on tree 9 does, however, suggest a rejection of CSR and an aggregated pattern. Fig 4.7 demonstrates for both tree 11 and 48 a more emphatic rejection of CSR due to aggregation. This is visually obvious for tree 48 as mentioned above but not so obvious for tree 11 [Fig 4.5(c)]. An interesting feature of the aggregated patterns reflected in Figs 4.6(b) and 4.7 is the less than expected, for an aggregated pattern, number of *nnd* less than 1cm [i.e. $\hat{G}_1(y)$ falls around or below $\bar{G}_1(y)$ at y=1]. This suggests a tendency for the male to space its gallery at least 1cm from already established galleries.

An approximate test of CSR can be obtained by comparing the observed mean *nnd* to that expected under CSR. Diggle (1983) used an approximation derived by

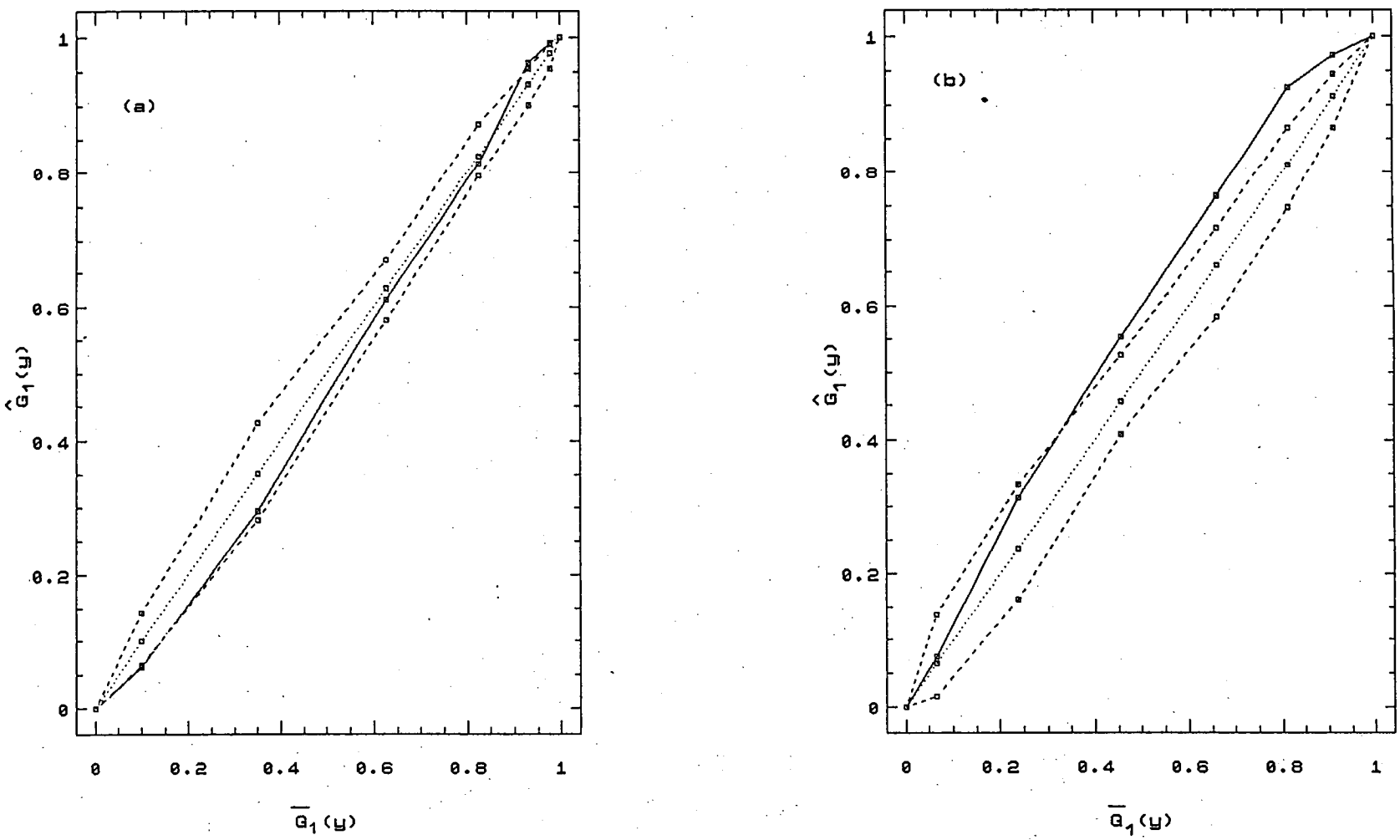

FIG 4.6 EDF of nearest neighbour distances _____, upper and lower simulation envelope ----- for tree 9 (a) all (b) Jan,Feb attack

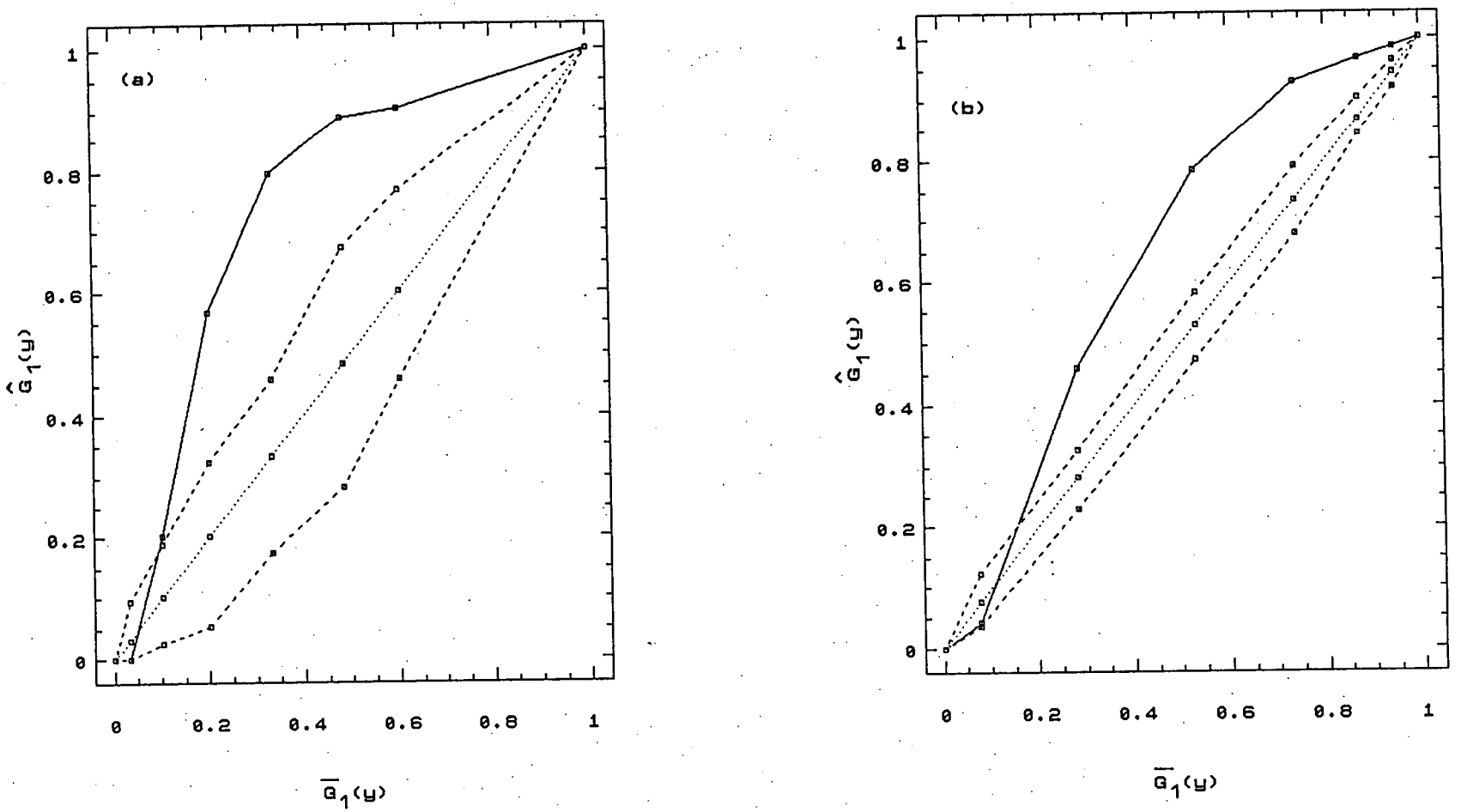

FIG 4.7 EDF of nearest neighbour distances _____, upper and lower simulation envelops ----- for tree (a) 11 (b) 48

Donnelly (1978) that mean *nnd*, $\bar{y}$, under CSR is normally distributed with expected value and variance given by

$$\mathcal{E}(\bar{y}) = 0.5(n^{-1}|A|)^{0.5} + (0.051 + 0.042n^{-0.5})\, n^{-1}\, l(A)$$

$$\mathcal{V}ar(\bar{y}) = 0.070\, n^{-2}|A| + 0.037(n^{-5}|A|)^{0.5}\, l(A)$$

where $|A|$ is surface area of the region, A, over which points (or pinholes) are distributed and $l(A)$ is the length of the boundary of the region A. The case of tree stems is slightly unusual since the vertical boundaries in Fig 4.4 and 4.5 are not real being required purely to display the map of attack in two dimensions. To calculate the above values of $\mathcal{E}(\bar{y})$ and $\mathcal{V}ar(\bar{y})$, the boundary of A was taken to be the length of the horizontal boundaries shown in Figs 4.4 and 4.5. Table 4.1 gives the observed mean *nnd*, $\mathcal{E}(\bar{y})$ and $sd(\bar{y})$ [$=\sqrt{\mathcal{V}ar(\bar{y})}$] and, in the case of trees 9, 11 and 48, values of $\mathcal{E}(\bar{y})$ and $sd(\bar{y})$ calculated using the 49 Monte Carlo simulations carried out to construct the $\hat{G}_1(y)$ versus $\tilde{G}_1(y)$ plot. The values in this last case are more reliable than Donnelly's approximation since they take into account the shape of A, but both estimates agree fairly well with the exception of $\mathcal{E}(\bar{y})$ for tree 11. This could be due to the low number of pinholes in this case. For the more densely attacked trees a mean *nnd* of about 2.5 cm appears to be a general value. A regular grid of 2.5x2.5 cm on an area of 1 m^2 with 2.5 cm boundary region would allow 38x38=1444 pinholes. Such a high density may occur locally (e.g. along the lines of attack in the inoculated trees) but is unlikely to occur over a large surface area.

4.2.3 Distribution of attack along the bole

The data collected by A.Slade in northwest Tasmania (Section 3.6) on the distribution of attack along the bole of 50 standing *N.cunninghamii* trees, showing various degrees of myrtle wilt symptoms, were used for the following. Slade recorded the diameter at 1.3m height, height and attacked bole length of each tree as well as the within-tree maximum density of attack recorded for 100 cm^2 areas within height classes along the bole of 0-5,5-10,10-15,15-20 and 20-25 m. Fig 4.8 shows the

Table 4.1 Statistics on nearest neighbour distance (nnd)

tree no.	number attacks	mean[a] *nnd*	$\mathscr{E}_1(\bar{y})$[b]	$sd_1(\bar{y})$[b]	Z[c]	$\mathscr{E}_2(\bar{y})$[d]	$sd_2(\bar{y})$[d]
9	406	2.773	2.724	0.073	0.69[f]	2.697	0.056
9[e]	255	2.934	3.446	0.116	-4.40[h]	-	-
10	472	2.260	2.470	0.061	-3.44[h]	-	-
11	74	3.371	4.176	0.266	-3.02[g]	5.603	0.373
12	129	4.685	5.581	0.267	-3.35[h]	-	-
26	277	2.938	3.568	0.115	-5.46[h]	-	-
40	295	2.533	3.410	0.107	-8.21[h]	-	-
45	188	3.165	4.085	0.161	-5.71[h]	-	-
48	471	2.347	2.862	0.071	-7.28[h]	3.092	0.067

a. Mean of observed nearest neighbour distances.

b. $\bar{y}$ is the mean nearest neighbour distance under CSR and $\mathscr{E}_1$ and sd_1 are Donnelly's approximations to the expected value and standard deviation of $\bar{y}$.

c. Statistic (mean- $\mathscr{E}_1$)/sd_1 compared to standard normal deviate

d. Mean and standard deviation of mean nearest neighbour distance based on 49 simulations of CSR.

e. Tree 9 early (January and February) attack.

f. Probability > 0.20

g. Probability < 0.002

h. Probability < 0.001

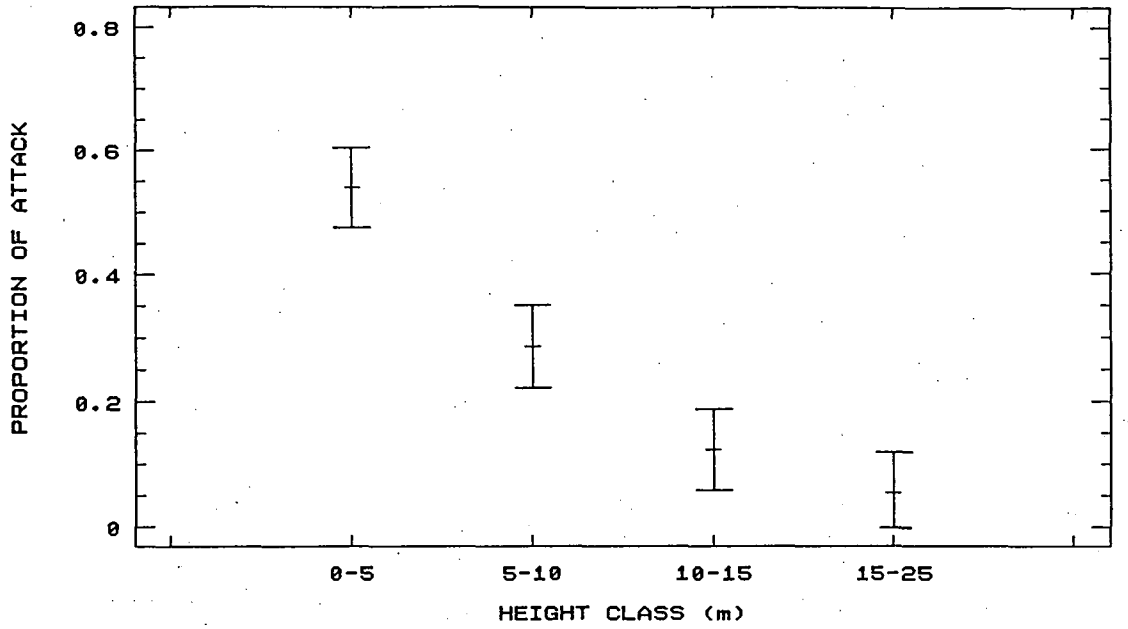

FIG 4.8 Proportion of attack along the bole for trees at least 20 metres tall (95% confidence bars shown)

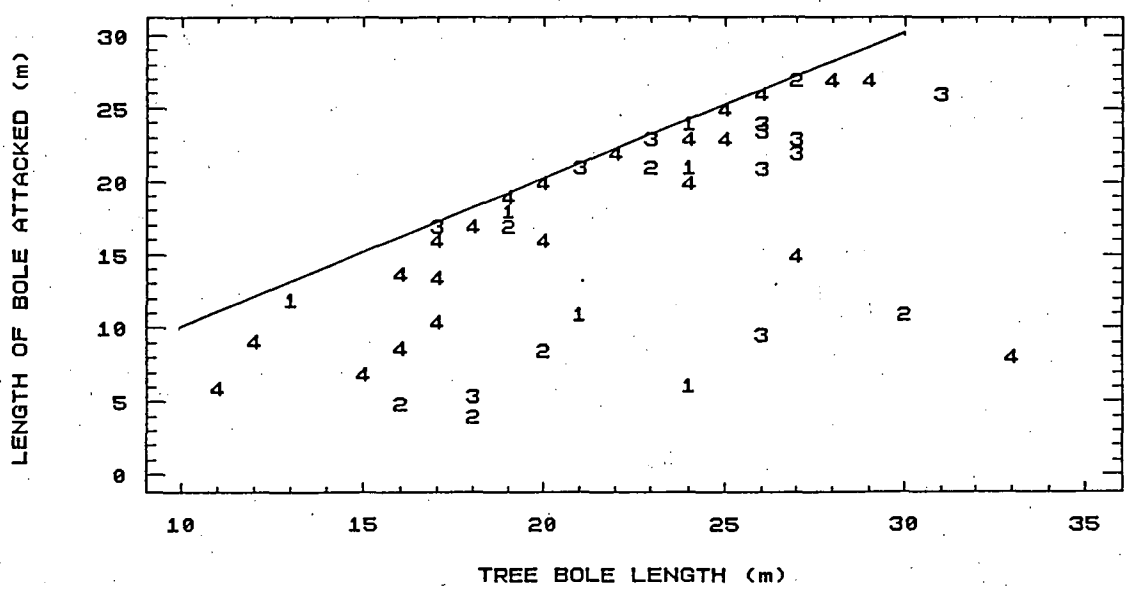

FIG 4.9 Length of bole attacked for health classes 1 to 4

proportion of total maximum attack versus bole height class where total maximum attack is the sum over the 5 bole height classes of the maximum recorded attack. Only trees at least 20m tall have been included in Fig 4.8. Fig 4.9 shows length of bole attacked versus tree bole height with numbers 1 to 4 representing myrtle wilt symptom classes ; 1 more than half the crown still green; 2 some green foliage remaining up to half of the crown; 3 foliage completely dead but over half still attached; and 4 less than half the dead foliage still attached.

4.3 Discussion

The results above show the close correlation of *P.subgranosus* attack and host tissue infection with *C.australis*. The highly aggregated pattern of attack on inoculated trees reflecting the movement of *C.australis* up the vascular system of the tree is quite striking. The exception to this was tree 9 where later attack did not strictly follow the streaming pattern of earlier attack. This could be the result of transverse flow of inoculum between vessels possibly aided by a more rapid development of galleries in this tree (Kile and Hall 1988).

The within-tree spatial pattern of *P.subgranosus* attack is also aggregated in trees uninfected by *C.australis* as demonstrated by the saprung sassafras (tree 11). This is probably due to the release of aggregation pheromones by pioneer beetles suggested by Elliott *et al.* (1982) as a secondary mechanism for inducing attack, the primary mechanism being the release of host produced volatiles. Hogan (1948) suggested pheromones as the explanation for the fact that females search for unmated males in a systematic fashion going directly from gallery to gallery without randomly searching in between. The release of anti-aggregation pheromones, for example as discussed by Borden (1988) for the striped ambrosia beetle *Trypodendron lineatum* Olivier, at high densities could be the cause of the regular pattern of total attack on tree 9, but contrary to this, tree 10 had a higher density of attack than tree 9 (Fig 4.3b) and did not exhibit

any tendency for regularity in spatial pattern as cumulative attack became more dense (Fig 4.4d).

The estimate of a minimum spacing between galleries of roughly one centimetre was based on the fact that the frequency of nearest neighbour distances in the 0-1cm class was less than expected under CSR while that for the 1-2cm classes and above was greater than expected (Figs 4.6a and 4.7). If aggregation occurs with no minimum spacing then the EDF plot should also lie outside the simulation limits for the 0-1cm class. Nearest neighbour distances less than 1cm were recorded but some of these could be due to errors introduced by the method of transcribing pinholes to plastic sheets (Section 3.4). Byers (1984) estimated a minimum distance between galleries of the bark beetle *Ips typographus* (L.) of 2.5cm. He noted that at high attack densities, galleries tend to be regularly spaced. In this study, aggregation was evident at low densities (tree 11) and remained so at high densities with the exception of tree 9. The fact that this was so despite the suggested minimum spacing of 1cm probably reflects the fact that densities did not reach a sufficient level for a minimum spacing of 1cm to have much impact on the spatial pattern of attack. As Borden (1988) has noted a spacing mechanism is probably more crucial for bark beetles which are limited to a 2-dimensional resource compared to wood boring beetles which can exploit the 3-dimensional resource of the wood. Once a sufficiently large diameter tree or log (i.e. greater than 12cm, Elliott *et al.* 1982) is colonised there is little competition for space between *P.subgranosus* galleries which are not restricted to the sapwood but can commonly extend through the heartwood.

Attack can occur along the entire length of the tree bole as demonstrated by the data of A.Slade but the intensity of attack declines rapidly with increasing height above the ground. This is probably a consequence of initial attack near the ground attracting further attack due to the release of aggregation pheromones and/or the possibility that a greater volume of primary attractant host volatiles are released nearer ground level.

5. DEVELOPMENT STAGES

In this section the natality and gallery development rates and phenology of immature stages of *P.subgranosus* are quantitatively described based on the data obtained by destructive sampling of galleries described in Section 3.1.2. Firstly the larval instars are classified numerically, using principally, head capsule width and, secondarily, body length. Numerical classification is required for all but the final instar because there are no morphological features which allowed instars to be classified as they were obtained. The final instar can be identified by the row of chitinous loops on the prothoracic segment (Section 2.2.2, Fig 2.7a). Quantitative descriptions of gallery development and initial oviposition are given. The phenology of the immature stages is then described in terms firstly, of simple statistics and secondly, probabilistic models. The general form of these models is described including a new model developed here. Finally, brood size and gallery failure rates are described.

5.1 Classification of larval instars

The general description of the larval instars was given in Section 2.2.2. This description assumed that there are 5 instars based on the work of Hogan (1948). Hogan obtained 50 larvae in the same way as those obtained in this study and by measuring head capsule width decided on 5 instars with mean widths given in Table 5.1. There is no need to use head capsule width to distinguish between the 4th and 5th (final) instars because of the chitinous loops on the prothoracic segment of the final instar which is absent in earlier instars as mentioned above. Individual larvae collected from disc dissections needed to be classified into an instar class. As mentioned in in Section 3.1.2, as individuals were extracted from galleries head capsule widths were measured for all instars except for the final instar for which a sample were measured. This gave 222 head capsule widths with 49 from final instars. For a further sample of 15 and 78 for each of the final and earlier instars, respectively, body length was also measured. To complement this sample all 50 preserved specimens in the Forestry Commission

Table 5.1 Statistics on larval head capsule width (mm)

Data/statistic	1st	2nd	3rd	4th	Final
Hogan/mean	0.346	0.439	0.587	0.772	0.945
author/sample	45	42	32	54	49
/mean	0.372	0.458	0.609	0.815	0.970
/median	0.36	0.44	0.60	0.83	0.96
/mode	0.36	0.44	0.60	0.83	0.996
/standard deviation	0.028	0.028	0.030	0.049	0.044
/standard error	0.0042	0.0043	0.0052	0.0067	0.0064
/minimum	0.28	0.44	0.56	0.72	0.83
/maximum	0.40	0.52	0.664	0.913	1.079

Table 5.2 Statistics on larval body length (mm)

statistic	1st	2nd	3rd	4th	Final
sample	24	31	17	25	45
mean	0.848	1.017	1.732	2.785	4.436
median	0.800	0.880	1.400	2.573	4.560
mode	0.800	0.800	1.400	2.490	4.150
standard deviation	0.138	0.285	0.639	0.502	0.594
standard error	0.028	0.051	0.155	0.100	0.089
minimum	0.640	0.760	1.080	1.743	2.573
maximum	1.160	1.740	3.400	3.760	5.440

collection, 30 of which were final instars, were also measured for both head capsule width and body length. Fig 5.1(a) shows the frequency of head capsule width where the frequency is the number of individuals at each unit on the x25 magnification scale. Fig 5.1(b) shows the classification of the first four instars obtained using the numerical classification procedure described below. Figs 5.2 and 5.3 show the relationship between head capsule width and body length on each of linear and logarithmic scales for body length. There are 5 definite peaks in Fig 5.1(a) which supports Hogan's conclusion. The difference between the first and second instar peak value is quite small. It can also be seen from Fig 5.1(a) that some individuals fall in the region between the peak frequencies where these peak values are taken to be the typical head capsule widths for the instars. The measurement error explains to a degree some of the overlap between 4th and final instar and the appearance of individuals between peak frequencies. For example a 4th instar with actual head capsule width of 0.83 mm (i.e. 10 units on the x12 scale), with a one unit measurement error on the x12 scale could have a measured value of 0.747, 0.83 or 0.913 mm. Measurement errors would be unbiased so that mean head capsule widths will reflect the actual typical instar value. The fact that the frequencies fall off symmetrically about the peak frequency values adds support to the unbiasedness of the measured values. Using the preserved specimens which were measured to greater precision (x50 scale, 1 unit =0.02 mm) measured values generally ranged 1 or 2 units either side of the typical values seen in Fig 5.1(a). This variation represents real population variation since variations of 2 units occurred too often to be purely measurement error.

It was possible to distinguish freshly hatched 1st instars (Section 2.2.2) from later instars but it was not possible to discriminate conclusively, using general appearance, between 2nd and 3rd, 3rd and 4th or even 2nd and a more developed 1st instar. For this reason when the individuals were collected an attempt to classify the

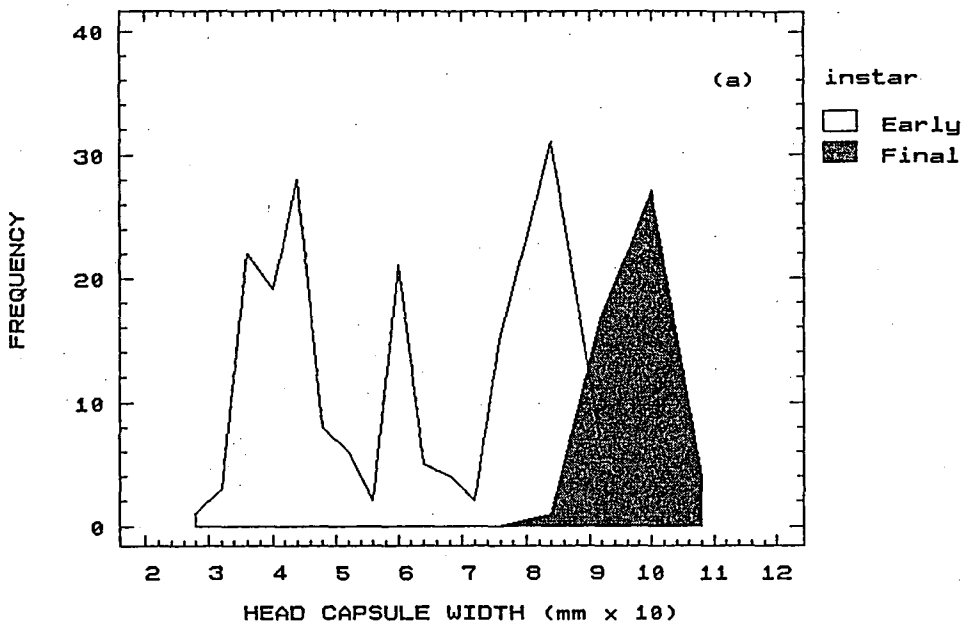

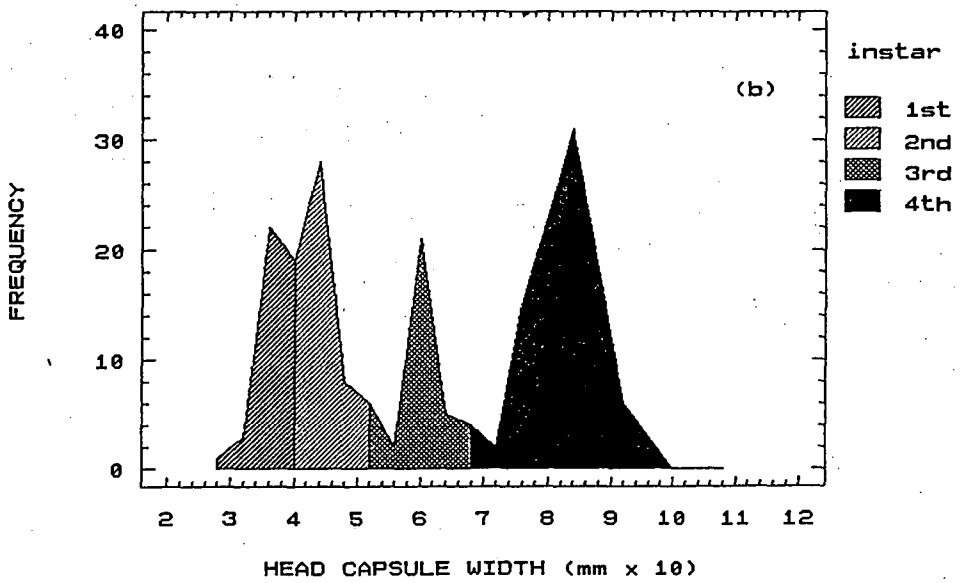

FIG 5.1 Frequency of head capsule width (a) early and final (b) classified 1st to 4th instars

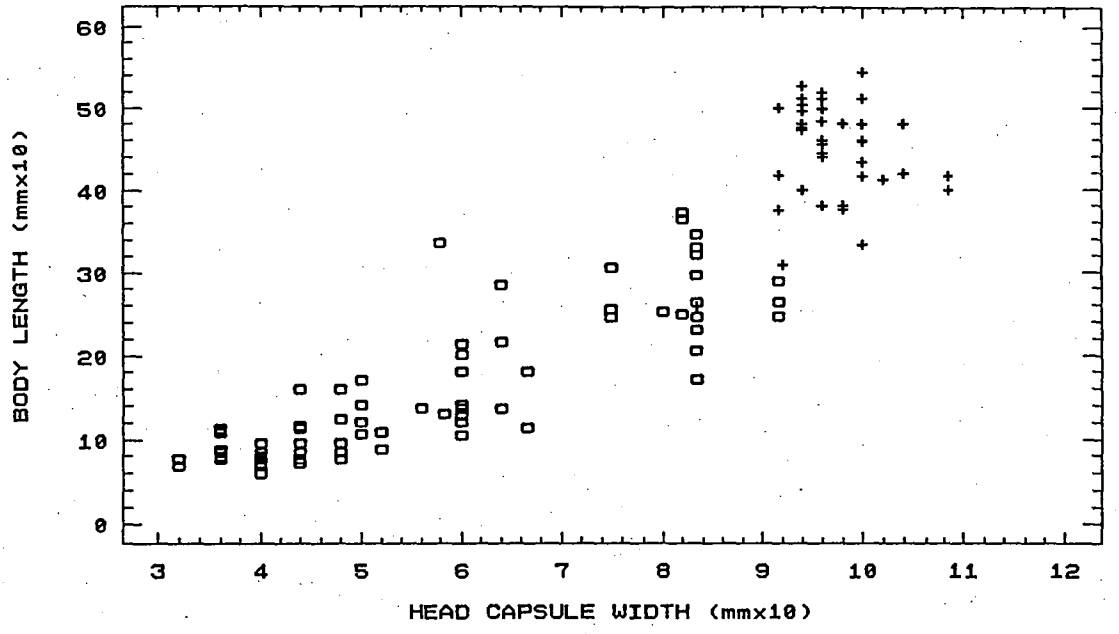

FIG 5.2 Head capsule width versus body length (+ final instar)

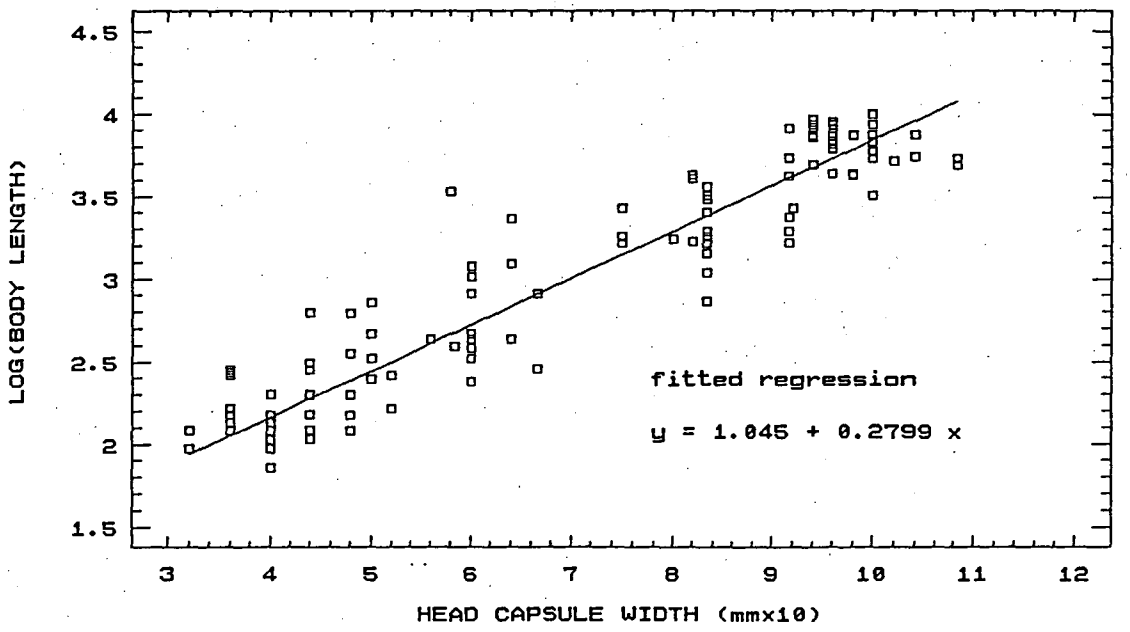

FIG 5.3 Head capsule width vs log(body length)

larva, with the exception of the final instar, was not made at that time, instead measurement of head capsule width was relied upon to allow larvae to be classed.

To aid classification a non-hierarchical classification procedure was employed. Since body length was measured for some individuals it was used along with head capsule width in this procedure to provide extra discrimination between instars. Since the procedure employed using GENSTAT does not allow missing values, for those individuals with no measured body length an estimate was used based on a regression of the logarithm of body length on head capsule width (Fig 5.3). The estimated coefficients for the regression were, with standard errors in brackets, 1.0447 (0.0565) for the intercept and 0.2799 (0.0078) for the slope with an R^2 value for this regression of 0.904. A regression of the log of body length on the log of head capsule width was tried but gave a worse fit ; R^2=0.894. These estimated body lengths do not provide extra discrimination to that of head capsule alone but they do allow the classification procedure to use both measurements. The algorithm used was one for which the criterion of goodness-of-fit of the classification is the within-class sums of squares and products which does not require assumptions that (a) the data is multi-normally distributed or (b) the within-class dispersion matrix is constant across classes. The algorithm used by GENSTAT alternates between transferring and swapping individuals between classes until no further improvement in the criterion can be made. The classification used to provide a starting point for the algorithm used the cut-points on the head capsule width scale of 0.4, 0.52, 0.68 and 0.9 mm. There were 5 obvious misclassifications from the procedure with a single final instar with width and length of 0.83 and 2.573 mm allocated to the 4th class and four, 4th instars each with width of 0.913 and lengths of 2.905, 2.656 and 2.49 (the last of the lengths was not measured) allocated to the 5th class. These individuals were reallocated to their correct class. Table 5.1 gives statistics for larval head capsule width for the 5 instar classes derived from the above classification procedure. Table 5.2 gives the corresponding statistics for

non-missing values of body length. The modes in Table 5.1 correspond to the peak frequencies in Fig 5.1. The classification of instars in Fig 5.4 is based on the minimum and maximum value of head capsule width for each instar class given in Table 5.1 and Fig 5.1(b). This is possible since using body length in the classification procedure has not caused any overlap in head capsule width between the derived classes but has assisted in determining the boundaries of the classes. Thus all 173 pre-final instar larvae were allocated to one of 4 instar classes.

All of the mean, median and mode values for each instar class derived in this study are larger than the values given by Hogan with the exception of the 2nd instar which had a mode and median value very similar to Hogan's value (Table 5.1). Hogan does not say how his values were calculated but it can be assumed that since they are quoted to 3 decimal places that they are means and not modes or medians where the precision is only that of the measuring instrument. Hogan also quotes an error of 0.003 for all 5 instar means which again must have been a standard error of the mean, where the number of individuals in each class was so similar that a single error for all classes could be quoted, since stereo light microscopes could not give such precision. Taking Hogan's values to be means, his values are consistently and significantly ($P<0.01$) below the means obtained here by roughly 0.02 mm. This difference at one unit on the x50 magnification scale could easily be due to a difference in instrument calibration rather than a real population difference.

Hogan, using Dyar's Rule (Dyar 1890) of a constant ratio of head capsule width for a given instar class to that of the preceding class, obtained a value of 1.29 for this constant ratio. Table 5.3 gives the values of this ratio for Hogan's data and for this study using class means. The mean value of the ratio in this study was calculated to be 1.27. The standard errors of the ratios given in Table 5.3 were approximated using eqn (10.12) of Kendall and Stuart (1977). According to Przibram's Rule (Chapman 1982) the ratio should be the cube root of 2 (i.e. approximately 1.26). The ratio

Table 5.3 Larval head capsule width and Dyar's Rule

Data/statistic	1st	2nd	3rd	4th	Final	mean
Hogan/mean	0.346	0.439	0.587	0.772	0.945	
/ratio[a]		1.269	1.337	1.315	1.224	1.286
/expected[b]	0.346	0.446	0.576	0.743	0.958	
author/mean	0.372	0.458	0.609	0.815	0.970	
/ratio[a]		1.230	1.329	1.339	1.190	1.272
/se(ratio)		0.119	0.103	0.104	0.090	
/expected[b]	0.372	0.474	0.603	0.766	0.975	

a. Ratio of this instar's width to that of previous instar
b. Using 1st instar mean width as the start of geometric series and common ratio given in the mean ratio column.

obtained in this study for each of instars 2 to 5 given in Table 5.3 did not differ significantly ($P>0.1$) from Przibram's Rule. Using the first instar mean head capsule width and a geometric series based on the above ratios for each of Hogan's and this study, the predicted 2nd to 5th instar widths are given in Table 5.3.

5.2 Gallery development and initial oviposition

The length of the initial section of the gallery up to initial oviposition (i.e. from the entry point to the end of the section excavated by the adults) was measured where the gallery was unbranched (Section 3.1.2). There were 244 such measured gallery sections of which 111 had eggs where, in most cases, these were located at the end of the gallery. One of the 111 galleries had two batches of 8 eggs each with one batch at the end of the gallery and one batch found one centimetre from the end. For two other galleries the eggs were found 2 to 3 cm from the end of the gallery. For the following, the gallery length at initial oviposition is also taken as the full length of gallery in these three exceptional cases. As well as the total of 870 eggs, 52 1st to 4th instars and 15 final instars were also found in these 111 galleries. For the remainder of this section on gallery development and initial oviposition, the number of eggs will be taken to be the combination of eggs and larvae above since negligible mortality of larvae was observed (Section 5.4). Fig 5.4 shows the relationship between gallery length and each of days and day-degrees above a threshold of 11°C (DD_{11}) (Section 3.3) where galleries in which eggs were found are identified separately. The threshold value of 11°C is based on the work described in Section 7.3. Table 5.4 gives some statistics on natality and length of gallery at initial oviposition. Fig 5.5 shows the relationship between the number of eggs and length of gallery. Above a minimum length of about 4cm the relationship appears linear so a linear regression was fitted with a Poisson error (Appendix 1) for the number of eggs using GLIM (NAG 1986). An adequate fit was obtained with 43% of the *deviance* (Appendix 1) explained and within the range of the

Table 5.4 Statistics[a] on natality and gallery development at initial oviposition

Variable	mean	median	s.d.[b]	minimum	maximum
natality[c]	8.44	7	6.57	1	36
gallery[d] length (cm)	12.13	12	3.93	5	26

a. Based on 111 measured galleries at the end of which eggs were found
b. Standard deviation
c. Number of eggs laid including larval instars found at the end of the adult section of the gallery
d. At initial oviposition

Table 5.5 Phenology of pre-adult stages

Stage	time unit	sample size	mean	median	s.d.[a]	minimum	maximum
egg	day	1457	229.0	216	90.9	37	651
	DD_{11}		862.7	575	669.2	89	3545
instar 1	day	47	301.4	295	60.5	161	414
	DD_{11}		1465.0	1389	630.3	300	2549
instar 2	day	36	264.1	257	73.7	161	405
	DD_{11}		1120.5	986	679.3	300	2447
instar 3	day	26	333.5	322	81.7	210	651
	DD_{11}		1732.9	1664	118.2	857	3545
instar 4	day	50	374.5	326	112.3	263	651
	DD_{11}		2021.3	1712	716.4	1241	3545
instar 5	day	319	457.3	405	131.4	263	651
	DD_{11}		2591.5	2448	735.2	1241	3545
pupa	day	83	639.9	651	16.3	609	651
	DD_{11}		3427.2	3545	170.0	3138	3545

a. standard deviation

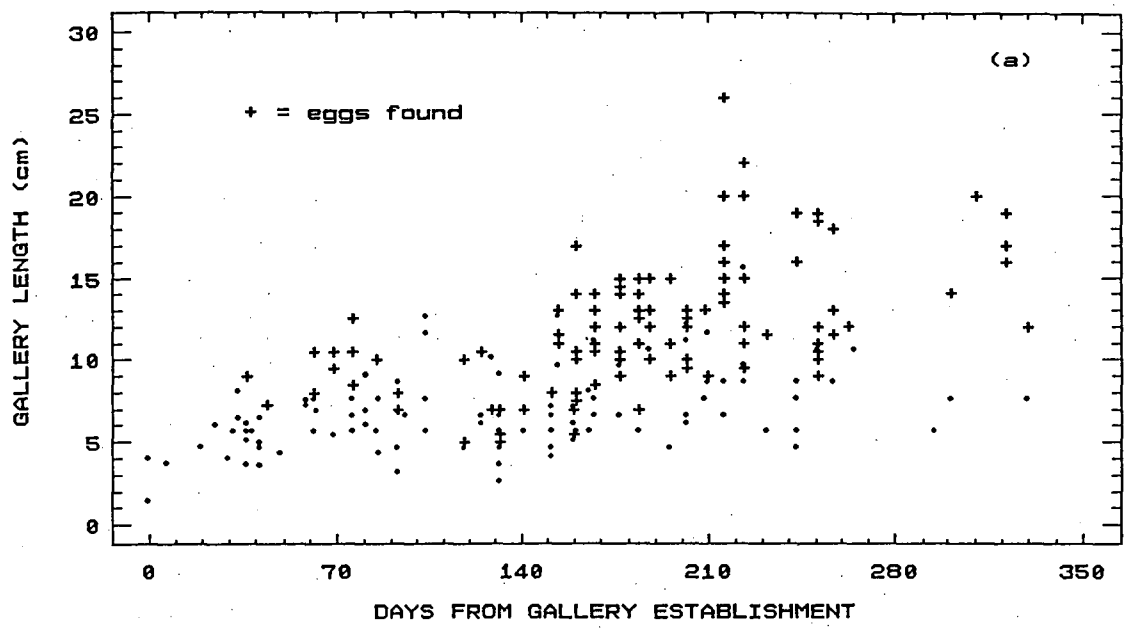

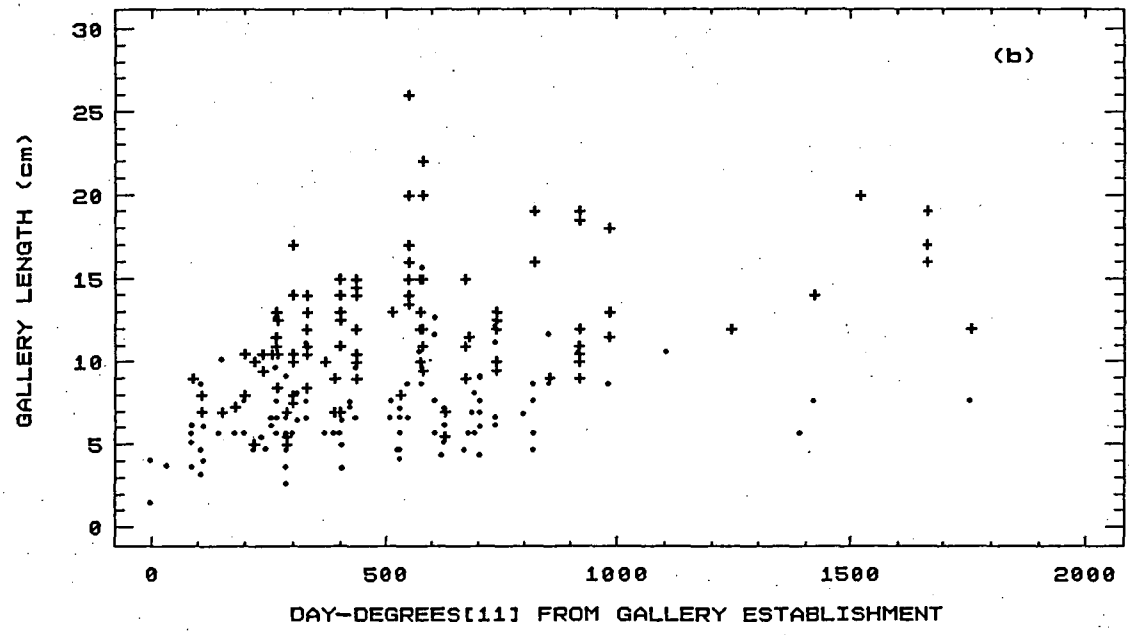

FIG 5.4 Length of gallery up to oviposition versus (a) days and (b) day-degrees[11] from gallery establishment

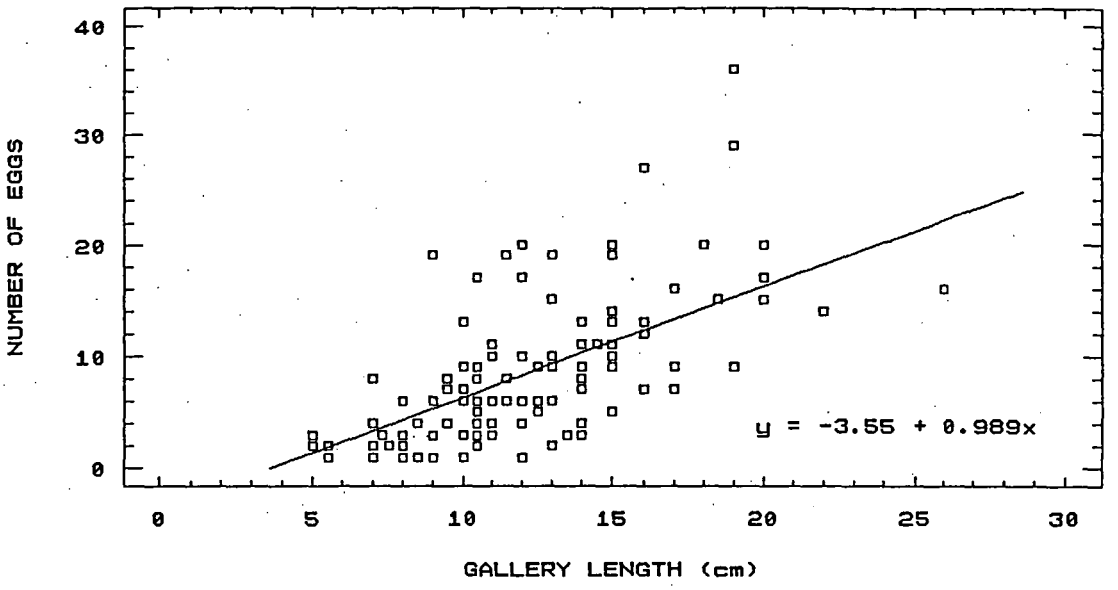

FIG 5.5 Number of eggs versus gallery length at oviposition

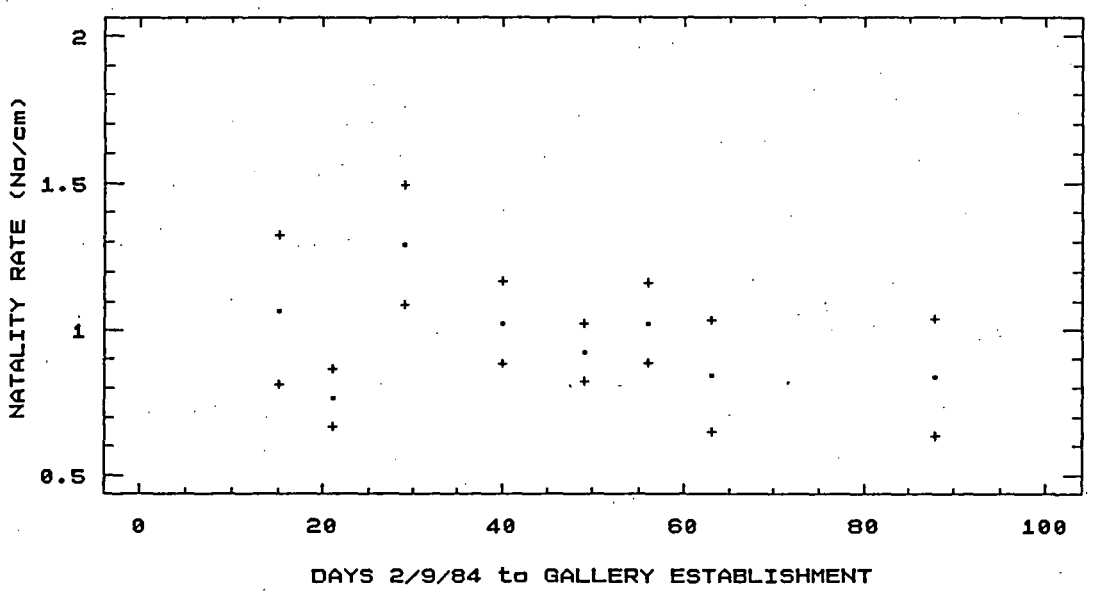

FIG 5.6 Natality rate (number eggs/cm gallery > 3.6) versus days from 1st to later gallery establishment, mean and (+) standard error bar

data sensible predicted values are obtained. Predictions below 3.6 cm, roughly the point where the regression line intercepts the abscissa, and above 30 cm should be constrained to zero and the predicted natality at 30cm respectively to give sensible predictions for these ranges. The corresponding log-linear (ie. log *link* Appendix 1) model gave a worse fit than the linear with 40% of the deviance explained.

The possibility that the diameter of the log could limit the development of the gallery and therefore affect natality was investigated. The relationship between each of length of gallery, number of eggs and natality rate [i.e. number eggs/(length-3.55)] at initial oviposition and the mid-diameter of the log in which the gallery was established was graphed. There were no obvious trends (graphs not shown) in all three cases. The smallest diameter in the sample was 12.8 cm.

The galleries were established over a 3 month period in the late summer/autumn of 1984 (Section 3.1.1) so to investigate any differences in gallery development and oviposition between galleries established early versus late in this period, for the 111 galleries above, the time, in units of both days and DD_{11}, from the first gallery establishment on 9/2/84 to initial oviposition was calculated. This data relates to 9 dates when gallery establishment was recorded (Section 3.1.1) ranging from 16/2/84 to 7/5/84 with corresponding days from 9/2/84 of 7,15,21,29,40,49,56,63,88 and number of galleries dissected being 1,8,14,12,14,21,19,9,13. Fig 5.6 compares the natality rate across the establishment dates. The single value for 16/2/84 (i.e. 7 days) was 3.52 and is not shown in Fig 5.6 to maintain a reasonable scale for the later dates. Figs 5.7 and 5.8 show the relationship between number of eggs and length of gallery, respectively, for each of days and DD_{11} from 9/2/84. These graphs do not show any striking differences between early and late establishment in natality rate, absolute number of eggs or length of gallery at oviposition. However, the mean time from gallery

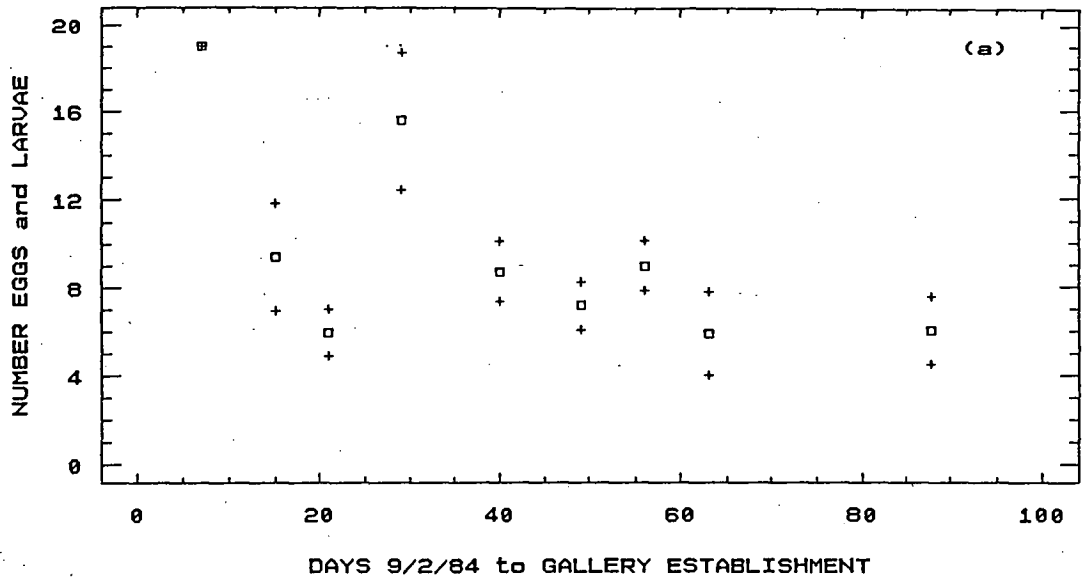

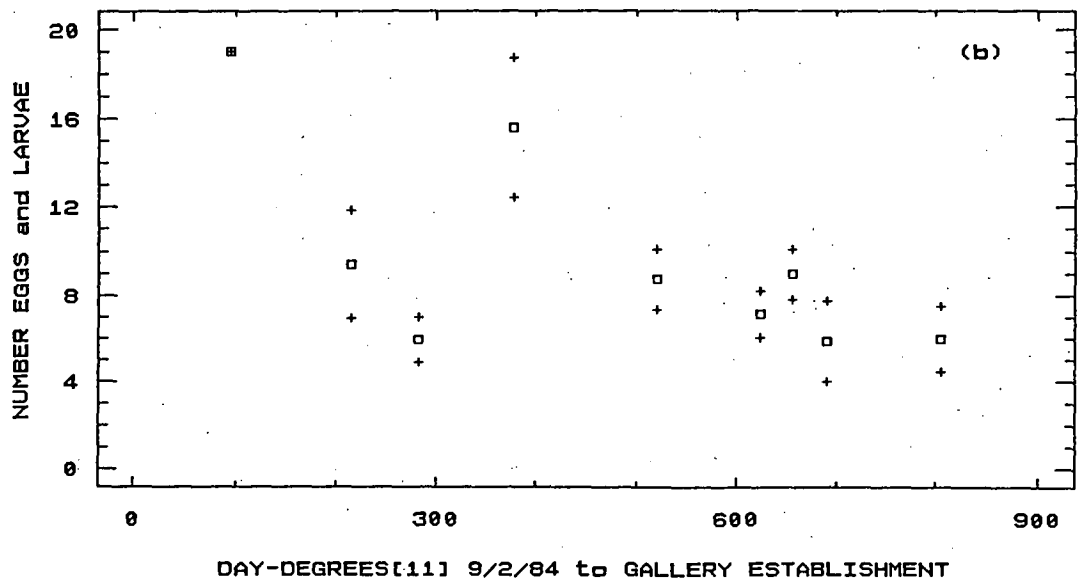

FIG 5.7 Number of eggs and larvae in gallery section up to oviposition versus time from 1st to later gallery establishment in units of (a) days (b) day-degrees above 11, means and (+) standard error bar

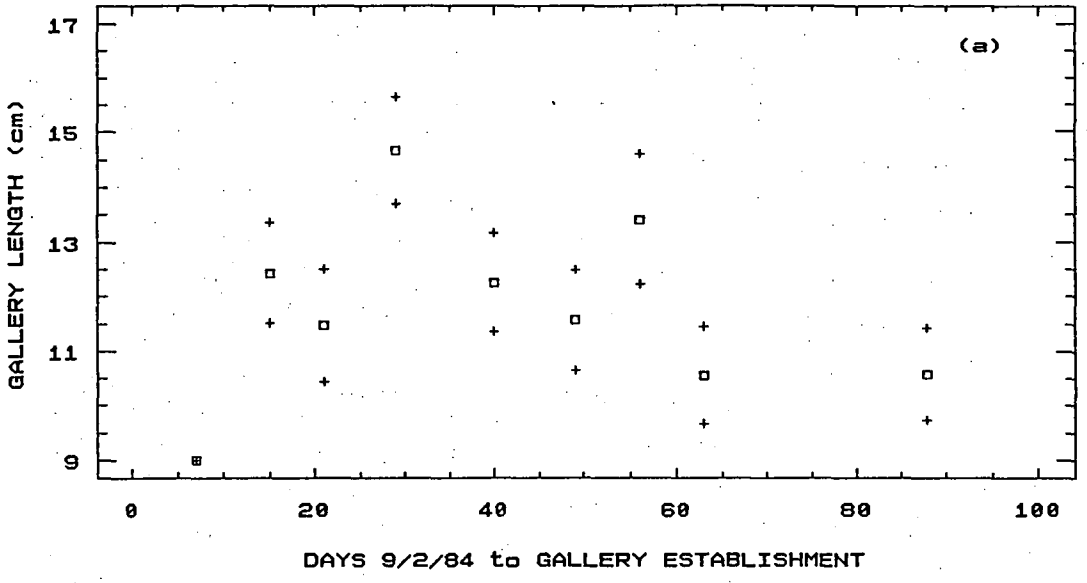

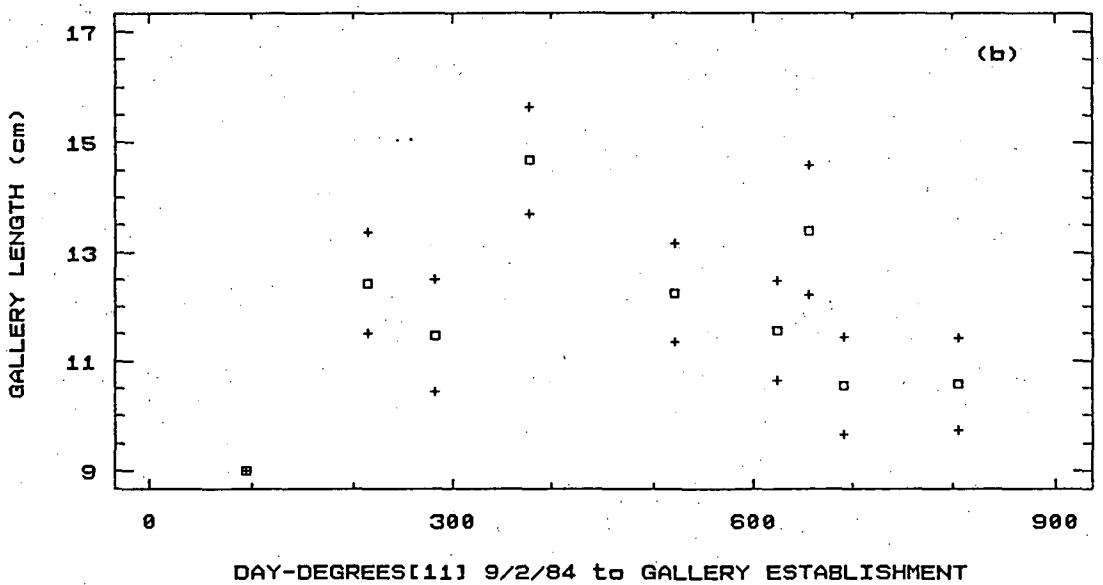

FIG 5.8 Length of gallery section up to oviposition versus 1st to later gallery establishment in units of (a) days (b) day-degrees above 11 degree threshold, means and (+) standard error bars

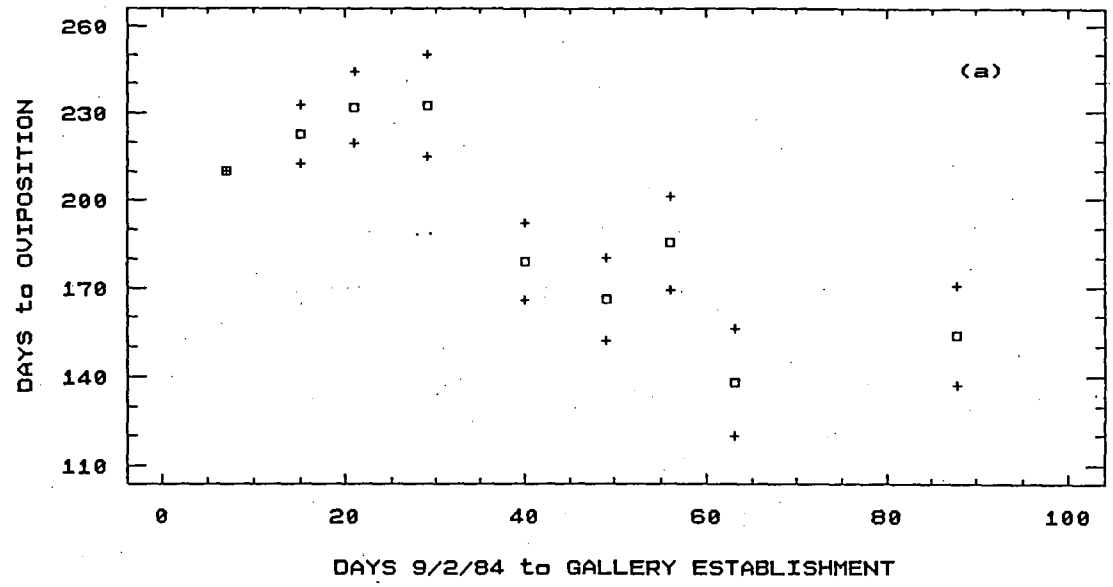

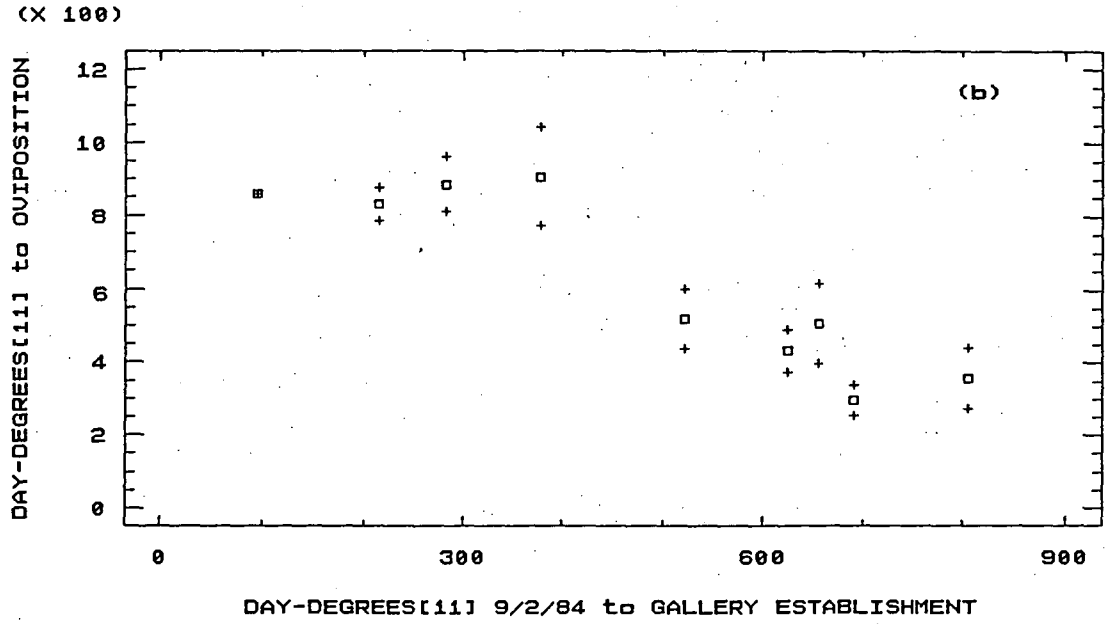

FIG 5.9 Time from gallery establishment to oviposition versus time from 1st to later establishment in units of (a) days (b) day-degrees above 11 degree threshold, mean and (+) standard error bar

establishment to initial oviposition (taken as the date of disc sampling if eggs were found in a single adult section of gallery) was found to decrease with later gallery establishment date as seen in Fig 5.9. Correspondingly the rate of gallery development taken over the period from establishment to initial oviposition in units of centimetre per time unit (i.e. day and DD_{11}) was found to increase with later establishment as seen in Fig 5.10. Fig 5.11 shows that there is no obvious difference in the calendar date of oviposition for early compared to late gallery establishment and as a result the difference in timing of establishment is reflected in the rate of gallery development. Since the galleries dissected were sampled randomly (Section 3.1.2) it is unlikely that the trends seen in Figs 5.9 and 5.10 are due to sampling bias. To confirm this, cross-tabulation of the 111 galleries by tree number and date of attack did not suggest that any particular tree was responsible for the trends. This trend of shorter time to initial oviposition with later gallery establishment was reflected in an analagous trend (Section 7.5) in the timing of emergence for caged galleries occurring in the same logs as those destructively sampled (Section 3.1.3). It was found that galleries established early in the late summer/autumn did not produce emergents, on average, any sooner than those established later in this period.

5.3 Phenology of immature stages

Data on each immature life stage were obtained by dissection of galleries of known establishment date (Section 3.1.2). Table 5.5 gives some statistics on the phenology of each immature stage in terms of days and DD_{11} from gallery establishment. The results in Table 5.5 have not been adjusted for the relationship of timing of initial oviposition with timing of gallery establishment as discussed in the previous section. A flow on effect to later stages would be expected, however, the numbers of galleries dissected at later sampling dates were too small, for reasons given in Section 3.1.2, to allow this to be investigated. Considering the timing of gallery establishment as random any resulting differences in phenology are incorporated in the

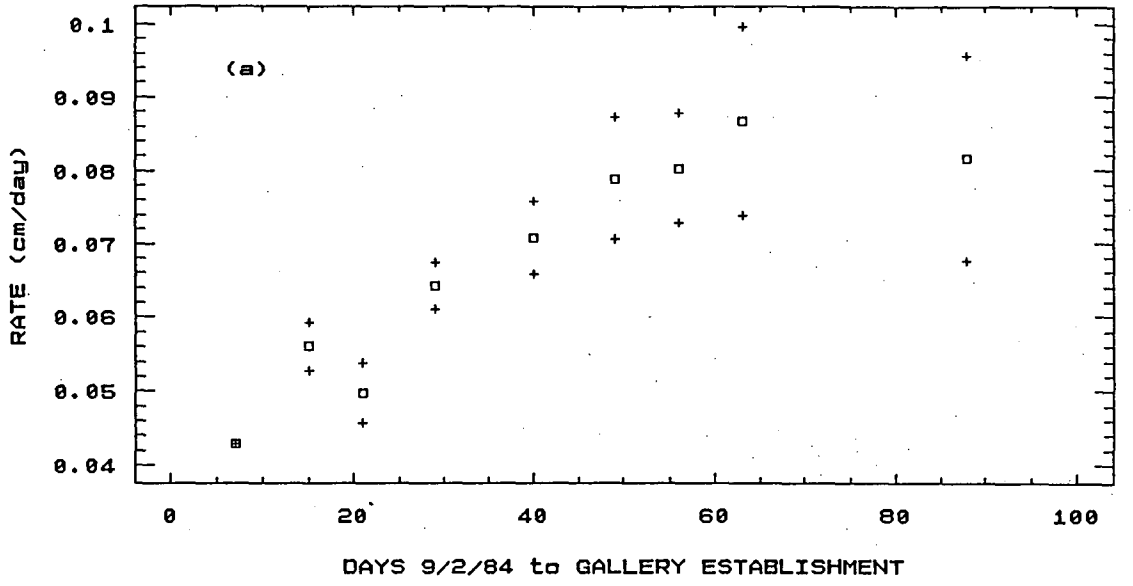

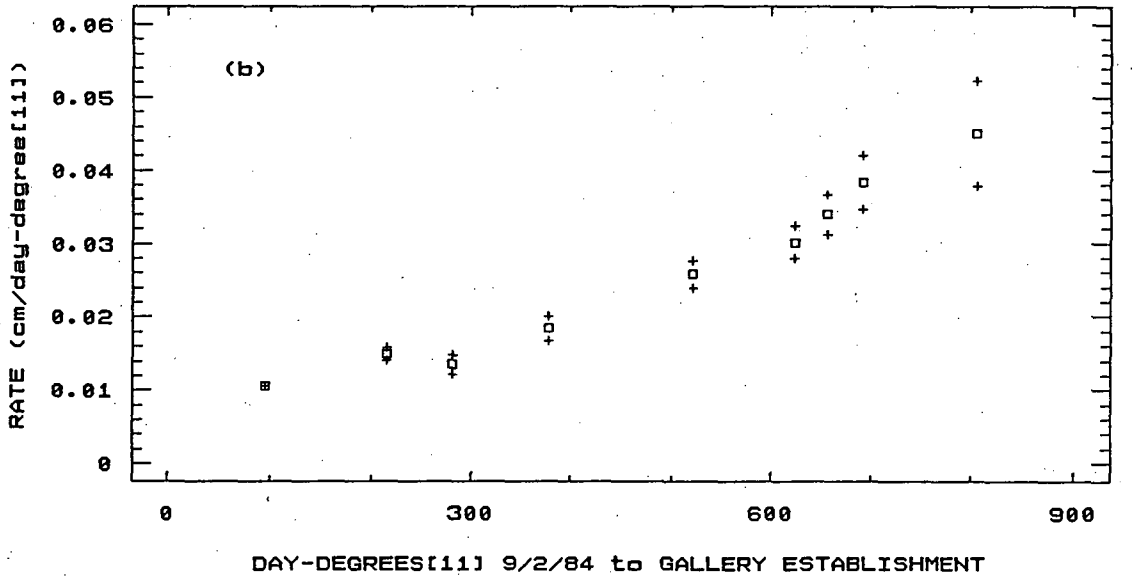

FIG 5.10 Rate of gallery development versus time from 1st to later gallery establishment in units of (a) days (b) day-degrees above 11 degree threshold, means and (+) standard error bars

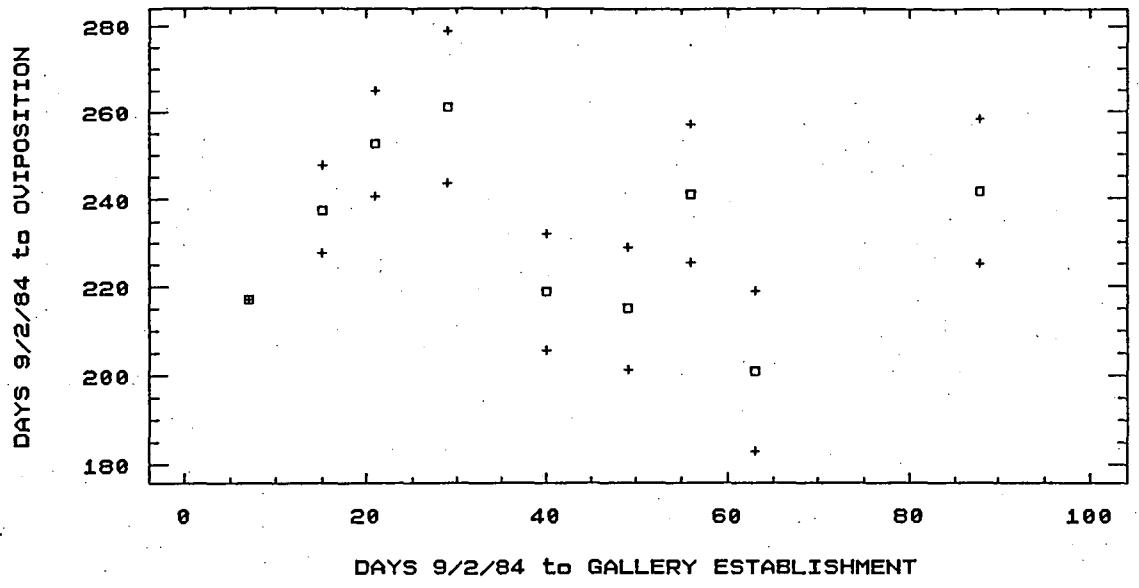

FIG 5.11 Days from 1st establishment to oviposition versus days from 1st to later establishment, means and (+) standard error bars

variation in time interval over which a particular stage occurs.

The sample sizes in Table 5.5 are the number of individuals collected in each stage from varying numbers of galleries at each sampling occasion. The large number of eggs obtained is a result of a large number of galleries dissected at the earlier sampling occasions, due to the simplicity of the gallery, while later sampling occasions where larvae were appearing involved fewer galleries, as mentioned above, because of their complexity (Section 3.1.2). The small number of early instars obtained is due, unfortunately, to the fact that the timing of their occurrence within the summer following gallery establishment was not well covered by the sampling. The 9th and 10th sampling occasions occurred on the dates of 9/11/84 and 25/1/85 which straddled the period during which most individuals passed through the 1st to 4th instar stages. Small sample size has caused the anomalous result in Table 5.6 where the 2nd instar has a mean time to occurrence which is less than the 1st instar. Fig 5.12 shows the number per gallery of each stage at each of the dates of sampling starting from the 4th sampling occasion at which eggs were first found. A logarithmic scale has been used in Fig 5.12 to allow mean number of early instars to be discernible on a common scale with mean number of eggs. Figs 5.13 and 5.14 show histograms of the timing of occurrence of the stages where the 1st to 4th instars have been combined because of their individually small sample size.

5.4 Models of insect phenology

5.4.1 Theory

Models of insect phenology are required within systems of models for simulating or predicting population dynamics. Models are also a useful way of summarising and/or smoothing phenological data as a means of determining general trends. When studying the life cycle in the field of a bark or wood boring insect such as *P.subgranosus* it is not possible to observe a cohort over time (i.e. longitudinally)

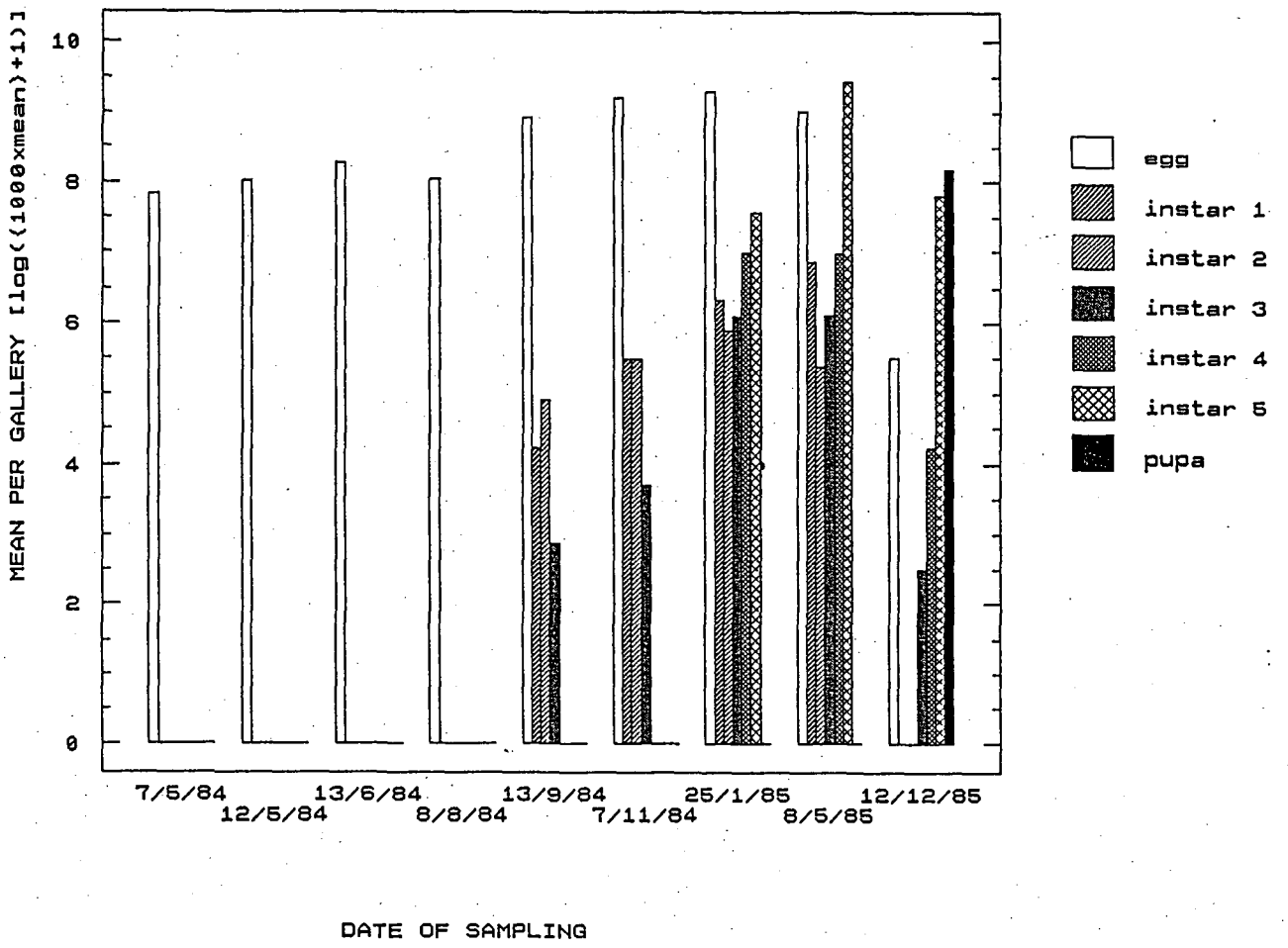

FIG 5.12 Mean number of stage per gallery on a logarithmic scale

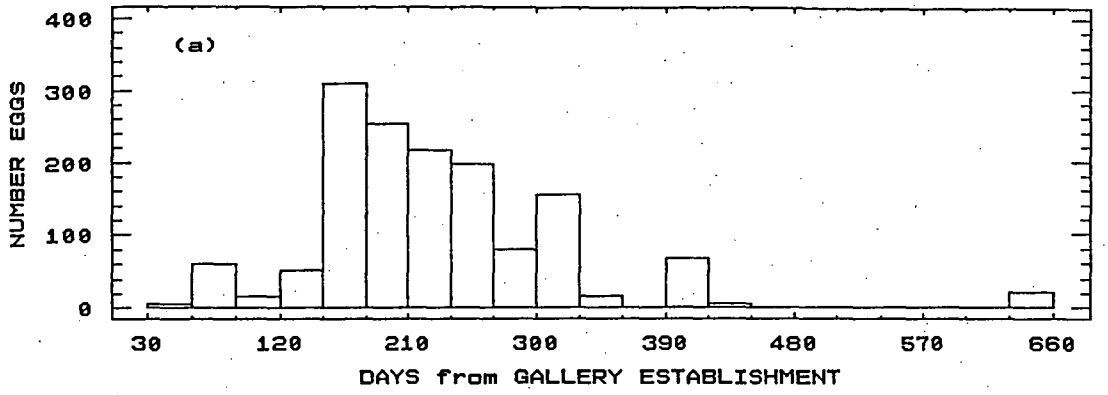

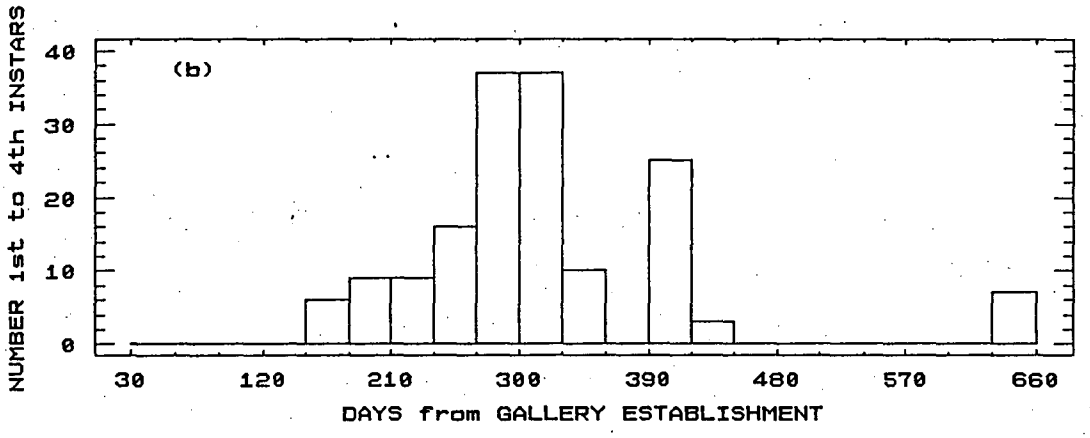

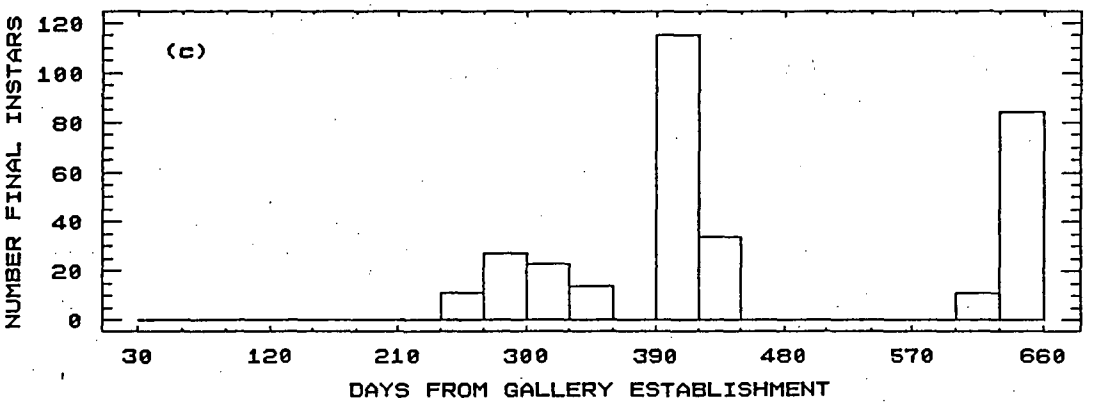

FIG 5.13 Frequency of stages across days from gallery establishment
(a) egg (b) 1st to 4th instar (c) final instar

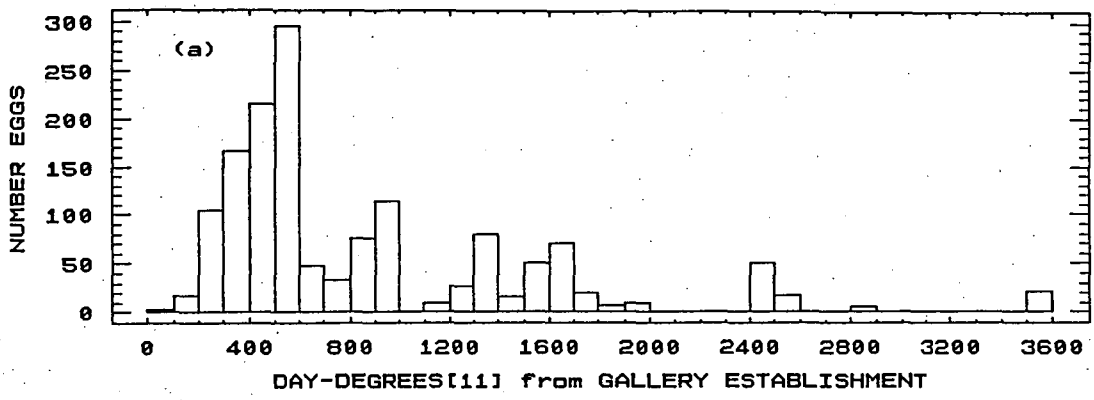

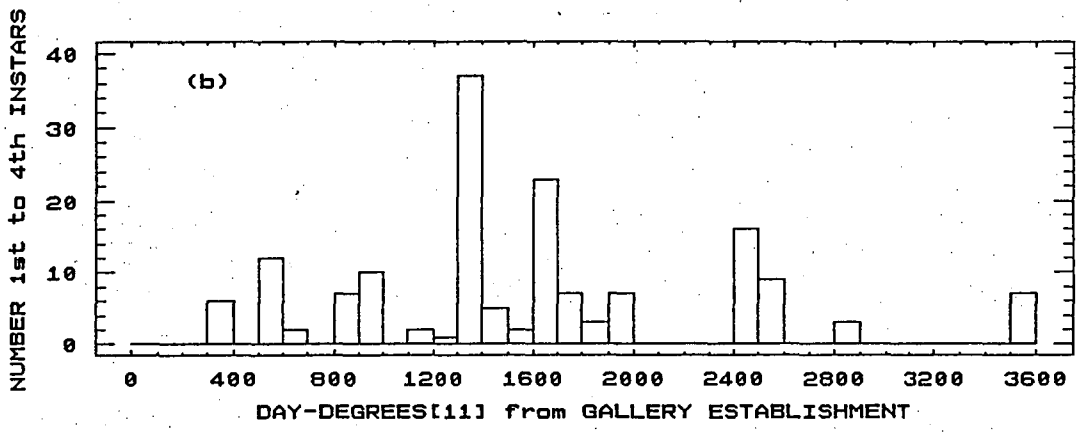

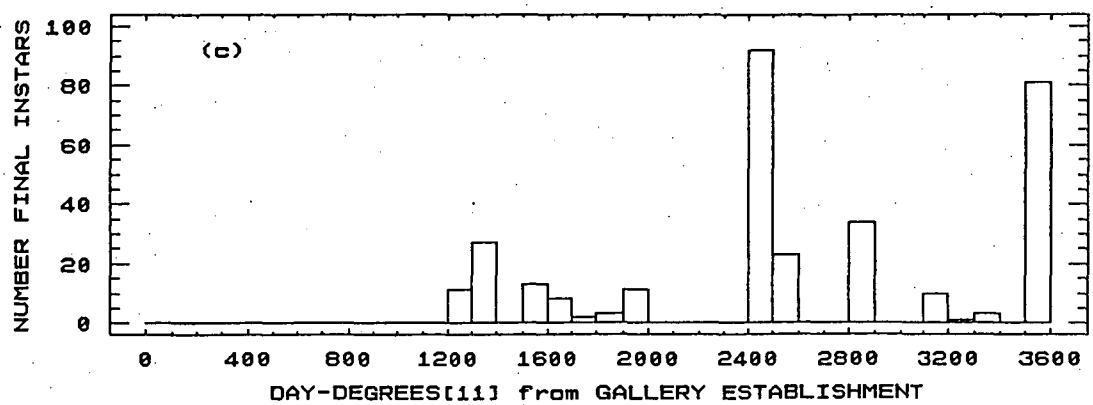

FIG 5.14 Frequency of stage across day-degrees[11] from gallery establishment (a) eggs (b) 1st to 4th instar (c) final instar

because destructive sampling of the galleries is required to observe pre-adult stages. The data obtained from destructive sampling is generally cross-sectional in nature whereby at each of a number of sampling occasions at times t_i , i=1,...,s , a sample of the population (e.g. a number of galleries are dissected) and the number of individuals, n_{ij} , in development stage j, j=1,...,a (e.g. egg, larval instars, pupa, adult) are observed.

Kempton (1979) developed a framework for modelling such data involving an initial population size given by unknown parameter N_0, and models for each stage of (i) the stage duration time and (ii) the stage death rate. Kempton made use of statistical distributions to model stage duration times (including entry time to the first stage) and in particular used the gamma distribution. Kempton used chronological time units but physiological time units such as day-degrees could equally well be used. The parameters in models of (i) and (ii) and the parameter N_0, because they are all estimated from the same data, are highly correlated and Kempton employed some simplifying assumptions to make the mathematics tractable and estimation feasible. In particular he assumed that the stage-specific mortality rate can be replaced by an age-specific mortality rate (i.e. the probability of death is a function of the individual's age and not its current stage) and that stage duration times are independent both between and within individuals and are gamma distributed with a common shape parameter across stages. Assumptions on the nature of the sampling are also implicit with Kempton's approach. These assumptions are (a) sampling efficiency is equal across stages (e.g. physically small stages such as eggs and early instars are not more easily missed or destroyed when sampling compared to late instars, pupae or adults); (b) sampling efficiency is equal across sampling occasions; and (c) individuals are correctly or unbiasedly allocated to their actual stage of development. Of the above (a) and (c) ensure that the proportion, p_{ij} , of individuals in each stage at each sampling occasion is an unbiased estimate of that in the population. The assumption in (b) is required for the unbiased estimation of initial population size (i.e. total brood size per

gallery, leaf etc.), age-specific mortality and recruitment to the first stage. Ensuring (b) is usually managed by employing a sampling unit relevant to population size, such as a gallery for wood boring insects or leaf for leaf-eating insects, and selecting sampling units randomly. In this context initial population size, N_0, is mean number of eggs laid per sampling unit. Kempton's simplified model is given by

$$\mathcal{E}(n_{ij}) = N_0\, \omega(t_i)\, p_j(t_i) \qquad (5.1)$$

where

$$p_j(t_i) = \mathcal{P}r(Y_j \le t_i < Y_{j+1} \mid \text{survival to age } t_i)$$

$$= \int_0^{t_i} [g_j(y) - g_{j+1}(y)]dy \qquad , j=1,...,a\text{-}1,$$

$$= \int_0^{t_i} g_j(y)dy \qquad , j=a \quad ,$$

$\omega(t)$ is the function determining the probability of surviving to age t, $g_j(y)$ is the probability density function (*pdf*) of $Y_j = \sum_{h=0}^{j-1} X_h$, Y_j is the time from t_0 to entry to the j^{th} stage, and X_h is the time spent (or duration) in the h^{th} stage. The reproductive property of the gamma distribution (Johnson and Kotz 1970) states that if the X_h are gamma distributed with index α_h (= Kempton's k_i) and common scale parameter β (= reciprocal of Kempton's b) so that

$$\mathcal{P}(X_h = x) = \frac{x^{\alpha_h - 1}\, exp\{-x/\beta\}}{\beta^{\alpha_h}\, \Gamma(\alpha_h)} \qquad \alpha_h, \beta > 0, x > 0,$$

then $g_j(y)$ is a gamma *pdf* with index $\sum_{h=0}^{j-1} \alpha_h$ and scale parameter β.

Kempton assumed the n_{ij} are approximately Poisson distributed with expected value given by eqn (5.1) and used maximum likelihood to estimate the parameters θ, t_0, x_0, N_1 and mean stage durations x_j, $j = 1,...,a$, where θ is the age-specific mortality rate assumed constant for all stages so that

$$\omega(t) = exp\{-\theta\,(t-t_0)\} \quad ,$$

t_0 is the time of the start of the process, x_0 is the mean time of entry to the first stage,

N_1 is the number entering the first stage where N_1 is given by

$$N_1 = N_0(1+\theta\beta)^{x_0/\beta} \quad ,$$

and $x_j = \alpha_j \beta$, j=1,...,a (i.e. the means of the gamma distributions for X_j , j=,1,...,a).

Summing the $p_j(t_i)$ in eqn (5.1) over j=1,...,a gives

$$\Sigma_j p_j(t_i) = G_1(t_i)$$

where

$$G_j(t_i) = \int_0^{t_i} g_j(y)dy$$

where $G_j(t_i)$ is simply the cumulative density function (*cdf*) corresponding to the gamma *pdf* $g_j(y)$. $G_1(t_i)$ is the proportion of the surviving population which is in *at least* stage 1 at time t_i . This proportion initially will be less than one (i.e. the remainder being individuals that have not entered stage 1 so that for these $X_0=Y_1 > t_i$) but increases with time until it reaches one when all surviving individuals have entered at least stage 1. Thus there is recruitment of new individuals to the first stage which operates through the distribution of X_0 and which offsets the effect of mortality in determining population size at time t_i . Recruitment in some insect species can continue while some individuals have already completed development but in general recruitment will decline to zero with time due to the decline in natality with age. Thus in general $p_j(t_i)$ in eqn (5.1) does not equal p_{ij} since the p_{ij} necessarily sum, across the a stages, to one. If we divide $p_j(t_i)$ by $G_1(y)$ to give $p^*_j(t_i)$ then this last term gives the probability of being in stage j conditional on being in at least stage 1. Summing the $p^*_j(t_i)$ across the stages now always gives one so that this, purely phenological model, is given by

$$p_{ij} = p^*_j(t_i) = \{G_j(t_i) - G_{j+1}(t_i)\}/G_1(t_i) \qquad (5.2)$$

This modification of Kempton's model is introduced because interest may lie in predicting only the proportion of the population, rather than the absolute number of individuals, in each stage over time. Predicting the average number of individuals in each stage, as seen above, requires estimation of the population size at time t_i via

estimation of initial population size, N_0 , survival, $\omega(t_i)$, and recruitment, $G_1(t_i)$. In fact it may not be possible to estimate population size over time if sampling assumption (b) above does not hold. Also, independently of the n_{ij}, direct observations of mortality rates may have been made and in this case a mortality model can be estimated separately to the model for p_{ij}. Two other models besides model (5.2) which predict the proportion of the population in each stage are discussed below.

We now, in contrast to Kempton's model given by eqn (5.1), model the n_{ij} conditional on N_i , the total number of individuals sampled at time t_i where $N_i = \sum_j n_{ij}$. Given random sampling where N_i is a small fraction of the total population then for each sampling occasion the n_{ij} are multinomially distributed given N_i . In this case no model of survival or initial population size is involved and the assumption (b) about sampling can be relaxed.

Dennis *et al.* (1986) adopted such an approach where the probability p_{ij} was obtained from a probability density function but with a completely different genesis to Kempton's $g_j(y)$. Dennis *et al.* based their model on the model of balsam fir bud phenology developed by Osawa *et al.* (1983). These models belong to a class of models called ordinal regression models in the statistical literature (McCullagh 1980). Ordinal regressions are used to describe data of the type considered here where a number, a, of ordered classes (e.g. insect life stages) are observed to contain a number of individuals for each of a number of samples or cohorts. Also, corresponding to each sample, one or more predictor variables (days or day-degrees in our case) may have been measured. An underlying, unobserved and continuously distributed variable X, with *pdf* $g(x)$, is assumed to be controlling the proportions in each ordinal class via a-1 unknown, ordered cut-point or signpost parameters, α_j, j=1,...,a-1, and parameters of $g(x)$ such as the mean and variance may be functions of the predictor variables. The variable X is often called a *latent* variable. Thus individuals at time t_i have a distribution of X with *pdf* $g(x,t_i)$, where X could be, for example, the unobserved level of a hormone

controlling development. Individuals with a value of X falling below α_1 fall in stage 1, between α_2 and α_3 in stage 2, and so on until those with X above α_{a-1} fall in the final stage. In effect the trajectories over time (in days or day-degrees) of the proportion in each stage are traced out by the changing values of proportions below α_1, between α_2 and α_3, and so on, as the mean of the distribution of X shifts with increasing t while the α_j remained fixed. An example of these trajectories is given in Fig 5.15. Fig 5.15 was derived from the model of Dennis *et al.* (1986) described below, which was fitted here to their published example data set on the phenology of the Western spruce budworm *Choristoneura occidentalis* Freeman. McCullagh (1980) defined the ordinal regression model in terms of the cumulative frequencies at each sample occasion, $m_{ij} = \sum_{h=1}^{j} n_{ih}$, and the *cdf* of X, $G(x)$ so that

$$\begin{aligned} \mathcal{E}(m_{ij}) &= N_i \, \mathcal{P}r(X_i < \alpha_j) \qquad , j=1,\ldots,a\text{-}1 \\ &= N_i \, G(\alpha_j + \beta z_i) \end{aligned} \tag{5.3}$$

where β and z_i are vectors of regression parameters and predictor variables respectively, and the final class is obtained by difference. If $\mu_{ij} = \mathcal{E}(m_{ij})/N_i$ and $\eta_{ij} = \alpha_j + \beta z_i$, then $G^{-1}(\mu)=\eta$ defines the *link function* in generalised linear model terminology (Appendix 1). Commonly used statistical distributions for X and their corresponding link functions are the normal/probit [$G^{-1} = \Phi^{-1}(\mu)$], logistic/logit [$G^{-1} = log(\mu/\{1-\mu\})$] and extreme value/complementary log-log [$G^{-1} = log\{-log(1-\mu)\}$]. Since X is not observed it is not strictly correct to say that X has a normal or logistic etc., distribution since only the link function has been specified in eqn (5.3) via G. The distribution of X, corresponding to the link functions given in the above order, could equally be log-normal, log-logistic or Weibull respectively (i.e. corresponding distributions on a logarithmic scale). Thus the data does not allow discrimination between smooth transformations of the underlying variable using a criterion of goodness of fit, but only between alternative link functions and models for η (i.e the model is unique up to a smooth transformation

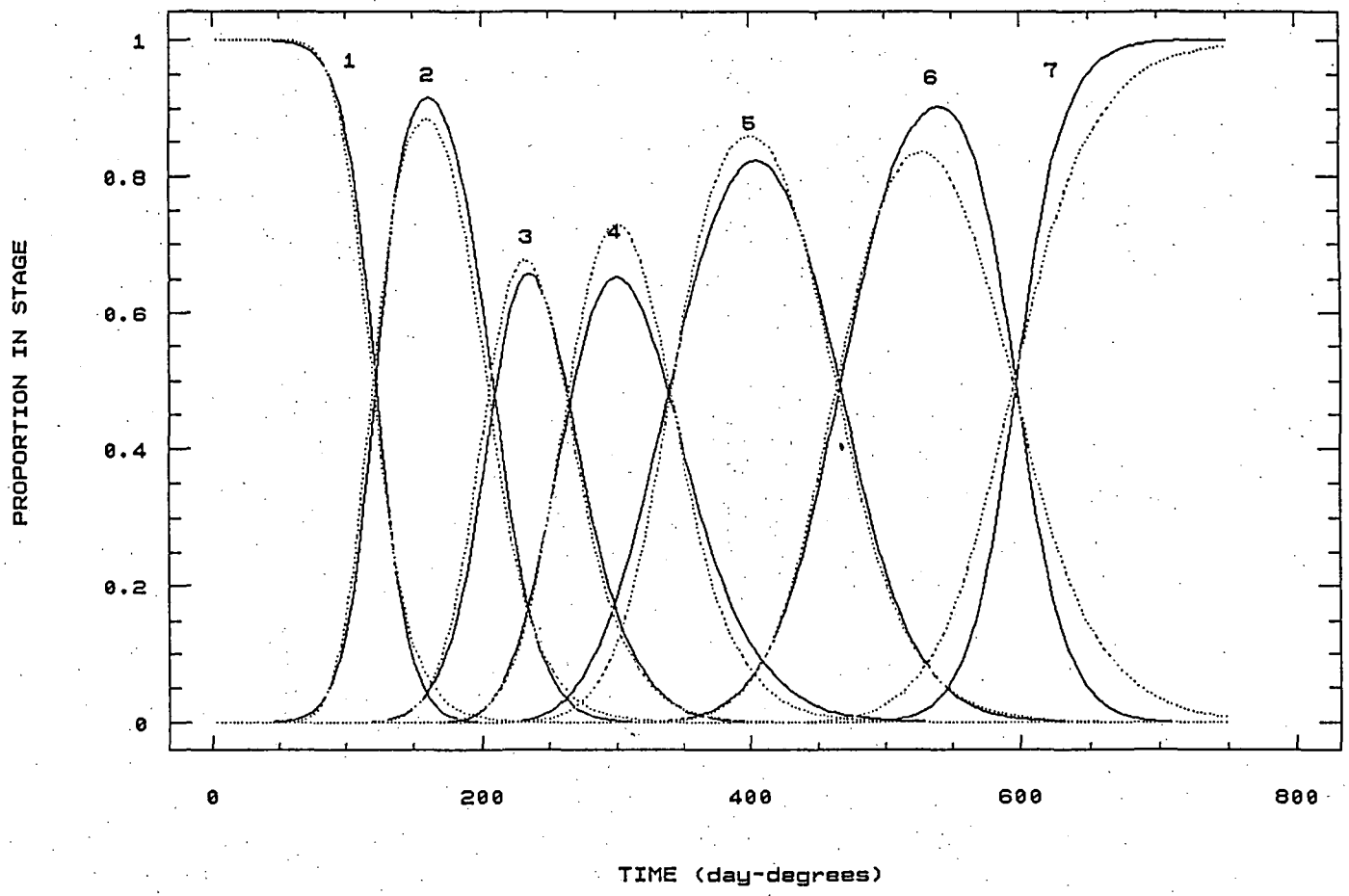

FIG 5.15 Conditional probability _____ and Dennis et al ..... models of spruce budworm phenology

of X). For the following the distribution of X will be referred to keeping in mind the above qualification.

When X belongs to the normal or logistic family of distributions the term in the model $\boldsymbol{\beta} z$, dropping the i^{th} subscript for the moment, specifies the mean of X, μ_x, (given unit variance for X) in terms of the regression equation $\mu_x = -(\beta_0+\beta_1 z_1+\beta_2 z_2+...)$, however, this model is over-parameterised with β_0 and the α_j parameters not uniquely defined so β_0 must be subsumed in one of the α_j, α_1 in GLIM and GENSTAT, to allow the model to be estimated. The constraint $\beta_0 \equiv \alpha_1$ can be achieved by the reparameterisation, $\overset{*}{\alpha}_j$, where $\overset{*}{\alpha}_1 = \alpha_1 = \beta_0$ and later cut-point parameters (i.e. j=2,...,a-1) are given by $\alpha_j = \overset{*}{\alpha}_1+\overset{*}{\alpha}_j$ (for the remainder the α_j will refer to this reparameterisation and the * will be dropped). The variance of X for normal and logistic distributions is necessarily unity in the above parameterisation (5.3) since it is not possible to add an extra unique parameter to specify the variance. In the case of the Weibull (used here as the reference distribution instead of the extreme value distribution because it is more familiar to most researchers) the term $\boldsymbol{\beta} z$ specifies $-ln(b)$ where b is the Weibull scale parameter (Johnson and Kotz 1970) rather than the mean of X and the shape parameter is necessarily a constant which is subsumed in α_1.

Dennis *et al.* (1986) used a different parameterisation of the logistic model, based on the model of Osawa *et al.* (1983) who used the normal *cdf* for $G(x)$. Dennis *et al.* define $G(x)$ as

$$G(x) = 1 / \{1 + exp[-(x - t)/\sqrt{(b^2 t)}]\}$$

so that the mean and variance of the logistic are t and $\pi^2 b^2 t/3$ respectively. This relationship between the mean and variance is retained when x is replaced by the cut-point parameters so that the model of Dennis *et al.* can be re-expressed as

$$\mathcal{E}(m_{ij}) = N_i \, exp(\alpha_j / \sqrt{t_i} + \beta z_i) / \{1 + exp(\alpha_j / \sqrt{t_i} + \beta z_i)\} \quad (5.4)$$

$\beta = -1/b$ and $z_i = \sqrt{t_i}$. The link function, G^{-1}, is therefore logit. The same number of parameters are involved in the ordinal regression model with unit variance, eqn (5.3), as that in eqn (5.4) so that the assumption of unit variance is no more restrictive than a mean of t and variance $\pi^2 b^2 t/3$. The choice of model can be based on the goodness of fit of each model if there is no *a priori* preference for one model over the other.

McCullagh (1980) described the maximum likelihood estimation of the ordinal regression model using the cumulative data, m_{ij} . His method takes into account the dependency between the values of the m_{ij} for a given sample occasion. Alternatively the models (5.3) and (5.4) can be expressed in terms of the expected value of the n_{ij} so that

$$\mathcal{E}(n_{ij}) = N_i \{G(\alpha_j + \beta z_i) - G(\alpha_{j-1} + \beta z_i)\}$$

and maximum likelihood (ML) estimation used, assuming a multinomial likelihood for the independent n_{ij}. This is the method used by Osawa *et al.* (1983) and Dennis *et al.* (1986) to fit their models. Thompson and Baker (1981) show how the above model can be fitted by maximum likelihood as a modified generalised linear model (Appendix 1) using a Poisson distribution for the n_{ij}. Given that the tails of the distribution are completed so that the ML estimates of the n_{ij} sum across j to the total N_i , which is ensured numerically by specifying an arbitrary but large positive (upper tail) and small, possibly negative, (lower tail) value to dummy parameters α_a and α_0 respectively, then the kernel of the Poisson likelihood (Appendix 1) is identical to that of the multinomial (Wedderburn 1974). This method was employed here using GLIM and used to fit eqn (5.4) to the spruce budworm data mentioned above.

A new approach to modelling insect phenology based on conditional probabilities is now described. We start from the same point as the ordinal regression model in that the N_i are considered fixed and the proportion in each stage is modelled

as a function of time. Taking each stage in turn, starting with the first stage, the probability of an individual being in stage j is modelled conditional on being in stage j or later. These conditional probabilities or continuation ratios (Fienberg 1980, contributions to discussion of McCullagh 1980 by Plewis, Fienberg and Pregibon) are modelled as functions of t so that

$$\mathcal{Pr}(\text{in stage } j \text{ at time } t_i \mid \text{in stage } j \text{ or later}) = G(\beta_{0j} + \beta_{1j}\, t_i)$$

where G^{-1} is a link function as described above and β_{0j} and β_{1j}, j=1,...,a-1, are unknown parameters. The expected value of n_{ij} is then given by

$$\begin{aligned} \mathcal{E}(n_{ij}) &= (N_i - \textstyle\sum_{k=1}^{j-1} n_{ik})\, G(\beta_{0j} + \beta_{1j}\, t_i) && , \; j = 2,...,a\text{-}1 \\ &= N_i\, G(\beta_{01} + \beta_{11}\, t_i) && , \; j = 1 \end{aligned} \qquad (5.5)$$

and the unconditional probabilities by p_{ij} where

$$\begin{aligned} p_{ij} &= G(\beta_{01} + \beta_{11}\, t_i) && , \; j = 1 \\ &= (1\text{-}\textstyle\sum_{k=1}^{j-1} p_{ik})\, G(\beta_{0j} + \beta_{1j}\, t_i) && , \; j = 2,...,a\text{-}1 \\ &= (1\text{-}\textstyle\sum_{k=1}^{a-1} p_{ik}) && , \; j = a. \end{aligned} \qquad (5.6)$$

The unconditional probability for the final stage is thus obtained by difference so that no model is required for it. The a-1 models given by eqn (5.5) can be fitted using maximum likelihood assuming binomial n_{ij} conditional on the N_i for the first stage and the $N_i^* = (N_i - \sum_{k=1}^{j-1} n_{ik})$ for the next a-2 stages. These models can be fitted as generalised linear models using GLIM or GENSTAT (Appendix 1). Note that the n_{ij} for which the binomial sample size, N_i^*, is zero must be weighted out of the regression. The estimate of n_{ij} given by $N_i \hat{p}_{ij}$, where the $\hat{p}_{ij}$ are calculated using eqn (5.6) with estimates of the β_{0j} and β_{1j} obtained from the fit of model (5.5), are directly comparable to the estimates obtained from the gamma entry time model, eqn (5.2), and ordinal regression models, eqns (5.3) and (5.4). The deviance (Appendix 1), based on a

multinomial distribution for n_{ij}, can be used to compare the fit of the three classes of model. Fig 5.15 compares the predicted proportion in each stage from model (5.4) to that from (5.6) (with G^{-1}=logit) obtained from the fit to the spruce budworm data.

The conditional probability model involves a-2 ($a \geq 3$) more parameters than the ordinal regression model. An assumption in this last case is that each stage responds equally to a common underlying variable X (i.e. controlled by the link function and β's which are common to each stage) which therefore allows a more parsimonious description of the data than the approach introduced here. A common underlying time scale and link function for each stage is also required in practice for the conditional probability model (i.e. so that the unconditional probabilities can be calculated) and either days or day-degrees must be chosen as the time units here. However, the fact that separate models are applied to each stage (i.e. common link function but separate β's for each stage), on a common time scale, results in the extra parameters required and a more flexible model than that of Dennis *et al.* since different stages can have a different response to the chosen time scale. However, any resultant improvement in fit must be balanced against the lesser degree of parsimony.

5.4.2 Application to immature stages of *P.subgranosus*

The ordinal, eqns (5.3) and (5.4), conditional probability, eqn(5.5), and the gamma entry time, eqn (5.2), models were fitted to *P.subgranosus* frequency data consisting of 191 sample occasions (i.e. number of dissected galleries, Section 3.1.2) at which immature stages were found. Kempton's complete model, eqn (5.1), was not fitted for reasons discussed later. To fit the above models it was found necessary to pool the number of 1st to 4th instar larvae with the number of eggs since the data on these early instars were inadequate in themselves to allow a reasonable model of their phenology to be constructed. When they were considered separately and the conditional model fitted the resulting probability trajectories were barely discernible above zero

when graphed on the same scale as those for eggs, final instar larvae and pupae. This was due to the fact that, as mentioned in Section 5.3, few early instars were found since the peak of their occurrence was missed by the sampling dates. Taking the three 'stages' consisting of (1) pooled egg and 1st to 4th instar larvae (2) final instar larva (3) pupa, a number of ordinal and conditional probability regression models were fitted as well as the gamma entry time model. In the case of the ordinal models combinations of logit or complementary log-log link, constant variance as in eqn (5.3) or mean and variance as in eqn (5.4), and the mean a function of days or DD_{11} were tried. Logit and complementary log-log links and both days and DD_{11} were used for the conditional probability model. Also each of days and DD_{11} were used in the gamma entry time model where in both cases t_0 was not estimated but set to zero since the first ovipositions occurred relatively soon after gallery establishment (Table 5.5). The data involved 573=191x3 frequencies; n_{ij} , i=1,...,191, j=1,2,3. Using the conditional probability approach the complementary log-log link was found to give a better fit than the logit link, however the choice between days and DD_{11} was not as straightforward. The fit of the model to the pooled egg and early instar larvae data suggested the DD_{11} scale was best while that for the final instar larva suggested the day scale was better. One constraint on the conditional probability models is that, as mentioned earlier, a common time scale is required for each stage even though the developmental response for each stage to this scale can vary as quantified by different estimates of β_0 and β_1. The presence of different threshold temperatures for development (Section 7.1) for each stage could be responsible for the difference in response to the DD_{11} scale seen here, however, it was not possible in this study to determine stage-specific thresholds.

The gamma entry time model (5.2) was fitted using a nonlinear optimisation algorithm which maximised the multinomial likelihood (or minimised the deviance). GENSTAT's FITNONLINEAR directive was used (Appendix 2) again employing the

Poisson distribution for n_{ij} given the constraint that the predicted proportions sum across the stages to one. Joint estimation of the gamma scale parameter β, and mean stage duration times x_0, x_1 and x_2 , proved difficult. It was found necessary to alternate between optimising β alone and then the x_j's. Even when this was done it was found using a contour plot of the likelihood surface that the x_0 and x_2 parameters were very highly negatively correlated and for this reason standard errors of these parameters could not be obtained.

To compare the fit of the conditional to ordinal and gamma entry time models, unconditional probabilities, p_{ij}, were calculated as given by eqn (5.6) and a value of the deviance calculated by summing the deviance contribution over the 573 observed and predicted frequency pairs; n_{ij} , $N_i \hat{p}_{ij}$. Table 5.6 gives the goodness of fit and Tables 5.7, 5.8 and 5.9 the parameter estimates for each of the above models. Table 5.8 also gives the deviance calculated using conditional probabilities. Table 5.6 shows that, of the ordinal regression models, the complementary log-log link with $z=DD_{11}$ gives the best fit to the data and is considerably better than the model of Dennis *et al.* (1986). The conditional probability model using complementary log-log link and DD_{11} gave the best fit of all the models requiring one extra parameter for a 4.1 drop in the deviance compared to the best of the ordinal regression models. Fig. 5.16 shows the trajectory and data for the proportion in each of the three stages for each of days and DD_{11} using the complementary log-log link ordinal model and Fig 5.17 compares the complementary log-log link ordinal and conditional probability models. On both the day and DD_{11} scales these two models produce very similar trajectories and as expected they give a similar fit to the data (Table 5.6). Fig 5.18 shows the trajectories for the gamma entry time model. In the case of the day scale (Fig 5.18a) the proportion in the combined egg/early instar stage declines more slowly and the final instar stage has a wider spread in time of occurrence than that seen in Fig 5.17. The gamma entry time model using the DD_{11} is totally inadequate for describing the phenology of

Table 5.6 Goodness of fit of three classes of regression model to *P.subgranosus* phenological data

model	eqn	Link	z	variance[a]	deviance	degrees of freedom[b]	%deviance[c] explained
ordinal	(5.3)	logit	days	constant	343.7	379	76.2
			DD_{11}		278.1	379	80.8
		clog[d]	days		234.5	379	83.8
		clog	DD_{11}		222.7	379	84.6
ordinal[e]	(5.4)	logit	$\sqrt{}$days	π^2b^2days/3	333.6	379	77.0
			$\sqrt{DD_{11}}$	$\pi^2b^2DD_{11}/3$	373.3	379	74.2
condit-ional	(5.5)	logit	days	-	325.7	378	77.5
		logit	DD_{11}	-	261.6	378	81.9
	(5.5)	clog	days	-	233.6	378	83.9
		clog	DD_{11}	-	218.6	378	84.9
gamma entry time	(5.2)	-	days	-	283.3	378	80.4
		-	DD_{11}	-	443.0	378	69.4

a. Scale parameter of the type 1 extreme value distribution and shape parameter of the Weibull distribution (Johnson and Kotz 1970) for the complementary log-log link, not applicable to the conditional probability model
b. Sample size (573) - no. regression parameters - no. constraints (191)
c. 100{(null deviance - deviance)/null deviance} where 'null deviance' is the deviance for the model consisting of common, across sample occasions, proportion in each stage estimated from stage totals as 0.807, 0.151 and 0.042 for the combined egg and early instar, final instar and pupa stages respectively.
d. Complementary log-log
e. Model of Dennis *et al.* (1986)

Table 5.7 Parameter[a] estimates for ordinal regression models of *P.subgranosus* phenology

model	link	z	α_1	α_2[b]	β
ordinal					
	logit	days	7.312 (0.223)	4.038 (0.194)	-0.0172 (0.0006)
		DD_{11}	6.090 (0.182)	3.251 (0.124)	-0.0025 (0.0001)
	clog[c]	days	3.744 (0.105)	2.409 (0.109)	-0.00986 (0.00031)
		DD_{11}	2.963 (0.085)	2.035 (0.070)	-0.00145 (0.00004)
Ordinal[d]	logit	$\sqrt{}$days	12.380 (0.420)	7.998 (0.368)	-0.300 (0.011)
	logit	$\sqrt{DD_{11}}$	6.199 (0.260)	4.859 (0.212)	-0.086 (0.004)

a. Standard errors given in brackets
b. Parameterisation which gives the cut-point between final instar and pupa stage as $(\alpha_1+\alpha_2)$
c. Complementary log-log
d. Model of Dennis *et al.* (1986)

Table 5.8 Parameter[a] estimates for conditional probability models of *P.subgranosus* phenology

stage[b]	link	t	β_0	β_1	deviance[c]
egg, instars 1-4	logit	days	6.817 (0.303)	-0.01571 (0.00082)	293.5 (189)
		DD_{11}	5.836 (0.260)	-0.00238 (0.00011)	203.1 (189)
final instar		days	12.09 (1.93)	-0.01851 (0.00304)	32.2 (27)
		DD_{11}	11.18 (1.46)	-0.00314 (0.00043)	58.6 (27)
egg, instars 1-4	clog[d]	days	3.779 (0.174)	-0.00997 (0.00051)	208.8 (189)
		DD_{11}	2.810 (0.135)	-0.00136 (0.00007)	170.6 (189)
final instar		days	5.443 (0.747)	-0.00887 (0.00121)	24.8 (27)
		DD_{11}	5.922 (0.682)	-0.00177 (0.00021)	48.0 (27)

a. Standard errors given in brackets
b. Proportion in pupa stage obtained by difference
c. Deviance based on conditional probabilities. Degrees of freedom given in brackets.
d. Complementary log-log

Table 5.9 Parameter[a] estimates for gamma entry time model of *P.subgranosus* phenology

t	β	x_0	x_1	x_2
days	23.5 (0.2)	134.8 -	299.3 (2.1)	217.6 -
DD_{11}	413.1 (4.5)	930.0 -	1871.6 -	750.0 -

a. Standard errors given in brackets. Some standard errors could not be estimated due to near singularity of the Hessian (Appendix 1).

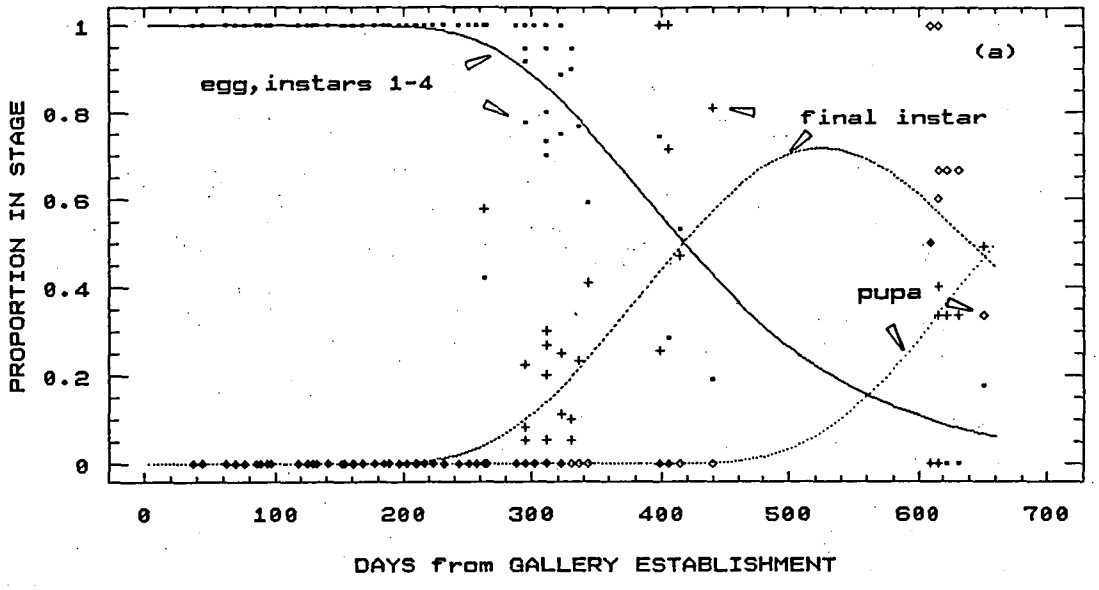

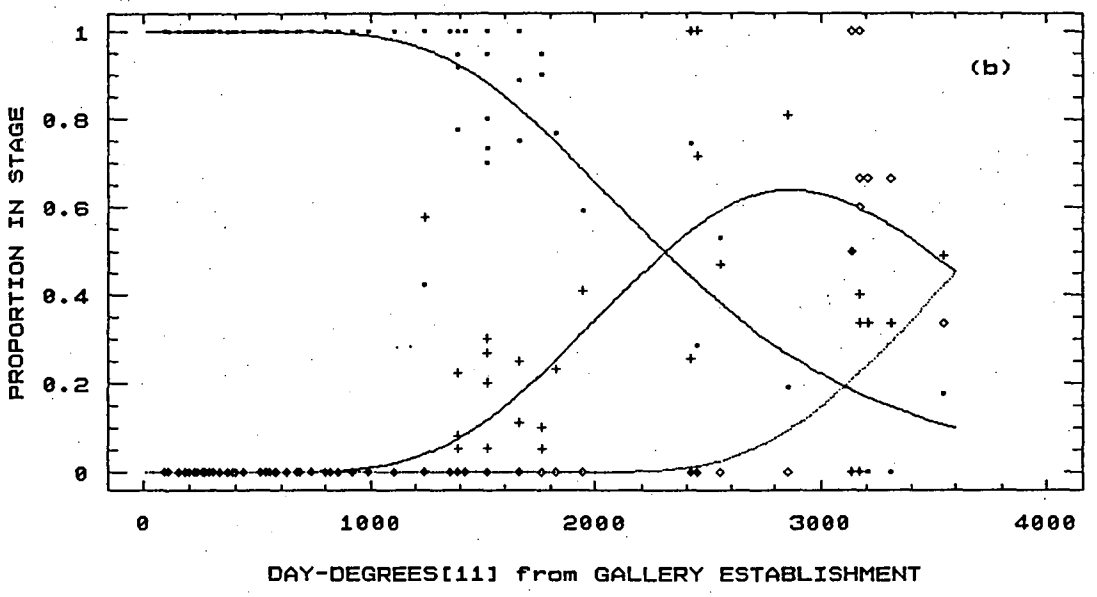

FIG 5.16 Observed and predicted proportions in each stage with predictions from the ordinal/complementary log-log model and time units of (a) days (b) day-degrees[11]

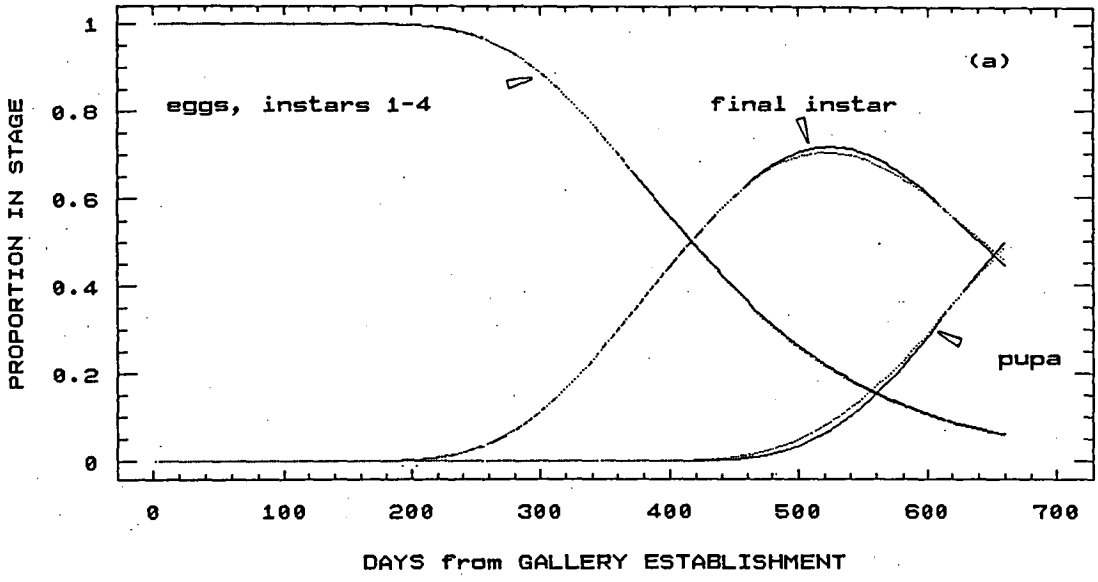

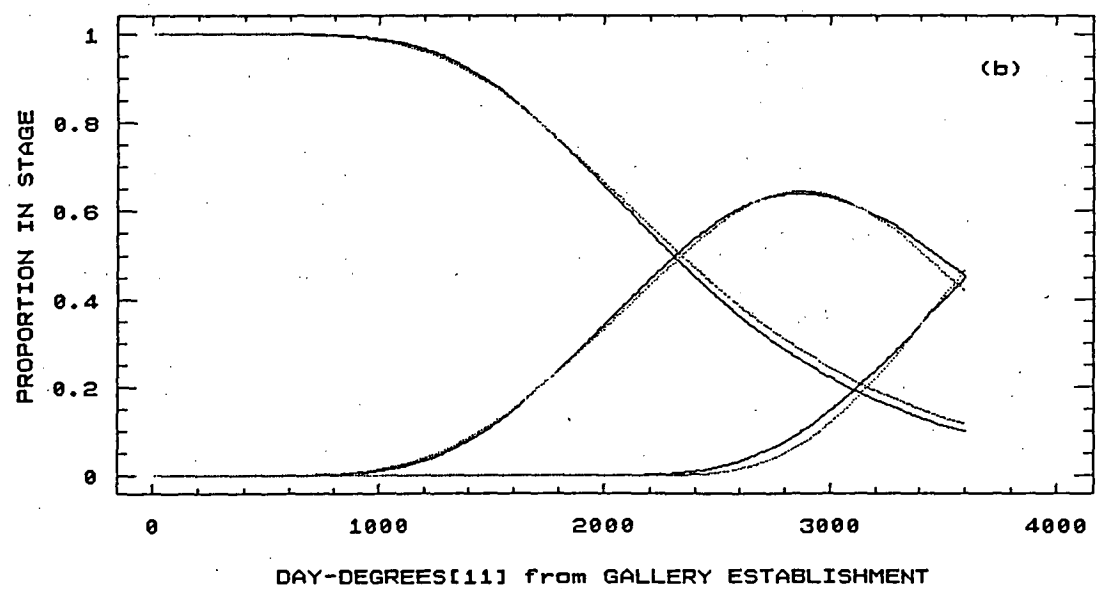

FIG 5.17 Proportion in each stage predicted from ordinal _____, and conditional probability ..... models with complementary log-log link and time units of (a) days (b) day-degrees[11]

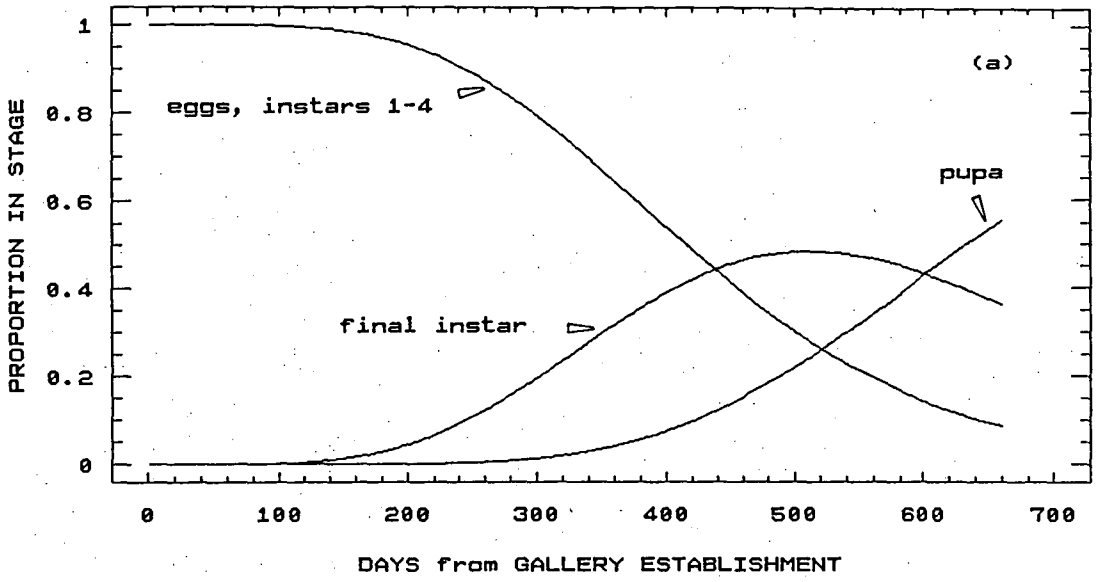

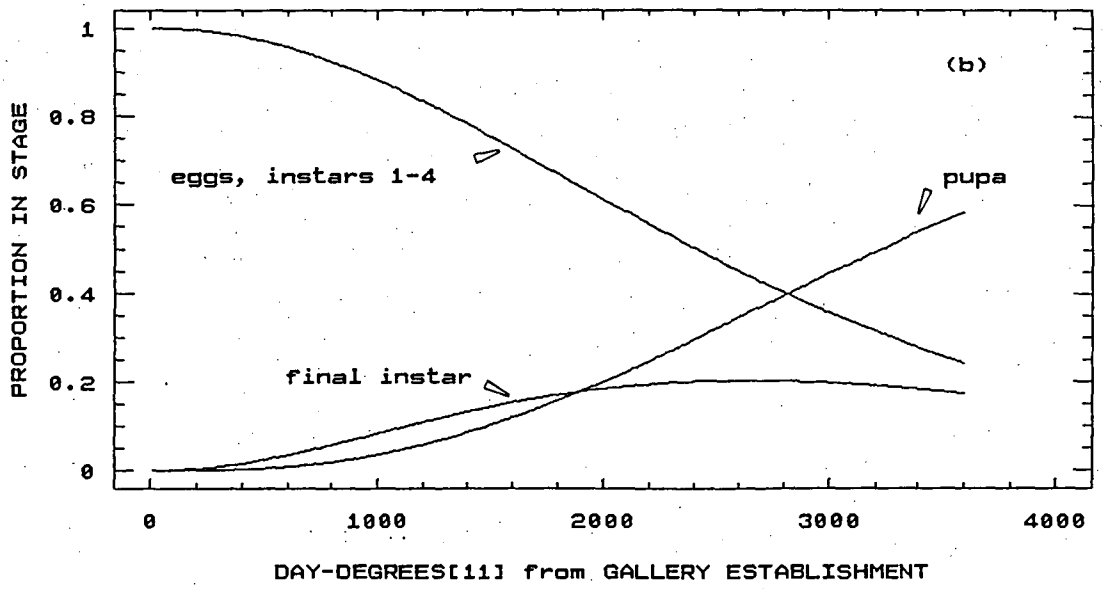

FIG 5.18 Proportion in stage predicted from the gamma entry time model in time units of (a) days (b) day-degrees[11]

P.subgranosus as indicated by its poor fit to the data and the unrealistic trajectories seen in Fig 5.18(b).

For comparison the model of Dennis *et al.* (1986) was fitted to their example data set on spruce budworm phenology and compared to the fit of the logit/constant variance/day-degree ordinal regression and logit/day-degree conditional probability models. The transcript of the GLIM session in which the model of Dennis *et al.* was fitted is given in Appendix 3. This model gave a better fit (deviance of 34.8 with 65 degrees of freedom) than the constant-variance ordinal model (deviance of 58.0) but a worse fit than the conditional probability model (deviance 25.9 with 60 degrees of freedom) using unconditional probabilities in this last case as was done above. These deviances cannot be compared in a formal test since the models are not nested (Appendix 1) so a judgment on which is the best model must rely on other factors such as built-up experience with each model, bias and precision of predictions and theoretical grounds such as a justification for an underlying variable X.

5.5 Brood size, mortality and gallery failure rate

As described in Section 2.3.3, after an initial oviposition at which a mean of roughly 8 eggs are laid the female continues to oviposit throughout the gallery. So countering any age- or stage-specific mortality is the continual recruitment of new individuals. Negligible mortality was observed in all immature stages with predation and parasitism very rare (Section 2.3.7). The only mortality observed in gallery dissections was for early instar larvae where three 1st, and one 2nd instar larvae were dead out of a total of 47 and 36 respectively. The cause of this mortality is uncertain. Although direct observations of mortality can be difficult, for example in the case of predation, it was felt that the very small amount of mortality observed was a genuine reflection of low mortality in the population.

Fig 5.19 shows a scatterplot of the total number of individuals in all stages (i.e.

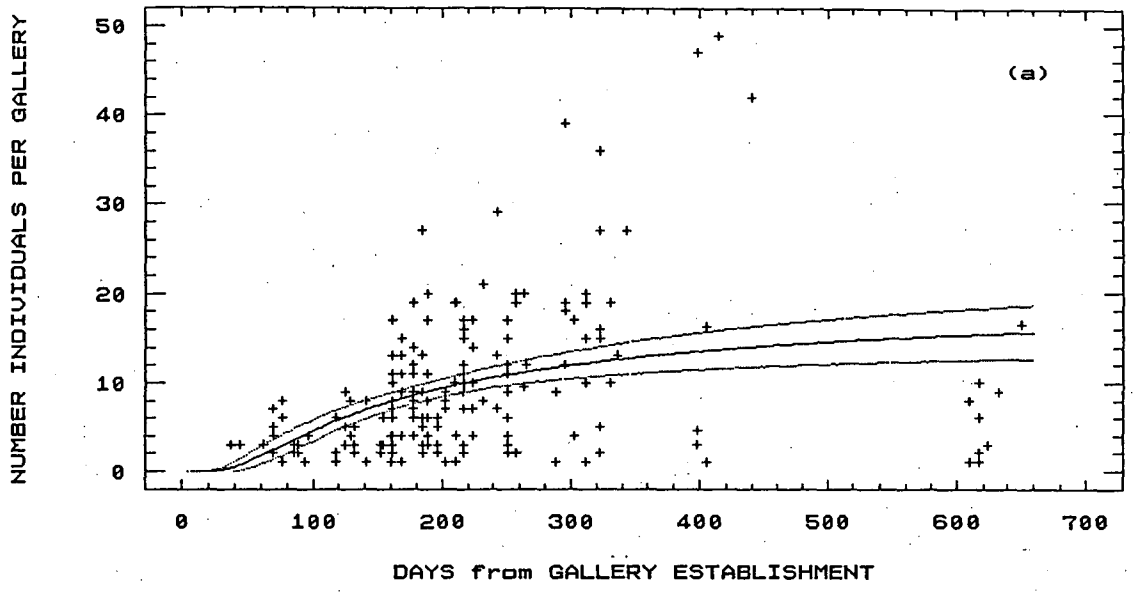

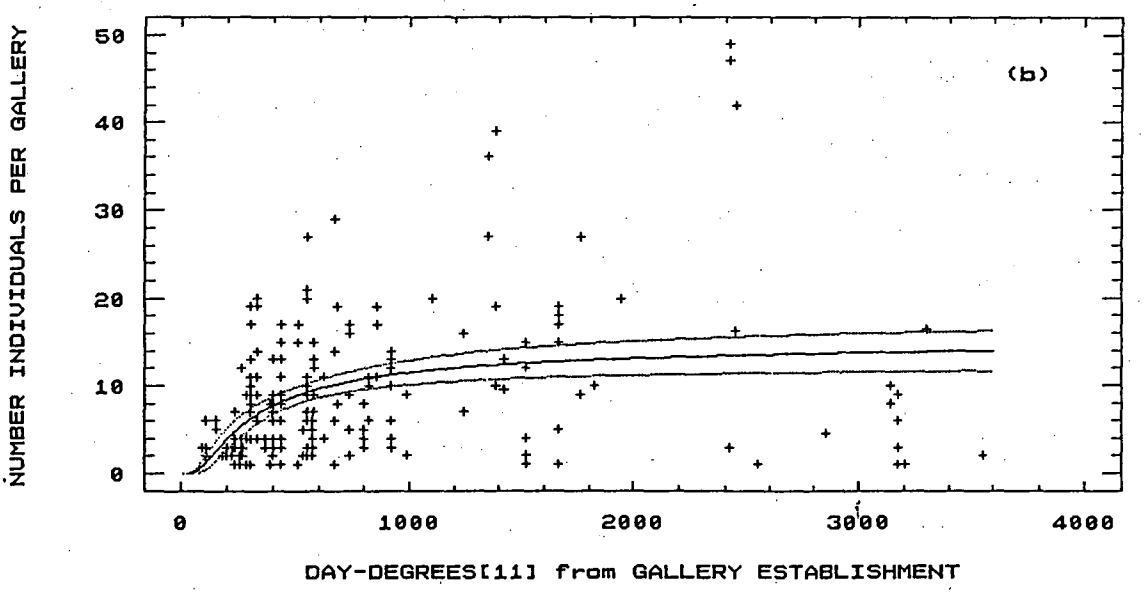

FIG 5.19 Total number of individuals per gallery and asymptotic regressions versus (a) days (b) day-degrees[11] from gallery establishment with ....., approximate 95% confidence region on predictions

brood size) for each of the above 191 sampled galleries against each of days and DD_{11}. The scatter in Fig 5.19 is very wide demonstrating the large between-gallery variance in brood size. Given zero or negligble mortality and a steadily declining recruitment the total brood size will, with time, approach from below an asymptotic value which should roughly equal the observed mean emergence rate (number per gallery). Asymptotic regressions were fitted to the scatterplot data shown in Fig 5.19. The best form of the model was found to be

$$N_i = \quad exp(\beta_0 + \beta_1 / t_i) \qquad (5.7)$$

where

N_i is total brood size, β_0 and β_1 are unknown regression parameters and t_i is either days or DD_{11}. Model (5.7) was fitted as a generalised linear model with Poisson error for N_i and logarithmic link function (Appendix 1). The parameter estimates and their standard errors are given in Table 5.10. The asymptote is given by $exp(\beta_0)$ which was estimated as 18.9 with approximate 95% confidence interval (including adjustment for over-dispersion, Appendix 1) of 15.2 to 23.6 using t=days. Corresponding estimates for $t=DD_{11}$ were 15.0 and 12.7 to 17.8. The trajectory of predicted mean brood size over time and the 95% confidence interval for predictions, based on the above regressions, are also shown in Fig 5.19.

Of the total of 381 galleries destructively sampled (Section 3.1.2) approximately 8% failed to produce any brood. Observed failure was due to either an unmated male (4%), which in some cases had extended the gallery to a length of 8 cm, or death of either parent (2%). A further 2% of galleries appeared to have been abandoned with the length of the tunnel at around 4 to 8 cm. This was probably due again to the male being unmated and then abandoning the gallery.

5.6 Discussion

Numerical classification using head capsule width is a standard technique for classifying larval instars when there are no instar-specific morphological features

Table 5.10 Parameter estimates[a] and fit of regression models[b] of brood size

regressor	β_0	β_1	deviance[c]	ϕ [d]	%deviance[e]
1/days	2.940 (0.110)	-141.14 (21.96)	974.9	5.158	22.1
$1/DD_{11}$	2.711 (0.083)	-268.10 (43.51)	1002.0	5.300	20.0

a. Standard errors adjusted for over-dispersion (Appendix 1) given in brackets
b. Poisson error, logarithmic link (Appendix 1)
c. Residual deviance, measure of goodness of fit (Appendix 1)
d. Dispersion parameter (Appendix 1)
e. Percentage of deviance for model consisting of $exp(\beta_0)$ only where $exp(\beta_0)$ gives average brood size over time.

which are easily observed (Imms 1964). An easily seen morphological feature specific to the final instar of *P.subgranosus* allowed this instar to be quickly and accurately identified. Visual inspection of frequencies of head capsule widths such as those displayed in Fig 5.1 is often sufficient to decide on the boundary values to be used to allocate individuals to an instar. The use of a non-hierarchical classification procedure to determine the boundary values allows objectivity and optimality in classification. Objectivity, in that the same criterion is used for any set of head capsule widths and optimality, in that the classification procedure optimises the above criterion where the optimum here was a minimum within-class (i.e. instar) sum of squares. The classification procedure used here generalises to a number of simultaneously measured and continuously varying morphological features. For example, larval body length was used here in addition to head capsule width to classify larvae. It is not possible to determine the extra discriminatory power of body length to that of head capsule width since instar number is not known *a priori*. It is therefore difficult to say how useful the addition of body length was in the classification but it is felt that it resulted in only a marginal improvement.

A problem with classification here was the fact that measurement error was a considerable percentage of head capsule width; for example around 10% for the early instars. Given this degree of measurement error the values of head capsule width between the peaks could be due largely to this error rather than real population variation. Even so there is little variation in head capsule width at the scale of measurement used here so that classification by visual inspection could, in practice, have been used without much difficulty (i.e. it is fairly easy to decide on class boundaries from Fig 5.1). However, the non-hierarchical classification technique used here would be more useful for a species for which there is more population variation than that seen here.

The observed relationship between number of eggs laid at initial oviposition and gallery length is fairly easily explained. The length of gallery determines the surface area of gallery wall on which ambrosia fungii can grow which thus determines the limit on food resources available to the larvae hatching from the initial batch of eggs. The number of eggs laid appears to be under the control of a physiological mechanism which is dependent on some way of determining the length of gallery excavated up to initial oviposition. The final instar larvae extend the gallery and it can be assumed that the length of these extensions is also related to the food requirements for growth and pupation.

The trend of delayed initial oviposition and corresponding slower gallery development rate for galleries established early in the late/summer autumn period cannot be fully explained at this time. The time from gallery establishment to initial oviposition is not known so time to disc sampling has been used to approximate this unobserved time. So in effect, the observed times are left-censored because initial oviposition could have occurred any time from soon after gallery establishment up until the sampling date. This means that time to initial oviposition and resultant gallery development rates have been over- and under-estimated respectively. However, the trends seen in Figs 5.4, 5.9 and 5.10 should be unaffected because the above bias should apply equally to all establishment dates. Also the fact that a corresponding trend in timing of first brood emergence was observed (Section 7.8) gives support to the above trend in timing of initial oviposition. Timing of initial oviposition does not depend on gallery length, allowing for the observation that at least 4 cm of gallery is required before oviposition can occur, since oviposition was observed to occur for a range of lengths between roughly 5 and 25 cm. One possible explanation for the delay in initial oviposition until winter is that summer oviposition could result in higher egg and early instar mortality due to desiccation. A trend of timing of initial oviposition to occur later for galleries in small diameter logs which are more susceptible to drying out

was not observed here. However, if under genetic control, timing of initial oviposition was preset to winter then selection for winter oviposition due to the resultant higher survival rate for eggs and early instar larvae might operate. Spring/early summer gallery establishment does occur and for this to result in emergence after as little as 10 months, as has been observed (Section 7.3), then initial oviposition in summer must presumably occur (Fig 2.9). However, spring/early summer emergence and gallery establishment is much less common than that in late summer/autumn which would suggest that there is selection for late summer/autumn emergence. Francke-Grossmann (1967) describes moisture content of the host plant as, in general, one of the most important factors for successful establishment and breeding of ambrosia beetles.

The mean number of eggs at initial oviposition of 8.4 is less than half the mean brood size and emergence rate (Section 6.1), both estimated at around 19, which indicates that subsequent oviposition is important in determining final brood size. The length of gallery excavations by final instar larvae probably determines the number of eggs from these later ovipositions.

The fact that the peak of occurrence of early instar larvae was missed by the sampling, having occurred early in the summer after gallery establishment, and that few early instars were found suggests that these stages are passed relatively quickly. Apart from the egg stage, the final instar larva is the predominant stage in terms of length of stage. This is understandable given that the final instar is responsible for the bulk of gallery excavations. Also time is required for feeding to allow this instar to build up fat reserves for pupation and, possibly, for emergence and flight of the brood adult although it is not known if brood adults feed before emerging.

Judging from Figs 5.12 to 5.14, 5.16 and 5.17 the ordinal and conditional probability models have been very useful in smoothing the highly variable phenological data obtained here. Both the ordinal and conditional probability models give a similar

fit to the data here and to the spruce budworm data. The complementary log-log link was superior, in terms of goodness of fit, to the logit link and thus presumably to the probit link since these last two links produce very similar predictions. One advantage of the conditional probability model is that the response of each stage to the time scale is quantified separately which can be more revealing than a common across-stage response. For example it was found that the DD_{11} scale gave a much poorer fit than the day scale for the final instar larva and *vice versa* for the combined egg and early instar class which suggests that the estimated 11°C development threshold (Section 7.3) might be too high for the final instar larva. The choice between ordinal and conditional probability models is not clear-cut. If the latent variable X exists and operates as described by the ordinal models then these models should be used but in the case of discrete stages, as is the case here, McCullagh (discussion to McCullagh 1980) suggests that the conditional probability (i.e. continuation ratio) model is more relevant. McCullagh suggests that the ordinal regression model is more suited to the case where the ordinal classes are the result of a coarse grouping of some finer scale. Also, it may be difficult to suggest a continuous variable which could result in the discrete processes of hatching and ecdysis. Even so, it is difficult to choose between the ordinal and conditional probability models other than on empirical grounds. An important practical advantage of the conditional model (5.5) is that initial parameter estimates are not required for GLIM's maximum likelihood estimation algorithm whereas good initial estimates are required for the ordinal regression models (5.3) and (5.4) to give the estimation algorithm a reasonable chance of success. Such good initial estimates are often difficult to obtain due to the unobserved nature of X.

The complete model of Kempton (1979) involving estimation of initial population size, mortality and stage durations was not used here because mortality of immature stages was virtually non-existent and the estimation of population size at time t was approached by using the asymptotic model of brood size given by eqn (5.7).

The reduced version of Kempton's model, called here the gamma entry time model, was used to predict the number in each stage conditional on sample size at time t which meant that it could be directly compared to the ordinal and conditional probability models in terms of fit to the data. The gamma entry time model gave a better fit to the *P.subgranosus* data than the logit ordinal and conditional probability models on the day time scale but a worse fit than the complementary log-log link versions of these models. A problem with gamma entry time model is the early appearance of final instar and pupa stages at about 100 and 300 days respectively (Fig 5.18a) whereas the ordinal and conditional probability models are much more in keeping with the data (Table 5.5, Fig 5.13) with the corresponding figures being 200 and 440 days respectively (Figs 5.16a and 5.17a). The gamma entry time model was totally inadequate using the DD_{11} time scale (Fig 5.18b). Stedinger *et al.* (1985) extended the ordinal regression model of Osawa *et al.* (1983) to allow for extra variation in the multinomial proportions, p_{ij} , due to spatial variation in insect development rates by using a Dirichlet-multinomial distribution. However, the variation in these proportions appears from the deviances in Table 5.6 to be adequately described by a multinomial.

The asymptotic regression model of brood size using the day time scale gave an estimate of total brood size per gallery of 18.9 which is not significantly different (P>0.1) from the estimate of mean number of emergents per gallery of 19.7 based on an independent data set (Section 6.1). A smaller estimate of total brood size of 15.0 was obtained using DD_{11}. This appears from Fig 5.19(b) to be due to a greater concentration of galleries at the lower end of the time scale than in Fig 5.19(a). Given the possibility of the threshold temperature of 11°C being too high for final instar larvae and the close correspondence of the asymptote obtained from the day time scale with the mean emergence rate, then the model based on the day time scale is considered to be the more reliable model of mean brood size over time and therefore recruitment.

6. EMERGENCE

6.1 Number of emergents per gallery

Estimating the total number of emergents per gallery is important in establishing the fecundity and reproductive potential for *P.subgranosus*. Data on total emergence for individual galleries were available from cages placed over the gallery entry holes. Two sets of cages were used; those established by the author (SGC) with emergence occurring in the 85/86 summer (Section 3.1.3) and those established by Elliott and Bashford (SILV) with emergence occurring between 1981 and 1985 (Section 3.2). Table 6.1 gives statistics on the number of emergents for each set of cages. Only cages for which emergence was greater than zero have been incorporated in Table 6.1. The number of unsuccessful galleries is estimated in Section 5.5 using data from destructive sampling of galleries (Section 3.1.2). The flooding of galleries in some cases, due to cages trapping rainwater, does not allow reliable estimation of the number of unsuccessful galleries from the cage data. The mean and median number of emergents is less for the author's cages since only a single year of emergence occurred (summer 1985/86). Desiccation of the logs resulted in no further emergence in the 1986/87 summer (Section 3.1.3). For this reason the SILV cage data gives a better estimate of total emergence because the logs were kept at the study site and individual galleries produced emergence up to the third summer after emergence began (i.e. first summer of emergence) . When emergence for only the first summer of emergence for these cages was used the results, with mean, standard error of the mean and median number of emergents 14.0, 2.0 and 9.0 respectively, were very similar to the corresponding figures, given in Table 6.1, for the author's cages. Fig 6.1 shows the distribution of number of emergents per gallery for the SILV cages. The mean number of emergents per gallery using the SILV data, was 19.7 with a median of 14.5 and ranged from 1 to 92.

Table 6.1 Statistics on emergence per gallery

Statistic	author's cages 1985/86	SILV cages 1981-85
sample size	59	58
mean	14.7	19.7
median	11.0	14.5
mode	1	1
standard deviation	14.7	18.7
standard error (of mean)	1.9	2.5
minimum	1	1
maximum	76	92
lower quartile	4	6
upper quartile	20	26

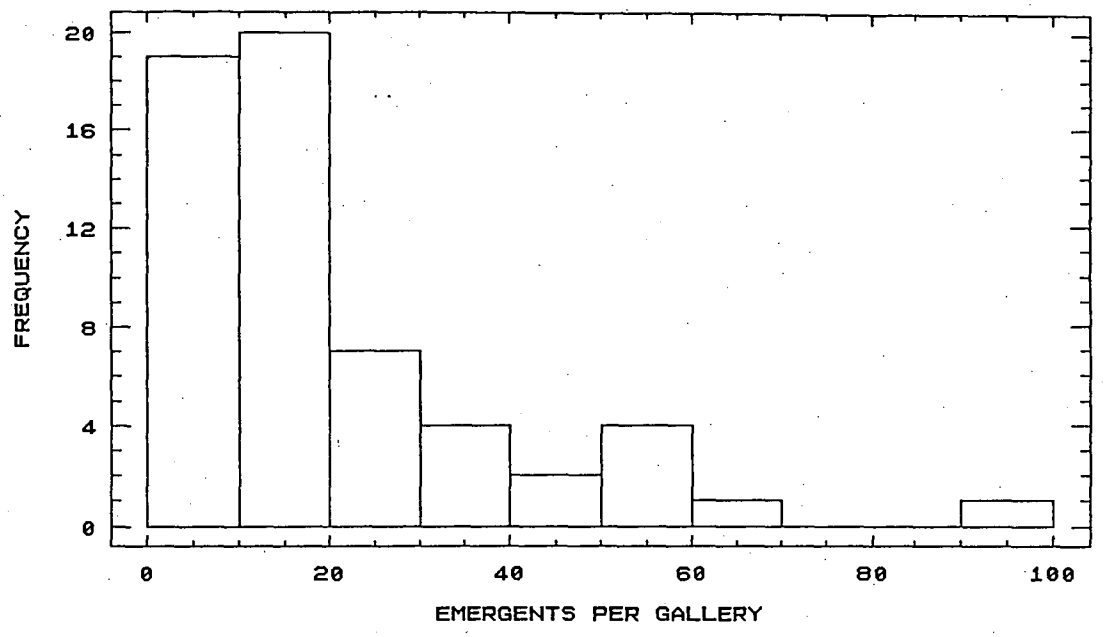

FIG 6.1 Frequency histogram of total emergents per gallery (1981-85)

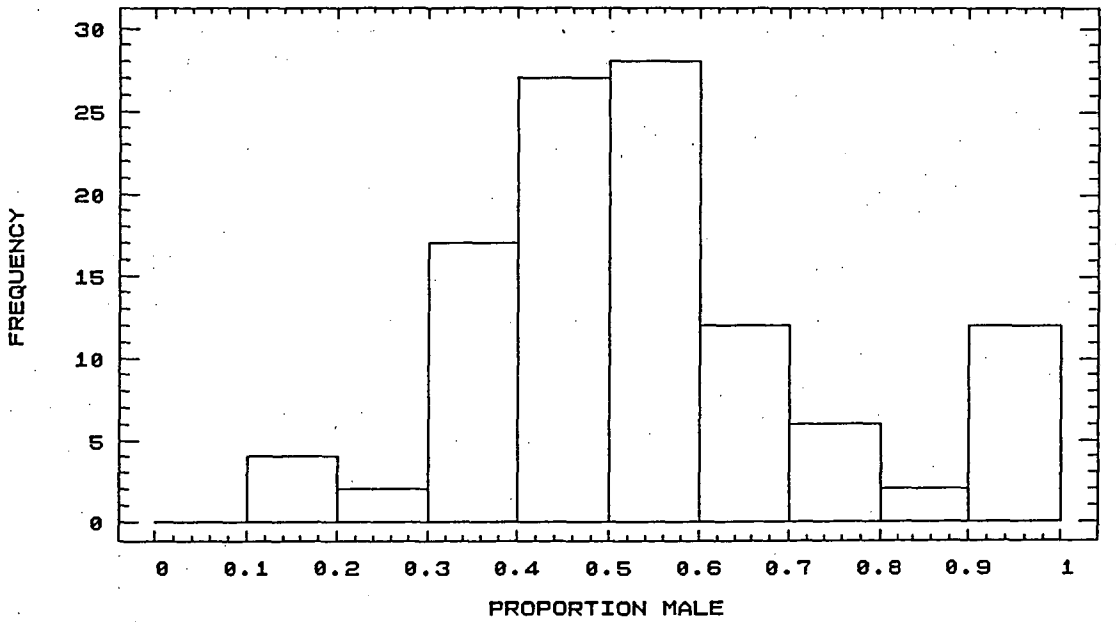

FIG 6.2 Frequency of galleries by proportion of males (81-85,85/86)

6.2 Sex ratio

A total of 2011 emergents were collected from the 117 cages (SGC 59, SILV 58) which had at least one emergent. Of this total 1042 were males. Fig 6.2 shows the frequency of galleries with a given proportion of total emergents that were male. The hypothesis of a sex ratio, which is defined here as the number of males divided by the number of females and is specified by the parameter Ψ, equal to one (H_0) is accepted at the 10% significance level (i.e. the probability of a random value from the χ^2_1 distribution being greater than the calculated statistic is at least 0.1) with $\hat{\Psi} = 1.0753$ and a single degree of freedom chi-square statistic (χ^2_1) of 2.65 ($P>0.1$). The figures for the two sets of cages separately were males (SGC 440; SILV 602), females (SGC 428; SILV 541) sex ratio (SGC 1.028 ; SILV 1.113) and chi-square (SGC 0.17 ; SILV 3.26). For each set of cages considered separately, H_0 is accepted at the 5% level but is rejected for the SILV traps at the 10% level. At the individual cage level, χ^2_1 values were calculated for each of the 70 cages (SGC 31; SILV 39) for which the number of emergents was 10 or more (i.e. giving an expected number of males under H_0 of at least 5). The remaining 47 cages were aggregated to give 97 males to 86 females with χ^2_1 of 0.66 ($P>0.1$). Of these 47 cages 12 had no females while 7 had no males. In the case of no males, there was in all cases only a single female while for the case of no females there were 8 cages with a single, 3 cages with 2 and one cage with 5 males. Of the 70 cages for which individual χ^2_1 values were calculated, 9 (12.9%) (SGC 4; SILV 5) had a χ^2_1 value greater than the nominal value at the 10% level (i.e. 2.706). The heterogeneity chi-square for these 70 cages with 69 degrees of freedom was calculated as 99.0 which indicates significant ($P<0.01$) between-gallery heterogeneity in sex ratio.

Although the chi-square statistics indicate that a sex ratio of unity cannot be rejected using this data it appears that there is a slight preponderance of males since 37 of the 70 cages mentioned above had a sex ratio greater than 1, 4 had a ratio of 1 and

the remainder of 29 had a ratio less than 1.

Over the population the sex ratio is very close to unity but there is some heterogeneity in sex ratios between galleries. For the SILV cages, two cages accounted for 64% of the difference between the number of males and females with number of males for the two galleries being 41 and 22 with corresponding number of females of 14 and 10.

When only emergence occurring in the same summer as the first emergence for a cage (i.e. the new emergence season was considered to start on the 1st of November) was considered, the sex ratio for the SILV cages was 1.02 resulting from 363 males compared to 355 females with a χ^2_1 value of 0.089 which is well below the nominal 10% value. The corresponding values for subsequent emergence were 239 males to 186 females with a sex ratio of 1.285 and a χ^2_1 value of 6.61 which is greater than the 1% nominal value.

The sex ratios for the 5 tent traps (Section 3.2) of 1.21, 1.59, 1.68, 1.26 and 1.46 with corresponding χ^2_1 values 69.1, 217.6, 185.7, 144.9 and 75.6 and with total number of emergents of 7340, 4148, 2893, 10697 and 2149 respectively, clearly demonstrates that males are caught more readily than females in the collecting container. The sex ratios for the individual cages, where there is no possibility for bias to enter the collection procedure, indicate that the sex ratios observed in the tent trap data do not reflect the population sex ratio which is very close to unity.

Investigation of the variation in sex ratio over the emergence period using the cage data indicated a slight trend for more males to emerge in the first few weeks after emergence begins for a gallery. The cumulative number of females after this period then, with some minor variations, gradually approaches that of the males involving an approach to 1 of the sex ratio. For the SILV data only emergence occurring in the same summer as first emergence for the gallery was considered. Various groupings of emergence within periods after first emergence were tried. Table 6.2 shows the number

Table 6.2 Sex ratio of emergents and its relationship to days from first emergence for cage

Days from 1st emergence	author's cages					SILV cages				
	♂♂	♀♀	Ψ	(Ψ[a])	χ^2_1	♂♂	♀♀	Ψ	(Ψ[a])	χ^2_1
0[b]-5	124	90	1.38	(1.38)	5.4[d]	83	78	1.06	(1.06)	0.2
5-10	48	56	0.86	(1.18)	0.6	43	36	1.19	(1.11)	0.6
10-15	44	63	0.70	(1.03)	3.4[c]	23	14	1.64	(1.16)	2.2
15-20	17	13	1.31	(1.05)	0.5	11	5	2.20	(1.20)	2.3
20-25	48	53	0.91	(1.02)	0.2	23	28	0.82	(1.14)	0.5
25-30	13	15	0.87	(1.01)	0.1	8	8	1.00	(1.13)	0.0
30-40	35	33	1.06	(1.02)	0.1	30	26	1.15	(1.13)	0.3
40-50	40	51	0.78	(0.99)	1.3	26	29	0.90	(1.10)	0.2
50-60	22	16	1.38	(1.00)	0.9	31	29	1.07	(1.10)	0.1
>60	49	38	1.29	(1.03)	1.4	85	102	0.83	(1.02)	1.5

Table 6.3 Sex ratio of emergents and its relationship to days at 15 degrees (C) from first emergence for cage

Days from 1st emergence	author's cages					SILV cages				
	♂♂	♀♀	Ψ	(Ψ[a])	χ^2_1	♂♂	♀♀	Ψ	(Ψ[a])	χ^2_1
0[b]-5	122	86	1.42	(1.42)	6.2[e]	83	78	1.06	(1.06)	0.2
5-10	49	58	0.84	(1.19)	0.8	13	21	0.62	(0.97)	1.9
10-15	39	56	0.70	(1.05)	3.0[c]	55	29	1.90	(1.18)	8.0[f]
15-20	19	20	0.95	(1.04)	0.0	11	5	2.20	(1.22)	2.3
20-25	35	37	0.95	(1.03)	0.1	25	31	0.81	(1.14)	0.6
25-30	19	20	0.95	(1.02)	0.0	1	4	0.25	(1.12)	1.8
30-40	35	28	1.25	(1.04)	0.8	39	30	1.30	(1.15)	1.2
40-50	17	33	0.52	(0.99)	5.1[e]	22	25	0.88	(1.12)	0.2
50-60	38	44	0.86	(0.98)	0.4	28	31	0.90	(1.09)	0.2
>60	67	46	1.46	(1.03)	3.9[d]	86	101	0.85	(1.02)	1.2

a. cumulative
b. includes 1st emergence for cage
c. significant at 10% level
d. significant at 5% level
e. significant at 2.5% level
f. significant at 1% level

of males and females, sex ratio for the period, sex ratio for cumulative emergence and the χ^2_1 value for each of the SGC and SILV data for 5-day periods to 30 days and then 10-day periods to 60 days and an above 60 days class. Table 6.3 shows the corresponding values grouped by the same classes as days but using units equivalent to days at 15 degrees (i.e. the number of day-degrees above a 0°C threshold divided by 15). The same data used to construct Tables 6.2 and 6.3 were also analysed using a binomial/logistic regression model (Appendix 1). The number of male emergents for a particular gallery and period was considered binomial conditional on the corresponding total number of emergents. The classes shown in Tables 6.2 and 6.3 were each used separately as a categorical factor, DAYS and DAYS15 respectively, as the regressor variable in the analysis along with the factor SOURCE specifying the source of the data, SILV or SGC, and the interaction of these two factors. Thus the number of males (N_m) was considered binomial conditional on the cumulative total emergence (N) and a logistic model in the above factors was used. Thus the logit of N_m [i.e. $log\{N_m/(N - N_m)\}$ is equivalent to $log(\Psi)$ which is sometimes called the log-odds since Ψ is the odds of an emergent being male. The generalized linear model (*glm*) (McCullagh and Nelder, 1983) with binomial error for N_m and logit link was used to fit the above model using *GLIM* so that in the usual *glm* notation $exp(\eta)$ gives the predicted odds or sex ratio where $\eta = log(\Psi)$ (Appendix 1). The *glm* approach differs from the simple chi-square tests given in Tables 6.2 and 6.3 in that a model for Ψ is constructed by progressively adding terms SOURCE, DAYS (or DAYS15) and the interaction SOURCE by DAYS (or DAYS15). Likelihood-ratio tests constructed from the above fits using deviances (Appendix 1) were used to determine the significance of the term added to the model. This approach complements the classic chi-square test in that the null hypothesis is not that $\Psi = 1$ but that Ψ , which may differ from 1, does not differ across classes in the factor added or in the case of the interaction the difference

in $log(\Psi)$ between SILV and SGC does not change across DAY (or DAY15) classes. The data need not have been grouped into classes but the actual days (or days-15) from first emergence observed for the particular gallery and period used as the regressor variable. However, grouping was carried out to smooth the data so that any trends in $log(\Psi)$ with DAY or DAY15 classes might be recognised. Table 6.4 shows the results of the *glm* analyses.

Both the classic chi-square tests of $\Psi = 1$ and the *glm* analyses show that any divergence from a sex ratio of one is minor. The *glm* analysis using DAYS indicated no significant differences in sex ratio between DAYS, SOURCE or their interaction and the minimal adequate model is a simple constant sex ratio which from Table 6.4 is not significantly different from 1. The individual chi-square tests in Table 6.2 have detected a significant departure from $\Psi = 1$ in the case of the author's data for the 0-5 and 10-15 day periods. In Table 6.3 the 40-50 and >60 classes also appear significant along with the 10-15 class for the SILV data. In both tables the trend is for more males emerging earlier with the females making up the difference later in the summer although this timing differs between data source. The *glm* analysis using DAYS15 did detect a highly significant interaction between SOURCE and DAYS15 factors. This was almost entirely due to the reversal of sex ratios for the 10-15 class (see Table 6.3) where in both cases the sex ratio was significantly different from one. Considering the period classes in Table 6.2 and the results for DAYS in Table 6.4, the results indicate no significant trends in, or departure from unity of the sex ratio remembering that of the 20, χ^2_1 values in Table 6.2 only 2 (or 10%) were greater than the nominal 10% significance level which is as expected if $\Psi = 1$. The evidence for departure from unity is stronger using DAYS15 classes where in Table 6.3 there are 5 (or 25%) χ^2_1 values above the nominal 10% level. The significant interaction between SOURCE and DAYS15 shown in Table 6.4 reflects the difference in timing in the recovery of the female emergence as mentioned above.

Table 6.4 Results of likeihood ratio tests for binomial/logistic regression of number of males on DAYS,DAYS15 by SOURCE.

additional model term	deviance (df)	deviance change (df)	$log(\hat{\Psi})$	se$\{log(\hat{\Psi})\}$[a]
constant	910.4 (594)	-	0.02522	0.05022
SOURCE	910.4 (593)	0.0 (1)		
DAYS	900.5 (584)	9.9 (9)		
SOURCE.DAYS	888.7 (575)	11.8 (9)		
replacing terms involving DAYS with DAYS15				
DAYS15	895.8 (584)	14.6 (9)		
SOURCE.DAYS15	872.3 (575)	23.5[b] (9)		

a. standard error
b. significant at 1% level

Table 6.5 Proportion of emergence by month based on data for 1981-86

month	proportion	s.e.(proportion)[a]
January	0.2412	0.1622
February	0.4447	0.1884
March	0.2300	0.1596
April	0.0325	0.0673
May	0.0209	0.0542
June	0.0027	0.0197
July	0.0000	0.0003
August	0.0000	0.0022
September	0.0010	0.0121
October	0.0131	0.0431
November	0.0067	0.0309
December	0.0071	0.0319

a. Multinomial standard errors scaled by multiplying by $\sqrt{\phi} = 64.83$

6.3 Timing of Emergence

Emergence data for both sets of individual cages and for the tent traps were classified according to the month and year in which emergence occurred. For the SILV cages emergence was recorded over the years 1981 to 1985 inclusive, for the author's cages 1985 and 1986 and for the tent traps 1981 to 1984. Fig 6.3 shows the number of male and female emergents by month and source of data. Fig 6.4 shows number of emergents by month and year. The peak of emergence occurs in early summer either in January or February. The peaks for males and females occur in the same month. The distribution of emergence across the months is skewed with relatively little emergence in late spring, early summer (Nov,Dec), a sudden pulse of emergence over January and February and then a gradual decrease until emergence ceases around June. These are general trends and as can be seen in Fig 6.4 variations in timing of emergence will occur from year to year. As discussed in Section 7, the length of time taken to complete development depends on the accumulated day-degrees and the timing of emergence will reflect year to year variation in accumulated day-degrees to a given month.

To test if the differences in the timing of emergence between years were statistically significant the number of emergents in the years by month contingency table was analysed using a log-linear model with Poisson errors and logarithmic link function (McCullagh and Nelder 1983, Appendix 1). After fitting the marginal factors YEARS and MONTHS the residual deviance indicated a significant departure from the no-interaction model. Thus the probability of emerging in a particular month varies significantly from year to year assuming a multinomial distribution of emergents across months. Without knowing the history of galleries (i.e. attack date and subsequent accumulated day-degrees) observing emergence by month can be viewed, across years, as sampling from a mixture of multinomial distributions. Taking the 6 years of data

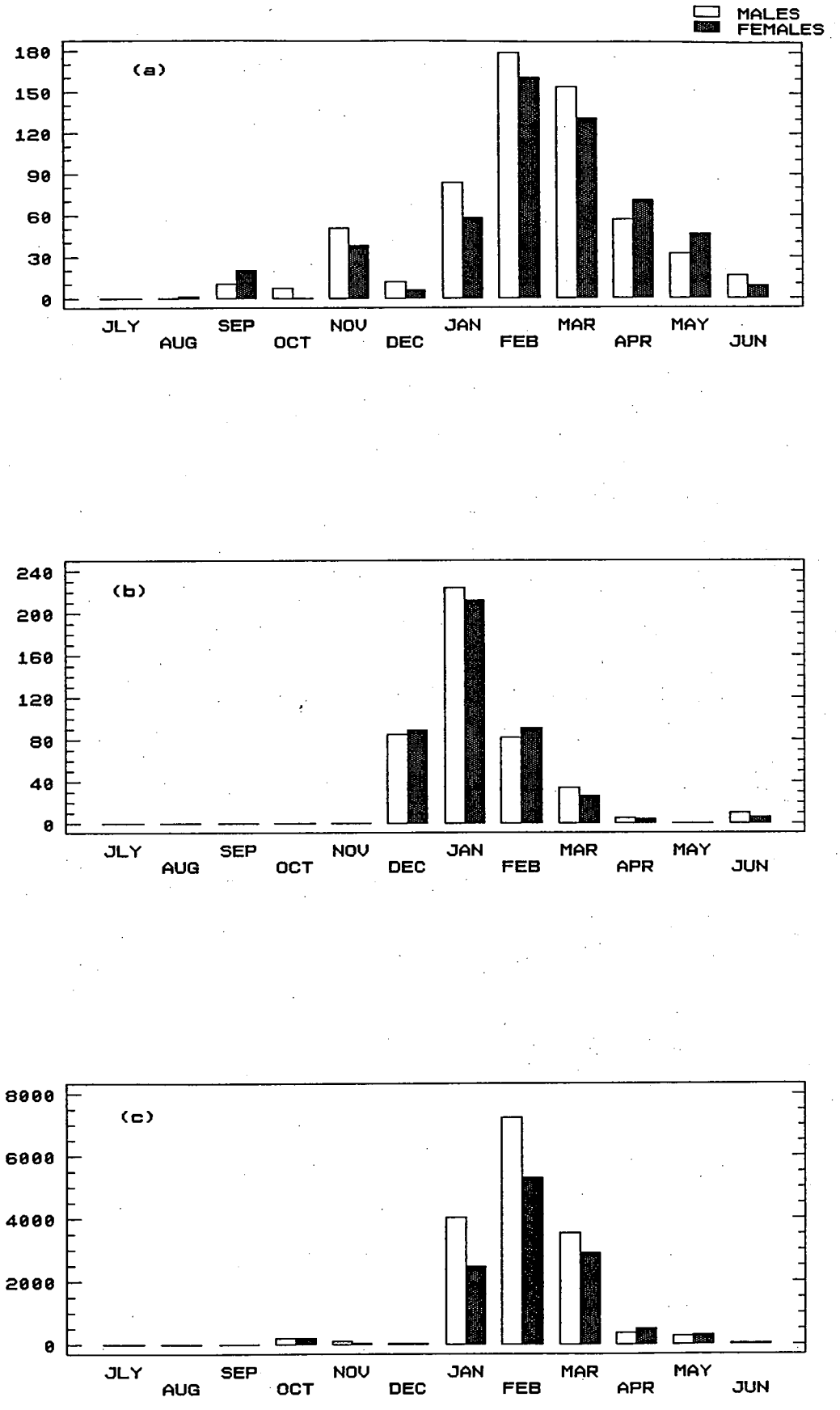

FIG 6.3 Number of emergents by month (a) 81-85 cages (b) 85/86 cages (c) 81-84 mass emergence tents

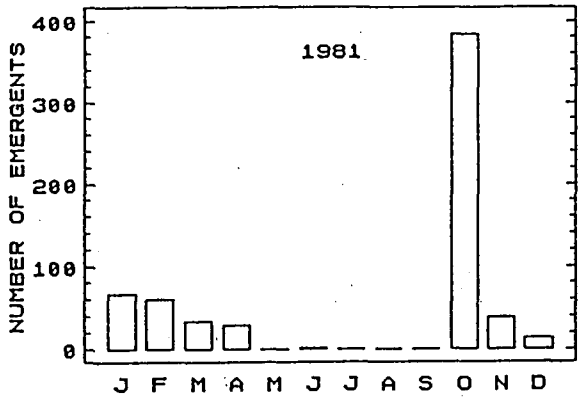

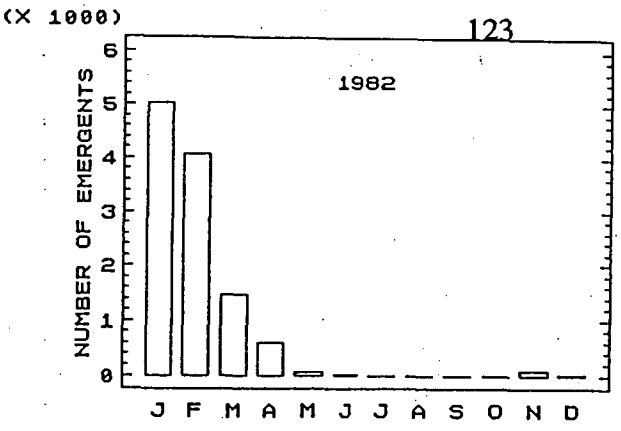

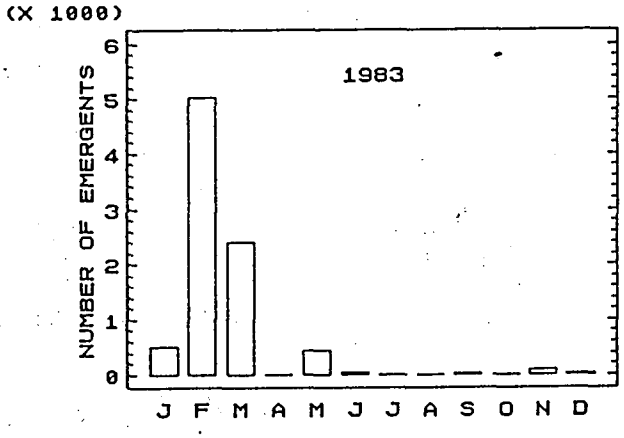

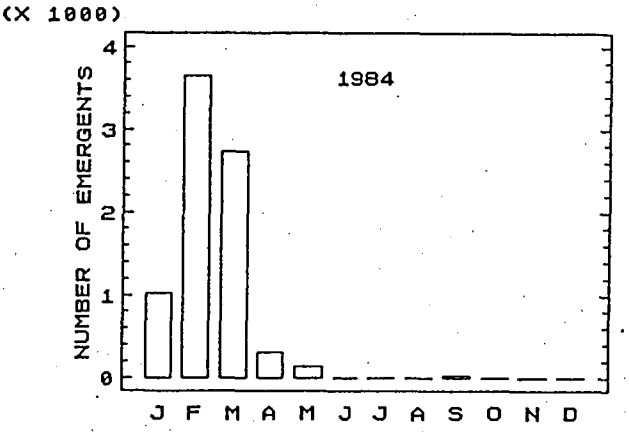

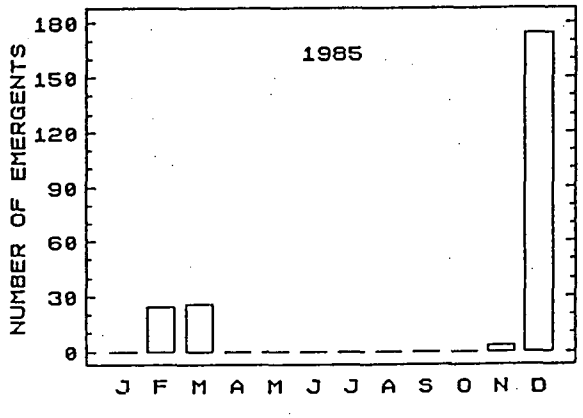

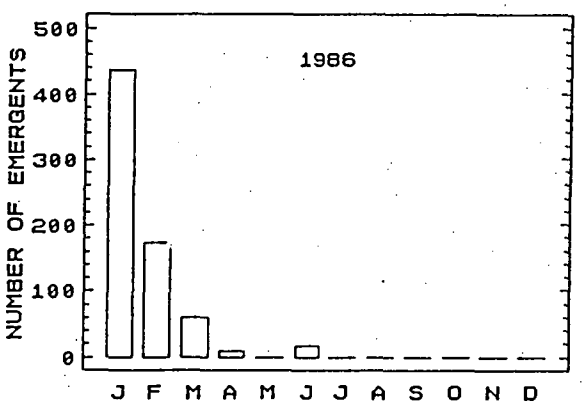

FIG 6.4 Total emergence by month and year

available here and using the residual deviance to estimate the dispersion parameter (McCullagh and Nelder 1983) ϕ, the probability of emergence by month is given in Table 6.5 with corresponding standard errors given by $\sqrt{(\hat{\phi}\ p_i(1-p_i)/N)}$ where p_i is the probability for month i and N is the total number of emergents collected over the 6 years which was 29238. The above standard errors assume that across years the p_i have a multivariate beta distribution. The total emergents over the j years in the ith month, $n_i = \sum_j n_{ij}$ and $N = \sum_i n_i$, then have, across the months, a compound multinomial distribution with variance proportional to a standard multinomial for the n_i (Mosimann 1962, Stedinger *et al.* 1985).

6.4 Mean temperature at the start of emergence

The mean ambient temperature at the Arve study site at the start of emergence for the author's cages, calculated for the period 3/12/85 to 8/12/85 was 15.2°(C). This figure was obtained by averaging the day-degrees (above zero) accumulated within each of the 6 days between the above dates. For the SILV cages the first emergence date observed for a cage (i.e. to exclude emergents which are late with respect to their cohorts) was obtained. Using the day-degrees, as described above, for each of the 6 days prior to each cage's first emergence date the mean temperature occurring during the 6-day period was calculated. These mean temperatures were then cross-classified by the year and month of emergence. For the 80/81, 81/82 and 84/85 summers the first emergence occurred in January with mean temperatures being 17.0, 17.0 and 13.4 respectively. For the 82/83 and 83/84 summers first emergence occurred in December and November respectively with mean temperatures of 11.6 and 12.4°C.

6.6 Length of emergence period for a gallery

As mentioned in Section 2.3.4, once emergence begins for a gallery it can continue over a period of several years. The author's emergence material was relocated to Hobart at the start of emergence early in the summer of 1985/86 and there was no further emergence the following summer probably due to desiccation of the logs

(Section 3.1.3). The emergence cages of Elliott and Bashford give a better indication of the total emergence period for a gallery. The longest period of emergence observed for their cages was 705 days for a gallery that first produced emergents on 15/4/82 and finally on 20/3/84 two years later. Fig 6.5 shows the frequency of male and female emergents by days since first emergence for the gallery from which they came for the 58 SILV cages. For these cages 36.4% of total emergence occurred in the second summer after emergence for the cage began and 0.8% in the third summer. There was no emergence recorded later than the third summer. Fig 6.6 shows the corresponding figure to Fig 6.5 for the author's cages.

6.6 Daily rate of emergence

Using the author's emergence data (Section 3.1.3) the daily rate of emergence was calculated for the periods over which emergence was observed in the summer of 85/86 at the Hobart Insectary. Starting from 17/12/85 for the 19 periods between dates at which cages were checked and cleared, which were mostly week-long periods with the exception of the first 3 which were single day periods, the rate of emergence was calculated as a per day and per gallery rate for each period and this rate, expressed as 100 x the number of emergents day^{-1} $gallery^{-1}$, is graphed against period mid-point in Fig 6.7(a). The mean temperature for the corresponding period, calculated as accumulated day-degrees above zero for the period divided by period length, is also shown in Fig 6.7(a). It would be expected that the emergence rate would increase from zero to a peak and then trail off to zero again as the pool of individuals which complete their development in the 85/86 summer and autumn dwindles to zero. There is such a general trend in Fig 6.7(a) but there is also a large amount of fluctuation about such a general trend. These fluctuations appear to be positively correlated to fluctuations in mean temperature although the correspondence between the peaks (and thus troughs) in emergence rate and mean temperature is not totally consistent. The sudden pulse in emergence starting at around the 70 day mark appears out of line with the general trend

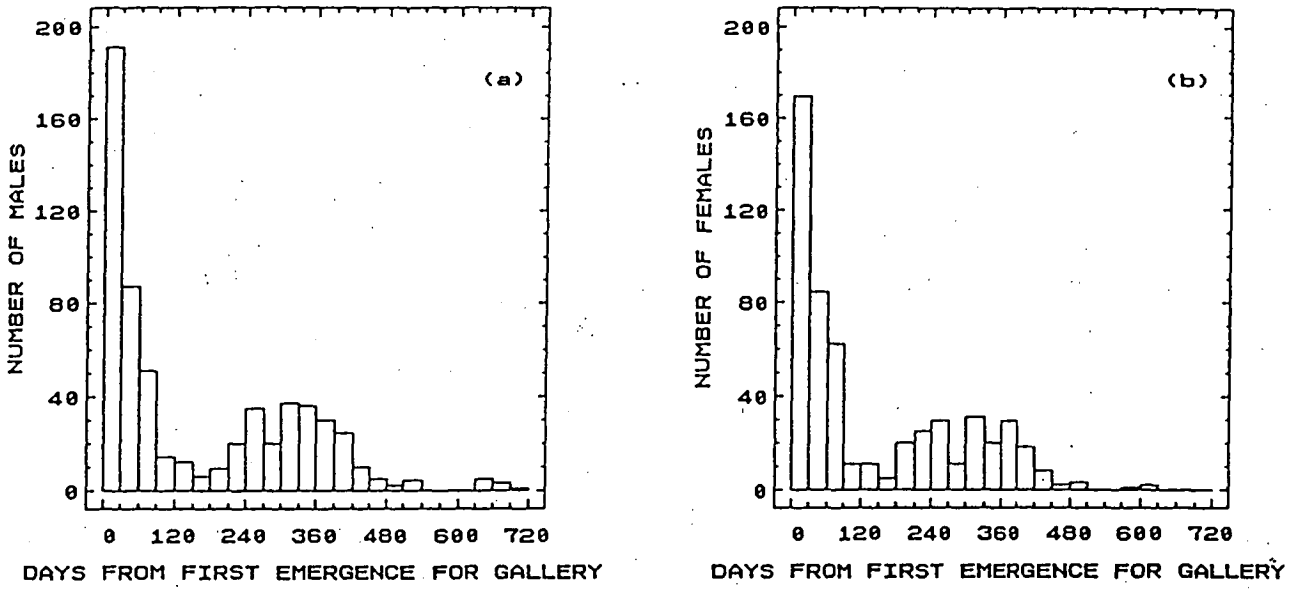

FIG 6.5 Number of (a) males (b) females emerging after emergence began for the gallery : 1981-85 data

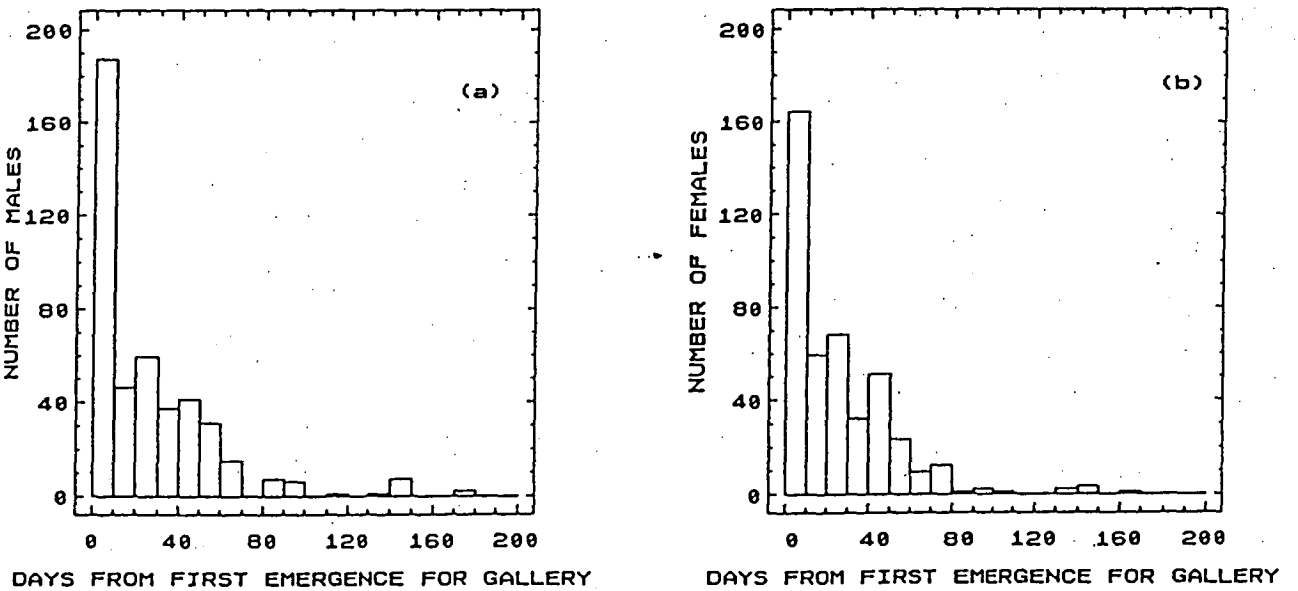

FIG 6.6 Number of (a) males (b) females emerging after emergence began for the gallery : 85/86 data

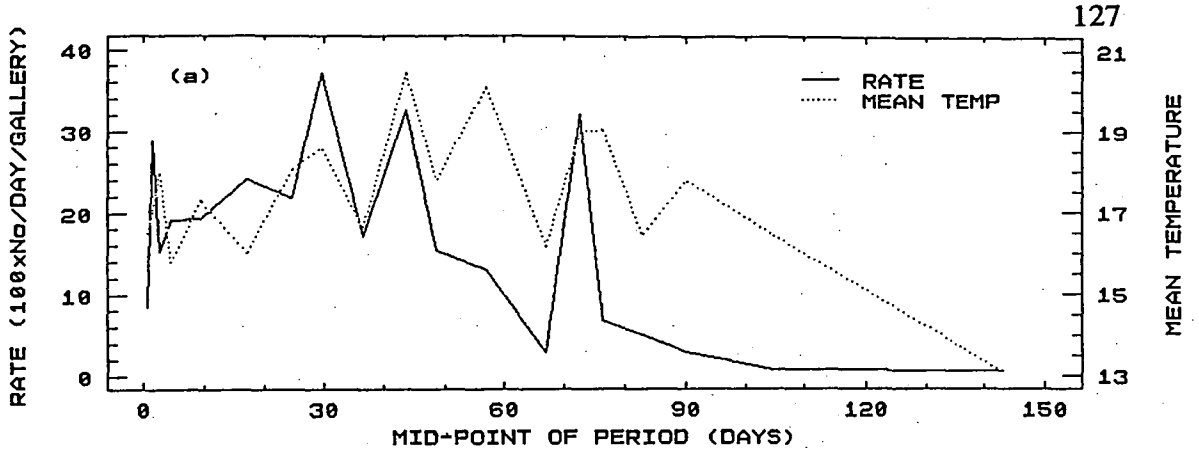

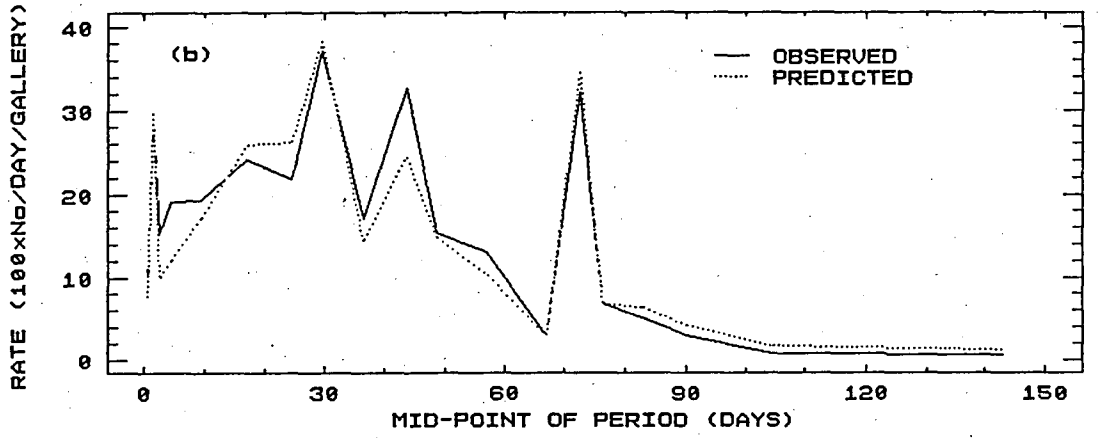

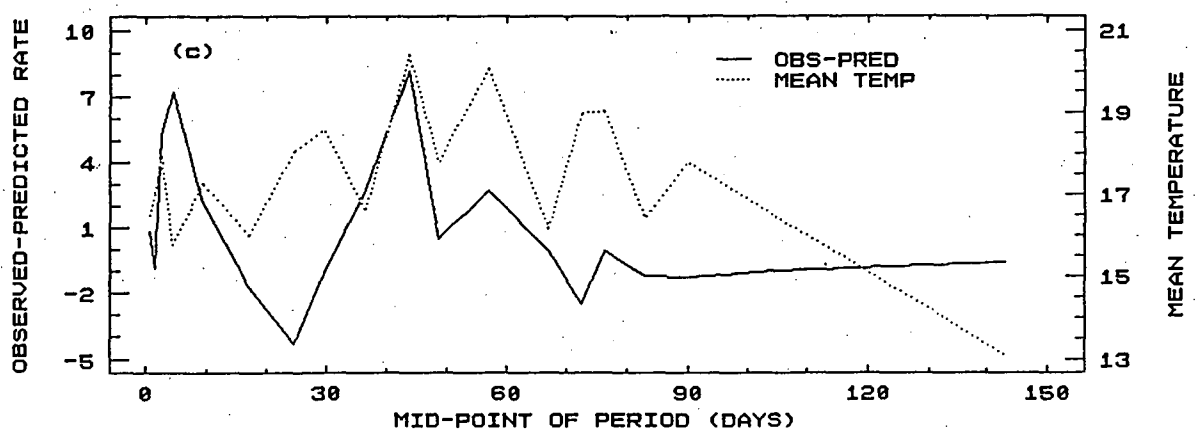

FIG 6.7 Emergence rate and mean temperature for periods in 85/86 summer, (a) observed (b) predicted (c) observed - predicted emergence rates with predictions from the log-odds model

of decreasing emergence, as mentioned above. To investigate these trends further the relationship between emergence for a gallery and period as a proportion, P_e, of the total pool of emergents remaining (i.e. the total emergence for a gallery minus the emergence that has already occurred to the start of the period) and the corresponding proportion, P_d, of the period length compared to the total period remaining (i.e. the total emergence period for the gallery minus the time from first emergence to the start of the period under consideration) was used. The values of P_e and P_d were obtained for each gallery and each period with the exception of the last period where P_e and P_d are both by definition equal to one. These proportions are analogous to those used earlier (Section 5.3.1) to model the phenology of each life stage using conditional probabilities (i.e. continuation ratios, Fienberg 1980) and they can be modelled as conditionally independent (i.e. for a gallery P_e for one period does not depend on that for the previous period) binomial proportions. These values of P_e were fitted using GLIM as a *glm* with binomial P_e , logit link function (Section 5.4, Appendix 1) and predictor variable $log\{P_d /(1-P_d)\}$. The model can be expressed as

$$log\{P_e /(1-P_e)\} = \beta_0 + \beta_1 log\{P_d /(1-P_d)\}$$

which expresses the odds of an emergent appearing in a given period compared to it appearing later (but within the total period of emergence for the gallery) as proportional to $\{P_d /(1-P_d)\}^{\beta_1}$. This model, therefore, takes into account the total number of emergents and the length of the period over which emergence occurs for each gallery. Using the above model and estimates of β_0 and β_1, with standard errors in brackets, of -0.171 (0.106) and 0.420 (0.045) respectively, the predicted number of emergents were aggregated across galleries for the 19 periods (the last period by difference) and the predicted rate of emergence calculated. Fig 6.7(b) shows observed (as in Fig 6.7a) and predicted rate for the period mid-points. It can be seen from the close correspondence of observed and fitted emergence rates in Fig 6.7(b) that the between-gallery variation in the total number of emergents, start, and length of emergence period, all of which

are involved in producing the predicted rates in Fig 6.7(b), are largely responsible for the observed fluctuations in observed emergence rate. With a larger sample of galleries these fluctuations would possibly be less pronounced. Fig 6.7(c) shows the difference between observed and predicted emergence rate as well as mean temperature for each period. Some extra variation in emergence rate beyond that explained by the factors mentioned above is explained by mean temperature but its effect is not consistent.

Fig 6.8 shows the emergence rate and mean temperature over the observed emergence period for the mass emergence tents. Since the number of galleries producing emergents is not known for each tent the emergence rate is expressed as the number per day. This rate is therefore not directly comparable to that in Fig 6.7 or between tents. Tents 2 and 3 are not shown in Fig 6.8 for brevity since they showed very similar trends to tent 1. An interesting feature seen in Figs 6.7(a) and 6.8 is the consistently occurring pulse in the emergence rate after the main peak of emergence. This pulse appears to be associated with an increase in mean temperature when such an increase occurs roughly a month after the main peak in emergence. With a much larger number of galleries involved the emergence rate over time appears much smoother, apart from the pulse mentioned above, for the mass emergence tents compared to the individual emergence cages.

6.7 Time of day of flight

Fig 6.9 shows the total number of males and females caught in a rotary trap at the Little Florentine study site (Section 3.5) over eight days of trapping between 24/2/86 and 26/3/86. It can be seen that females are less readily caught than males and that males were mostly caught after midday while females were caught mostly before midday. The low number of females caught explains the sporadic trend with time of day. In contrast there is a clear trend of males reaching a peak in mid-afternoon (1400-1600 hours) and then declining towards evening. These trends were also reported by Hogan (1948).

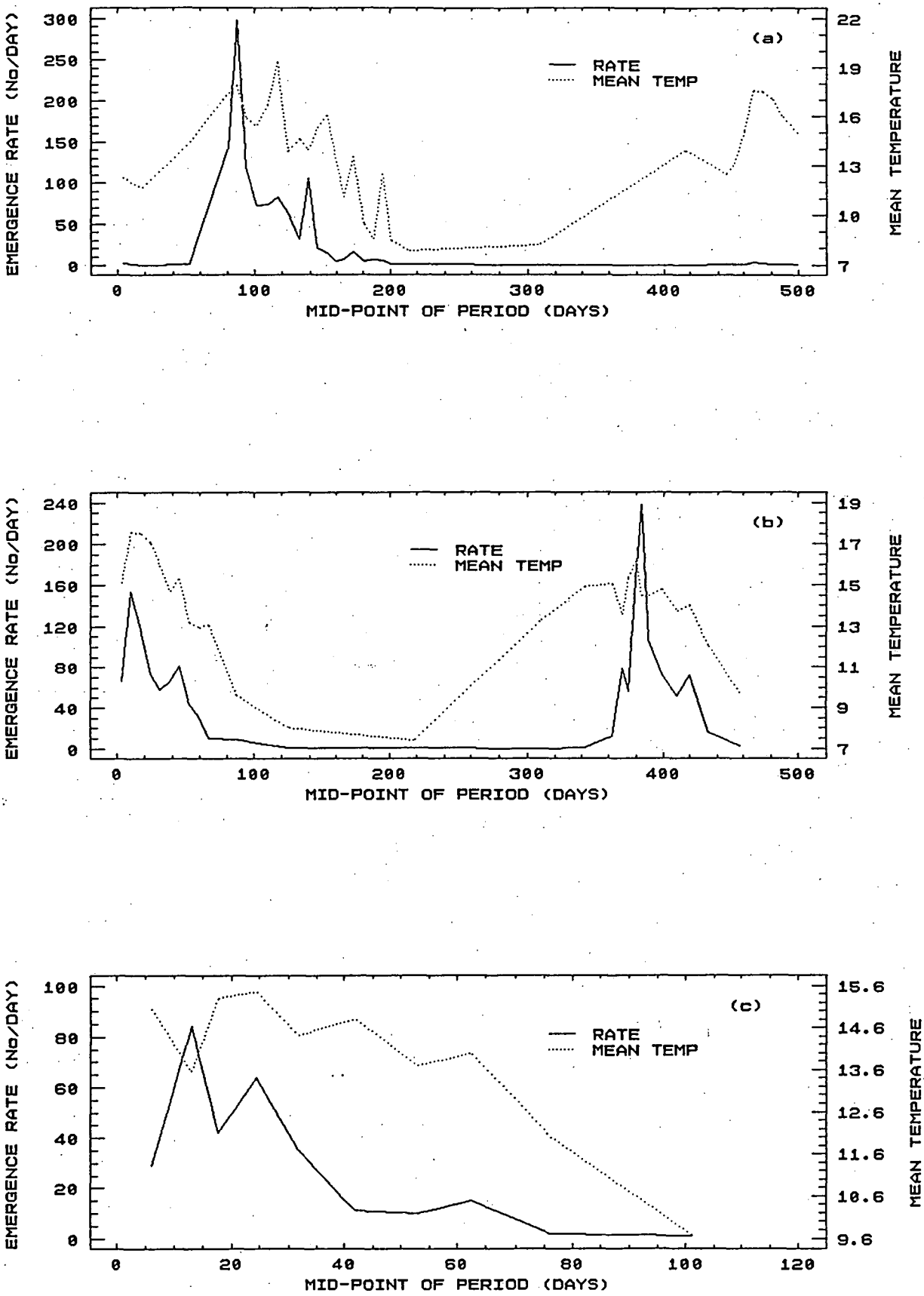

FIG 6.8 Emergence rate and mean temperature over the emergence period for mass emergence tents (a) 1 (b) 4 (c) 5

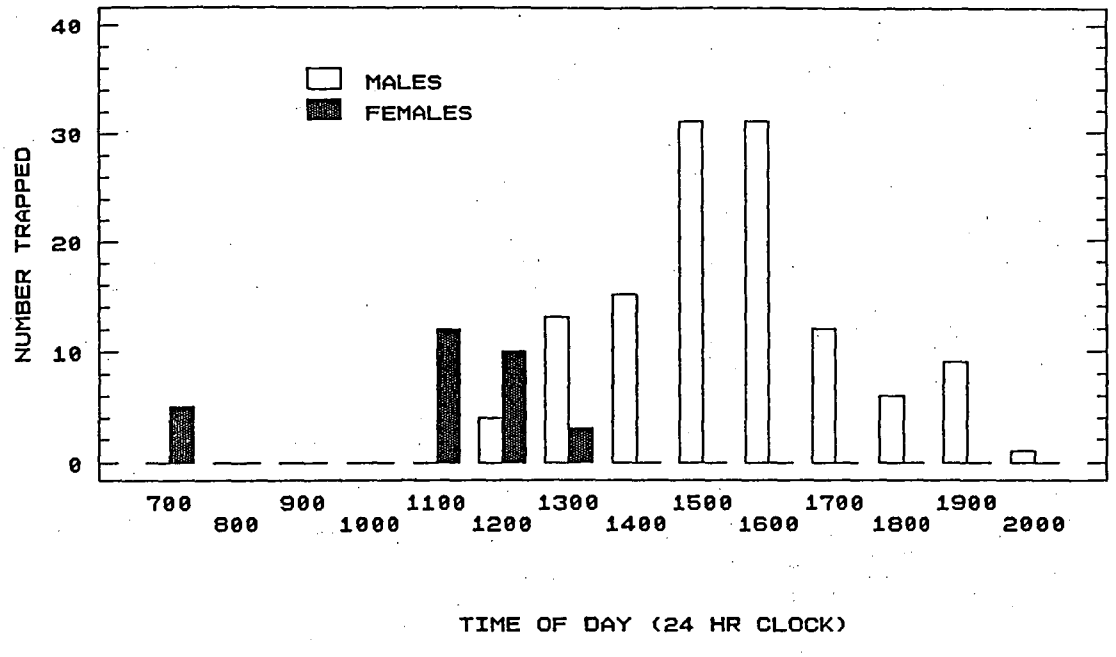

FIG 6.9 Total number of P.subgranosus caught in rotary trap

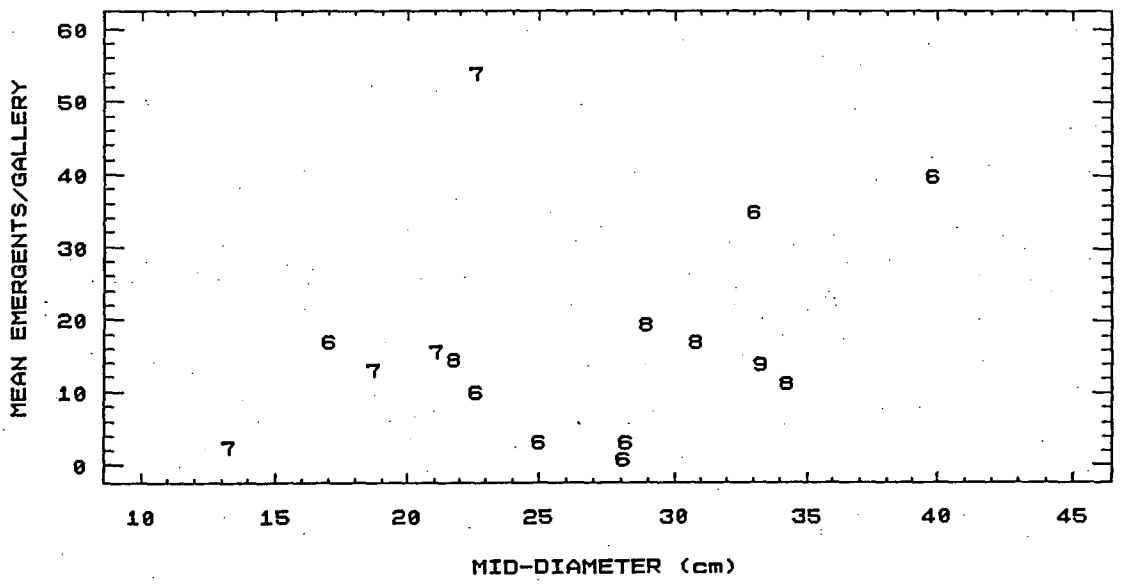

FIG 6.10 Mean number of emergents per gallery versus mid-diameter of log with tree numbers shown

6.8 Emergence and log diameter

In Section 5.2 it was reported that natality at initial oviposition was a function of gallery length. If smaller diameter logs restrict the development of the gallery and/or caused higher mortality due to desiccation of immature stages then the number of emergents per gallery would reflect this. No evidence was found for a lower mean number of eggs or gallery length at initial oviposition in smaller compared to larger diameter logs (Section 5.2). Fig 6.10 shows the number of emergents per gallery, averaged over cages with at least one emergent, for each log which was sampled by cages (Section 3.1.3). Tree numbers from which the logs were taken (Section 3.1.1) are shown in Fig 6.10. There is a weak overall trend for mean number of emergents to increase with increasing diameter of the log but within trees this trend is inconsistent with only tree 7 showing such a trend. The high value of emergence of 54 for tree 7 seen in Fig 6.10 was obtained from a single cage. The lowest value for tree 7 was for a log with a diameter of 12.8 cm where the mean emergence was calculated from four cages with consistently low values of 1,3,4 and 5 emergents. It appears then, that above a limit of approximately 15 cm for diameter of log, brood production is not limited by diameter but below this it can be drastically reduced. Low values of mean emergence at larger diameters are possibly due to other factors such as the suitability of the wood for boring.

6.9 Discussion

The mean number of emergents per gallery is consistent with the estimate of brood size obtained from destructively sampled galleries (Sections 5.5 and 5.6) and is very similar to that obtained by Holloway (W.A. Holloway, Forest Research Institute, unpublished data) for *P.caviceps* obtained from *Nothofagus* spp. logs in New Zealand. Holloway obtained a mean of 21.4 emergents per gallery from 23 of a total of 25 cages. The two excluded cages had one and zero emergents respectively. The mean including the single emergent cage was calculated here as 20.6. Hogan (1948) reported a mean

emergence of insectary reared *P.subgranosus* of 9.8 but conceded that parasitic mites, which were a serious problem for insectary rearing, could have reduced final brood size compared to field conditions. The number of progeny per gallery observed in this study is also similar to that reported by Borden (1988) for the striped ambrosia beetle *T.lineatum* of Europe and North America.

The distribution of the number of emergents per gallery is reverse J-shaped and is similar to that reported by Milligan (1979) for *P.apicalis*, *P.caviceps* and *P.gracilis* for which roughly two thirds of total emergence is produced by a highly productive one third of galleries. This is comparable to that obtained here where the mean for the SILV cages in Table 6.1 is half way between the median and the upper quartile.

Milligan (1979) reported a population sex ratio very close to unity but with considerable between-gallery heterogeneity as was the case here. He also reported a similar trend to that reported here for males of *P.gracilis* to predominate in the first 2 weeks of the flight season. Also similar to observations here, *P.apicalis* and *P.caviceps* begin emergence in the second summer after gallery establishment (not counting the summer when establishment occurs) with 25% (*P.caviceps*) and 40% (*P.apicalis*) of total emergence occurring in the third and fourth summer where most of this occurs in the third summer.

Considerable variation was observed here in the timing and duration of emergence within the first summer of emergence. Emergence rates per gallery over the summer were predicted accurately by a model which incorporated, for each gallery, time of the start and duration of emergence combined with total number of emergents. Mean temperature beyond these factors did not consistently correlate with emergence rate.

Given that extra variation is involved when galleries producing first, second and, a small number, third summer emergence are acting in combination then it is not surprising that definite brood flights are not observed (Hogan 1948). Although with a

large number of galleries sampled by mass emergence cages a definite peak in emergence was observed.

The reason for the late pulse in emergence, which occurred consistently over a number of years during the general slow-down in emergence in the latter part of the summer, is not clear. The association of this pulse with a peak in temperature roughly one month previous is also consistent over a number of years. A possible explanation is that the pulse represents the brood resulting from oviposition occurring after initial oviposition (Sections 2.3.3 and 5.2).

The average field temperature at the start of the emergence season can be used for some insect species as an indication of the lower threshold temperature for development, τ_0, (Gilbert 1988). With τ_0 set as the average temperature then the variation in development rates produced by variation in individual values of τ_0, which is under genetic control (Gilbert 1986), will be ensured whereas low values of τ_0, relative to field temperatures, will not produce such variation. Gilbert (1988) suggests this variation is beneficial at a time of year when survival is erratic. With the early spring emergence in species such as the small white butterfly *Pieris rapae* L., that Gilbert (1988) is referring to, development will initially be slow and matched to food availability. Gilbert (1988) also maintains that given the selective advantage of early emergence, then emergence will begin as early as individuals can possibly hope to survive. The relationship between development rate and temperature is examined in detail in Section 7.3, but suffice it to say here that the average field temperature at the start of the emergence season observed in this study is in general far too high to be a realistic value for τ_0. *P.subgranosus* begins emergence mostly in January or later when average field temperatures are high. Given the above arguments, if there were no advantage but instead a disincentive to early emergence then the average field temperatures at the start of emergence will be higher than τ_0 as was observed here (Section 6.4 and 7.3). Such a possible disincentive, mentioned earlier (Section 2.3.3,

2.3.4 and 5.6), is the higher mortality of eggs and early instar larvae from desiccation when oviposition occurs in summer. This disincentive will be balanced to a degree by the reproductive advantage that early summer gallery establishment and subsequent same summer oviposition obtains by producing an emergent brood after only one year instead of two (Section 7.3). This could explain why risky summer oviposition occurs at all.

7. DEVELOPMENT TIME

In the general description of the life cycle of *P.subgranosus* given in Section 2.3.4, the development time from gallery establishment to first emergence was described as ranging from approximately 10 months to 2 years. The development time for individuals from egg to adult is not directly observable since laboratory rearing was not possible and destructive sampling of galleries was the only way of obtaining immature stages (Section 3.1.2). Gallery establishment and emergence for the same gallery are observable (Sections 3.1.1 and 3.1.3) and, initially, attention here is concentrated on this observed 'development time', however, the development time from egg to adult can be inferred from observing the time from gallery establishment to oviposition (Section 5.2). Development observed for some galleries to be completed in a single year compared to the usual time of two years was implied to be the result of spring/early summer attack in the first case as opposed to late summer/autumn attack in the latter case in Section 2.3.4 (Fig. 2.9). Different gallery establishment dates result in different temperature profiles, over time, that galleries are exposed to. Models relating development rate to temperature are introduced in the following section. A maximum likelihood procedure developed here to estimate the parameters of the day-degree model from emergence data obtained under ambient temperatures in the field is then described. This procedure is then applied to emergence data obtained by the author (Section 3.1.3) combined with data collected by Elliott and Bashford (Section 3.2). The resulting day-degree model is used to explain the observed chronological development time in terms of *physiological* time units.

7.1 Development time as a function of temperature

Temperature is a major determinant of the rate at which physiological processes proceed and is thus a major determinant of the length of time taken for insect development which occurs within a definite temperature range. Various mathematical models have been used to describe the relationship of development time and

temperature. The simplest and most widely used model is the thermal-summation or day-degree model or method (Howe 1967). This approach integrates the temperature (T) over time (t) (which numerically involves summing the temperature for small time intervals) above a threshold temperature (τ_0). The threshold temperature is the temperature below which no development occurs and above τ_0 the rate of development, λ, is linear on (or proportional to) temperature. The rate parameter λ can be expressed as the proportion development per day-degree above τ_0. The total day-degrees above threshold τ_0 required to complete development in time l is given by $D(\tau_0)$ where

$$D(\tau_0) = \int_0^l \{T(t)-\tau_0\}\,\delta(t)dt \qquad (7.1)$$

where $\delta(t) = 1$ for $T(t)>\tau_0$

$= 0$ otherwise.

The rate of development is given by $\lambda=1/D(\tau_0)$. A consequence of this relationship is that the proportion of development up to time t', $P(t')$, is given by

$$P(t') = \lambda\int_0^{t'} \{T(t)-\tau_0\}\,\delta(t)dt \qquad (7.2)$$

where $t'\leq l$ and $\delta(t) = 1$ for $T(t)>\tau_0$

$= 0$ otherwise.

In laboratory studies the relationship between temperature and development can be studied by exposing a number of cohorts each to a separate fixed temperature and observing the time for individuals from each cohort to completely develop. The generalised relationships between each of development time, l, and rate λ and temperature is shown in Fig 7.1. As temperature approaches a lower limit for development l increases to infinity (development cannot be completed) and the λ versus T curve asymptotes to zero. At the other end of the temperature scale as T increases above the optimum, T_{opt} , for the species (or individuals since T_{opt} will vary within and between populations) then λ will start to decrease (and l increase). Ignoring for the moment the slight curvature in the λ versus T relationship and assuming a linear

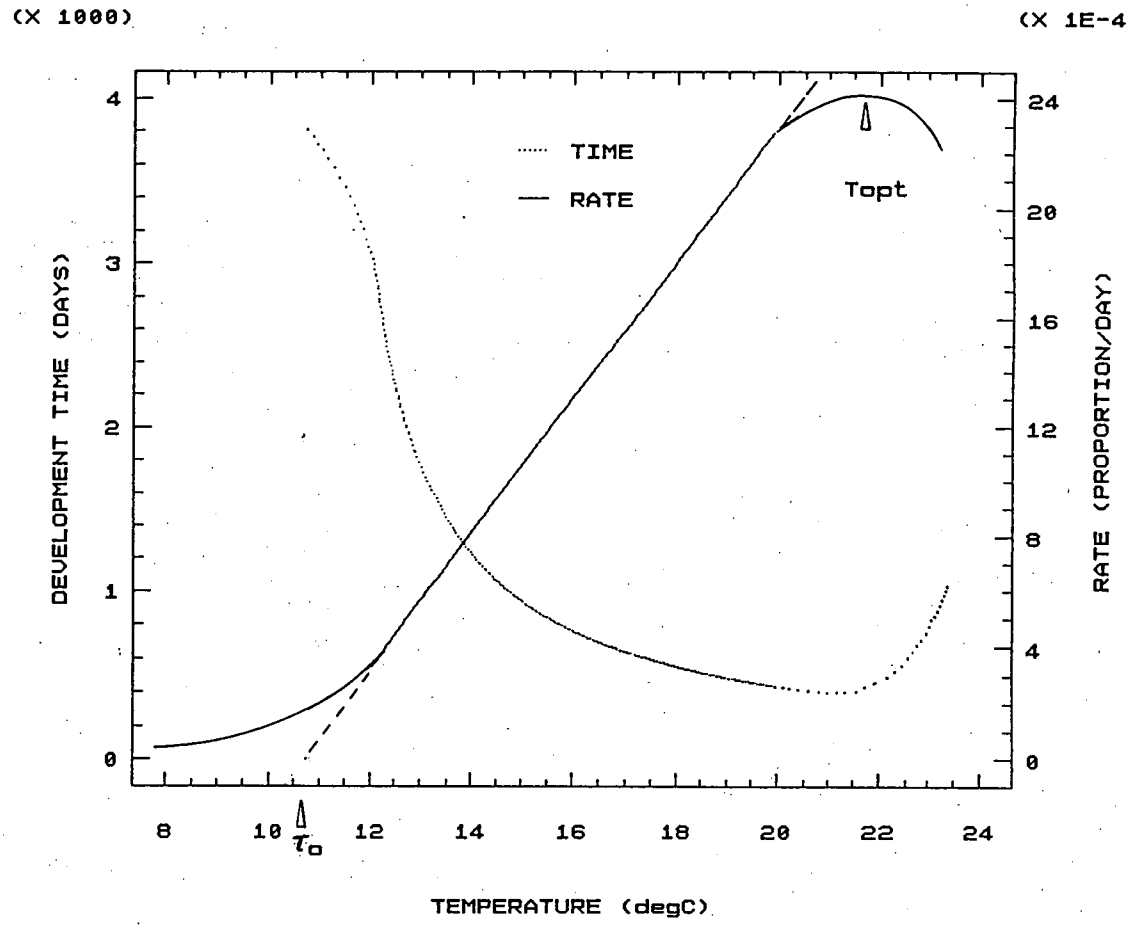

FIG 7.1 General development time and rate versus temperature relationships

relationship passing through the development zero point ($l \to \infty$ as $T \to \tau_0$) with slope λ, the parameters λ and τ_0 can be estimated from data on length of development time collected under constant temperature regimes by regressing observed development rate, r (i.e. $1/l$), on T. For each cohort the mean of the individual values of r can be used as the regressand in a least squares fit. The regression equation is

$$r_i = \alpha + \beta T_i \qquad (7.3)$$

where r_i is the mean rate for the i^{th} cohort,

T_i is the temperature for the i^{th} cohort,

$\alpha = -\lambda\tau_0$ and $\beta = \lambda$.

Since temperature is fixed over time, eqn (7.3) can be obtained from the integral on the right hand side of eqn (7.1) which gives

$$1/\lambda = l_i (T_i - \tau_0)$$

which is a re-arrangement of eqn (7.3).

Nonlinear models of the relationship between development rate and temperature have been used (see Wagner *et al.* 1984 for a review) to take into account the observed nonlinearity in the relationship between r and T mentioned above. This nonlinearity is not directly observable in data obtained under fluctuating temperatures, which can be either artificially produced or are those obtained under ambient conditions in the field (Allsopp 1986), since a graph equivalent to Fig 7.1 cannot be constructed. The nonlinearity produced by temperatures approaching and exceeding T_{opt} is not of great importance for field based studies where temperatures very rarely approach this value (Gilbert 1988). The nonlinearity at lower temperatures is more relevant to field based studies but the error introduced by assuming the day-degree model as an approximation to the real situation may not have any practical significance. Attention is therefore restricted to the day-degree model for the moment and the implications of the assumptions involved for this study are discussed later.

7.2 Estimation of the day-degree model using ambient temperatures.

In the field temperature varies continuously with time so it is not possible to estimate λ and τ_0 in the way described above. The model in this case is expressed for an individual emergent as

$$1 = \int_0^l \lambda\{T(t) - \tau_0\}\delta(t)dt \qquad (7.4)$$

which is the sum of the proportional components of development, given by eqn (7.2), until development is completed when $P(t'=l)=1$, assuming that development starts at time zero without loss of generality.

The integral in eqn (7.4) can be approximated using numerical integration via the trapezoidal rule given a value for τ_0 such that

$$1 \simeq \lambda D(\tau_0) \qquad (7.5)$$

where

$$D(\tau_0) = \Sigma_k \delta_k\{(T_k-\tau_0)+(T_{k+1}-\tau_0)\}\Delta t/2 \quad , \qquad (7.6)$$

$$\delta_k = 1 \text{ for } T_k, T_{k+1}>\tau_0 \, ,$$

$$= 0 \text{ otherwise} \quad ,$$

k is a subscript referring to the k^{th} point taken from the observed temperature/time trace, Δt is a small time interval t_{k+1}-t_k, T_k is the temperature at time t_k and δ_k is an indicator variable and the summation proceeds until $\Sigma_k \Delta t = l$. When a recorded continuous temperature/time trace from an instrument such as a thermograph is not available T_k can be obtained by a number of methods (Section 3.3) including fitting a sine curve to daily maximum and minimum temperatures, linear interpolation between typical shape values of the daily temperature cycle or fitting spline curves to daily minima and maxima temperatures using time of day of the maximum and minimum as the abscissa scale. This last method was used in this study (Section 3.3).

For n emergents with length of development time l_j , j=1,...,n days, least squares estimates of τ_0 and λ obtained by minimisation of the following function, with respect

to the parameters,

$$\Sigma_{j=1}^{n}\{1 - \lambda D_j(\tau_0)\}^2 \qquad (7.7),$$

is used by the computer program DEVAR (Dallwitz and Higgins 1978, Allsopp 1986). In the case of nonlinear models the term $\lambda D_j(\tau_0)$ in eqn (7.7) is replaced by the integral $\int_0^l \mathcal{I}(T)\,dt$ where $\mathcal{I}(T)$ is a nonlinear function relating proportional development to temperature T which is itself a function of time t. The distributional assumptions underlying the above least squares fit are not clear. Sharpe *et al.* (1977), using constant temperature data, developed distributional theory for development time, l, from assumptions about the distribution of individual development rates, $r=1/l$. The random variable considered for the following is, dropping the subscript, $D(\tau_0)$, the day-degrees above τ_0 required for an individual to complete development. Distributions of development times tend to be positively skewed while distributions of rates show little skew (Stinner *et al.* 1975, Sharpe *et al.* 1977). It was therefore thought likely that the distribution of $D(\tau_0)$ would also be positively skewed. Two alternative distributional models were used here. Firstly, a normal probability density function (*pdf*) was used for $X=1/D(\tau_0)$ and the *pdf* of $Y=D(\tau_0)$ can then be obtained from the distribution of X and the transformation $Y=1/X$ as shown by Sharpe *et al.* (1977). The distribution of Y is then positively skewed (Sharpe *et al.* 1977). Alternatively a gamma *pdf*, which was used by Howe (1967) and which also exhibits positive skew, was used directly for $Y=D(\tau_0)$.

Maximum likelihood estimation is employed in each case using the assumed distribution for each of X and Y, however, since $D(\tau_0)$ is not directly observed if τ_0 is unknown, the likelihood is obtained for the observed variable, l. This likelihood is obtained by expressing X or Y as a transformation of l.

Considering first the case of X normal, mean λ and variance σ^2, then the *log-likelihood*, $\mathcal{L}$, for the l_j is given by

$$\mathcal{L} = -n\log(\sigma^2)/2 + \sum_{j=1}^{n}\{-(x_j - \lambda)^2/2\sigma^2 + \log[\{T(l_j) - \tau_0\}\delta(l_j)] + 2\log(x_j)\} \quad (7.8)$$

where $x_j = 1/D_j(\tau_0)$, $T(l_j)$ is the temperature at emergence and $\delta(l_j)$ is as described for eqn (7.1). The first two terms in eqn (7.8) are simply those derived from the normal *pdf* for X. The last two terms[1] are due to the transformation relating X and l, that is $X=1/D(\tau_0)$ where l appears as a limit in the integral (7.1) used to obtain $D(\tau_0)$. These terms combined are the logarithm of the *Jacobian*, $\mathcal{J}$, of the transformation where

$$\mathcal{J} = |dx/dl| = [T(l_j)-\tau_0]\delta(l_j)/D_j^2(\tau_0) \quad (7.9),$$

where $|.|$ denotes the 'absolute value of'. The term $\delta(l_j)$ ensures that $dx/dl \geq 0$ so the absolute value operation is no longer required. However, $\mathcal{J}$ is zero if $T(l_j) \leq \tau_0$ which means that there is a zero probability, according to the model, of observing $T(l_j) \leq \tau_0$ (i.e. emergence when temperature is below the threshold). This is logical if τ_0 is a fixed constant as given in the above development. Further discussion of this point is left to the discussion section.

As far as maximum likelihood estimation is concerned, the Jacobian term effectively sets an upper limit to $\hat{\tau}_0$ as the minimum observed value of $T(l_j)$, called $T_{min}(l)$ for the following. This can be seen to be the result of maximising the likelihood $\mathcal{L}$ with respect to τ_0. This is achieved in part by maximising the term $2\log(x)$ since increasing $\log(x)$ [i.e. decreasing $D(\tau_0)$] is achieved by increasing τ_0. Alternatively maximising the term $T(l_j)-\tau_0$ in $\mathcal{L}$ will tend to force τ_0 downwards. Experience with log-likelihood (7.8) in this study showed that the term $2\log(x)$ dominates all other terms in $\mathcal{L}$ causing τ_0 to increase to the point where $\mathcal{L}$ becomes undefined when $\hat{\tau}_0 \geq T_{min}(l)$. When field emergence dates are all that are known, then $T_{min}(l)$ also provides an upper limit for τ_0. In this case the usual estimate of τ_0 is the mean field temperature when

---

[1]I am indebted to Stephen Wallace for pointing out the need to include $\mathcal{J}$ in the likelihood.

emergence begins (Gilbert 1988, Section 6.9 this study). However, extra information on τ_0 is available when l and the temperature profile from time zero to l are known as is the case here. A value for τ_0 which gives emergents, which have completed development in either one or two calendar years, the same mean $D(\tau_0)$ is the objective here. It is the term $-\sum_{j=1}^{n}(x_j-\lambda)^2/2\sigma^2$ in $\mathscr{L}$ which in effect attempts to give all emergents a common mean value for $D(\tau_0)$, so for the following it alone was used in the maximum likelihood estimation procedure and will be taken to be equivalent to $\mathscr{L}$. It is in fact the *kernel* (Appendix 1) of the log-likelihood for normal X. The effect of the Jacobian on estimation of τ_0 was maintained by restricting τ_0 to be less than $T_{min}(l)$. Maximising this likelihood is then simply equivalent to least squares estimation.

In this study a number of emergents were observed to have emerged between dates on which emergence cages were checked and, if necessary cleared. Taking m to be the number of emergents relating to l then the log-likelihood is now

$$\mathscr{L} = -\sum_{j=1}^{n} m_j (x_j - \lambda)^2/2\sigma^2 \qquad (7.10)$$

Incorporating m_j in the above way in eqn (7.10) assumes that each of the m_j individuals emerge at the same time (i.e. after l_j days). This approximation should not seriously affect the estimates if the time between observations is short relative to l_j. Howe (1967) suggested this interval should not be more than 1/10th of l which was easily satisfied in this study with a value of around 1/100th of l.

The variance of X, σ^2, can be ignored for the moment since it does not affect the MLE's of either λ or τ_0. Considering for the moment fixed τ_0, the MLE of λ is simply $\hat{\lambda} = \sum_j m_j x_j / \sum_j m_j$ which is obtained by solving the partial differential equation $\partial\mathscr{L}/\partial\lambda = 0$. The MLE $\hat{\lambda}$ is an unbiased estimate of λ since the x_j are assumed independent with expected value λ. The least squares estimate of λ obtained from (7.7) as used by DEVAR, including now the weighting factor m_j as in (7.10), is given by

$$\hat{\lambda}_s = \sum_j m_j D_j(\tau_0) / \sum_j m_j D_j^2(\tau_0) \quad ,$$

the ratio of the weighted sum to the weighted sum of squares of the $D_j(\tau_0)$, which is

different to $\hat{\lambda}$. The calculation of the expected value of $\hat{\lambda}_s$ does not appear to be analytically tractable but even so using the approximation that the expected value of the ratio is the ratio of expected values and the variance of $D(\tau_0)$ is approximately σ^2/λ^4 [based on eqns (10.11) and (10.12) of Kendall and Stuart 1977] gives $\mathcal{E}(\hat{\lambda}_s) \equiv \lambda/(1+\sigma^2/\lambda^2)$. This represents an under-estimation by approximately $100\{1-1/(1+\sigma^2/\lambda^2)\}$ percent.

Removing the constraint that τ_0 is fixed, the joint estimates of τ_0 and λ can be found using a one-dimensional search along τ_0 for the maximum of the log-likelihood (7.10) with a maximum value for τ_0 set to $T_{min}(l)$ as mentioned above. The reason the search is only one-dimensional is that while the MLE's are the joint solution to the simultaneous equations $\partial\mathcal{L}/\partial\tau_0=0$, $\partial\mathcal{L}/\partial\lambda=0$, substituting the solution to $\partial\mathcal{L}/\partial\lambda=0$, given above as $\Sigma_j m_j y_j / \Sigma_j m_j$, into the expression for $\partial\mathcal{L}/\partial\tau_0$ makes $\partial\mathcal{L}/\partial\tau_0$ a function of, in terms of the parameters of interest, only τ_0.

An estimate of σ^2 is given by the usual residual mean square, $\{\Sigma_j m_j (x_j - \lambda)^2\}/(n-2)$, where this estimate in the general setting of likelihood is equivalent to the residual mean deviance (Appendix 1).

The probability density function (*pdf*) for $Y = D(\tau_0)$ using a gamma distribution is given by

$$\mathcal{P}(Y=y) = \frac{(y-\xi)^{\theta-1} exp\{-(y-\xi)/\beta\}}{\beta^\theta\ \Gamma(\theta)} \qquad (7.11)$$

where $\theta,\beta,\xi > 0,\ y>\xi$,

θ,β,ξ are the shape, scale and location parameters respectively and $\Gamma(.)$ is Euler's gamma function. The expected value of Y is given by $\theta\beta+\xi$ which is equivalent to $1/\lambda$ where λ is given in equation (7.2) as the rate parameter. A location parameter is required since the value of Y for the first individuals that complete development will be a considerable proportion of the mean of Y. The kernel of the log-likelihood of l assuming the above gamma distribution for Y is shown in Appendix 4 to be equivalent

to

$$\mathcal{L} = \theta \sum_j \{m_j log(\mu_j) - \mu_j\} \qquad (7.12),$$

where $\mu_j = m_j\, y_j\, \lambda$ and θ can be treated like σ^2 in eqn (7.10) as a nuisance parameter and estimated separately from λ and τ_0. The logarithm of the Jacobian of the transformation between Y and l plus the term $-log(y-\xi)$ have been excluded from $\mathcal{L}$ (Appendix 4) for the same reason that the Jacobian was excluded from $\mathcal{L}$ in the case of normal X.

Eqn (7.12) is equivalent to the kernel of the log-likelihood assuming a Poisson distribution for m_j with expected value μ_j. The Poisson likelihood and the fact that λ appears linearly in μ were exploited using GENSTAT's FITNONLINEAR directive (Appendix 5) to obtain MLE's of λ and τ_0. Note also that there is no need to estimate ξ in this parameterisation of the gamma.

For fixed τ_0 the MLE of λ is given by $\hat{\lambda}_g = (\sum_j m_j\, y_j / \sum_j m_j)^{-1}$ which is simply the inverse of the mean day-degrees above τ_0. The estimator $1/\hat{\lambda}_g$ has expected value $\theta\beta+\xi$, and is thus an unbiased estimator of the expected value of Y. From the theory of maximum likelihood (Bickell and Doksum 1977) $\hat{\lambda}_g$ is an asymptotically unbiased estimate of λ. A similar duality occurs for $1/\hat{\lambda}$ which is an asymptotically unbiased estimate of the expected value of Y.

The joint MLE's of λ and τ_0 can again be found using a one-dimensional search along τ_0 for the same reason that was given for the normal likelihood for X.

A practical problem with the specification of the model above is that fitting the model requires the calculation of the integral $D_j(\tau_0)$ and this generally requires a special purpose computer program such as DEVAR which uses the trapezoidal rule, eqn (7.6), and the least squares estimation given by eqn (7.7). Even if such is available the memory required for some data sets can be enormous. In this study (Section 3.3) numerical integration of a combination of temperature/time traces and spline curves fitted through daily minimum and maximum temperatures using 15 minute time

intervals for a range of roughly 400 to 850 days resulted in a very large database for the calculation of $D_j(\hat{\tau}_0)$. In the iterative ML estimation algorithm described above, $D_j(\hat{\tau}_0)$ needs to be re-calculated when $\hat{\tau}_0$ is updated at each iteration. The computational burden this imposes on the algorithm could make it impractical to implement. An alternative method used in this study, which does not require the integration to obtain $D_j(\hat{\tau}_0)$ to be carried out within the ML estimation procedure, involves carrying out the integration given in eqn (7.6) prior to using the ML estimation procedure by using pre-specified integer values of τ_0 ranging from say, 0 to 20 degrees. Then employing the resultant values of $D_j(f)$, f=1,...,21, where f indexes the integer values of τ_0, in the search for the MLE of τ_0 involves using the current iteration's estimate of τ_0 and linear interpolation to obtain $\tilde{D}_j(\hat{\tau}_0)$, where

$$\tilde{D}_j(\hat{\tau}_0) = D_j(f_\tau)+\{\hat{\tau}_0-int(\hat{\tau}_0)\}[D_j(f_\tau+1)- D_j(f_\tau)] \quad ,$$

$$f_\tau = int(\hat{\tau}_0) + 1, \qquad int(.) \text{ means 'integer part of ',}$$

and searching for the value of $\tilde{D}_j(\hat{\tau}_0)$ which maximises the log-likelihood. This allows the algorithm to be implemented using standard optimisation software such as the FITNONLINEAR directive in GENSTAT which was used in this study. Appendix 5 gives the GENSTAT commands to implement the algorithm for log-likelihood (7.12) using the data obtained for this study and described in the results section.

For the following the fit of the model is expressed in terms of the deviance, $\mathscr{D}$ (Appendix 1), rather than the log-likelihood, $\mathscr{L}$. When $\mathscr{L}$ is given by (7.10) then

$$\mathscr{D} = \Sigma_j\, m_j(x_j - \hat{\lambda})^2 \qquad (7.13)$$

and when $\mathscr{L}$ is given by (7.12) then

$$\mathscr{D} = \Sigma_j\{m_j log(m_j /\hat{\mu}_j)-(m_j - \hat{\mu}_j)\} \qquad (7.14).$$

The deviance divided by the degrees of freedom (n-2) gives an estimate of ϕ which is equivalent to σ^2 in the case of X normal and $1/\theta$ when Y is gamma (McCullagh and Nelder 1983, Appendices 1 and 4 here). Maximizing $\mathscr{L}$ (with respect to λ and τ_0) is equivalent to minimizing $\mathscr{D}$

7.3 Fitting the day-degree model to *P.subgranosus* emergence data

7.3.1 Data

Data on the time from attack to emergence were provided firstly by the author's emergence cages of which 59 produced emergents all occurring in the second summer (85/86) after attack (Feb-May,1984) (Section 3.1.3) and secondly by 12 out of the 58 emergence cages of Elliott and Bashford (SILV) for which the time of attack was known (Section 3.2). Only emergence occurring in the same summer in which emergence for the cage began for both sets of cages (i.e. the first brood from the gallery) is considered for the following. Of the 12 SILV cages, 11 produced emergents in the first summer after attack. Attack for the SILV cages occurred early to mid-summer (28/12/80 for 11 cages and 12/1/81 for the remaining cage) and emergence began late in the following summer with the exception of one cage where the gallery was established on 28/12/80 and only produced a single male and female collected on 16/2/83, two summers later. For the author's cages, attack occurred late in the summer of 83/84 and the first emergents did not appear until December 1985.

Fig 7.2 shows the distribution of days from attack to emergence separately for each set of cages where the SILV cages are identified by the years 80-83 and the author's cages by the years 84-86 which in each case is the period during which cages were established and observed. Each of gallery establishment and emergence were observed at roughly weekly intervals. Considering only the first year of emergence for a gallery, a total of 381 emergence occasions (i.e. the number of galleries with at least one emergent totalled over the collection dates), producing a total of 952 emergents, were recorded. The majority of these data came from the 59, 84-86 emergence cages which accounted for 334 of the emergence occasions and 865 of emergents.

For a particular gallery and emergence occasion m_j individuals are observed to have emerged (completed development) between the date the gallery was checked and

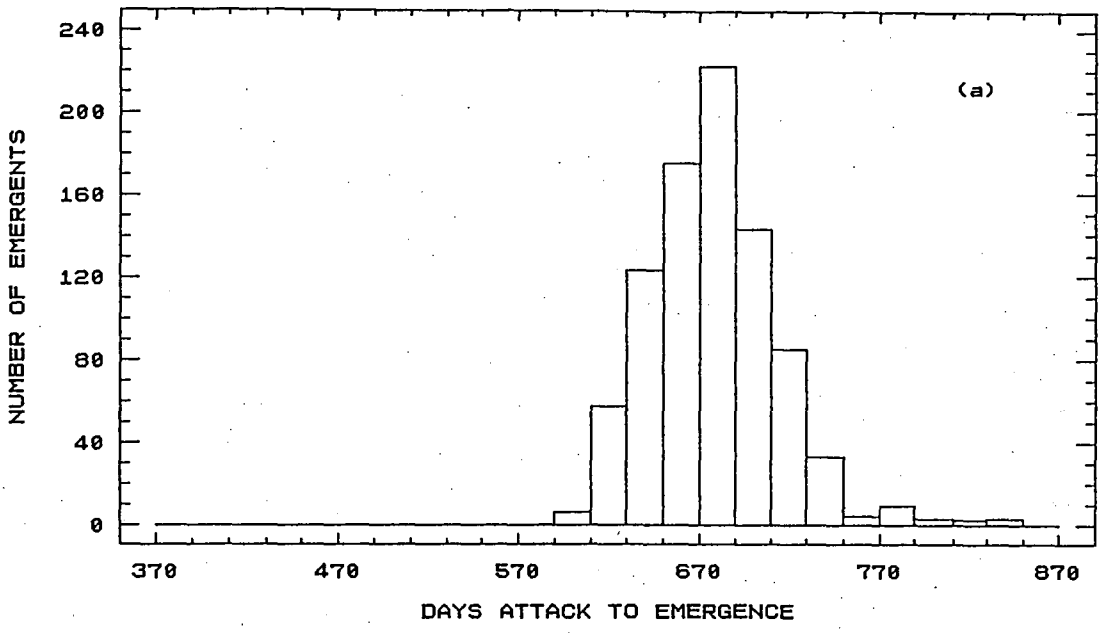

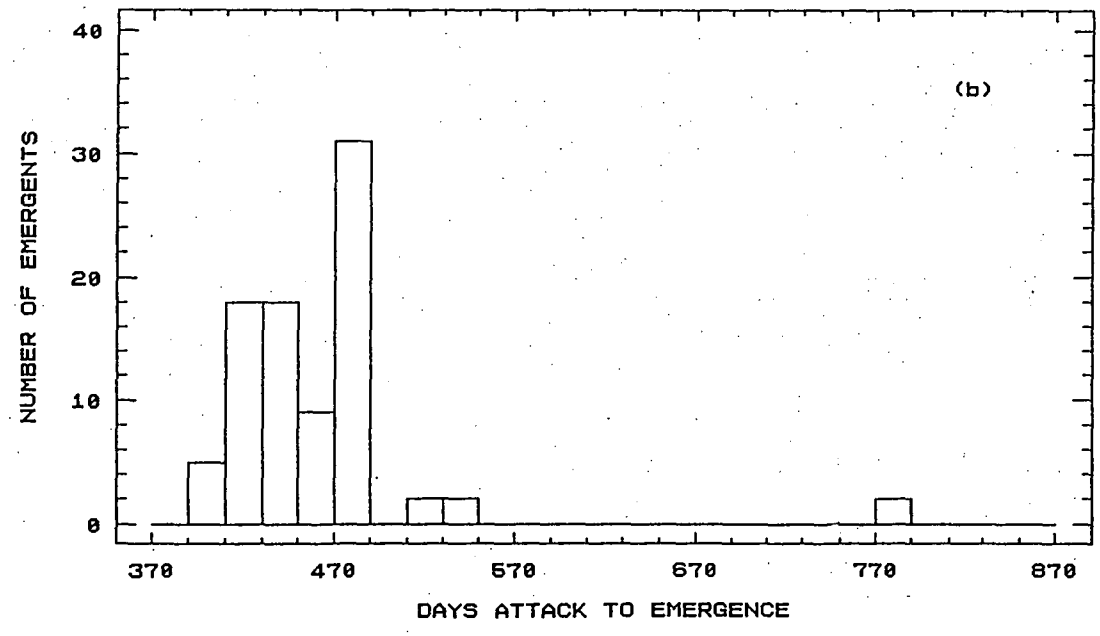

FIG 7.2 Days from attack to emergence (a) 84-86 (b) 80-83 first year emergence data

the date it was previously checked and, if necessary, cleared. For each individual the date on which it emerged is unobserved. The parallel situation applies to attack for which only the period between checking dates in which gallery establishment occurred was known. Since the period between checks of attack and emergence was roughly a week in each case and this is a short time interval relative to total development time, for the following the approximation that all m_j individuals emerged on the date when they were collected and that gallery establishment occurred on the date it was discovered will be used. The difference between these two dates gives l_j. This approximation should have little effect on the estimation of the parameters as mentioned earlier.

7.3.2 Maximum likelihood estimation

Initially all 381 values of m and corresponding values of $D(\tau_0)$ for τ_0=0,...,16 were used in the fit of the model. Fig. 7.3 shows the value of the deviance (7.14) for integer values of τ_0 and the corresponding MLE of λ. The corresponding figure for deviance (7.13) (graph not shown) was very similar to Fig. 7.3. It can be seen from Fig 7.3 that there is not a clear optimum value (in terms of minimum deviance) for τ_0 other than a general region somewhere below 10 or 11 degrees. As would be expected under these conditions the iterative search algorithm using linear interpolation did not converge for either of log-likelihoods (7.10) or (7.12).

The minimum temperature at which emergence was observed to occur, $T_{min}(l)$, was calculated as the minimum, over the 381 emergence occasions, of the maximum temperature occurring in the period between the dates on which the cages were checked. These maxima were used because emergence could have occurred at any time in the period so a conservative minimum value for τ_0 should be based on the maximum of the daily maxima for the period. The value so obtained was 13°C for emergence occurring between the 15th and 22nd of April 1982. $T_{min}(l)$ thus provides an upper limit for τ_0 consistent with Fig 7.3.

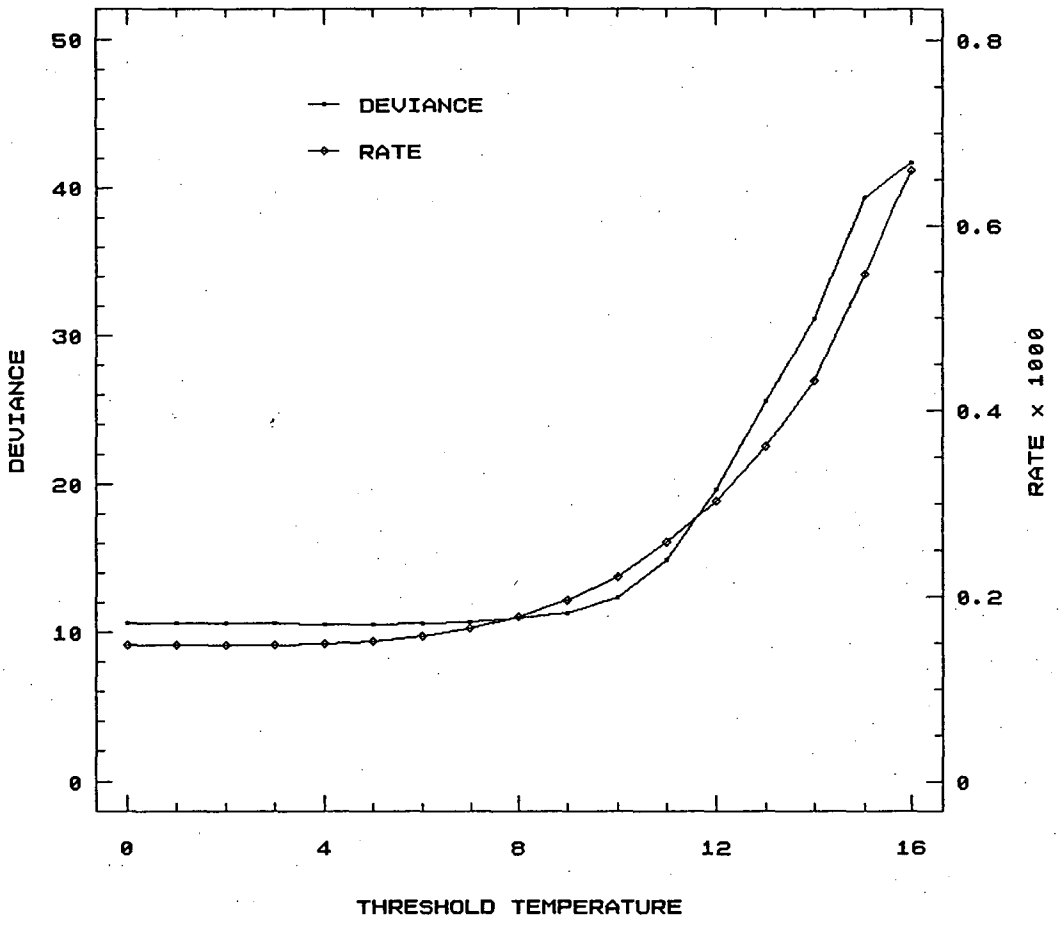

FIG 7.3 Deviance and development rate versus threshold for all first year emergence data

The problem of a lack of a clear optimum value for τ_0 was recognised to be the dominance of the 84-86 data in the fit. As mentioned earlier, all the emergents in the author's data set were exposed to the same winter periods but different proportions of the two summers (i.e. attack and emergence both occurred in summer) so the differences in the length of development within this data set can be assumed to largely reflect differences, apart from individual variation in thermal requirements for development, in the proportion of time spent in the upper end of the temperature scale (i.e. different length of time exposed to summer temperatures) rather than at the lower temperature range. In other words the 1984-86 data alone does not provide much information about τ_0. Where the ambient temperature ranges above and below τ_0 the time below τ_0 does not, according to the model, contribute to development which explains the large difference in number of days taken for development between the 84-86 data and the 80-83 data shown in Fig 7.2. A similar separation on a day-degrees above 0°C scale is apparent in Fig 7.4. It is this difference reflected in the different exposures to winter temperatures between the two data sets that will allow τ_0 to be estimated. So to make the data more balanced between the two data sets, which could be considered samples from two temperature regimes, 47 of the m values were randomly selected from the 84-86 data and these data were combined with the 47 values in the 80-83 data to give 94 values of m and corresponding values of $D(\tau_0)$ for τ_0=0,...,16. The above random selection was repeated 10 times to give 10 such data sets. Fig 7.5 shows deviance (7.14) versus integer values of τ_0 for the 10 data sets. Fig 7.6 shows the mean, over the 10 data sets, of deviance (7.14) and $\hat{\lambda}_g$ versus τ_0. There is now a clear optimal region for τ_0 somewhere between 9 and 11 degrees. Fig 7.7(a) shows the deviance (7.14) surface, for one of the 10 data sets, for a grid of τ_0 and λ values and Fig 7.7(b) shows the corresponding deviance contours. Again the optimal region for τ_0 lies roughly between 9 and 11 degrees with corresponding region for λ roughly between 0.00020 and 0.00025. The direction of contours in Fig 7.7(b)

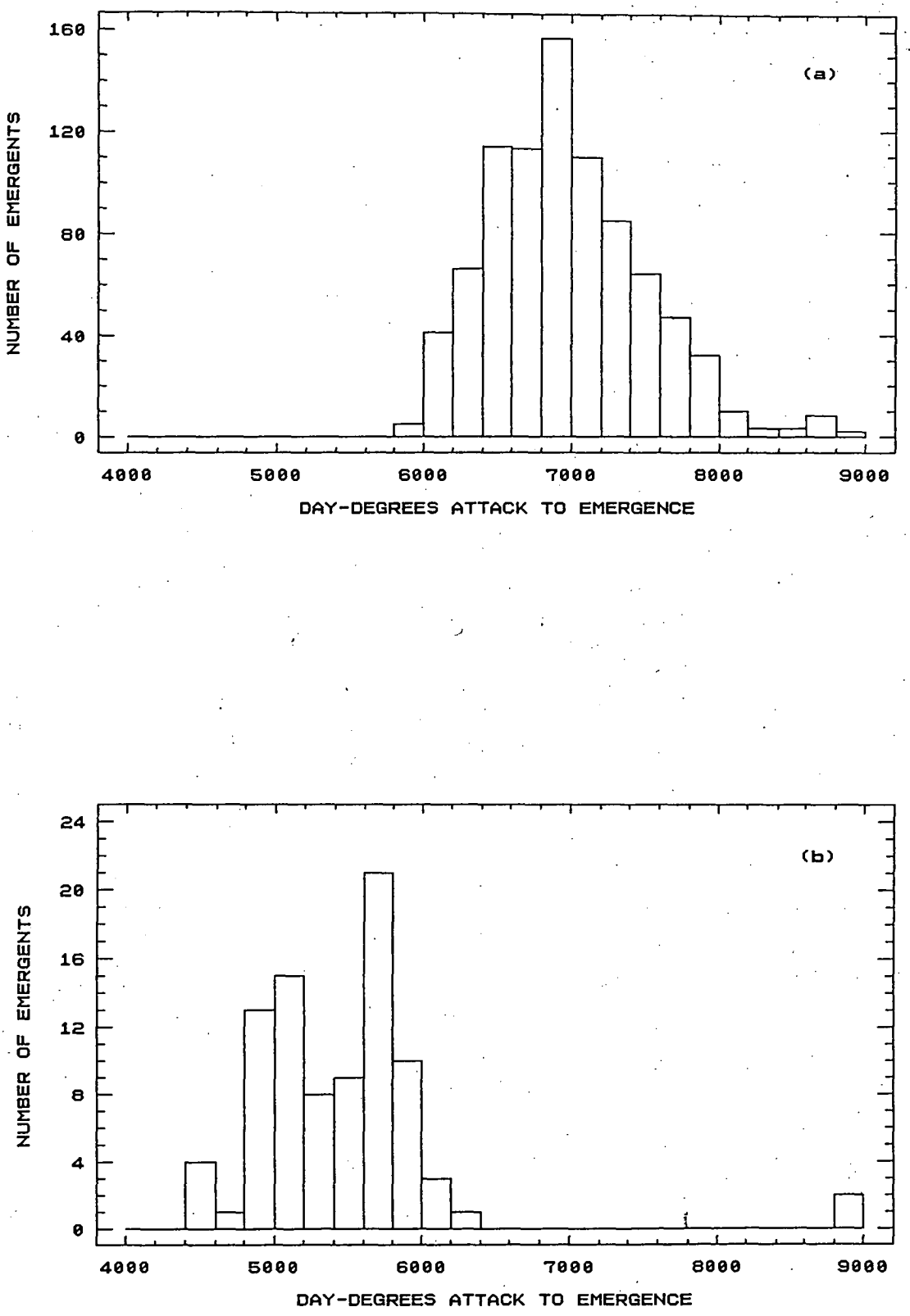

FIG 7.4 Day-degrees above a 0degC threshold from attack to emergence
(a) all 84-86 data (b) 80-83 first year emergence data

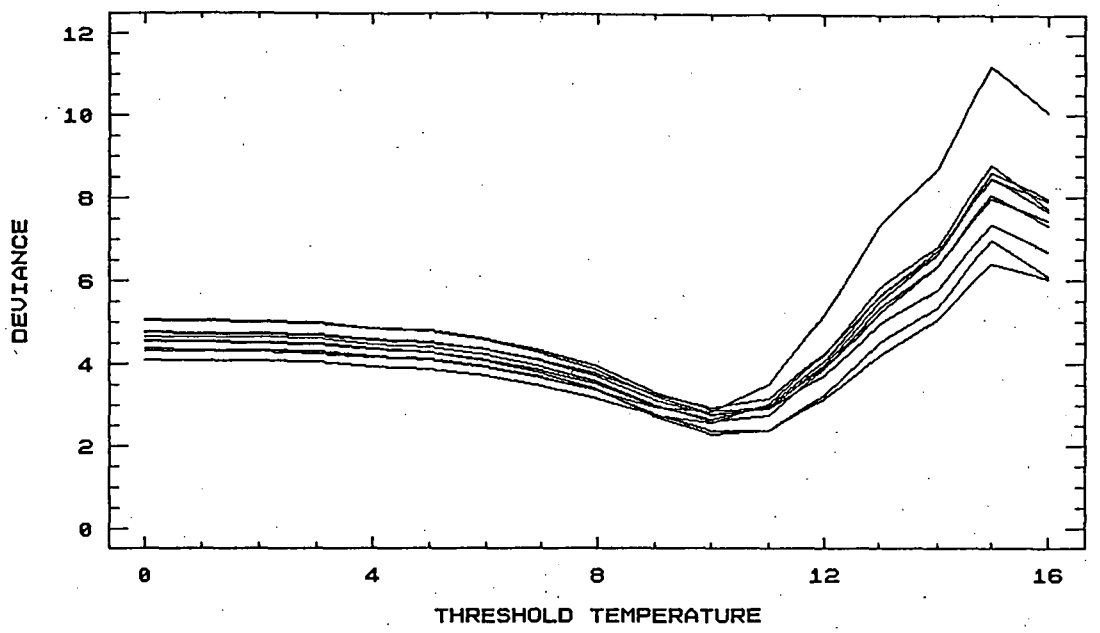

FIG 7.5 Deviance versus threshold using 80-83 data and 10 samples from the 84-86 data

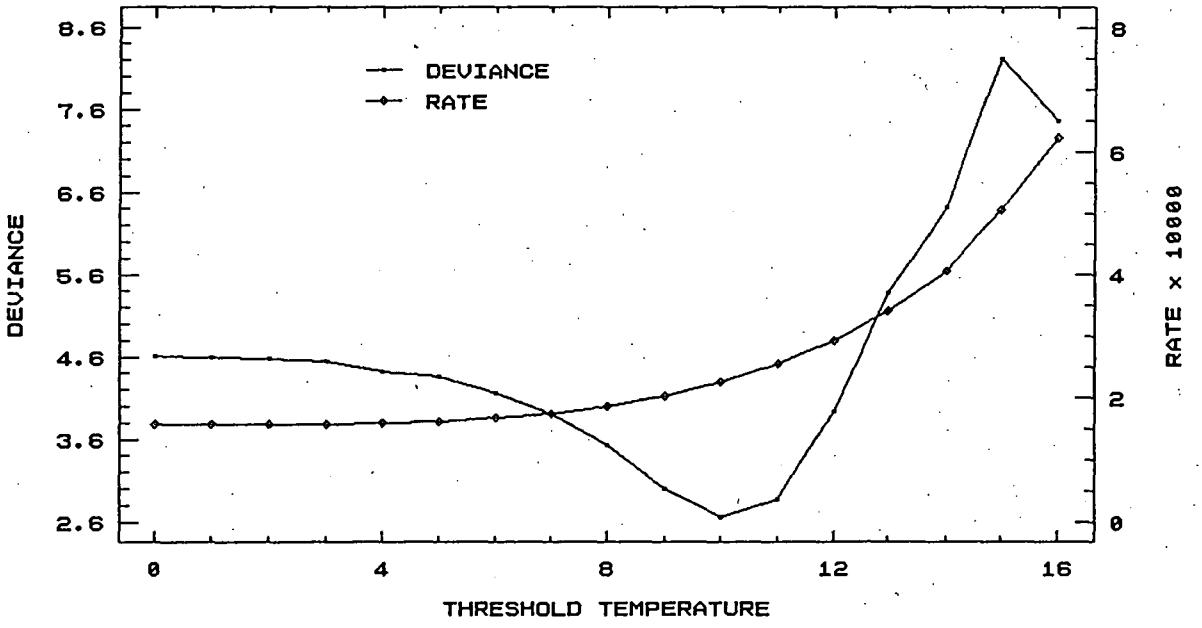

FIG 7.6 Deviance and development rate averaged over 10 data sets

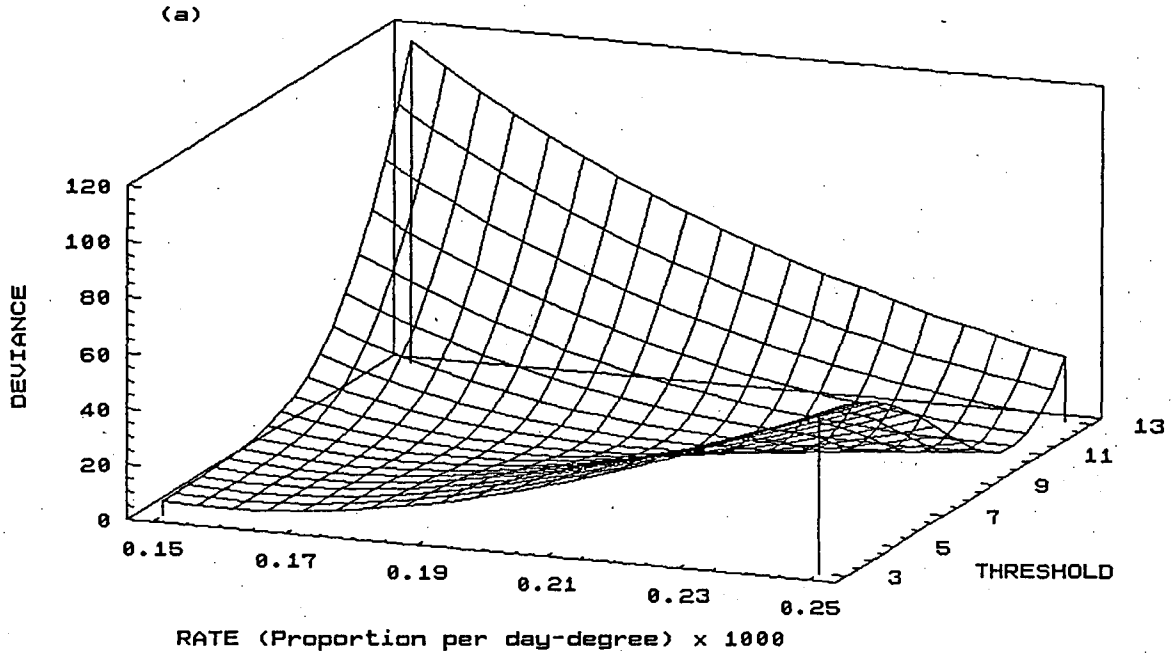

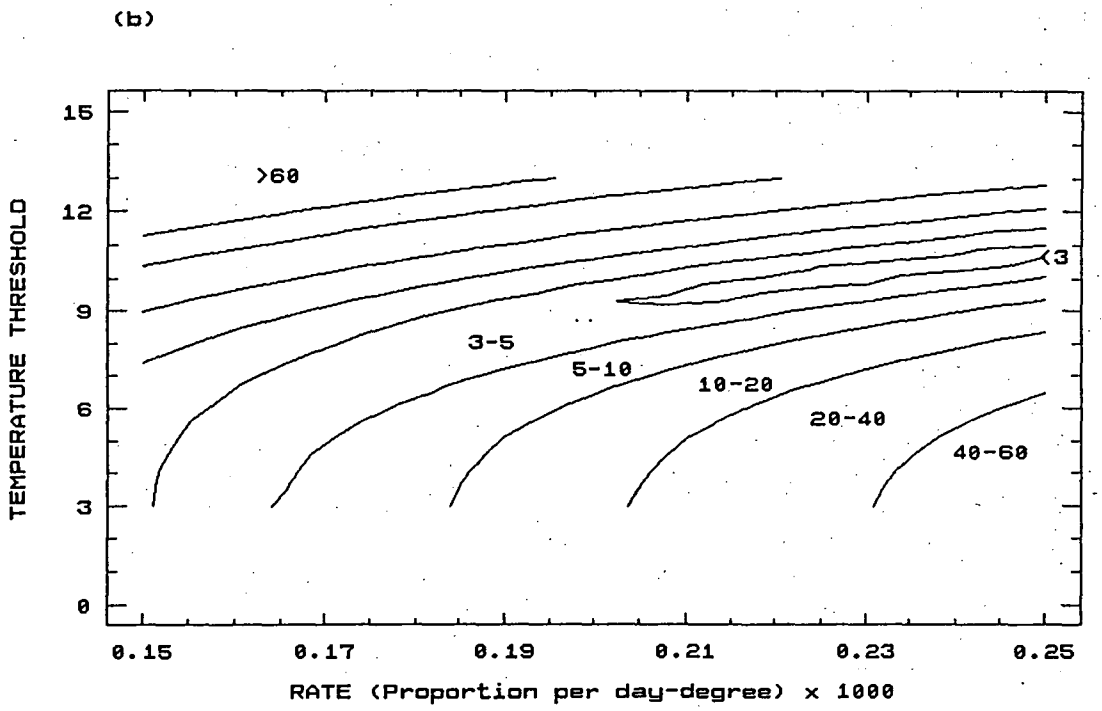

FIG 7.7 Deviance (a) surface (b) contours for rate and threshold grid using one sample from 84-86 and all 80-83 data

demonstrates the positive correlation between $\hat{\tau}_0$ and $\hat{\lambda}_g$ as would be expected : as $\hat{\tau}_0$ increases $D(\hat{\tau}_0)$ decreases and $\hat{\lambda}_g$ therefore increases. The iterative search algorithm using log-likelihood (7.12) was employed in GENSTAT (Appendix 5). For the case of log-likelihood (7.10) the random subsampling did not improve the estimation of τ_0. The graphs (not shown) corresponding to Figs 7.5 and 7.6 did not show a clear optimum region but looked very similar to Fig 7.3 and as a result the search based on log-likelihood (7.10) failed to converge for every subsample. The reason for the failure of the algorithm based on normal X is not clear but possible explanations are discussed later.

Table 7.1 gives some statistics on the subsample MLE's of τ_0 based on log-likelihood (7.12) along with those for the corresponding MLE's of λ. Taking the mean of the $\hat{\tau}_0$'s gives a point estimate of 10.74, however very little difference in goodness of fit would be obtained whatever value was used for τ_0 in the range 10 to 11. For the following the abbreviation DD_{11} will be used to denote the value of $\tilde{D}(\hat{\tau}_0)$, where $\hat{\tau}_0$ is taken as 10.74°C, obtained by the interpolation given in Section 7.2.

7.3.3 Adequacy of the day-degree model, inverse normal and gamma distributions

Individual values of DD_{11} were used to construct histograms one for each of the 80-83 and 84-86 data using all 334 emergence occasions in this last case. These histograms are shown in Fig 7.8 and it can be seen that there is now a large degree of overlap in the histograms for the two data sets. Table 7.2 gives statistics separately for each data set for days from attack to emergence, DD_0 (i.e. τ_0=0) and DD_{11}. It can be seen from Table 7.2 that only for DD_{11} is there no significant difference in the means between the two data sets. The range of values of DD_{11} is also very similar for both data sets. The day-degree model given by eqn (7.5) with a value of $\hat{\tau}_0$ around 10 or 11°C has been able to explain the large difference in mean development time between the two data sets as seen in Fig. 7.2.

Fig. 7.9 shows the observed frequency histogram of Y=DD_{11} using all 952

Table 7.1 Statistics for MLE's of temperature threshold (τ_0) and rate (λ) parameters estimated from 1981-85 emergence data combined with 10 random samples from the 1985/86 data.

	mean	standard deviation	minimum	maximum
Threshold ($\hat{\tau}_0$)	10.7408	0.5177	9.6734	10.9983
se($\hat{\tau}_0$)	1.4754	0.1766	0.0866	1.8731
Rate ($\hat{\lambda}_g$)	0.2237_x10^{-3}	0.1341_x10^{-5}	0.2215_x10^{-3}	0.2256_x10^{-3}
se($\hat{\lambda}_g$)	0.0487_x10^{-3}	0.1271_x10^{-5}	0.0467_x10^{-3}	0.0511_x10^{-3}
Deviance	2.6506	0.2116	2.2645	2.9280

Table 7.2 Statistics on days and cumulative day-degrees from attack to emergence based on all first year emergence data with known attack date.

	sample size	mean	standard deviation	standard error	min	max
Days (81-85)	87	458.1	58.8	6.3	393	780
Days (85/86)	865	679.5	35.4	1.2	610	841
DD_0[a] (81-85)	87	5486	662	71	4560	8888
DD_0 (85/86)	865	6980	557	19	5993	9443
DD_{11} (81-85)	87	4056	473	51	3239	6207
DD_{11} (85/86)	865	4046	511	17	3210	6282
DD_{11} (81-84), (85/86)	952	4047	507	16	3210	6282

a. Day degrees accumulated above a τ_0=0 threshold temperature

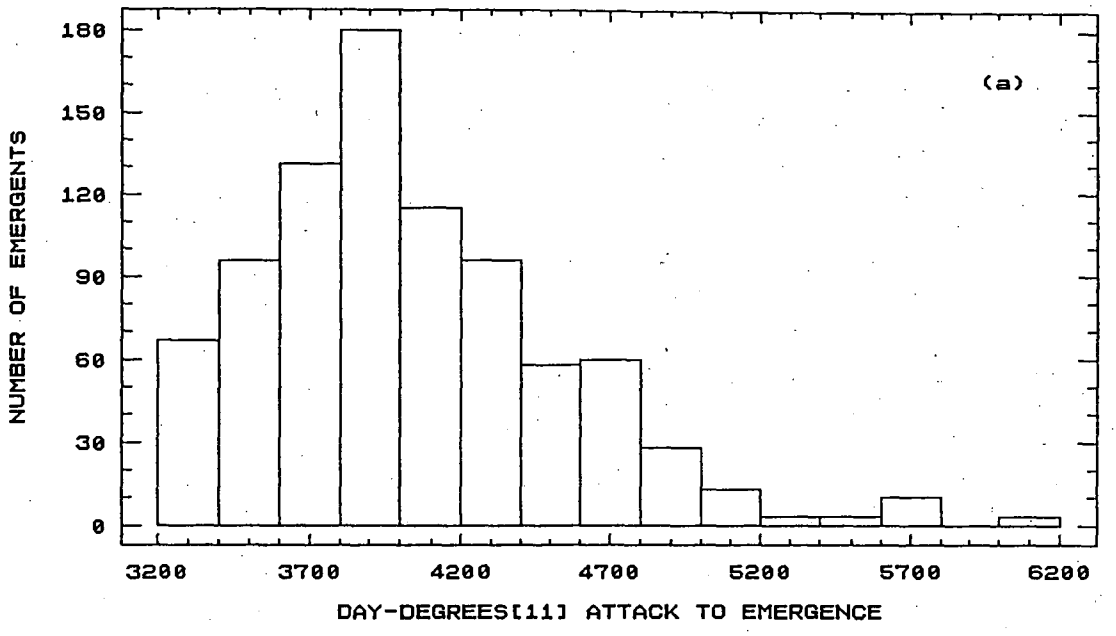

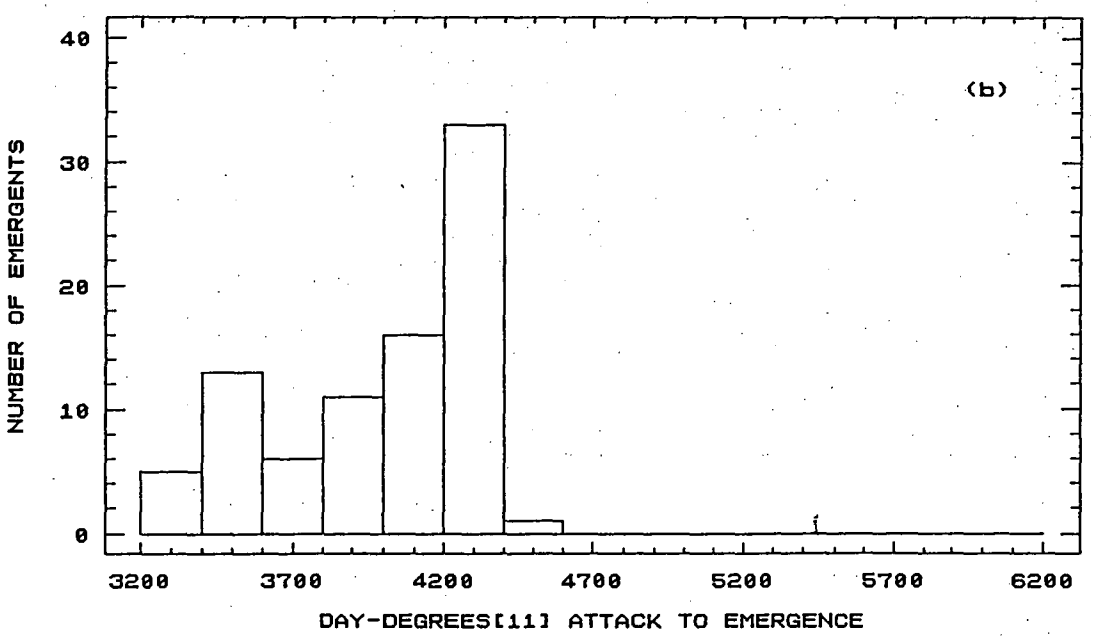

FIG 7.8 Frequency of time from attack to emergence in units of day-degrees[11] (a) all 84-86 data (b) 80-83 first year

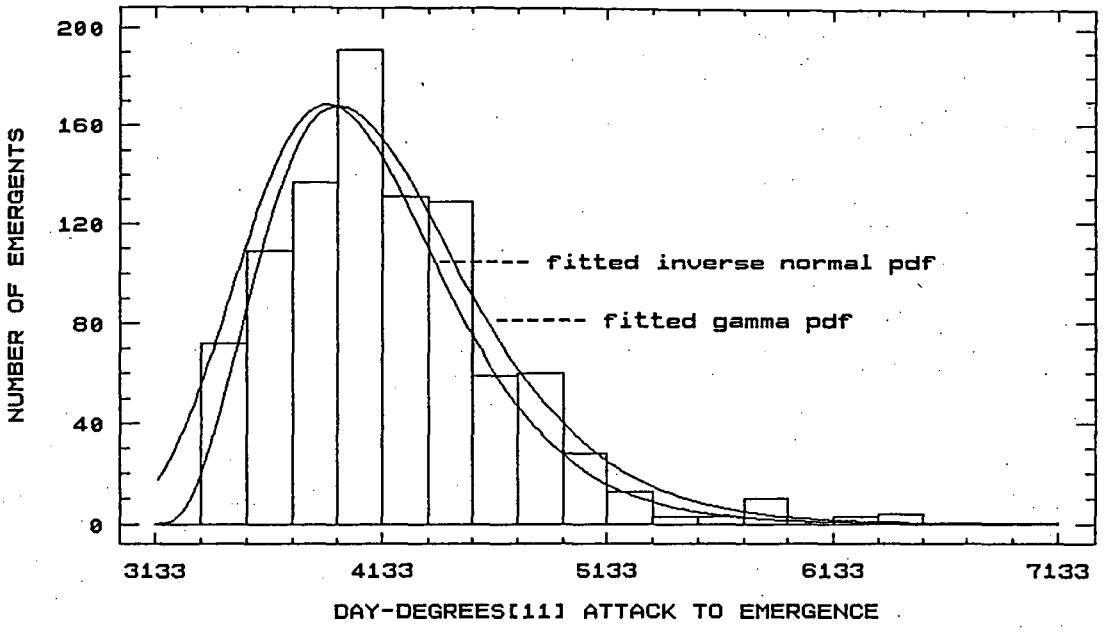

FIG 7.9 Distribution of time from attack to emergence in units of day-degrees[11] : all data

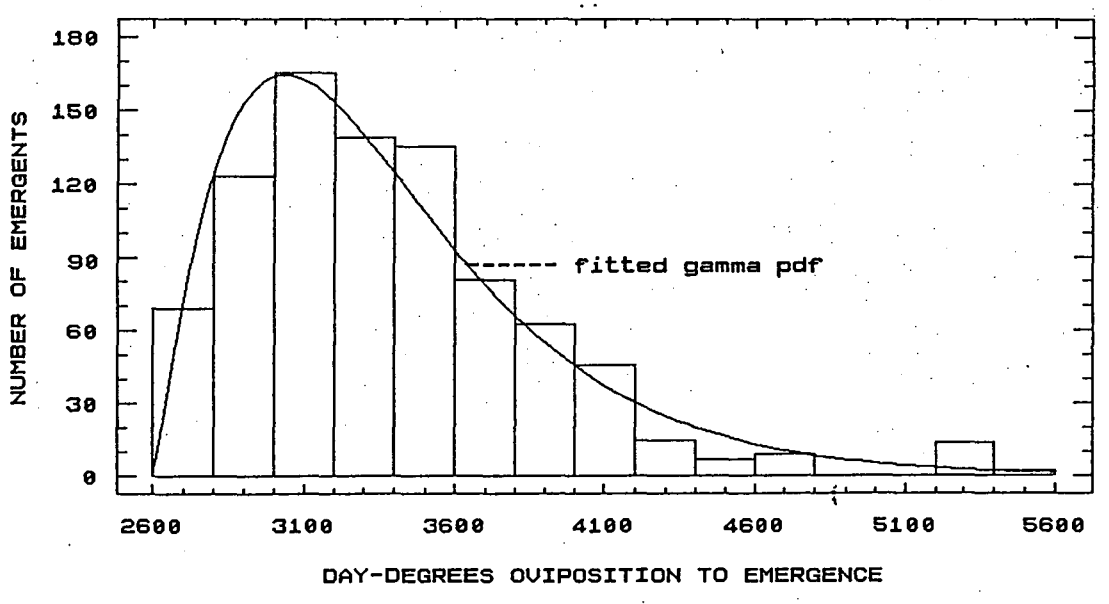

FIG 7.10 Distribution of development time in units of day-degrees[11] : 1984-86 data

($=\sum_{j=1}^{381} m_j$) values along with fitted frequencies for each of the inverse normal, based on the transformation $Y=1/X$ with X normal with mean λ and variance σ^2 (Sharpe *et al.* 1977), and gamma distribution models. For the gamma an estimate of ξ was obtained using the method of moments (Johnson and Kotz 1970) as 3133. The frequencies for the inverse normal were obtained using estimates of λ and σ^2 obtained simply as the mean and variance of the 952 values of $1/DD_{11}$. The two models produce similar shaped distributions each of which appears visually to be an adequate representation of the empirical distribution. Using a modified Kolmogorov-Smirnov test with statistic $d_{max} = \max|\tilde{F}_j - F_j|$, where $\tilde{F}_j$ is the cumulative probability under the model to x_j or y_j, as the case may be, and F_j is the observed cumulative probability given by $\sum_{i=1}^{j} m_i / \sum_{i=1}^{n} m_i$ where n=381, the fit of the normal to $1/DD_{11}$ was slightly superior (d_{max}= 0.038) to the fit of the gamma to DD_{11} (d_{max}= 0.065). Stinner *et al.* (1975) used a beta distribution for development time under constant temperature regimes. Using the beta here for DD_{11}, with lower and upper limits of 3200 and 6290 respectively, the fit of the beta was worse (d_{max}= 0.192) than either of the above models. In the case of the normal and gamma distributions the d_{max} statistic did not lead to a rejection (P>0.05) of the null hypothesis that the empirical was not different from the theoretical distribution.

7.4 Development time from initial oviposition to emergence

Attention above has been restricted to development time from gallery establishment to first brood emergence because these events are observed externally. Also any simulation/prediction system based on field data is likely to have as starting point for development, observations on gallery establishment rather than difficult-to-observe oviposition. Nevertheless, development time from initial oviposition (Sections 2.3.3 and 5.2) to first brood emergence, assuming the initial batch of eggs laid produces the first brood of emergents, is also of interest. The distribution

of times, in units of DD_{11}, from initial oviposition to emergence based on the 865 emergents obtained in the 85/86 summer is given in Fig 7.10 along with a fitted gamma distribution using a value for ξ of 2600. The values of DD_{11} used to construct Fig 7.10 were calculated by subtracting the mean value of DD_{11} accumulated from gallery establishment to initial oviposition for the particular establishment date for the gallery (Section 5.2) from the observed value of DD_{11}, for the individual emergent, accumulated from gallery establishment to emergence. An average time to initial oviposition was not used because of the relationship between establishment date and time to oviposition (Section 5.2). As can be seen in Fig. 7.10 the gamma fits quite well.

7.5 Effect of timing of attack on timing of emergence

Given the effect of timing of attack on the timing of initial oviposition reported in Section 5.2, the possibility that a similar effect occurred for timing of emergence was investigated. Attention was restricted to the 84-86 data because there were only two attack dates for the 80-83 data, both of which were in early summer. Fig 7.11 shows the mean time from attack to emergence versus time from the first observed attack over all galleries (i.e. 9/2/84). Mean time from attack to emergence was calculated as the mean, over all galleries with same attack date, of mean time for the gallery (i.e. over all first year emergents). A similar trend to that seen in Fig 5.9 is obvious in Fig 7.11 in that development time is longer for early versus later attack within the late summer/autumn period. The longer development time was found (graph not shown) to be due to the time difference between attack dates since earlier attack produced emergents no sooner than later attack. This is contrary to the case of spring/early summer versus late summer/autumn attack where in the former case the extra exposure to summer temperatures allows shorter calendar time to emergence as quantified by the day-degree model above. The 'thermal advantage' of earlier established galleries within the late summer/autumn period is not similarly exploited.

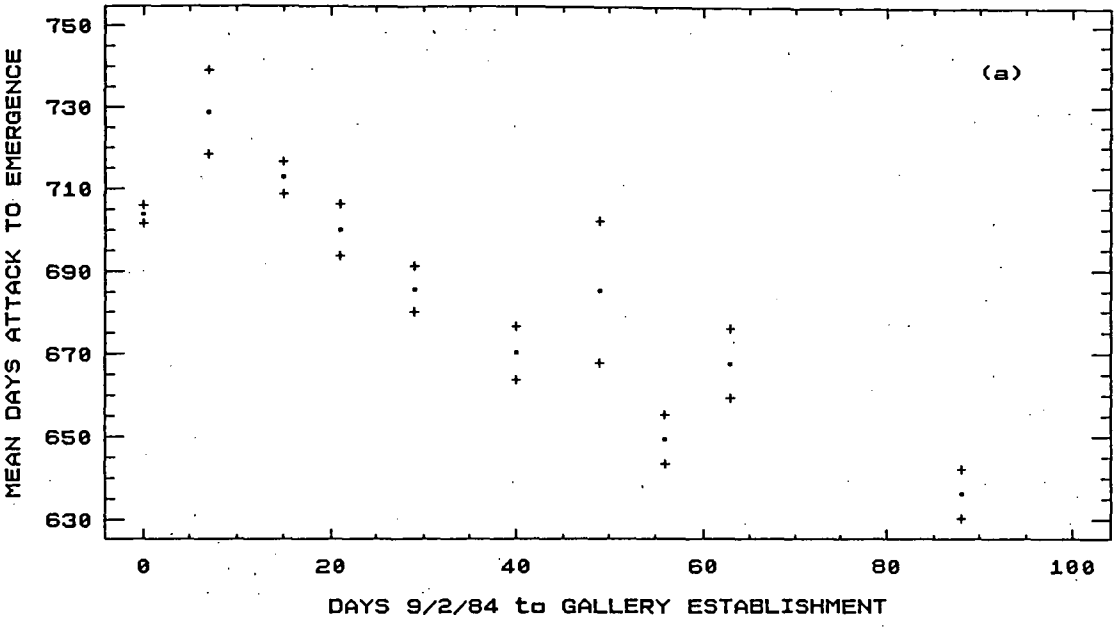

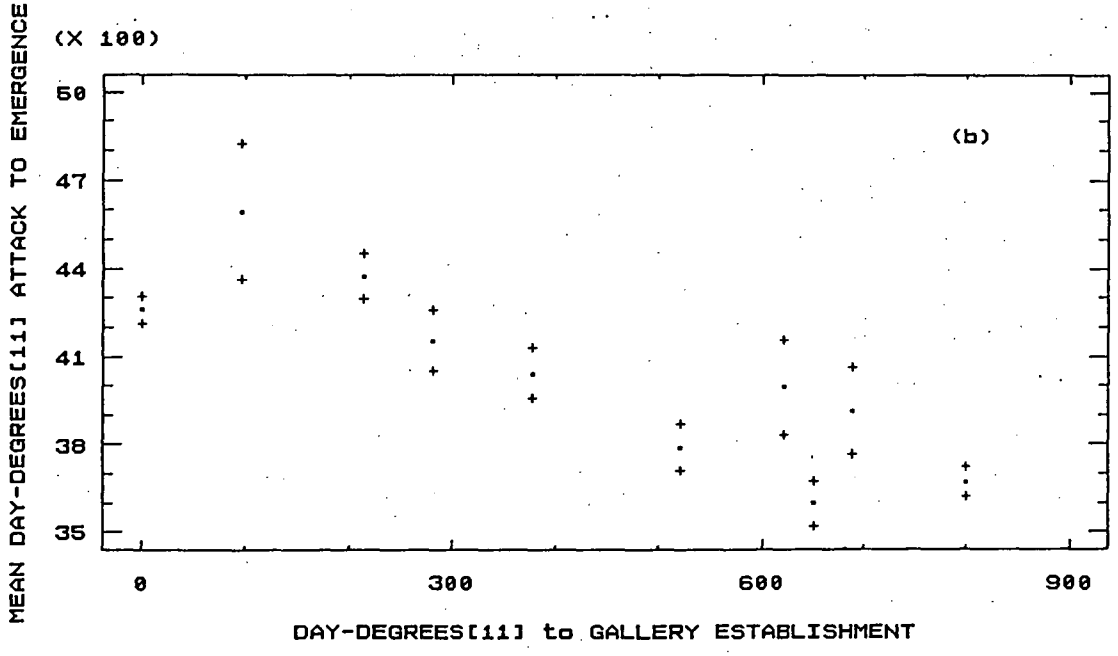

FIG 7.11 Mean of gallery mean time from attack to emergence versus time from 1st to later gallery establishment in units of (a) days (b) day-degrees[11], with (+) standard error bars

7.6 Discussion

The day-degree model of the development rate/temperature relationship has been criticised for its inability to account for curvature in the observed rate versus temperature relationship obtained in laboratory studies (Wagner *et al.* 1984). Nonlinear models such as the general model of poikilotherm development of Sharpe and DeMichele (1977) have been used to account for the above nonlinearity. However, temperatures above the optimal temperature at which the insect is adversely affected (Fig 7.1) rarely occur in the field (Gilbert 1988) and this is especially so here where both the rainforest canopy and surrounding wood damps temperature extremes inside the galleries. The simple day-degree model, though, will under-estimate development rate near the lower threshold, τ_0 (see Fig 7.1) (Howe 1967) so it is the adequacy of this model at temperatures around τ_0 that is more important here. However, Howe (1967) questioned the extra efficacy of purely empirical nonlinear models such as those based on the cumulative density functions of statistical distributions such as the logistic and normal. It is not easy to see the biological significance of the parameters of these purely empirical nonlinear models. A lower threshold temperature on the other hand has a natural interpretation and, given that it is under genetic control, is a useful concept for genetic studies (Gilbert 1984, 1986 and 1988). Also the curvature in the development rate versus temperature relationship at lower temperatures can be explained in terms of individual variation in τ_0 (Howe 1967, Gilbert 1984). The day-degree model assumes τ_0 is constant but a version of the day-degree model that allows τ_0 to have a statistical distribution could be developed using stochastic differential equations [i.e. since τ_0 appears within the integral in eqn (7.2)]. It was, however, beyond present resources to investigate such a model here. A further advantage of the day-degree model is that it gives a physiological time scale which was exploited here to allow estimation to be based on the assumed distribution of $D(\tau_0)$. Nonlinear models do not necessarily perform better than the day-degree model

for all development stages (Allsopp 1986, Richmond and Bacheler 1989) and given the greater difficulty of fitting these models often due to the large number of parameters involved, Sharpe and DeMichele's (1977) model [reparameterised by Schoolfield *et al.* (1981)] has six parameters, they may not be a practical alternative to the day-degree model in the case of field-collected data. The practical problem of fitting any model when the development time is as long as that seen here was overcome using the linear interpolation method described here for the day-degree model where the accuracy in the calculation of day-degrees for different threshold temperatures was maintained without a large requirement for computer memory. The day-degree model was found to adequately describe the data in this study, in particular the difference in development time resulting from early summer versus late summer/autumn gallery establishment. The gamma and normal distributions both adequately described the empirical distribution of development time and rates respectively but the reason(s) for the failure of the maximum likelihood estimation procedure in the case of the normal is not clear at this time. The estimation based on the gamma distribution on the other hand was highly successful in locating an optimum value for τ_0. A possible explanation of the failure of normal X (inverse normal $Y=1/X$) is the scale of X. Since X is the inverse of development time in physiological time units, $D(\tau_0)$, where $D(\tau_0)$ is large but decreasing with increasing τ_0, then the weighted sum of squares, eqn (7.13), used to estimate the parameters will be very small. The role of the Jacobian is to account for the change of scale as $D(\tau_0)$ varies with τ_0, however, the adjustment to the likelihood due to the Jacobian only managed to provide an upper limit for τ_0 as mentioned in Section 7.2. The reason for the success of the gamma likelihood could be due to the way it was expressed in eqn (7.12) as that of a Poisson for the number of emergents m_j which, like l_j , is observed.

The least squares minimisation given by eqn (7.7) and used by DEVAR gives a biased estimate, $\hat{\lambda}_s$, of the rate parameter λ. The bias of $\hat{\lambda}_s$ was approximated earlier by

a formula given in terms of λ and σ^2, the variance of X. Using the mean and variance of $X=1/D_{11}$ this bias is roughly -1.3%. The ML estimate of λ based on the normal distribution for X and gamma distribution for Y have the advantage that they are respectively unbiased and asymptotically unbiased.

The day-degree model here has been based on ambient temperatures under the canopy, however, it is the air temperature within the gallery that *P.subgranosus* is directly exposed to. The temperature inside the gallery would be damped by surrounding wood compared to outside temperatures and would probably also lag behind outside temperatures. It was beyond the resources of this study to collect within-gallery temperatures but in practice, if the day-degree model is used to predict *P.subgranosus* emergence, as discussed in Section 8.3, then temperature recording would also be restricted to ambient temperatures outside the tree or log.

The observation that attack and subsequent gallery establishment early in the late summer/autumn period did not translate into earlier emergence compared to galleries established late in this period has been discussed earlier (Section 2.3.3 and 5.6). To reiterate, this observation is explained as a flow on effect of initial oviposition being delayed for early establishment to about the same calendar dates as late establishment. This winter oviposition was hypothesised to be a response to high summer mortality of eggs and early instars due to desiccation.

8. IMPLICATIONS FOR RAINFOREST ECOLOGY AND FOREST MANAGEMENT

8.1 *P.subgranosus* and myrtle wilt

The role that *P.subgranosus* plays in the ecology of Tasmania's cool temperate rainforests depends to a large degree on its role in the spread of myrtle wilt. Myrtle wilt is recognised as a major factor in the ecology of these rainforests. It can be locally severe with cumulative deaths reaching roughly 50% of the myrtle component of the stand. The gaps in the canopy caused by myrtle wilt are important in regeneration processes (Hickey and Felton 1987) and can result in locally altered stand structure. Given a low and stable incidence of myrtle wilt in undisturbed rainforest, myrtle wilt may be viewed simply as a component of natural regeneration processes along with other natural disturbances such as wildfire and windthrow. Alternatively, the mean incidence of dying *N.cunninghamii* observed in undisturbed rainforest of roughly 2.4 trees ha^{-1} or 1.6% of live trees per year (Elliott *et al.* 1987), being of the same order as serious epidemics such as Dutch Elm Disease in Great Britain, could represent part of a trend for myrtle wilt to be increasing to a serious epidemic. Kile *et al.* (1990a) suggest that if this is true it could be due to the development of new, more aggressive strains of the pathogen or promotion of disease development through greater human access to, and disturbance of rainforest. Current research by the Silvicultural Division of the Forestry Commission, Tasmania, is addressing the problem of the status of myrtle wilt using rate-of-spread plots in which the spread of the disease is monitored on permanent plots. In rainforest managed for timber production or public amenity, any silvicultural management practices will need to consider the impact of myrtle wilt on stand health and timber production. Kile *et al.* (1990a) have discussed possible management practices which will reduce the incidence and impact of myrtle wilt. As for the role of *P.subgranosus* in the spread and management of myrtle wilt, current opinion is that, quoting Kile *et al.* (1990a),

'..*while* P.subgranosus *is not a direct vector of* C.australis *it has the potential to*

be of significance in disease spread through liberation of contaminated frass, creation of wounds (pinholes) in stressed trees, and through promotion of spread within trees already infected.', and

'*As* P.subgranosus *is a secondary agent it seems unlikely that attempts to manage beetle populations would have a significant effect on disease development, except possibly if frass contaminated with* C.australis *is important as inoculum.*'

It can be seen from the above that the most important task in *P.subgranosus* research is determining the role of the beetle in the spread of myrtle wilt. Strategies for controlling *P.subgranosus* populations and infestations may be required within a management programme for the control of myrtle wilt if *P.subgranosus* is important in the spread of myrtle wilt. Such strategies should be similar to those discussed below for controlling *P.subgranosus* infestations of freshly cut logs in current forest operations.

8.2 Possible measures to control degrade of valuable logs due to *P.subgranosus* attack

A moratorium on logging in rainforest, excluding mixed forests with more than 5% eucalypt crown cover which are harvested and regenerated to eucalypt, is currently due to end. Given current logging of mixed stands and future logging of pure rainforest including possible clearfell, selective logging and thinning in pole sized stands, *P.subgranosus* attack of, and gallery development in high value logs is an important problem for forest operation managers. Valuable sawlogs and veneer logs of species, including the eucalypts *E.regnans*, *E.obliqua*, *E.delegatensis* and rainforest species *N.cunninghamii*, *A.moschatum* (sassafras) and *P.aspleniifolius* (celery top pine), can be seriously degraded by *P.subgranosus* attack. No estimate of economic losses due to such degrade is available and no organised programme of control of such degrade is currently practiced. Removal of logs from landings and marshalling yards from winter operations before the flight season begins in summer and quickly processing logs in summer operations are currently recommended to minimise damage due to

P.subgranosus attack (Elliott *pers. comm.*). Given the dwindling supply of eucalypt sawlogs from old-growth stands in Tasmania and the pressure from sawmillers to exploit the large resource of rainforest species, the largest volume of these being myrtle, the logging of high quality rainforest set aside for timber production will require a more organised programme to protect valuable logs from pinhole borer attack.

Pest-management strategies have been adopted with mixed success to control the damage caused to high grade logs by the striped ambrosia beetle *T.lineatum* in British Columbia (Borden 1988). These strategies have been based on observations or hypotheses on *T.lineatum* population behaviour (Table 1 of Borden 1988). There are some similarities in the biology and habits of *P.subgranosus* to that of *T.lineatum*. In particular the hypothesis that population levels are dependent on the supply of host material (i.e. logs, stumps, dead or dying *N.cunninghamii* infected with *C.australis*) is as relevant to *P.subgranosus* as *T.lineatum*. There is only circumstantial evidence for this hypothesis both in the case of *T.lineatum* (Borden 1988) and *P.subgranosus* and this is largely by default given that no other significant population control mechanisms have been observed. Brood mortality is very low for *P.subgranosus* and of the few parasites and predators associated with *P.subgranosus*, as with *T.lineatum* (Borden 1988), none appear to play any significant role in regulating populations. Apart from the lack of suitable host material, the only other suggested factor which could limit brood production is egg and early instar larvae mortality due to desiccation (Section 5.6). A modified version of Table 1 of Borden (1988) which sets out pest-management strategies based on observed or hypothesised population behaviour is given in Table 8.1. Probably the most important strategy in the control of damage to high value logs is to limit the resource of suitable host material available during the flight season. This involves good forest hygiene by removing slash from logging and quick processing of logs. However, given that summer logging is most often required in wet forests, there will always be a time when some logs are vunerable to attack. In these cases it may be

Table 8.1 Pest–management strategies and tactics that exploit observed or hypothesised behaviour of *P.subgranosus* populations.

Observation or hypothesis	Pest management	
	Strategy	Tactic
Regulation levels depend on supply of suitable host material	Regulate the amount of host resource	Reduce logging slash Winter logging where possible Remove logs from landings as soon as possible Process logs at mills as soon as possible
	Protect host from attack	Kill beetles on host with residual insecticide Repel beetles from hosts using artificial repellents
Aggregation of population on available hosts is odor mediated	Manipulate host–seeking population by providing a false chemical message	Attract beetles to water–soaked waste or pulp logs which are then removed Intercept host–seeking beetles by mass–trapping them using ethanol–baited traps

necessary to employ other tactics. Browne (1952) reported that creosote, pentachlorphenol, sodium pentachlorphenate, and possible formaldehyde can be partially effective in inhibiting ambrosia beetle attack on debarked tropical hardwood logs. Browne suggested that these substances inhibited attack by countering the effect of primary attractants. Repelling attack using turpentine oil (a mixture of monoterpenes) has been found effective against *T.lineatum* (Borden 1988) for up to five days. Experiments to investigate various artificial repellents should be carried out in Tasmanian rainforest to determine if a similar tactic can be employed against *P.subgranosus*. Water misting of logs has been used as a cheap method of deterring attack by *T.lineatum* (Borden 1988) but operational problems have meant that this method has not been widely adopted. A possible problem with water misting logs in mill yards or log marshalling yards for the case of *P.subgranosus* is that logs with established galleries, if left long enough might be allowed to produce a brood which can then emerge and attack other logs in the yard. If the logs are left to dry in the exposed environment of the log yard then survival of such broods will be minimal. This tactic is based on the hypothesis, given support in this work, that brood survival is dependent on a high humidity within the galleries during, in particular, the time when eggs and early instar larvae are present.

Exploiting the chemical host-seeking mechanism of ambrosia beetles is another way of protecting exposed logs. Aggregation of attack is due firstly to primary attraction due to volatiles released by stressed or dying trees and decaying logs. Elliott *et al.* (1982) have identified ethanol as a primary attractant for pinhole borer attack. Soaking logs speeds up the fermentation process and trap logs of suitable size (i.e. large enough to allow a large number of beetles to establish their galleries) soaked over the winter and moved to strategic locations between flight paths of the beetle and landings or log yards could be used to reduce attack on valuable logs cut and stored in summer.

Given the known problem of a high incidence of defect in myrtle (Walker and Candy 1982) there would be little difficulty in finding reasonably sized waste and pulp logs which could be used as trap logs.

Alternatively, or in combination, ethanol baited traps could be designed to mass trap the beetle. Aggregating pheromones are suspected as being a secondary attractant (i.e. after pioneer beetles have begun boring) for *P.subgranosus* attack (Elliott *et al.* 1982). Mass trapping using pheromone-baited trap logs is an important tactic in the control of *T.lineatum* (Shore and McLean 1985, Borden 1988), however, the pheromone(s) of *P.subgranosus* has yet to be identified so a similar use of pheromone-baited traps is not yet possible.

It should be emphasised at this point that given the ubiquity and enormous population size of *P.subgranosus* the only effective method of protecting high value logs may be simply removing them from landings and processing them through mills before the beetle has a chance to attack.

8.3 Monitoring *P.subgranosus* populations

Given the costs associated with any pest-management programme using tactics such as those given in Table 8.1, a cost-effective method of monitoring *P.subgranosus* populations may be useful in deciding if control measures are required in any particular year. The relatively long development time of one or, more often, two years for *P.subgranosus*, as mentioned by Milligan (1974) for the case of the New Zealand *Platypus* spp. which have similarly long development times, allows a good amount of lead time for control measures to be implemented which can defuse potential population explosions. Such a lead time is not available in the case of *T.lineatum* with a development time of around 9-10 weeks (Borden 1988). A monitoring programme to assess population levels combined with built up experience on the relationship between population levels and damage would allow forest managers to determine the risks associated with various forest operations and whether control measures are required.

Any monitoring programme would need to be quick and cheap, involve a minimum of equipment, and be able to forecast population levels one and two summers ahead. In logged coupes assessment of the number of pinholes on logs left by the operation could be combined with routine logging residue assessments. These are currently carried out using line intersect sampling and De Vries (1979) gives an example of such a sampling scheme combined with subsampling to assess bark beetle populations. In surrounding rainforest, line transect sampling could be used in a multi-stage sampling scheme. For example, in the first stage all trees on the transect are sampled and their disease status with regard to myrtle wilt assessed. In the second stage a subsample of trees suffering myrtle wilt are sampled and an estimate of the total number of pinholes determined. This could be done by delimiting the main area of attack on the bole and randomly sub-sampling small areas using a calibrated plastic sheet. Sampling would be best carried out at the end of the last summer or in winter so that emergence in the following summer can be predicted. The number of pinholes can be easily and cheaply estimated as seen in the suggested sampling schemes above, however, the number of emergents produced from these galleries for any future period is not so easily estimated. Firstly, the proportion of active galleries needs to be estimated. This can be done relatively easily by observing if there is any fresh frass produced by the gallery, or by testing if there is a live male at the gallery entrance. If the abdomen of the male is seen it can be gently prodded with say a toothpick or probe to test if it is alive. Given that the gallery is active, the stage of its development needs to be known. The time taken from gallery establishment to first brood emergence will depend on the day-degrees accumulated from gallery establishment (Section 7.3). Also galleries which have already produced their first brood emergence in the previous summer will produce only an average of 36.4% of the total of emergence for the gallery in the coming summer, 62.8% occurring in first brood emergence and 0.8% in the third year of emergence (Section 6.5). Therefore the expected number of emergents

for a gallery will depend on which brood, if any, will emerge in the next summer. The timing of first brood emergence cannot be predicted from the models developed in this study unless the date, or more roughly the period in which, gallery establishment occurred and the accumulated day-degrees from this date (Section 7) are known. The date or period within which gallery establishment occurred is not available from a single sampling occasion, however, a rough guide to the age of the gallery can be obtained by examining the type of frass being produced. If the frass is fibrous then it can be assumed that the gallery was established in the previous summer and first brood emergence will not occur until the summer following the next summer. Alternatively, if granular frass is evident it indicates that final instar larvae are present which means that pupation and emergence should occur in the next summer. The difficulty in this last case is that it would not be known if the larval frass was from later broods than those emerging in the first summer of emergence for the gallery unless the frass can be reliably aged. Old frass tends to form a solid, faded mass and determining the age of frass based on such appearances could be sufficiently accurate to allow the estimates of mean emergence per gallery in the first and second summer of emergence, obtained in this study (Section 6.1 and 6.5), to be applied.

From such a classification of the development stage of the gallery using frass an overall estimate of total emergence for each of the next two summers can be obtained. If more detail on the timing of emergence within the summer is required, for instance, to allow scheduling of operations to avoid, or mass trapping to coincide with the main period of emergence, then the models of the distribution of development times (i.e. the day-degree and gamma distribution models developed in Section 7) could be employed to predict emergence rates for periods within the summer period. This would require a database of time of attack to be accumulated and estimates of daily minimum and maximum temperature to be obtained as was done in this study (Section 3.3). In the first case this database could be obtained by repeat sampling, say monthly through the

summer and at the end of the summer, at which time the number of new galleries could be estimated using the multi-stage sampling discussed above. Day-degrees can be accumulated using daily minimum and maximum temperatures as was done in this study (Section 3.3). Given an estimate of total emergence for the summer then this total can be distributed over the summer using the cumulative density function of the gamma distribution and the day-degree time scale (Section 7.2) with a development threshold temperature estimated in this study at 11°C (Section 7.3.2).

In conclusion, although *P.subgranosus* does not have the biotic potential of *T.lineatum* and many bark beetles in terms of generation time, even though brood production is similar, it has the potential to reach very high population levels given enough resource of suitable host material. Dead and dying myrtle infected with *C.australis* are highly attractive to attack by *P.subgranosus* and high densities of attack can occur on these trees (Section 4). Disturbances such as logging and roading as well as providing host material in the form of logs and slash increase the incidence of myrtle wilt. There is therefore the potential for *P.subgranosus* to cause serious damage to saw and veneer logs and, given a possible contributory role in the spread of myrtle wilt, cause elevated levels of this disease in adjacent rainforest. From the above it can be seen that more refined control measures must wait until the type and extent of future rainforest management, the relationship between *P.subgranosus* and myrtle wilt, the effectiveness of measures to control myrtle wilt, and the generality of the results from this study, are better known.

9. CONCLUDING REMARKS

No study of this nature can hope to be complete as populations and the environmental conditions to which they are exposed are dynamic and, given the long development time of *P.subgranosus*, it was only possible to follow a single cohort in detail in this study. Even so, a number of observations in this study have led to interesting and plausible hypotheses on the behaviour of *P.subgranosus* at the population level. In particular, the relationship between gallery length and brood size at initial oviposition and the delay in initial oviposition until winter are useful new observations. Combined with the lack of relationship between timing of gallery establishment and timing of first brood emergence for late summer/autumn establishment and infrequent spring/early summer establishment these observations have led to the hypothesis that egg and early instar mortality due to desiccation is an important factor in the timing of gallery establishment and initial oviposition. Indirectly, this mortality would exert some control on populations given that late/summer autumn gallery establishment causes first brood emergence to take two years rather than a single year which limits population growth.

The attractiveness of host tissue infected with *C.australis* to *P.subgranosus* attack has been demonstrated by Kile *et al.* (1990b) and the more detailed statistical analyses of their data carried out in this study reinforces their conclusions. Their work gives further support to the hypothesis that *P.subgranosus* is not a vector of *C.australis*. The observation that myrtle wilt is always associated with *P.subgranosus* attack is thus explained by the primary attractant role of *C.australis* infection rather than Howard's (1973) original hypothesis that the platypodid beetle attacking myrtle is a vector of the pathogen which causes myrtle wilt.

The mathematical and statistical modelling techniques used in this study were found to be very useful in summarising, at times, highly variable data. In particular, the

day-degree model of development and the models of the distribution of development rate and time, in day-degree time units, using normal and gamma density functions respectively, adequately explained observed development time from attack to first brood emergence. The maximum likelihood estimation procedure for estimating the threshold and rate parameters of the day-degree model from field data which was developed in this study could be used in similar field based studies. Also the comparison of models of insect phenology carried out in this study is particularly relevant to insect pest species in which the timing of control measures requires accurate prediction of the timing of occurrence of immature stages. For wood boring insects this is of less interest from a pest control viewpoint since there is little ability to target immature stages with control measures. For insects such as the Tasmanian eucalyptus leaf beetle, *Chrysophtharta bimaculata* Olivier (Coleoptera: Chrysomelidae), a serious defoliator of eucalypts (Elliott and deLittle 1984), models of phenology are very important for the prediction of the optimum timing of control measures and the models and methodology used in this study could be applied in this way. The introduction in this study of the complementary log-log link and the conditional probability model, which in both cases proved superior to two existing phenological models, may be of interest to other population modellers and researchers.

REFERENCES

Allen, J.C. 1976. A modified sine wave method for calculating degree days. *Environ. Entomol.* 5: 388-96.

Allsopp, P.G. 1986. Development, Longevity and Fecundity of the False Wireworms *Pterohelaeus darlingensis* and *P. alternatus* (Coleoptera : Tenebrionidae) IV. Models for larval and pupal development under fluctuating temperatures. *Aust. J. Zool.*, 34: 815-25.

Baskerville, G.L. and Emin, P. 1969. Rapid estimation of heat accumulation from maximum and minimum temperatures. *Ecology* 50: 514-7.

Bickel, P.J. and Doksum, K.A. 1977. *Mathematical Statistics*: *Basic Ideas and Selected Topics*. Holden-Day, San Francisco.

Borden, J.H. 1988. The striped ambrosia beetle. Pp 579-96 in *Dynamics of Forest Insect Populations*: *Patterns*, *Causes*, *Implications*. Berryman, A.A. (Ed.), Plenum Press, New York.

Browne, F.G. 1952. Suggestions for future research in the control of ambrosia beetles. *Malayan Forester* 15: 197-206.

Byers, J.A. 1984. Nearest neighbour analysis and simulation of distribution patterns indicates an attack spacing mechanism in the bark beetle, *Ips typographus* (Coleoptera: Scolytidae). *Environ. Entomol.* 13: 1191-200.

Chapman, R.F. 1982. *The Insects*, *Structure and Function*. Third Edition. Harvard University Press, Cambridge, Massachusetts. xvi, 919 pp.

Dallwitz, M.J. and Higgins, J.P. 1978. User's guide to DEVAR. A computer program for estimating development rate as a function of temperature. *CSIRO Aust. Div. Entomol. Rep.* 2: 1-23.

Dennis, B., Kemp, W.P., and Beckwith, R.C. 1986. Stochastic model of insect phenology : estimation and testing. *Environ. Entomol.* 15: 540-6.

De Vries, P.G. 1979. Line intersect sampling - statistical theory, applications and suggestions for extended use in ecological inventory. Pp. 1-154 in *Sampling Biological Populations*. Cormack, R.M., Patil, G.P., and Robson, D.S. (Eds.). Satellite Program in Statistical Ecology, International Co-operative Publishing House, Fairland, Maryland.

Diggle, P.J. 1983. *Statistical Analysis of Spatial Point Patterns*. Academic Press, London.

Donnelly, K. 1978. Simulations to determine the variance and edge-effect of total nearest neighbour distance. Pp. 91-5 in *Simulation Methods in Archaeology*. Hodder, I. (Ed.) Cambridge University Press, London.

Dyar, H.G. (1890) The number of moults of Lepidopterous larvae. *Psyche*, 5: 420-2.

Elliott, H.J., Kile, G.A., and Madden, J.L. 1982. Ambrosia beetle attack on myrtle. Pp. 67-73 in *Tasmanian Rainforests - Recent Research Results*. Forest Ecology Research Fund, Hobart.

Elliott, H.J., Madden, J.L., and Bashford, R. 1983. The association of ethanol in the attack behaviour of the mountain pinhole borer *Platypus subgranosus* Schedl (Coleoptera: Curculionidae: Platypodinae). *J. Aust. ent. Soc.*, 22: 299-302.

Elliott, H.J. and deLittle, D.W. 1984. *Insect Pests of Trees and Timber in Tasmania*. Forestry Commission, Tasmania, Hobart 90pp.

Elliott, H.J., Kile, G.A., Candy, S.G., and Ratkowsky, D.A. 1987. The incidence and spatial pattern of *Nothofagus cunninghamii* (Hook.) Oerst. attacked by *Platypus subgranosus* Schedl in Tasmania's cool temperate rainforest. *Aust. J. Ecology* 12: 125-138.

ESRI (1987) *ARC/INFO Version 4.0*. Environmental Systems Research Institute, California.

Fienberg, S.E. 1980. *The Analysis of Cross-classified Categorical Data.* 2nd ed. Cambridge, Mass. M.I.T. Press.

Francke-Grossmann, H. 1967. Ectosymbiosis in wood-inhabiting insects. Pp. 141-205 in Henry, S.M. (Ed.) *Symbiosis*. Vol. II. Academic Press, New York.

Genstat 5 Committee (1987) Genstat 5 Reference Manual. Clarendon, Oxford.

Gilbert, N. 1984. Control of fecundity in *Pieris rapae*. II. Differential effects of temperature. *J. Anim. Ecol.* 53: 589-97.

Gilbert, N. 1986. Control of fecundity in *Pieris rapae*. IV. Patterns of variation and their ecological consequences. *J. Anim. Ecol.* 55: 317-29.

Gilbert, N. 1988. Control of fecundity in *Pieris rapae*. V. Comparisons between populations. *J. Anim. Ecol.* 57: 395-410.

Hickey, J.E. and Felton K.C. 1987 Management of Tasmanian cool temperate rainforest. Pp. 327-42. *Proceedings of Conference of the Institute of Foresters of Australia*, Perth, Western Australia, Sept. 1987.

Hogan, T.W. 1944. Pin-hole borers of fire-killed mountain ash. I. Survey and field observations. *J. Dep. Agric. Vict.*, **42**: 513-20, 524.

Hogan, T.W. 1948. Pin-hole borers of fire-killed mountain ash. The biology of the pin-hole borer, *Platypus subgranosus* S. *J. Dep. Agric. Vict.*, **46**: 373-80.

Howard, T.M. 1973. Accelerated tree death in mature *Nothofagus cunninghamii* Oerst. forests in Tasmania. *Vict. Nat.* **90**: 343-5.

Howe, R.W. 1967. Temperature effects on embryonic development in insects. *Annual Review of Entomology*, 12: 15-42.

Imms, A.D. 1964. *A General Textbook of Entomology*. Revised by Richards, O.W. and Davies, R.G. Methuen & Co. Ltd., London.

Jarman, S.J., Brown, M.J., and Kantvilas G. 1984. *Rainforest in Tasmania*. National Parks aand Wildlife Service, Hobart, Tasmania.

Johnson, N.L. and Kotz, S. 1970. *Continuous Univariate Distributions-1*. John Wiley and Sons. New York.

Kempton, R.A. 1979. Statistical analysis of frequency data obtained from sampling an insect population grouped by stages. Pp 401-18 in. *Statistical Distributions in Ecological Work*, Ord, J.K., Patil, G.P, and Taillie, C. (Eds.) Satellite Program in Statistical Ecology, International Co-operative Publishing House, Fairland, Maryland.

Kendall, M. and Stuart, A. 1977. *The Advanced Theory Of Statistics 1* : *Distribution Theory*. Charles Griffith & Co., London.

Kile, G.A. 1989. Infection of exotic and Tasmanian native tree and shrub species by the vascular stain fungus *Chalara australis*. *Eur. J. For. Path.* 19: 98-104.

Kile, G.A. and Walker, J. 1987. *Chalara australis* sp. nov. (Hyphomycetes), a vascular pathogen of *Nothofagus cunninghamii* (Fagaceae) in Australia and its relationship to other *Chalara* species. *Aust. J. Bot.*, 35: 1-32.

Kile, G.A. and Hall, M.F. 1988. Assessment of *Platypus subgranosus* as a vector of *Chalara australis*, causal agent of a vascular disease of *Nothofagus cunninghamii*. *N.Z. J. For. Sci.* 18: 166-86.

Kile, G.A., Packham, J.M., and Elliott, H.J. 1990a. Myrtle wilt and its possible management in association with human disturbance of rainforest in Tasmania. *N.Z. J. For. Sci.*(In press).

Kile, G.A., Elliott, H.J., Candy, S.G., and Hall, M. 1990b. Treatments influencing susceptibility of *Nothofagus cunninghamii* to attack by the ambrosia beetle, *Platypus subgranosus*.(In preparation).

Lawrence, J.F. 1985. The genus *Teredolaemus* Sharp (Coleoptera: Bothrideridae) in Australia. *J. Aust. ent. Soc.*, 24: 205-6.

McCullagh, P. 1980. Regression models for ordinal data (with discussion). *J. R. Statist. Soc.*, B, 42: 109-42.

McCullagh, P. and Nelder, J.A. 1983. *Generalized Linear Models*. Chapman and Hall, London.

Milligan, R.H. 1974. The purposes of research on Platypus pinhole borers. *Beech Research News*, 2: 17-19.

Milligan, R.H. 1979. *Platypus apicalis* White *Platypus caviceps* Broun *Platypus gracilis* Broun (Coleoptera : Platypodidae) The native pinhole borers. *Forest and Timber Insects in New Zealand*, 37. Forest Research Institute, New Zealand Forest Service.

Morgan, F.D. 1966. The biology and behaviour of the beech buprestid, *Nascioides enysi* (Sharp) (Coleoptera: Buprestidae) with notes on its ecology and possibilities for its control. *Trans. Roy. Soc. N.Z., Zool.*, 7: 159-70.

Mosimann, J.E. 1962. On the compound multinomial distribution, the multivariate β-distribution, and correlations among proportions. *Biometrika* 49: 65-82.

NAG (1986) *The GLIM System*, Release 3.77. Numerical Algorithms Group, Oxford.

Nelder, J.A. and Wedderburn, R.W.M. 1972. Generalized linear models. *J.R. Statist. Soc.*, A, 135: 370-384.

Osawa, A., Shoemaker, C.A., and Stedinger, J.R. 1983. A stochastic model of balsam fir bud phenology utilizing maximum likelihood parameter estimation. *For. Sci.* 21: 478-90.

Pal, T.K. and Lawrence, J.F. 1986. A new genus and subfamily of mycophagus Bothrideridae (Coleoptera: Cucujoidea) from the Indo-Australian region with notes on related families. *J. Aust. ent. Soc.* 25: 185-210.

Richmond, J.A. and Bacheler, J.E. 1989. A comparison of two temperature-dependent development models for immature stages of the Nantucket pine tip moth (Lepidoptera: Tortricidae). *J. Entomol. Sci.* 24: 117-23.

Samson, P.R. 1984. Interpolating temperatures for simulation of the developmental progress of *Pieris rapae* (L.) (Lepidoptera: Pieridae). *J. Aust. ent. Soc.*, 22: 299-302.

Schedl, K.E. 1936. Scolytidae and Platypodidae. Contribution 35. The collection of the South Australian Museum. Records of the South Australian Museum. 5: 513-535.

Schoolfield, R.M., Sharpe, P.J.H., and Magnuson, C.E. 1981. Non-linear regression of biological temperature-dependent rate models based on absolute reaction-rate theory. *J. Theor. Biol.* 88: 719-31.

Sharpe, P.J.H., Curry, G.L., DeMichele, D.W., and Cole, C.L. 1977. Distribution model of organism development times. *J. Theor. Biol.* 66: 21-38.

Sharpe, P.J.H. and DeMichele, D.W. 1977. Reaction kinetics of poikilotherm development. *J. Theor. Biol.* 64: 649-70.

Shore, T.L. and Mclean, J.A. 1985. A survey for the ambrosia beetles *Trypodendrum lineatum* and *Gnathotrichus retusus* (Coleoptera: Scolytidae) in a sawmill using pheromone-baited traps. *Can. Ent.* 117: 49-55.

Slade, A. 1978. Survey of myrtle die-back. Forestry Commission, Tasmania report.

Stedinger, J.R., Shoemaker, C.A., and Tenga, R.F. 1985. A stochastic model of insect phenology for a population with spatially variable development rates. *Biometrics* 41: 691-701.

Stinner, R.E., Gutierrez, A.P., and Butler, JR. G.D. 1974. An algorithm for temperature-dependent growth rate simulation. *Can. Ent.* **106**: 519-24.

Stinner, R.E., Butler, Jr. G.D., Bacheler, J.S. and Tuttle, C. 1975. Simulation of temperature-dependent development in population dynamics models. *Can. Ent.* **107**: 1167-74.

Thompson, R. and Baker, R.J. 1981. Composite link functions in generalised linear models. *Appl. Statist.*, **30**: 125-31.

Wagner, T.L., Hsin-i wu, Sharpe, P.J.H, Schoolfield, R.M. and Coulson, R.N. 1984. Modeling insect development rates: A literature review and application of a biophysical model. *Ann. Ent. Soc. Amer.*, 77: 208-25.

Walker, B.B. and Candy, S.G. 1982. Investigating methods of assessing rainforest in Tasmania. Pp. 7-33 in *Tasmanian Rainforests - Recent Research Results*. Forest Ecology Research Fund, Hobart.

Webb, S. 1945. Australian ambrosial fungi (*Leptographium lundbergii* Lagerberg et Melin and *Endomycopsis* spp. Dekker). *Proc. R. Soc. Victoria* **57** (N.S.), Pts I and II, 57-78.

Wedderburn, R.W.M. 1974. Generalized linear models specified in terms of constraints. *J. R. Statist. Soc. B*, 36: 449-454.

Zervos, S. 1980. *Bispiculum inaequale* n.gen & sp. (Nematoda: Tetradonematidae) from New Zealand wood-boring beetles (Curculionidae: Platypodinae). *N.Z. J. Zoology*, 7: 155-64.

APPENDIX 1. Generalised Linear Models

Generalised linear models and modelling are a class of models and modelling techniques developed originally by Nelder and Wedderburn (1972). A number of the models such as log-linear models for contingency tables and probit analysis for bioassay were commonly used prior to the 1972 but Nelder and Wedderburn unified these and other models into one general class of models called generalised linear models or *glm's*. The *glm's* of Nelder and Wedderburn should not be confused with the *General Linear Model* which is a matrix based class of models which incorporates both linear regression modelling and analysis of designed experiments. There is some overlap between *glm's* and the *General Linear Model*. There was nothing essentially new in the method of estimation and hypothesis testing used by Nelder and Wedderburn (1972), estimation was by maximum likelihood using Fisher's scoring algorithm and hypothesis testing used Neyman-Pearson likelihood ratio tests. However, the attraction of Nelder and Wedderburn's *glm* was the fact that a wide class of models could be fitted using a single algorithm: iteratively re-weighted least squares (*IRLS*), and these models could be tested using the likelihood ratio statistic to generalise the residual sum of squares to the *deviance*. This allowed the familiar regression analysis of variance table to be constructed for error distributions other than the normal. The use of *glm's* are available in the computer packages GLIM and GENSTAT.

A *glm* is specified by (i) the linear predictor η, (ii) the link function $\eta = g(\mu)$ where μ is the expected value of y the dependent variable, and (iii) the error distribution of y. The linear predictor is simply the linear combination of regressor or predictor variables, $x_1,...,x_p$, and unknown regression parameters so that

$$\eta_i = \Sigma_j \beta_j x_{ij}$$

where the i^{th} subscript refers to the sampling unit of y. Note that *glm's* are univariate models (i.e. one dependent variable only) and that the x's can be qualitative, called *factors*, as well as quantitative (i.e. *variates*) variables.

The link function, $g(.)$, must be a one-to-one differentiable function such as the logarithmic, exponential, reciprocal or power functions with a positive exponent in this last case. In the case of log-linear models $g(.)$ is the exponential function. For bioassay where the expected value of the proportion of response is $\mu=p$ then commonly used link functions are the ; *probit* $\eta = \Phi^{-1}(p)$ where Φ is the cumulative normal integral; the *logit* $\eta = log\{p/(1-p)\}$; and the *complementary log-log* $\eta = log\{- log(1-p)\}$. Note that since the transformation or link is applied to the expected value, which is itself given by the model, there is usually no problem with the transformation being undefined which can be a problem if the transformation is applied to the data (e.g. if y is zero or one in the above case). Problems with the link function can occur for example if the exponential link is used and for a particular sample all the regressor variables are zero. However, most of these problems can be overcome by selecting a link function which is sensible given the nature of y and the x's. The logit link function has the property, employed in Section 6.2, that the linear predictor is equivalent to the expected log-odds where $p/(1-p)$ is the odds of say death, success or being male (Section 6.2) depending on the definition of y. The logit and complementary log-log links are also used extensively in Section 5.4 where in the case of the ordinal regression models these links are used as cumulative density functions on an unknown metric scale given by X. In the case of the conditional probability models the inverse of these links define transformations of the time scale t.

The error distribution, as originally specified by Nelder and Wedderburn (1972), must belong to the class of exponential distributions so that the probability density function (*pdf*) of y, is given by

$$\mathcal{P}(y_i) = exp\{[y_i\,\theta_i - b(\theta_i)]/\alpha_i\,(\phi) + c(y_i, \phi)\} \qquad \text{(A1.1)}$$

where θ is called the canonical parameter, which involves the β since the expected value of y is given by $b'(\theta)$ where the prime denotes differentiation with respect to θ, ϕ is a dispersion parameter which does not involve the β and is therefore considered a

nuisance parameter, the function $\alpha_i(\phi)$ is usually specified by ϕ/w_i where the w_i are known *prior weights* (for example for the normal distribution ϕ is usually denoted by σ^2) and the term $c(y_i, \phi)$ is used to collect terms in the *pdf* not involving the β's. The log-likelihood is given by

$$\mathcal{L} = [y_i \theta_i - b(\theta_i)]/\alpha_i(\phi) + c(y_i, \phi).$$

The *kernel* of the log-likelihood is that part of $\mathcal{L}$ involving only the parameters of interest and is given by dropping the term $c(y_i, \phi)$ from $\mathcal{L}$ above. The variance of y is given by $\phi\tau_i^2/w_i$ where τ_i^2 is the *variance function* given by $b_i''(\theta)$ the second derivative of $b_i(\theta)$. Since the expected value of y_i, μ_i, is given by $b_i(\theta)$ then, ignoring the w_i for the moment, the variance of y is a function only of μ_i and ϕ. This is the basis of quasi-likelihood theory (McCullagh and Nelder 1983) which relies purely on the functional relationship between the mean and the variance to provide the *iterative weights* for the Fisher scoring algorithm. The Fisher scoring algorithm is a method of obtaining the maximum likelihood estimates of the β's. It involves a Newton-Raphson search in which the expected rather than observed value of the Hessian matrix is inverted to determine the step size along the steepest descent gradient given by the vector derivative $\partial\mathcal{L}/\partial\beta$. The Hessian is given by the matrix derivative with $(i,j)^{th}$ element $\partial\mathcal{L}^2/\partial\beta_i\,\partial\beta_j$.

Some commonly used distributions and their variance functions are the normal ($\tau_i^2 = 1$), Poisson ($\tau_i^2 = \mu$), gamma ($\tau_i^2 = \mu^2$) and binomial [$\tau_i^2 = \mu(1-\mu)$]. Less commonly used is the inverse Gaussian distribution for which $\tau_i^2 = \mu^3$. Several distributions can share the same variance function, for example the gamma, log-normal and Weibull distributions. Thus quasi-likelihood requires the weaker assumption of a given variance function compared to likelihood which assumes a given distribution for y. For the Poisson and binomial distributions the *scale* or *dispersion* parameter, ϕ, is one and does not need to be estimated. However, in some cases the residual variation in y after fitting the model is either greater than or less than expected for a Poisson or

binomial which is termed *over-dispersion* and *under-dispersion* respectively. In the case of over- or under-dispersed data standard errors of parameter estimates can be adjusted by multiplying them by $\sqrt{\phi}$. In general ϕ will be unknown but it can be estimated as described below.

One of the most useful features of *glm's* is the *deviance*. The deviance is a generalisation of the familiar residual sum of squares and is based on the likelihood ratio statistic in a way that exploits the special structure of *glm*'s. The likelihood ratio statistic is given by $exp(\mathscr{L}_a - \mathscr{L}_b)$ where $\mathscr{L}_a$ is the log-likelihood for the model with parameters $\beta_1,...,\beta_a$ [called model(a) for the following] and $\mathscr{L}_b$ is the log-likelihood for that with parameters $\beta_1,...,\beta_b$ and $a<b$. Thus the parameters in model(a) are *nested* within model(b). The deviance for a model, say model(a) above, is defined as $\mathscr{D} = -2\,(\mathscr{L}_a - \mathscr{L}_f)$ where $\mathscr{L}_f$ is the log-likelihood for the model which is *saturated* with parameters (i.e. there are as many parameters as observations so that $\hat{\mu}_i \equiv y_i$). In some cases, such as y normal, $\mathscr{L}_f$ will be zero and $\mathscr{D}$ is then simply, in the case of y normal, the familiar residual sum of squares. The above likelihood ratio statistic is asymptotically chi-square distributed with b-a degrees of freedom and from this it follows that $\mathscr{D}$ is in general asymptotically chi-square distributed with n-a degrees of freedom. For the case of the normal and inverse Gaussian distributions the distribution of the deviance is exactly chi-square. An estimate of the dispersion parameter can be obtained by dividing the deviance of the finally selected model by its degrees of freedom (McCullagh and Nelder 1983). The significance of adding extra terms to the linear predictor can be tested by the change in deviance. This change when scaled by dividing by the dispersion parameter is approximately chi-square distributed with b-a degrees of freedom when the null hypothesis $\mathscr{H}_0$: $\beta_{a+1}=,...,=\beta_b=0$ is true and when ϕ is known. If ϕ is estimated then the scaled change in deviance divided by (b-a) should be compared with an F-distribution with $\{(b\text{-}a),(n\text{-}b)\}$ degrees of freedom.

A number of distributions other than those with *pdf* given by eqn (A1.1) can be

fitted as *glm*'s. An important example employed in this study is the case of the multinomial. Models for which the data is sampled as a multinomial do not fit directly into the *glm* framework which is restricted to univariate distributions. However, if the fitted values from the model are constrained to sum to the marginal total representing the multinomial sample size, then the Poisson error structure can be used since it gives the same kernel log-likelihood as the multinomial in this case. Constraining the fitted values in this way occurs in a number of contexts. For contingency table data (e.g. Section 6.3) if a Poisson error and logarithmic link function (i.e. canonical link function for the Poisson distribution) are used then the fitted values are constrained in the above way as long as a factor which corresponds to the margin defining the multinomial sample size is included in the model. In the case of the ordinal regression models used in Section 5.4 the fitted values are constrained to total the multinomial sample size by completing the tails of the distribution for X using suitable end-point parameters (pg.92).

A number of extensions to generalised linear models in terms of the systematic component (i.e. the model for μ) have also been developed. In particular, the composite link functions developed by Thompson and Baker (1981) were employed to fit the ordinal regression models in Section 5.4. The composite link function allows the expected value μ to be a linear combination of a number of link functions each with their own linear predictor. Where μ is the expected proportion of a population distributed along X which lies between α_{j-1} and α_j, and G defines the cumulative density function for the distribution of X, then the difference between cumulative probabilities at abscissa values of α_{j-1} and α_j gives the required proportion in the $(\alpha_{j-1},\alpha_j]$ interval. Thus μ is a linear combination (i.e. a difference) of two link functions which both have the same form but have different linear predictors.

APPENDIX 2. GENSTAT program to fit the gamma entry time model to *P.subgranosus* phenological data

```
" open data file "
OPEN 'LIFE.DAT' ; 2 ; I
UNITS[573]
" data consists of 573 records (see Section 5.4.2  pg.95) of
DAYS (days from gallery establishment to sampling), DDEG
(day-degrees above 11°C threshold corresponding to DAYS),
NUM (number of individuals in each of 3 'stages'), and TOT
(total number of individuals) "
READ[LAY=f ; CHAN=2 ; SKIP=* ; END=*] DAYS,DDEG,NUM,TOT \
      ; FIELD=6,8,2(4) ; SKIP=8,3(0) ; DECIMALS=0,2,2(0)
" starting values for t0, β, and x0, x1 and x2 "
SCALAR T0,B,X[1,2,3] ; VALUE=0,416,930,1871.6,750 & \
      GYI[1,2,3]
VARIATE PR[1,2,3],FVV[1,2,3]
" factor defining stage "
FACTOR[LEVELS=3] LSF ; VALUE=!((1,2,3)191)
" expression defining the model :
  gamma cdf values obtained via a chi-square distribution
  where GYI gives the degrees of freedom for the stages "
EXPRESSION GG[1...12] ; VALUE=!E(GYI[1]=2*X[1]/B), \
      !E(GYI[2]=2*(X[1]+X[2])/B), \
      !E(GYI[3]=2*(X[1]+X[2]+X[3])/B), \
      !E(Y=2*(TIME-T0)/B), \
      !E(PR[1]=CHISQ(Y;GYI[1])),!E(PR[2]=CHISQ(Y;GYI[2])), \
      !E(PR[3]=CHISQ(Y;GYI[3])),!E(FVV[1]=PR[1]-PR[2]), \
      !E(FVV[2]=PR[2]-PR[3]),!E(FVV[3]=PR[3]), \
      !E(FV=(LSF.EQ.1)*FVV[1]+(LSF.EQ.2)*FVV[2] \
            +(LSF.EQ.3)*FVV[3]), \
      !E(FV=TOT*FV/PR[1])
CALC TIME=DDEG
"calculate fitted values using initial parameter estimates"
CALC #GG[1] & #GG[2] & #GG[3] & #GG[4] & #GG[5] & #GG[6]
CALC #GG[7] & #GG[8] & #GG[9] & #GG[10] & #GG[11] & #GG[12]
```

```
" calculate Poisson (=multinomial due to scaling in GG[12])
  likelihood "
CALC PD=LLPOISSON(NUM;FV)
PRINT PD
" fit gamma entry time model "
MODEL[DIST=poisson] NUM ; FITTED=FV
RCYCLE B
FITNONLINEAR[PRINT=mod,est,mon ; CALC=GG ; CONST=omit]
```

APPENDIX 3. Transcript of GLIM run used to fit the model of Dennis *et al.* (1986) to their spruce budworm data

```
[o] GLIM 3.77 update 1 (copyright)1985 Royal Statistical
[o]           Society, London
[o]
[i] ? $units 84 $
[i] ! read data consisting of
[i] ! DDEG day-degrees, TOT total individuals in stage,
[i] ! LSF stage number 1-5 instars, 6 pupa, 7 adult
[i] ! NUM total individuals in stage
[i] $data DDEG TOT LSF NUM $
[i] $read
[i]  58  16  1 16  58  16  2  0  58  16  3  0  58  16  4  0
[i]  58  16  5  0  58  16  6  0  58  16  7  0  82  10  1 10
[i]  82  10  2  0  82  10  3  0  82  10  4  0  82  10  5  0
[i]  82  10  6  0  82  10  7  0 107  30  1 23 107  30  2  7
[i] 107  30  3  0 107  30  4  0 107  30  5  0 107  30  6  0
[i] 107  30  7  0 155  47  1  3 155  47  2 44 155  47  3  0
[i] 155  47  4  0 155  47  5  0 155  47  6  0 155  47  7  0
[i] 237  64  1  0 237  64  2  6 237  64  3 45 237  64  4 13
[i] 237  64  5  0 237  64  6  0 237  64  7  0 307  74  1  0
[i] 307  74  2  2 307  74  3  9 307  74  4 48 307  74  5 15
[i] 307  74  6  0 307  74  7  0 342  72  1  0 342  72  2  0
[i] 342  72  3  1 342  72  4 34 342  72  5 37 342  72  6  0
[i] 342  72  7  0 388 103  1  0 388 103  2  0 388 103  3  1
[i] 388 103  4 10 388 103  5 87 388 103  6  5 388 103  7  0
[i] 442  81  1  0 442  81  2  0 442  81  3  0 442  81  4  7
[i] 442  81  5 53 442  81  6 21 442  81  7  0 518  76  1  0
[i] 518  76  2  0 518  76  3  0 518  76  4  0 518  76  5 10
[i] 518  76  6 65 518  76  7  1 609  40  1  0 609  40  2  0
[i] 609  40  3  0 609  40  4  0 609  40  5  0 609  40  6 14
[i] 609  40  7 26 685  42  1  0 685  42  2  0 685  42  3  0
[i] 685  42  4  0 685  42  5  0 685  42  6  0 685  42  7 42
[i] ! note that there appears to be an error in Dennis et
[i] ! al. (1986) where the total number of individuals, NUM
[i] ! here, does not correspond to the sum across the 7
[i] ! stages for DDEG=388,442. The numbers in each stage
[i] ! have been assumed correct and the total adjusted
[i] ! here.
[i] $fac LSF 7 $
[i] $yvar NUM $
[i] ! set up macros to fit composite link functions
[i] ! using Poisson deviance
[i] ! see Candy, S.G. 1985. Using factors in composite link
[i] ! function models. GLIM Newsletter, 11: 24-8.
[i] $MAC M2 $calc %DR=1 $endmac $
[i] $MAC M3 $calc %VA=%FV $endmac $
[i] $MAC M4 $calc %DI=2*(%YV*%log(%YV/%FV)-(%YV-%FV)) $
[i] $endmac $
[i] $MAC MEXT $extract %PE $endmac $
[i] $MAC M1 $
[i] $calc %L=%ne(%PL,0) $swi %L MEXT $
[i] !
```

```
[i] !
[i] $calc LP1=%PE(7)*X $
[i] $calc LP1=LP1+%PE(1)*(1+CUL)/X+%PE(2)*%eq(LSF,2)/X $
[i] $calc LP1=LP1+%PE(3)*%eq(LSF,3)/X+%PE(4)*%eq(LSF,4)/X $
[i] $calc LP1=LP1+%PE(5)*%eq(LSF,5)/X+%PE(6)*%eq(LSF,6)/X $
[i] $calc LP1=LP1*%le(LP1,20)+21*%gt(LP1,20) $
[i] $calc LP2=%PE(7)*X $
[i] $calc LP2=LP2+%PE(1)*(1+CLT)/X+%PE(2)*%eq(LSF,3)/X $
[i] $calc LP2=LP2+%PE(3)*%eq(LSF,4)/X+%PE(4)*%eq(LSF,5)/X $
[i] $calc LP2=LP2+%PE(5)*%eq(LSF,6)/X+%PE(6)*%eq(LSF,7)/X $
[i] $calc LP2=LP2*%le(LP2,20)+20*%gt(LP2,20) $
[i] $calc F1=%exp(LP1)/(1+%exp(LP1)) $
[i] $calc F2=%exp(LP2)/(1+%exp(LP2)) $
[i] $calc FD1=%exp(LP1)/(1+%exp(LP1))**2 $
[i] $calc FD2=%exp(LP2)/(1+%exp(LP2))**2 $
[i] $calc WC2=TOT*(FD1*%eq(LSF,2)-FD2*%eq(LSF,3))/X $
[i] $calc WC3=TOT*(FD1*%eq(LSF,3)-FD2*%eq(LSF,4))/X $
[i] $calc WC4=TOT*(FD1*%eq(LSF,4)-FD2*%eq(LSF,5))/X $
[i] $calc WC5=TOT*(FD1*%eq(LSF,5)-FD2*%eq(LSF,6))/X $
[i] $calc WC6=TOT*(FD1*%eq(LSF,6)-FD2*%eq(LSF,7))/X $
[i] $calc WGM=TOT*(FD1*(1+CUL)-FD2*(1+CLT))/X $
[i] $calc WB=TOT*(FD1-FD2)*X $
[i] $calc %LP=%PE(1)*WGM+%PE(2)*WC2+%PE(3)*WC3 $
[i] $calc %LP=%LP++%PE(4)*WC4+%PE(5)*WC5 $
[i] $calc %LP=%LP+%PE(6)*WC6+%PE(7)*WB $
[i] $calc %FV=TOT*(F1-F2) $
[i] $calc %FV=%FV*%gt(%FV,0)+0.0001*%le(%FV,0) $
[i] $endmac $
[i] !
[i] !
[i] $own M1 M2 M3 M4 $
[i] ! initial estimates of cut-point parameters α_i
[i] ! and regression parameter β
[i] $assign %PE=45,80,125,190,250,300,-0.6 $
[i] $calc X=%sqrt(DDEG)  $
[i] ! specify abitrarily small (CLT) and large (CUL)
[i] ! starting and finishing points for X
[i] $calc CLT=-%eq(LSF,1) : CUL=10*%eq(LSF,7) $
[i] $use M1 $use M4 $
[i] ! deviance using initial estimates
[i] $calc %S=%cu(%DI) $print %S $
[o]    355.3
[i] $cycle 8 1 $
[i] ! fit the model
[i] $fit -%GM+WGM+WC2+WC3+WC4+WC5+WC6+WB $disp me $
[o] deviance = 79.995 at cycle  1
[o] deviance = 38.343 at cycle  2
[o] deviance = 34.883 at cycle  3
[o] deviance = 34.841 at cycle  4
[o] deviance = 34.841 at cycle  5
[o]     d.f. = 77
[o]
[o] Current model:
[o]
```

```
[o]   number of units is  84
[o]
[o]   y-variate  NUM
[o]   weight     *
[o]   offset     *
[o]
[o]   probability distribution is defined via the macros
[o]   M1, M2, M3 and M4
[o] scale parameter is to be estimated by the mean deviance
[o]
[o]   terms =  WGM + WC2 + WC3 + WC4 + WC5 + WC6 + WB
[o]
[o]          estimate        s.e.     parameter
[o]     1       101.0       4.025     WGM
[o]     2       71.22       4.770     WC2
[o]     3       121.6       5.285     WC3
[o]     4       186.2       6.677     WC4
[o]     5       289.9       9.555     WC5
[o]     6       400.3       13.35     WC6
[o]     7     -0.8416     0.02689     WB
[o]     scale parameter taken as  0.4525
[o]
[i] ! Note that GLIM's degrees of freedom for the deviance
[i] ! is incorrect since the constraint that the fitted
[i] ! values sum to the sample size at each sampling
[i] ! occasion, produced using CLT (=α0) and CUL (=αa),
[i] ! has not been taken into account. The correct degrees
[i] ! of freedom here is 84-7-12=65.
[i] ! Also, if a multinomial error structure is assumed
[i] ! then the standard errors in the above table should be
[i] ! divided by √ 0.4525
[i] $return
[i] ? $stop
```

APPENDIX 4. Equivalence of likelihoods for gamma $D(\tau_0)$ and Poisson m

Considering for the moment a single emergent and its contribution to the *log-likelihood* based on the *pdf* (7.11). The *pdf* (7.11) can be re-expressed as

$$\mathcal{P}(Y = y) = \frac{\theta^{\theta}\ \mu'^{\theta}\{exp(-\mu')\}^{\theta}}{(y-\xi)\Gamma(\theta)} \qquad \text{(A4.1)}$$

where

$$\mu' = (y-\xi)\lambda',\ \lambda' = 1/\beta' \text{ and } \beta' = \theta\beta.$$

The individual's contribution to the *log-likelihood* for l, $\mathcal{L}$, is

$$\mathcal{L} = \theta\{log(\mu') - \mu'\} - log(y-\xi) + log\{[T(l)-\tau_0]\delta(l)\} + \Phi(\theta) \qquad \text{(A4.2)}$$

where the term $\Phi(\theta)$ is used to collect components of $\mathcal{L}$ which do not involve the parameters of interest, λ' and τ_0. The third term in eqn (A4.2) is the logarithm of the Jacobian of the transformation from y to l. Only the first term in eqn (A4.2) is required for maximum likelihood estimation for the same reasons discussed in Section 7.2 for the likelihood for l based on normal X. Note that the term $2log(x)$ in the log-likelihood (7.8) has a similar effect to $-log(y-\xi)$ here. Considering the first term of eqn (A4.2) as equivalent to $\mathcal{L}$ without loss of generality and summing over the data, assuming the m_j individuals have common value of y_j, gives

$$\begin{aligned}\mathcal{L} &= \theta\Sigma_j\{m_j log(\mu_j')-m_j\mu_j'\} \\ &= \theta\Sigma_j\{m_j log(\mu_j)-\mu_j\}\end{aligned} \qquad \text{(A4.3)}$$

where $\mu_j=m_j\mu_j'$ and noting that $m_j log(m_j)$ does not involve the μ_j' and thus λ' and can therefore be ignored. The right-hand side of eqn (A4.3) is proportional to the kernel of the log-likelihood for Poisson m_j, the number of emergents, where μ_j is the expected value of m_j and is given by $\mu_j = m_j(y_j-\xi)\lambda'$ remembering that $y_j = D_j(\tau_0)$. The scaling constant in (A4.3) is θ, the shape parameter of the gamma distribution and thus ϕ $(=1/\theta)$ does not have the usual interpretation of a dispersion parameter for the Poisson (McCullagh and Nelder, 1983). Since θ appears as a scaling constant within the

expression for the log-likelihood, it can be estimated independently of μ_j as the reciprocal of the residual mean deviance (Appendix 1). Equivalencing m_j to its expected value and re-arranging terms the model for m_j can be re-parametrised as $\mu_j = m_j\, y_j\lambda$ where $\lambda=\lambda'/(1+\xi\lambda')$. Expressing λ in terms of the gamma *pdf* parameters gives $\lambda=1/(\theta\beta+\xi)$. Note that μ_j is simply the sum of eqn (7.5) over m_j emergents. Therefore ML estimation of λ and τ_0 using the log-likelihood (7.12, A4.3), representing Poisson m_j with expected value $m_j D_j(\tau_0)\lambda$, is equivalent to fitting a gamma distribution using ML to $D(\tau_0)$ while simultaneously obtaining the MLE of τ_0. The parameterisation is different in each case so that separate estimates of the gamma distribution parameters β and ξ cannot be obtained from MLE's of λ and τ_0 obtained in the above fit, however, it is these last two parameters that are of direct interest because they specify the day-degree model. Separate estimates of β and ξ are required to inspect the adequacy of the gamma as a model of the distribution of $D(\tau_0)$ (Section 7.3.3).

APPENDIX 5. GENSTAT commands to fit the day-degree model using Poisson *m*.

```
JOB 'P.subgranosus day-degree linear model '
" day-degree data {DDEG[f]=D_j(f), f=1,...,17 see Section 7.2
pg. 146} is on two files HADDEG1.DAT and HADDEG2.DAT the
day-degrees for each threshold temperature from 0 to 16
degrees (0 to 8 on HADDEG1.DAT and 9 to 16 on HADDEG2.DAT)
from attack to emergence date. The 3rd file DDEGSEL.DAT
holds the 10 random subsample codes where ISEL[]=1 include,
=0 exclude observation (Section 7.3.2 pg. 151). MF is the
number of emergents (i.e. m) "
OPEN 'HADDEG1.DAT' ; CHAN=2 ; WIDTH=120
OPEN 'HADDEG2.DAT' ; CHAN=3 ; WIDTH=120
OPEN 'DDEGSEL.DAT' ; CHAN=4
OUTPUT[WIDTH=130] 1
UNITS[381]
TEXT DATE
READ[LAY=f ; CHAN=2 ; SKIP=* ; END=*] DATE,MF,DDEG[1...9] \
            ; FIELDWIDTH=8,3,9(10)
READ[LAY=f ; CHAN=3 ; SKIP=* ; END=*] DATE,MF, \
           DDEG[10...17]  ;  FIELDWIDTH=8,3,8(10)
READ[LAY=f ; CHAN=4 ; SKIP=* ; END=*] GND,DATE, \
           ISEL[1...10]  ;  FIELDWIDTH=4,8,10(2)
" scale day-degrees to avoid large numbers "
CALCULATE DDEG[1...17]=DDEG[1...17]/1000
" set up initial values (T0=τ0), DDI is an index to DDEG
where DDI[1] is the integer value of T0+1 and DDI[2] the
integer value of T0+2 (see Section 7.2 pg. 146) "
SCALAR DDI[1,2],T0 ; VALUE=10,11,9.0
" set up model calculation in DDL "
EXPRESSION DDL[1...5] ; VALUE=!E(DDI[1]=INT(T0+1.0)), \
   !E(DDI[2]=INT(T0+2.0)),!E(DIF=T0-INT(T0)), \
   !E(DDEGL=DDEG[DDI[1]]+DIF*(DDEG[DDI[2]]-DDEG[DDI[1]])), \
```

```
   !E(Fitted=MF*DDEGL)
MODEL[DISTRIBUTION=Poisson] Y=MF
RCYCLE[METHOD=g ; TOL=0.0004] T0 ; 0 ; 16 ; 0.2 ; 9.0
SCALAR I ; VALUE=1  & SPSE[1...4]
" for each random selection fit the model
  and extract the parameter estimates and their s.e.
  Note that the rate parameter, λ, is estimated using
  Fitted as the linear component of the model "
FOR[NTIMES=10]
  RESTRICT MF,Fitted ; COND=ISEL[I].EQ.1
  FITNONLINEAR[PRINT=model,summary,estimates ;   \
          CONSTANT=omit ; CALC=DDL ; SELIN=y] Fitted
  RKEEP EXIT=EX ; ESTIMATES=PAR ; SE=SEP ; DEVIANCE=DEV
  EQUATE OLD=!P(PAR,SEP) ; NEW=SPSE
  PRINT EX
  RESTRICT MF,Fitted
  CALCULATE I=I+1
ENDFOR
STOP
```